



UNIL | Université de Lausanne

Unicentre

CH-1015 Lausanne

<http://serval.unil.ch>

Year : 2019

Molecular mechanisms of insect egg-triggered cell death

Groux Raphaël

Groux Raphaël, 2019, Molecular mechanisms of insect egg-triggered cell death

Originally published at : Thesis, University of Lausanne

Posted at the University of Lausanne Open Archive <http://serval.unil.ch>

Document URN : urn:nbn:ch:serval-BIB_AB02A844A7950

Droits d'auteur

L'Université de Lausanne attire expressément l'attention des utilisateurs sur le fait que tous les documents publiés dans l'Archive SERVAL sont protégés par le droit d'auteur, conformément à la loi fédérale sur le droit d'auteur et les droits voisins (LDA). A ce titre, il est indispensable d'obtenir le consentement préalable de l'auteur et/ou de l'éditeur avant toute utilisation d'une oeuvre ou d'une partie d'une oeuvre ne relevant pas d'une utilisation à des fins personnelles au sens de la LDA (art. 19, al. 1 lettre a). A défaut, tout contrevenant s'expose aux sanctions prévues par cette loi. Nous déclinons toute responsabilité en la matière.

Copyright

The University of Lausanne expressly draws the attention of users to the fact that all documents published in the SERVAL Archive are protected by copyright in accordance with federal law on copyright and similar rights (LDA). Accordingly it is indispensable to obtain prior consent from the author and/or publisher before any use of a work or part of a work for purposes other than personal use within the meaning of LDA (art. 19, para. 1 letter a). Failure to do so will expose offenders to the sanctions laid down by this law. We accept no liability in this respect.



UNIL | Université de Lausanne

Faculté de biologie
et de médecine

Département de Biologie Moléculaire Végétale

Molecular mechanisms of insect egg-triggered cell death

Thèse de doctorat ès sciences de la vie (PhD)

présentée à la

Faculté de biologie et de médecine
de l'Université de Lausanne

par

Raphaël GROUX

Master en Sciences Moléculaires du Vivant de l'Université de Lausanne.

Jury

Prof. Jan-Willem VEENING, Président
Prof. Philippe REYMOND, Directeur de thèse
Dr. Sébastien MONGRAND, Expert
Dr. Fabrice ROUX, Expert

Lausanne
2019



UNIL | Université de Lausanne

Faculté de biologie
et de médecine

Ecole Doctorale

Doctorat ès sciences de la vie

Imprimatur

Vu le rapport présenté par le jury d'examen, composé de

Président·e	Monsieur	Prof.	Jan-Willem	Veening
Directeur·trice de thèse	Monsieur	Prof.	Philippe	Reymond
Expert·e·s	Monsieur	Dr	Sébastien	Mongrand
	Monsieur	Dr	Fabrice	Roux

le Conseil de Faculté autorise l'impression de la thèse de

Monsieur Raphaël Groux

Maîtrise universitaire en sciences moléculaires du vivant, Université de Lausanne

intitulée

**Molecular mechanisms
of insect egg-tiggered cell death**

Lausanne, le 14 février 2020

pour le Doyen
de la Faculté de biologie et de médecine

Prof. Jan-Willem Veening

Content

SUMMARY	4
RÉSUMÉ	5
GENERAL INTRODUCTION	6
The plant immune system	6
Plant responses to herbivory.....	10
Plant responses to insect eggs	11
Programmed cell death and immunity.....	15
Aim and structure of the thesis.....	17
References	19
CHAPTER 1: ROLE OF SPHINGOLIPIDS IN <i>PIERIS BRASSICAE</i> EGG-INDUCED CELL DEATH IN <i>ARABIDOPSIS THALIANA</i> AND <i>BRASSICA NIGRA</i>.....	26
Abstract	27
Introduction	28
Material and methods	30
Results	36
Eggs of <i>P. brassicae</i> induce biotic cell death markers in a SA- and ET-dependent manner	36
Oviposition by <i>P. brassicae</i> induces transcriptomic alterations in lipid metabolism genes.....	37
HR-like induction is independent from MYB30 and oxylipin synthesis	39
Egg perception alters transcription of sphingolipid metabolism genes	40
Ceramide synthase mutants show reduced cell death but intact upstream signaling	42
Fatty acid hydroxylation modulates egg-induced responses	43
Sphingolipidome analysis reveals an accumulation of C16:0-containing ceramides in response to <i>P. brassicae</i> eggs	44
The impact of sphingolipid mutants during biotic stress depends on the interaction	47
Discussion	49
Acknowledgments	52
References	53
Supplementary Figures	59
Supplementary Tables	68
CHAPTER 2: <i>GLUTAMATE RECEPTOR-LIKE 2.7</i> IS ASSOCIATED WITH INSECT EGG-INDUCED RESPONSES AND IS UNDER BALANCING SELECTION.	76
Abstract	77
Introduction	78
Material and methods	81
Results	85
Arabidopsis accessions display natural variation in response to <i>P. brassicae</i> eggs	85
GWA mapping and identification of associated loci	86
Different haplotypes of <i>GLR2.7</i> segregate in Arabidopsis populations.....	89
Haplotype-specific <i>GLR2.7</i> expression correlate with HR-like symptoms	90
Signatures of balancing selection at the <i>GLR2.7</i> locus.....	92
<i>GLR2.7</i> regulates HR-like in a background-dependent manner	94
<i>P. brassicae</i> egg-extract triggers long lasting cytosolic calcium influxes in leaves	96
Symptoms and survival of <i>P. brassicae</i> eggs on different accessions	97
Discussion	98
The potential role of <i>GLR2.7</i> in insect egg-induced responses	100
Acknowledgments	101

References	102
Supplementary Figures	107
Supplementary Tables	119

CHAPTER 3: L-TYPE LECTIN RECEPTOR KINASE-I.1 CONTRIBUTES TO INSECT EGG-INDUCED CELL DEATH 127

Abstract	128
Introduction	129
Material and methods	132
Results	136
Identification of a minor genetic locus associated with <i>P. brassicae</i> egg-induced symptoms	136
LecRK-I.1 is involved in cell death triggered upon egg perception	137
<i>LecRK-I.1</i> haplotypes correlate with egg-induced symptoms	138
<i>LecRK-I.1</i> variants are not associated with altered expression	141
Signatures of selection at the <i>LecRK-I.1</i> locus	141
LecRK-I.1 and LecRK-I.8 function in the same pathway	142
Discussion	144
Acknowledgments	147
References	148
Supplementary figures	152
Supplementary Tables	156
GENERAL DISCUSSION	158
References	162
ACKNOWLEDGMENTS	164

Summary

In contrast to animals, plant defenses completely rely on the induction of innate immunity to fend off herbivores or pathogens. As a consequence, plants have evolved different immune strategies to protect themselves against external biotic stressors. While immunity to herbivorous insects and pathogens has received a great deal of attention in the past decades, other sectors of plant defense remain vastly overlooked. In particular, it was found that *Arabidopsis thaliana* plant react differently to caterpillars or eggs of the large white butterfly *Pieris brassicae*. Upon perception of egg-derived cues, the defense response share similar components and outputs with plant responses to pathogens, or pathogen-triggered immunity (PTI), and culminates in the induction of cell death in a process called hypersensitive-like response (HR-like). The induction of HR-like has been reported in different plant species from outside of *Brassicaceae* and results in decreased egg survival and/or increased egg parasitism. While the activation of this sophisticated defense mechanism can be effective at reducing egg load, the underlying molecular mechanisms are poorly understood. The aim of this thesis was to identify novel molecular components involved in the induction of cell death in response to insect eggs.

We first observe that sphingolipids, a class of lipids that are known to control cell death induction during immune responses in eukaryotes, play a key role in egg-induced responses. A subset of these lipids accumulate in response to eggs in two *Brassicaceae* species, and we confirm genetically that they are involved in the execution of cell death, indicating that sphingolipids act as downstream components during HR-like. In a second step, we make use of the existence of natural variation in HR-like responses among wild *Arabidopsis* accessions to better characterize the genetic structure of this trait. By performing a genome-wide association study (GWAS), a widely used technique which helps to dissect complex trait by looking for association between genetic polymorphisms and phenotypes, we identify two loci in the *Arabidopsis* genome that are associated with the severity of HR-like in response to eggs of *P. brassicae*. While demonstrating that *LecRK-1.1* is involved specifically in the regulation of cell death, the role of the second locus is still unclear although it displays characteristics which are fully compatible with a potential role in cell death. Moreover, we provide evidence that these genes are under natural selection, indicating that they may be ecologically important.

Altogether, our result provide additional information on the identity of up- and downstream signaling components involved in the response to insect eggs. Identification of genomic regions important in the regulation of this trait provides an important resource for further research on the exact mechanisms regulating HR-like in plants. This knowledge may also prove useful in developing novel strategies to prevent egg-laying by insect pests.

Résumé

Contrairement aux animaux, les défenses des plantes reposent entièrement sur l'induction d'une immunité innée pour lutter contre les herbivores et les agents pathogènes. En conséquence, les plantes ont développé différentes stratégies immunitaires pour se protéger contre différents agresseurs. Alors que l'immunité contre les insectes herbivores et les pathogènes a fait l'objet de beaucoup d'attention au cours des dernières décennies, d'autres secteurs restent largement ignorés. En particulier, il a été constaté que la plante *Arabidopsis thaliana* réagit différemment aux chenilles qu'aux œufs de la piéride du chou *Pieris brassicae*. Lors de la perception de signaux dérivés des œufs, l'induction de mécanismes de défenses est très similaires à l'immunité déclenchée par les agents pathogènes, et aboutit à l'induction de la mort cellulaire dans un processus appelé réponse de type hypersensible (HR-like). L'induction de HR-like a été rapportée chez différentes plantes de la famille du chou (les Brassicacées) et entraîne une augmentation de la mortalité des œufs et/ou une augmentation du parasitisme des œufs. Bien que l'activation de ce mécanisme de défense sophistiqué puisse être efficace pour réduire la charge en œufs, les mécanismes moléculaires sous-jacents sont encore mal compris. Le but de cette thèse était d'identifier de nouveaux composants moléculaires impliqués dans l'induction de la mort cellulaire en réponse aux œufs d'insectes.

Nous observons dans un premier temps que les sphingolipides, une classe de lipides connue pour contrôler l'induction de la mort cellulaire durant les réponses immunitaires chez les eucaryotes, jouent un rôle clé dans les réponses induites par les œufs. Un sous-ensemble de ces lipides s'accumule en réponse aux œufs chez deux espèces de Brassicacées et nous confirmons génétiquement qu'ils sont impliqués dans l'exécution de la mort cellulaire, démontrant que les sphingolipides agissent en tant que composants en aval de la signalisation lors d'une réaction HR-like. Dans un deuxième temps, nous nous servons de l'existence de variation génétique entre des accessions sauvages d'*Arabidopsis* afin de mieux caractériser la structure génétique de la HR-like induite par les œufs d'insectes. En réalisant une étude d'association pangénomique (GWAS), une technique désormais courante qui permet d'analyser la structure génétique d'un trait, nous identifions deux loci du génome d'*Arabidopsis* associés à la sévérité de la mort cellulaire en réponse aux œufs de *P. brassicae*. Nous démontrons que le récepteur immunitaire LecRK-I.1 est impliqué spécifiquement dans la régulation de la mort cellulaire, néanmoins le rôle du deuxième gène n'est toujours pas clair, bien qu'il présente des caractéristiques parfaitement compatibles avec un rôle potentiel dans la mort cellulaire. De plus, nous apportons la preuve que ces gènes sont sous sélection dans la nature, indiquant qu'ils peuvent avoir une importance du point de vue de l'écologie de la plante.

Globalement, nos résultats fournissent des informations supplémentaires sur l'identité des composants de signalisation en amont et en aval impliqués dans la réponse aux œufs d'insectes. L'identification des régions génomiques importantes dans la régulation de ce trait constitue une ressource importante pour la poursuite des recherches sur les mécanismes régulant la HR-like chez les plantes. Ces connaissances pourraient également s'avérer utiles pour élaborer de nouvelles stratégies visant à prévenir la ponte des œufs par les insectes nuisibles dans des plantes d'intérêt agronomique.

General introduction

Plants are central components of our ecosystems and play several major roles for life. The overall biomass of plants represents ~450Gt and is by far the most abundant life kingdom on Earth (Bar-On et al., 2018). Plants are essential primary producers as they perform photosynthetic assimilation of atmospheric carbon. In addition, photosynthesis is also responsible for the production of the high levels of oxygen found in Earth's atmosphere. As primary producers, they also provide nutrient and carbon-based molecules to other heterotrophic organisms that feed on pre-existing organic compounds and are therefore at the basis of our trophic system. As such, plants directly and indirectly provide most of humanity's calorie intake. Besides these roles, they also provide humans with materials such as wood or fibers but also many chemical compounds essential for the production of drugs and many everyday products. It is estimated that ~30% of crop yield is lost due to pest and pathogens (Oerke and Dehne, 2004), however this figure is only correct in the context of plant protection. As a result of the development of modern agricultural practices, the use of pesticides and herbicides has significantly contributed to the increase in crop yields. In this perspective, it is estimated that pest control strategies are responsible for a reduction in crop losses of 30-70% (Oerke, 2006). Besides these practices, crop domestication and improvement has also significantly contributed to agricultural yields through the improvement of physiological processes that results in better plant stature or higher grain/fruit number and size (Pingali, 2012). As a consequence of pest control together with advances in breeding techniques, the production of cereal crops for instance has increased by a factor of 2-3 in the last half century (Pingali, 2012; Oerke, 2006). Unfortunately, despite these large improvements in plant productivity, it is generally accepted that domestication and breeding has frequently increased plant susceptibility to pests (Chen et al., 2015; Moreira et al., 2018).

The plant immune system

In comparison to animals, plants lack circulating immune cells and do not possess adaptive immunity. Besides being equipped with constitutive defensive proteins and metabolites, plants rely on innate immunity that can be triggered upon perception of various attackers. As a result, virtually all cells are able to induce some form of immune responses. The current model relies on the existence of membrane and cytoplasmic receptors that recognize specific molecules indicative of pathogen, insect or damage presence (Bigéard et al., 2015; Jones and Dangl, 2006; Erb and Reymond, 2019). For sake of clarity, the model presented here is based on the Zig-Zag model proposed by Jones and Dangl in the 2006. More recent iterations of the model have been proposed and simplify certain concepts related to plant

immunity (Thomma et al., 2011; Kanyuka and Rudd, 2019). Moreover, most present literature on immunity still rely on the Zig Zag model in terms of concepts and nomenclature.

In the zig zag model, a distinction is made between transmembrane and cytoplasmic immune receptors (Jones and Dangl, 2006, Fig. 1). Accordingly, plants rely on a suite of pathogen recognition receptor (PRRs) that monitor the extracellular space for molecular signatures of pathogens. These molecular signatures consist of conserved patterns harbored by pathogens that unequivocally signal the presence of a potentially damaging microbial agent. Once pathogens penetrate the first structural defense barriers such as the cuticle and the cell wall (Serrano et al., 2014), pathogen-triggered immunity (PTI) can be activated upon the perception of so called pathogen-associated molecular patterns (PAMP, Pieterse et al., 2012; Zipfel, 2014; Bigeard et al., 2015). The archetype of plant PAMPs is the short peptide named flg22, which is a 22 amino acid fragment of bacterial flagelin, but other PAMPs include chitin, lipopolysaccharides (LPS), bacterial proteins... etc. These molecules are typically conserved patterns or molecules that cannot be modified without impacting fitness. Different PRR have been successfully identified, the most well characterized being FLS2 which senses flg22 (Chinchilla et al., 2006; Zipfel et al., 2004). A substantial part of these receptors belong to the family of leucine-rich repeats receptor kinases (LRR-RK), but advances in the field revealed that other classes of receptors can also bind PAMPs (Ranf, 2017). Recently, the G-type Lectin-like receptor kinase LORE was shown to be responsible to immunity triggered by bacterial LPS by binding short-chain hydroxyl-fatty acids (Kutschera et al., 2019). Upon ligand binding, most PRR interact with the co-receptor BAK1 to transduce downstream responses (Roux et al., 2011). PTI induction typically results in the mitogen-

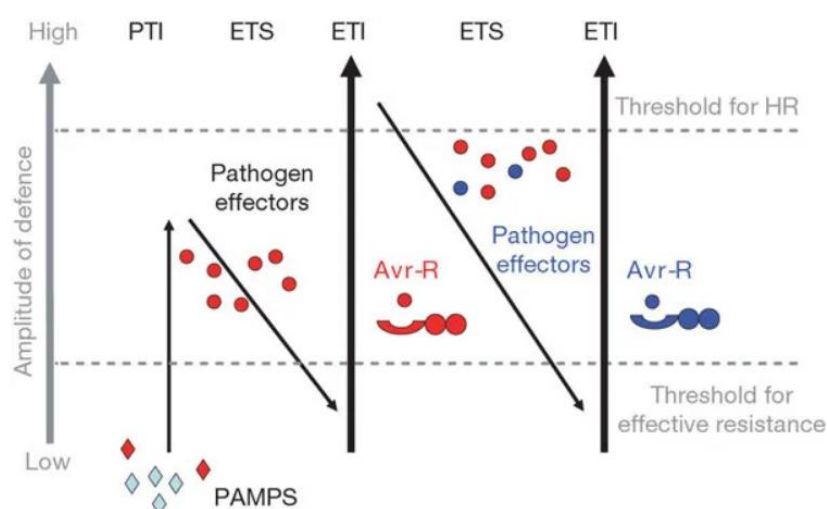


Figure 1. The zig-zag model, see text for details. PTI: pathogen-triggered immunity; ETS: effector-triggered susceptibility; ETI: effector-triggered immunity; PAMP: pathogen-associated molecular patterns. Adapted from Jones and Dangl 2006

activated protein kinase (MPK) activation, generation of reactive oxygen species (ROS), modification of intracellular calcium levels, accumulation of salicylic acid (SA), transcriptional changes, and ultimately to the production of defense proteins and metabolites (Pieterse et al., 2012). SA biosynthesis is initiated from chorismate, and it is mainly produced through the isochorismate pathway during immunity (Bürger and Chory, 2019). The rate-limiting step of this pathway, the conversion of chorismate into isochorismate, is mainly performed by the enzyme ISOCHORISMATE SYNTHASE (ICS1/SID2). Indeed, during infection, SID2 activation is the major contributor of SA pools (Wildermuth et al., 2001). SA-dependent signaling is largely controlled by NPR1 which, upon SA-dependent redox changes, monomerizes and thereby translocates into the nucleus where it functions as a transcriptional activator (Bürger and Chory, 2019). As a central component, NPR1 was previously reported to control the transcription of ~95% of SA-responsive genes (Wang et al., 2006). Interestingly, natural variation in the response to exogenously applied SA was observed in *Arabidopsis* accessions (van Leeuwen et al., 2007). NPR1, together with the homologous proteins NPR3 and NPR4, have been shown to function as SA receptors *in planta* (Wu et al., 2012; Fu et al., 2012). While NPR1 functions as a direct defense activator, NPR3 and NPR4 mediate SA-dependent NPR1 degradation in low or high SA conditions (Fu et al., 2012). The degradation of NPR1 is thought to act as a control for the induction of programmed cell death whereas its stabilization results in systemic acquired resistance (SAR) establishment (Boatwright and Pajerowska-Mukhtar, 2013), whereby a primary infection leads to a systemic resistance to subsequent attacks against a variety of pathogens (Shah and Zeier, 2013). Inside the nucleus, NPR1 associates with TGA transcription factors to control the expression of defense genes, including the expression of *PR* (pathogenesis-related) genes (Zhang et al., 2003). PTI is also usually associated with the induction of SAR. SAR induction was reported to be dependent on the production of several small metabolites, including pipecolic acid (Pip) and its hydroxylated form NH-Pip, which serve as a central regulators of the response in systemic tissues (Hartmann et al., 2018; Navarova et al., 2012; Bürger and Chory, 2019).

As a result of coevolution, adapted pathogens have evolved so-called effector proteins that target various components of defense signaling pathways (Jones and Dangl, 2006; Cui et al., 2015). Effectors aim at dampening defense reactions in order to promote virulence. The recognition of adapted pathogens is mediated by NLR (nucleotide-binding leucine-rich repeat) receptors which detect the presence or the activity of effectors that modulate plant immune responses (Cui et al., 2015). This process is called effector-triggered immunity (ETI). Quantitatively, ETI is described as a faster and stronger form of PTI, as shown by the large overlap between both responses (Thomma et al., 2011; Tsuda and

Katagiri, 2010; Tao et al., 2003). ETI thus reinstates and amplifies signaling, which is often associated with localized cell death, a phenomenon called the hypersensitive response (HR) (Mur et al., 2008; Balint-Kurti, 2019). HR is thought to restrict pathogen proliferation at the infection site although this is still subject to debate. Effectors can function by interfering with different aspects of PTI. For instance, the effector AvrPtoB was shown to directly target and ubiquitinate NPR1, thereby addressing it for subsequent proteosomal degradation (Chen et al., 2017). Interestingly, the interaction between NPR1 and AvrPtoB was facilitated by SA. Other effectors may target transcription factors needed for defenses or modulate phytohormone pathways by taking advantage of existing hormonal antagonisms (Kazan and Lyons, 2014). In particular, SA signaling is known to be antagonistic on the jasmonate (JA) pathway, another hormonal pathway important for defense against insects (Robert-Seilaniantz et al., 2011). Coronatine, for instance, is a well-documented bacterial toxin/effector that is structurally similar to JA-Ile. It functions by promoting JA signaling in infected leaves, thereby inhibiting an efficient induction of SA and therefore PTI (Cui et al., 2005; Zheng et al., 2012). NLRs fall into two classes based on the structure of their N terminal domain: either they contain a Toll-interleukin 1 (TIR) domain, or a coiled-coil (CC; Cui et al. 2015). Signaling downstream of NLR activation is dependent on the EDS1/PAD4 or NDR1 depending on the NLR class (Hofius et al., 2009; Cui et al., 2015)

From the previously discussed mechanisms, it is therefore not surprising that SA mediates defenses against biotrophic pathogens that rely on living tissues for their survival (Glazebrook, 2005; Boatwright and Pajerowska-Mukhtar, 2013). As a consequence, biotrophs usually possess mechanisms to maintain their host alive and to suppress cell death induction (Dickman and Fluhr, 2013). In contrast SA-dependent signaling and cell death induction does not protect against necrotrophs, organisms that obtain nutrients from dead tissues (Bürger and Chory, 2019). Instead, it appears that cell death promotes the susceptibility to necrotrophs (Glazebrook, 2005; Dickman and Fluhr, 2013; Govrin and Levine, 2000). Interestingly, many of such pathogens produce toxins that actively kill their host. For instance, the necrotrophic fungus *Alternaria alternata* produces two toxins called AAL and Fumonisin B1 (FB1) which both induce host cell death (Berkey et al., 2012). Interestingly, both toxins function through the inhibition of an early metabolic step in sphingolipid synthesis which promotes the accumulation of cell death inducing precursors (Magnin-Robert et al., 2015; Saucedo-García et al., 2011). In consequence, plant cells cannot successfully resist necrotroph attack through the induction of HR, rather the response promotes cell survival and toxin accumulation (Veloso and van Kan, 2018).

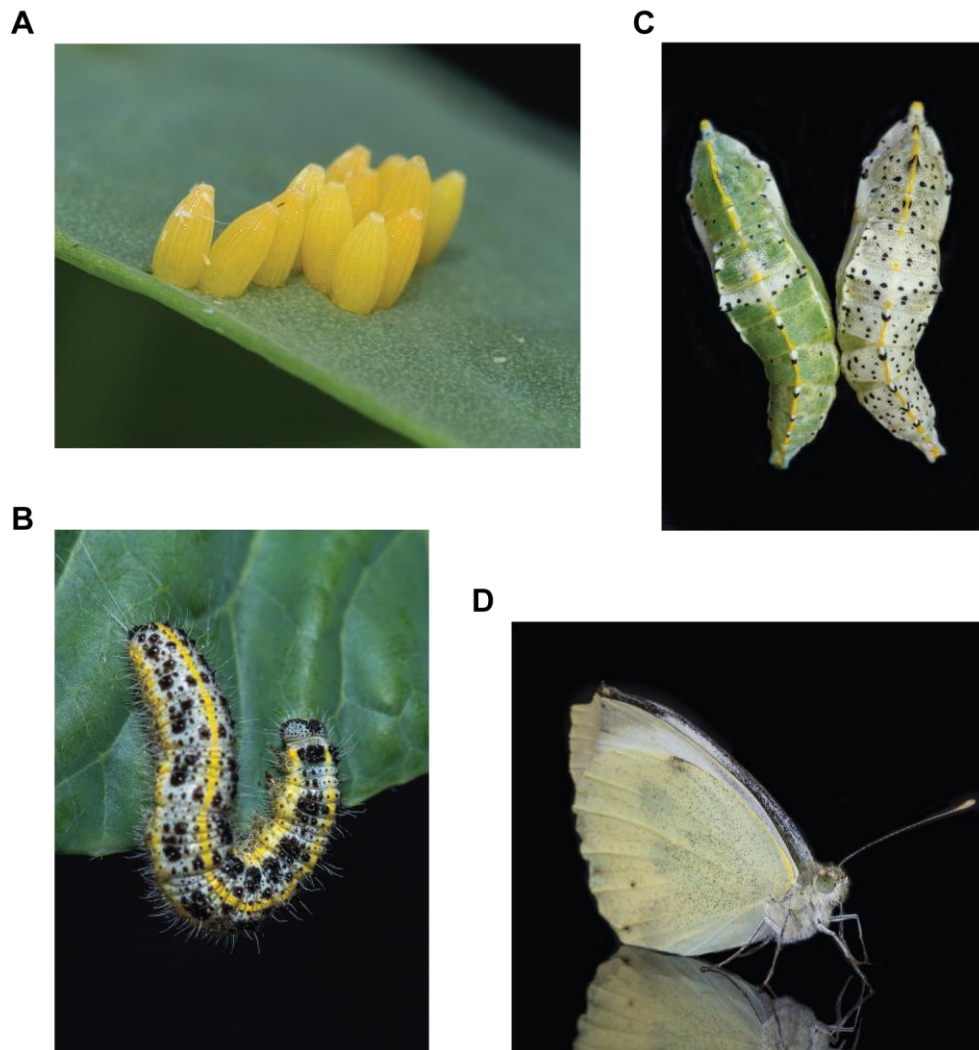


Figure 2. Pictures of different *P. brassicae* developmental stages: eggs (A), fourth instar larva (B), young and mature chrysalis (C), and butterfly (D). Pictures courtesy of Zigmunds Orlovskis.

Plant responses to herbivory

Defenses against herbivorous insects (and also necrotrophs) is coordinated by the JA pathway (Bürger and Chory, 2019; Erb and Reymond, 2019). Upon wounding, JA is formed via the oxidation of poly-unsaturated fatty acids in the chloroplast through the action of lipoxygenases (LOX) proteins. The metabolic intermediate OPDA is then translocated into the peroxisome, where it undergoes several cycles of β -oxidation and results in the formation of JA. JA is then further activated by the conjugation with isoleucine through the activity of the amino acid conjugase JAR1. JA-Ile, which is the biologically active component of this hormonal pathway, binds to a receptor complex SCF^{COI1} inside the nucleus. This leads to the ubiquitination and the degradation of JAZ transcriptional repressors, releasing the repression of bHLH MYC transcription factors (Erb and Reymond, 2019; Dombrecht et al., 2007; Lorenzo et al., 2004). Most of JA-dependent responses are controlled by COI1 and MYC2/3/4, although other transcription factors contributing to the JA pathway have been

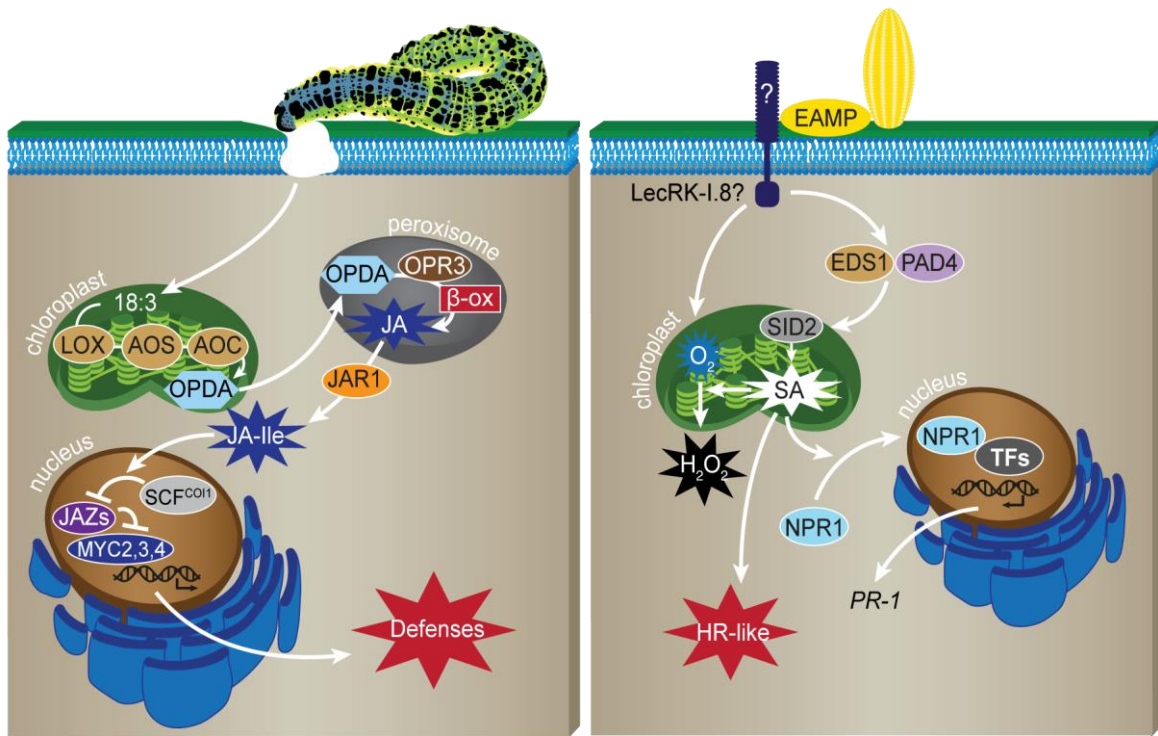


Figure 3. Simplified model of the molecular mechanisms at work during immunity against a herbivore (left panel) or against insect eggs (right panel) in *A. thaliana*. Refer to the text for details. Modified from Stahl et al. 2018 with permission.

described (Schweizer et al., 2013b, 2013a). In particular, MYC2/3/4 control the biosynthesis of glucosinolates, a major class of defense compounds in *Brassicaceae*, and the increased insect performance on a *myc234* mutant revealed a major contribution of these compounds and transcription factors (Fig. 3). Interestingly, glucosinolates were found to be effective against the generalist insect *Spodoptera littoralis* but did not negatively affect the growth of the specialist *P. brassicae* (Schweizer et al., 2013b, Fig. 2). Insect feeding, as during SAR establishment, triggers the induction of fast systemic responses leading to the systemic induction of defenses against herbivores. This process was recently shown to be dependent on the generation of electrical and concomitant Ca^{2+} signals that travel from the wound site to distant tissues (Mousavi et al., 2013; Nguyen et al., 2018; Toyota et al., 2018). Interestingly, the generation of both signals is dependent on the function of two GLUTAMATE-LIKE RECEPTORS: GLR3.3 and GLR3.6.

Plant responses to insect eggs

Despite representing a future threat, eggs of herbivorous insects deposited on plant surfaces are immobile and inert structures (Fig. 4). Plants can sense the presence of eggs on their tissues and can trigger immune responses accordingly. Defenses against insect eggs fall into two categories: direct defenses, which directly harm the eggs; and indirect defenses which involves the attraction of egg predators (Reymond, 2013; Hilker and Fatouros, 2015). Direct

defenses include the induction of tissue growth (Desurmont and Weston, 2011; Petzold-Maxwell et al., 2011; Doss et al., 2000) or cell death (Shapiro and DeVay, 1987; Fatouros et al., 2014; Garza et al., 2001). These responses directly affect egg mortality by causing egg desiccation/drop off or egg crushing, respectively. The induction of cell death, a process that is called hypersensitive-like response (HR-like) based on the similarity to HR triggered by certain pathogens, is commonly found in plants from the *Brassicales* and *Solanales* orders (Fatouros et al., 2016, 2014; Kalske et al., 2014; Petzold-Maxwell et al., 2011; Garza et al., 2001). Indirect defenses, on the other hand, involve the release of volatile chemicals and/or changes in leaf chemistry that lead to the attraction of natural egg predators such as parasitoid wasps (Fatouros et al., 2012; Hilker and Meiners, 2006; Blenn et al., 2012). A fascinating recent study reported that insectivorous birds can also be attracted by egg-deposited plants, and the authors conclude that this could be due to either changes in chemical volatiles or in the reflectance of oviposited tissues (Mäntylä et al., 2018). The latter hypothesis is supported by other studies showing that oviposition can affect the optical properties of plant tissues (Peschiutta et al., 2018).

Although in most cases the exact cause of the decrease in egg survival is not known, studies in *Brassica nigra* suggest that it could be due to water removal at the oviposition site when HR-like is induced (Griese et al., 2017), consistent with the decrease in water potential



Figure 4. Pictures of eggs from different insect species deposited on plant tissues. Pictures were obtained on Google Image.

observed during HR (Wright and Beattie, 2004). Another study using *Solanum dulcamara*, revealed that ROS production, in particular H₂O₂, at oviposition sites was responsible for the increased egg mortality observed (Geuss et al., 2017). In consequence, this effect was independent from ambient humidity and was decreased upon incubation of the eggs with catalase. In *Oryza sativa*, plants respond to eggs of the Whitebacked Planthopper *Sogatella furcifera* through the formation of water lesions and the production of benzyl benzoate, an ovicidal substance (Suzuki et al., 1996; Yamasaki et al., 2003). Finally, the beetle *Pyrrhalta viburni* lays eggs in cavities created in twigs of *Viburnum spp.* and subsequent wound tissue growth was found to result in egg-crushing (Desurmont and Weston, 2011). While these defense mechanisms increase egg mortality individually, some studies found that the co-induction of both direct and indirect defense strategies synergistically impact egg survival (Fatouros et al., 2014).

In addition to these defense strategies, insect oviposition can function as a signal for imminent herbivory, and recent studies have reported that they can prime defenses against larval feeding (Altmann et al., 2018; Kim et al., 2012). For instance, prior oviposition by *Spodoptera exigua* on *Nicotiana attenuata* plants resulted in a decreased insect performance and increased mortality as compared to egg-free plants (Bandoly et al., 2015). This increased resistance to insect feeding was independent on JA levels, but was functionally dependent on a higher inducibility of defense traits. Interestingly, this effect was not dependent on egg load (Bandoly and Steppuhn, 2015). A similar enhancement of resistance against larval was observed upon oviposition on *S. dulcamara*, except that resistance was independent from defense priming (Geuss et al., 2018). Similar effects were reported in *B. nigra*, however the mechanisms of this response were not investigated (Pashalidou et al., 2013). Interestingly, oviposition by the generalist insect *Mamestra brassicae* did not alter larval performance, suggesting that plants can induce specific responses depending on the identity of the insect. In contrast, an increase in larval performance of the generalist herbivore *Spodoptera littoralis* was observed in *Arabidopsis* upon treatment with *P. brassicae* or conspecific egg extract, and this response was dependent on a functional SA-JA crosstalk (Bruessow et al., 2010). However, no impact of prior oviposition on larval growth was observed for the specialist *P. brassicae*. Other studies reported a decrease of *P. brassicae* performance on oviposited *Arabidopsis* plants (Geiselhardt et al., 2013; Lortzing et al., 2019), in line with the effects observed in other plant species. Surprisingly, this effect was dependent on SA accumulation, and authors provide evidence that flavonoid metabolism may be involved in this response.

Genetically, the response of plants to oviposition is still poorly understood (Reymond, 2013; Hilker and Fatouros, 2015). Transcriptomic analyses have shown that insect oviposition on various plants species trigger changes in gene expression (Geuss et al., 2018; Firtzlaff et al., 2016; Little et al., 2007; Altmann et al., 2018; Fatouros et al., 2008; Baruah et al., 2017; Nallu et al., 2018). Even though defenses against the specialist herbivore *Pieris brassicae* (Fig. 2) at the larval stage are dependent on a functional JA pathway, it was recently found that eggs of the same species induce a largely different transcriptional reprogramming, together with SA and ROS accumulation in Arabidopsis (Little et al., 2007; Bruessow et al., 2010). Interestingly, the response of Arabidopsis to *P. brassicae* eggs was found to be dependent on components such as SID2, NPR1, EDS1 and NUDT7, all known regulators of PTI (Gouhier-Darimont et al., 2013, Fig. 3). Furthermore, the expression of several early PTI markers was induced as early as 3h after treatment with egg extract. Interestingly, the induction of cell death was also dependent on PTI regulators, demonstrating that SA signaling is required for HR-like induction in Arabidopsis. Interestingly, *P. brassicae* oviposition resulted in the induction of 41 RLK (receptor-like kinase) genes, and among these it was found that LecRK-I.8 participates in egg-induced *PR1* (Little et al., 2007; Gouhier-Darimont et al., 2013). Characterization of mutant plants showed that LecRK-I.8 is required for ROS and SA accumulation, cell death induction and also SAR establishment following egg perception (Gouhier-Darimont et al., 2019). These results therefore demonstrate that LecRK-I.8 is an upstream component of egg-induced signaling in Arabidopsis.

While addressing the mechanisms that regulate these responses can be challenging in most species due to the lack of proper genetical/molecular tools, the existence of natural variation in the expression of direct defenses was reported in different species. Geuss et al. (2017) reported that egg-killing was affected on one *S. dulcamara* plant genotype, and this effect correlated with a decreased ROS accumulation in eggs. In several *Brassicaceae* species including *B. nigra*, the expression of HR-like symptoms varied according to plants genotypes (Griese et al., 2017, 2019). In Arabidopsis, several natural accessions were shown to display very severe symptoms, with large patches of cell death and chlorosis, while others (including the widely used background Col-0) did not (Reymond, 2013). Volatiles from maize landraces oviposited by the stemborer *Chilo partellus* varied in their ability to attract a parasitoid wasp (Tamiru et al., 2015). Finally, rice varieties were found to vary in their ability to produce water lesions and benzyl benzoate (Yamasaki et al., 2003). The existence of natural variation in the inducibility of direct defenses against eggs demonstrates two important things: (i) the response to insect eggs has a genetic basis and therefore can be under selection; (ii) this variation can be used to explore the genetic basis egg-killing traits.

Recent developments in sequencing and genotyping technologies has vastly improved our ability to perform quantitative trait loci (QTL) and genome-wide association (GWA) mapping, two techniques that allow the identification of genomic regions underlying the variation in a given phenotype. Interestingly, QTL mapping was performed on rice varieties and allowed the identification of several regions implicated in the formation of watery lesions (Yamasaki et al., 2003; Yang et al., 2014)

Programmed cell death and immunity

Plant cell death (PCD) has been extensively studied at the molecular level, although current knowledge is still scattered in contrast to animal models (Huysmans et al., 2017). Based on this observation, the description of PCD in plants is fragmented and many processes appear to have dual functions. PCD can occur during development (dPCD), such as in the formation of sieve elements in xylem cells, or upon pathogen recognition (pPCD; (Huysmans et al., 2017). Recently, a meta-analysis of diverse PCD-inducing conditions revealed that transcriptional signatures of dPCD and pPCD were distinct, demonstrating that these processes are under the control of different pathways (Olvera-Carrillo et al., 2015). For sake of clarity, all processes described below correspond to pPCD mechanisms. One of the most studied form of cell death is the HR. This response, triggered upon the recognition of adapted pathogens, is usually associated with pathogen resistance and the induction of localized cell death (Balint-Kurti, 2019). The observed pathogen growth restriction during HR was historically attributed to the induction of cell death, where dying cells would constrain pathogen spread and survival (Balint-Kurti, 2019). However, it was later realized that in many cases disease resistance could be uncoupled from cell death induction, demonstrating that cell death is not always the cause of resistance (Coll et al., 2010; Künstler et al., 2016; Jurkowski et al., 2004). HR leads to distinct cellular features, such as cytoplasmic shrinkage, chromatin condensation, mitochondrial swelling, cytochrome c release, vacuole rupture and the formation of autophagic vesicles (Mur et al., 2008; Salguero-Linares and Coll, 2019).

Morphologically, several types of PCD exist in animals, ranging from ordered/controlled reactions in the case of apoptosis, pyroptosis and autophagic cell death, to “disordered” in the case of necrosis (Dickman and Fluhr, 2013; Reape et al., 2008; Coll et al., 2011). Apoptosis is the result of tightly controlled cellular checkpoints that ultimately decide whether the cell enters cell death program. One important feature of apoptosis is the formation of so-called apoptotic bodies, which address potentially dangerous cellular components to phagocytosis by macrophages. Plants, however, lack phagocytic pathways and therefore apoptosis in the conceptual sense does not exist (Coll et al., 2011; Dickman and Fluhr, 2013). Despite this major difference, apoptotic-like features such as DNA

laddering (through its degradation by endogenous nucleases) also occurs in plants in response to diverse stresses. In contrast, pyroptosis is triggered by the activation of Toll-like/Nod receptors, which are the structural and functional homologs of plants PRR and NLR respectively. This form of PCD is associated with rapid cell collapse through pore formation at the membrane and the subsequent cell lysis. During autophagy, cellular components are embedded into two-membrane vesicles and cleared through the fusion with peroxisomes in animals or vacuoles in plants. Finally, necrosis is usually seen as the result of cellular injury, where cell death occurs as the result of loss of membrane integrity

In plants, several forms of PCD have been recognized as homologous to animal PCD. While apoptosis *per se* does not exist, apoptotic-like cell death occurs and shares different features of animal apoptosis (Dickman and Fluhr, 2013; Coll et al., 2011). Interestingly, pyroptosis shares similarities with HR triggered upon ETI induction. Recently, the plant NLR ZAR1 was shown to form a macromolecular complex called “resistosome” (Wang et al., 2019). Structural analysis of this complex revealed the exciting possibility that, similar to animal inflammasomes, plant resistosome(s) could directly induce cell death by forming pores in the membrane. However, outside of this elegant possibility, other processes by which cell death is executed remain unclear. For instance, while the induction of different cell death modes is largely dependent on the activation of caspases in animal cells, true caspases are lacking in plant genomes (Coll et al., 2011; Salvesen et al., 2015). Instead, plants possess a variety of proteases that may fulfill similar functions (Salguero-Linares and Coll, 2019). The type I metacaspase MC1 and MC2 were recently shown to regulate cell death in response to exogenous SA and avirulent pathogens (Coll et al., 2010). Notably, their role was specific to the induction of cell death, as pathogen loads were not different in *mc1* and *mc2* plants. Another family of protease named vacuolar processing enzymes (VPE) was also reported to influence cell death in response to *P. syringae*, *B. cinerea* and the turnip mosaic virus (Rojo et al., 2004; Hatsugai et al., 2004). Despite increasing evidences that various proteases regulate PCD, the mechanisms by which they are activated and how they control cell death is still unclear (Thomas and van der Hoorn, 2018; Salguero-Linares and Coll, 2019).

Many other cellular processes and proteins were shown to impact the induction of PCD during immunity. Autophagy (from the greek “self eating”) is a cellular process that functions in the degradation and recycling of cellular material in stressful conditions (Hofius et al., 2007). The role of autophagy during PCD is dual: in certain context it functions as a pro-survival mechanism, while in others it promotes cell death (Hofius et al., 2011). Autophagy was found to be required for the induction of HR downstream of EDS1, while ETI

responses dependent on NDR1 were not (Hofius et al., 2009). In contrast, exogenous SA-induced cell death was negatively regulated by autophagic components (Yoshimoto et al., 2009). The seemingly opposite roles of autophagy during cell death highlight the complex nature of PCD regulation in plants. ROS also play a central role during immunity by regulating redox-dependent processes and by inducing cell death (Dickman and Fluhr, 2013).

Indeed, ROS accumulation is a common signature of PCD, and these reactive molecules are produced mainly through the activity of NADPH oxidases (Torres et al., 2002; Morales et al., 2016) but also from other cellular sources (Dickman and Fluhr, 2013). While ROS are usually thought to function as pro-death signals, they can also promote cell survival in different contexts (Vellosillo et al., 2010). SA, despite being an important signal during for immune responses, also plays a role during PCD. Similar to ROS, SA can function both as a pro-death or pro-survival signal in various contexts. For instance, many mutants displaying spontaneous lesions accumulate SA (Bruggeman et al., 2015), however lesion formation in certain mutants was found to be independent from SA levels. The identification of the SA receptors NPR3 and NPR4 further provides evidence for this dual role (Fu et al., 2012). As mentioned, despite the existence of a large amount of literature regarding plant PCD, the mechanisms involved in its regulation are still fragmented. Moreover, many central PCD components during immunity appear to play opposite roles in different contexts.

Aim and structure of the thesis

As mentioned, the molecular mechanisms leading to the induction of cell death upon the perception of insect eggs are largely unknown. In particular, the identity of upstream and downstream components of this response are elusive. From previously published results, we now know that eggs of *P. brassicae* induce a response in *Arabidopsis* that is dependent on SA accumulation and downstream signaling components, which forms the “central” part, or core, of the response to eggs. In addition, while *lecRK-I.8* plants showed reduced cell death, ROS production and SA accumulation, these responses were not totally abolished thus showing that additional receptors may play a role during this response. Despite the conceptual achievement of this finding, *LecRK-I.8* is the only known upstream component of this signaling cascade, and how it signals further downstream is unknown. Furthermore, the mechanisms implicated in cell death induction downstream of SA are unknown.

The aim of this thesis was thus to gain a better mechanistical understanding of how HR-like cell death is regulated. To this end, we chose to follow two different strategies: (i) identification of processes potentially involved in cell death induction using previously

published transcriptomes of oviposited plants, (ii) exploit natural variation in HR-like responses among Arabidopsis accession. This thesis was written as a compilation of three different manuscripts representing the major findings of the project, and these will serve as a basis for future publications. In consequence, results were selected and arranged in order to build the different stories. Although more directions were explored based on a prior-knowledge basis, these results are not shown here for sake of clarity. Yet, some preliminary data will be discussed in the general discussion at the end of this document as they could represent interesting future extensions of this work.

Chapter 1 reports the identification of sphingolipids as downstream executors of cell death during HR-like responses in Arabidopsis and *B. nigra*. These findings provide a first description of late responses involved in the execution of cell death *per se*. In a second part of this PhD thesis, we discuss the identification through GWA of two new loci involved in the regulation of HR-like. Chapter 2 and 3 are thus dedicated to the validation and description of these loci and their involvement in the response to eggs. Based on our data, the identified loci seem to participate in upstream signaling mechanisms in response to eggs.

References

- Altmann, S., Muino, J.M., Lortzing, V., Brandt, R., Himmelbach, A., Altschmied, L., and Hilker, M.** (2018). Transcriptomic basis for reinforcement of elm antiherbivore defence mediated by insect egg deposition. *Mol. Ecol.* **27**: 4901–4915.
- Balint-Kurti, P.** (2019). The plant hypersensitive response: concepts, control and consequences. *Mol. Plant Pathol.* **0**: 1163–1178.
- Bandoly, M., Hilker, M., and Steppuhn, A.** (2015). Oviposition by *Spodoptera exigua* on *Nicotiana attenuata* primes induced plant defence against larval herbivory. *Plant J.*: n/a-n/a.
- Bandoly, M. and Steppuhn, A.** (2015). A push-button: *Spodoptera exigua* oviposition on *Nicotiana attenuata* dose-independently primes the feeding-induced plant defence. *Plant Signal. Behav.* **2324**: 0–4.
- Bar-On, Y.M., Phillips, R., and Milo, R.** (2018). The biomass distribution on Earth. *Proc. Natl. Acad. Sci. U. S. A.* **115**: 6506–6511.
- Baruah, I.K., Panda, D., Jagadale, M. V., Das, D.J., Acharjee, S., Sen, P., and Sarmah, B.K.** (2017). Bruchid egg induced transcript dynamics in developing seeds of black gram (*Vigna mungo*). *PLoS One* **12**: 1–17.
- Berkey, R., Bendigeri, D., and Xiao, S.** (2012). Sphingolipids and plant defense/disease: the “death” connection and beyond. *Front. Plant Sci.* **3**: 68.
- Bigeard, J., Colcombet, J., and Hirt, H.** (2015). Signaling mechanisms in pattern-triggered immunity (PTI). *Mol. Plant* **8**: 521–539.
- Blenn, B., Bandoly, M., Küffner, A., Otte, T., Geiselhardt, S., Fatouros, N.E., and Hilker, M.** (2012). Insect egg deposition induces indirect defense and epicuticular wax changes in *Arabidopsis thaliana*. *J. Chem. Ecol.* **38**: 882–92.
- Boatwright, J.L. and Pajeroska-Mukhtar, K.** (2013). Salicylic acid: an old hormone up to new tricks. *Mol. Plant Pathol.* **14**: 623–34.
- Bruessow, F., Gouhier-Darimont, C., Bruchala, A., Metraux, J.-P., and Reymond, P.** (2010). Insect eggs suppress plant defence against chewing herbivores. *Plant J.* **62**: 876–885.
- Bruggeman, Q., Raynaud, C., Benhamed, M., and Delarue, M.** (2015). To die or not to die? Lessons from lesion mimic mutants. *Front. Plant Sci.* **6**: 1–22.
- Bürger, M. and Chory, J.** (2019). Stressed Out About Hormones: How Plants Orchestrate Immunity. *Cell Host Microbe* **26**: 163–172.
- Chen, H. et al.** (2017). A Bacterial Type III Effector Targets the Master Regulator of Salicylic Acid Signaling, NPR1, to Subvert Plant Immunity. *Cell Host Microbe* **22**: 777-788.e7.
- Chen, Y.H., Gols, R., and Benrey, B.** (2015). Crop Domestication and Its Impact on Naturally Selected Trophic Interactions. *Annu. Rev. Entomol.* **60**: 35–58.
- Chinchilla, D., Bauer, Z., Regenass, M., Boller, T., and Felix, G.** (2006). The *Arabidopsis* receptor kinase FLS2 binds flg22 and determines the specificity of flagellin perception. *Plant Cell* **18**: 465–476.
- Coll, N.S., Eppele, P., and Dangl, J.L.** (2011). Programmed cell death in the plant immune system. *Cell Death Differ.* **18**: 1247–56.
- Coll, N.S., Vercammen, D., Smidler, A., Clover, C., Van Breusegem, F., Dangl, J.L., and Eppele, P.** (2010). *Arabidopsis* Type I Metacaspases Control Cell Death. *Science* (80-.). **330**: 1393–1397.
- Cui, H., Tsuda, K., and Parker, J.E.** (2015). Effector-Triggered Immunity: From Pathogen Perception to Robust Defense. *Annu. Rev. Plant Biol.* **66**: 487–511.

- Cui, J., Bahrami, A.K., Pringle, E.G., Hernandez-Guzman, G., Bender, C.L., Pierce, N.E., and Ausubel, F.M.** (2005). *Pseudomonas syringae* manipulates systemic plant defenses against pathogens and herbivores. *Proc. Natl. Acad. Sci. U. S. A.* **102**: 1791–6.
- Desurmont, G.A. and Weston, P.A.** (2011). Aggregative oviposition of a phytophagous beetle overcomes egg-crushing plant defences. *Ecol. Entomol.* **36**: 335–343.
- Dickman, M.B. and Fluhr, R.** (2013). Centrality of Host Cell Death in Plant-Microbe Interactions. *Annu. Rev. Phytopathol.* **51**: 543–570.
- Dombrecht, B., Xue, G.P., Sprague, S.J., Kirkegaard, J. a., Ross, J.J., Reid, J.B., Fitt, G.P., Sewelam, N., Schenk, P.M., Manners, J.M., and Kazan, K.** (2007). MYC2 Differentially Modulates Diverse Jasmonate-Dependent Functions in Arabidopsis. *Plant Cell Online* **19**: 2225–2245.
- Doss, R.P., Oliver, J.E., Proebsting, W.M., Potter, S.W., Kuy, S., Clement, S.L., Williamson, R.T., Carney, J.R., and DeVilbiss, E.D.** (2000). Bruchins: Insect-derived plant regulators that stimulate neoplasm formation. *Proc. Natl. Acad. Sci.* **97**: 6218–6223.
- Erb, M. and Reymond, P.** (2019). Molecular Interactions Between Plants and Insect Herbivores. *Annu. Rev. Plant Biol.* **70**: 1–31.
- Fatouros, N.E., Broekgaarden, C., Bukovinszky, G., van Loon, J.J. a, Mumm, R., Huigens, M.E., Dicke, M., and Hilker, M.** (2008). Male-derived butterfly anti-aphrodisiac mediates induced indirect plant defense. *Proc. Natl. Acad. Sci. U. S. A.* **105**: 10033–8.
- Fatouros, N.E., Cusumano, A., Danchin, E.G.J., and Colazza, S.** (2016). Prospects of herbivore egg-killing plant defenses for sustainable crop protection. *Ecol. Evol.* **6**: 6906–6918.
- Fatouros, N.E., Lucas-Barbosa, D., Weldegergis, B.T., Pashalidou, F.G., van Loon, J.J. a, Dicke, M., Harvey, J. a, Gols, R., and Huigens, M.E.** (2012). Plant volatiles induced by herbivore egg deposition affect insects of different trophic levels. *PLoS One* **7**: e43607.
- Fatouros, N.E., Pineda, A., Huigens, M.E., Broekgaarden, C., Shimwela, M.M., Candia, I.A.F., Verbaarschot, P., and Bukovinszky, T.** (2014). Synergistic effects of direct and indirect defences on herbivore egg survival in a wild crucifer. *Proc. R. Soc. B Biol. Sci.* **281**: 20141254.
- Firtzlaff, V., Oberländer, J., Geiselhardt, S., Hilker, M., and Kunze, R.** (2016). Pre-exposure of Arabidopsis to the abiotic or biotic environmental stimuli “chilling” or “insect eggs” exhibits different transcriptomic responses to herbivory. *Sci. Rep.* **6**: 28544.
- Fu, Z.Q., Yan, S., Saleh, A., Wang, W., Ruble, J., Oka, N., Mohan, R., Spoel, S.H., Tada, Y., Zheng, N., and Dong, X.** (2012). NPR3 and NPR4 are receptors for the immune signal salicylic acid in plants. *Nature* **486**: 228–32.
- Garza, R., Vera, J., Cardona, C., Barcenas, N., and Singh, S.P.** (2001). Hypersensitive response of beans to *Apion godmani* (Coleoptera: Curculionidae). *J. Econ. Entomol.* **94**: 958–962.
- Geiselhardt, S., Yoneya, K., Blenn, B., Drechsler, N., Gershenzon, J., Kunze, R., and Hilker, M.** (2013). Egg Laying of Cabbage White Butterfly (*Pieris brassicae*) on Arabidopsis thaliana Affects Subsequent Performance of the Larvae. *PLoS One* **8**: e59661.
- Geuss, D., Lortzing, T., Schwachtje, J., Kopka, J., and Steppuhn, A.** (2018). Oviposition by Spodoptera exigua on Solanum dulcamara Alters the Plant’s Response to Herbivory

and Impairs Larval Performance. *Int. J. Mol. Sci.* **19**: 4008.

- Glazebrook, J.** (2005). Contrasting mechanisms of defense against biotrophic and necrotrophic pathogens. *Annu. Rev. Phytopathol.* **43**: 205–27.
- Gouhier-Darimont, C., Schmiesing, A., Bonnet, C., Lassueur, S., and Reymond, P.** (2013). Signalling of *Arabidopsis thaliana* response to *Pieris brassicae* eggs shares similarities with PAMP-triggered immunity. *J. Exp. Bot.* **64**: 665–74.
- Gouhier-Darimont, C., Stahl, E., Glauser, G., and Reymond, P.** (2019). The *Arabidopsis* Lectin Receptor Kinase LecRK-I.8 Is Involved in Insect Egg Perception. *Front. Plant Sci.* **10**: 1–10.
- Govrin, E.M. and Levine, A.** (2000). The hypersensitive response facilitates plant infection by the necrotrophic pathogen *Botrytis cinerea*. *Curr. Biol.* **10**: 751–757.
- Griese, E., Dicke, M., Hilker, M., and Fatouros, N.E.** (2017). Plant response to butterfly eggs: inducibility, severity and success of egg-killing leaf necrosis depends on plant genotype and egg clustering. *Sci. Rep.* **7**: 7316.
- Griese, E., Pineda, A., Pashalidou, F.G., Iradi, E.P., and Hilker, M.** (2019). Plant responses to butterfly oviposition partly explain preference-performance relationships on different brassicaceous species. *bioRxiv*.
- Hartmann, M., Zeier, T., Bernsdorff, F., Reichel-Deland, V., Kim, D., Hohmann, M., Scholten, N., Schuck, S., Bräutigam, A., Hölzel, T., Ganter, C., and Zeier, J.** (2018). Flavin Monooxygenase-Generated N-Hydroxypipicolinic Acid Is a Critical Element of Plant Systemic Immunity. *Cell*: 1–14.
- Hatsugai, N., Kuroyanagi, M., Yamada, K., Meshi, T., Tsuda, S., Kondo, M., Nishimura, M., and Hara-Nishimura, I.** (2004). A Plant Vacuolar Protease, VPE, Mediates Virus-Induced Hypersensitive Cell Death. *Science* (80-). **305**: 855–858.
- Hilker, M. and Fatouros, N.E.** (2015). Plant Responses to Insect Egg Deposition. *Annu. Rev. Entomol.* **60**: 493–515.
- Hilker, M. and Meiners, T.** (2006). Early herbivore alert: insect eggs induce plant defense. *J. Chem. Ecol.* **32**: 1379–97.
- Hofius, D., Munch, D., Bressendorff, S., Mundy, J., and Petersen, M.** (2011). Role of autophagy in disease resistance and hypersensitive response-associated cell death. *Cell Death Differ.* **18**: 1257–1262.
- Hofius, D., Schultz-Larsen, T., Joensen, J., Tsitsigiannis, D.I., Petersen, N.H.T., Mattsson, O., Jørgensen, L.B., Jones, J.D.G., Mundy, J., and Petersen, M.** (2009). Autophagic Components Contribute to Hypersensitive Cell Death in *Arabidopsis*. *Cell* **137**: 773–783.
- Hofius, D., Tsitsigiannis, D.I., Jones, J.D.G., and Mundy, J.** (2007). Inducible cell death in plant immunity. *Semin. Cancer Biol.* **17**: 166–187.
- Huysmans, M., Lema A, S., Coll, N.S., and Nowack, M.K.** (2017). Dying two deaths — programmed cell death regulation in development and disease. *Curr. Opin. Plant Biol.* **35**: 37–44.
- Jones, J.D.G. and Dangl, J.L.** (2006). The plant immune system. *Nat. Rev.* **444**: 323–329.
- Jurkowski, G.I., Smith, R.K., Yu, I.C., Ham, J.H., Sharma, S.B., Klessig, D.F., Fengler, K.A., and Bent, A.F.** (2004). *Arabidopsis* DND2, a second cyclic nucleotide-gated ion channel gene for which mutation causes the “defense, no death” phenotype. *Mol. Plant-Microbe Interact.* **17**: 511–520.
- Kalske, A., Muola, A., Mutikainen, P., and Leimu, R.** (2014). Preference for outbred host plants and positive effects of inbreeding on egg survival in a specialist herbivore. *Proc. R. Soc. B Biol. Sci.* **281**: 20141421.

- Kanyuka, K. and Rudd, J.J.** (2019). Cell surface immune receptors: the guardians of the plant's extracellular spaces. *Curr. Opin. Plant Biol.* **50**: 1–8.
- Kazan, K. and Lyons, R.** (2014). Intervention of Phytohormone Pathways by Pathogen Effectors. *Plant Cell* **26**: 2285–2309.
- Kim, J., Tooker, J.F., Luthe, D.S., De Moraes, C.M., and Felton, G.W.** (2012). Insect eggs can enhance wound response in plants: a study system of tomato *Solanum lycopersicum* L. and *Helicoverpa zea* Boddie. *PLoS One* **7**: 1–8.
- Künstler, A., Bacsó, R., Gullner, G., Hafez, Y.M., and Király, L.** (2016). Staying alive – is cell death dispensable for plant disease resistance during the hypersensitive response? *Physiol. Mol. Plant Pathol.* **93**: 75–84.
- Kutschera, A. et al.** (2019). Bacterial medium-chain 3-hydroxy fatty acid metabolites trigger immunity in *Arabidopsis* plants. *Science* (80-.). **181**: 178–181.
- van Leeuwen, H., Kliebenstein, D.J., West, M.A.L., Kim, K., van Poecke, R., Katagiri, F., Michelmore, R.W., Doerge, R.W., and St Clair, D.A.** (2007). Natural variation among *Arabidopsis thaliana* accessions for transcriptome response to exogenous salicylic acid. *Plant Cell* **19**: 2099–110.
- Little, D., Gouhier-Darimont, C., Bruessow, F., and Reymond, P.** (2007). Oviposition by pierid butterflies triggers defense responses in *Arabidopsis*. *Plant Physiol.* **143**: 784–800.
- Lorenzo, O., Chico, J.M., Sánchez-Serrano, J.J., and Solano, R.** (2004). JASMONATE-INSENSITIVE1 encodes a MYC transcription factor essential to discriminate between different jasmonate-regulated defense responses in *Arabidopsis*. *Plant Cell* **16**: 1938–1950.
- Lortzing, V., Oberländer, J., Lortzing, T., Tohge, T., Steppuhn, A., Kunze, R., and Hilker, M.** (2019). Insect egg deposition renders plant defence against hatching larvae more effective in a salicylic acid-dependent manner. *Plant. Cell Environ.* **42**: 1019–1032.
- Magnin-Robert, M., Le Bourse, D., Markham, J.E., Dorey, S., Clément, C., baillieul, fabienne, and Dhondt-Cordelier, S.** (2015). Modifications of sphingolipid content affect tolerance to hemibiotrophic and necrotrophic pathogens by modulating plant defense responses in *Arabidopsis*. *Plant Physiol.* **169**: pp.01126.2015.
- Mäntylä, E., Kleier, S., Lindstedt, C., Kipper, S., and Hilker, M.** (2018). Insectivorous Birds Are Attracted by Plant Traits Induced by Insect Egg Deposition. *J. Chem. Ecol.* **44**: 1127–1138.
- Morales, J., Kadota, Y., Zipfel, C., Molina, A., and Torres, M.** (2016). The *Arabidopsis* NADPH oxidases RbohD and RbohF display differential expression patterns and contributions during plant immunity.
- Moreira, X., Abdala-Roberts, L., Gols, R., and Francisco, M.** (2018). Plant domestication decreases both constitutive and induced chemical defences by direct selection against defensive traits. *Sci. Rep.* **8**: 1–11.
- Mousavi, S.A.R., Chauvin, A., Pascaud, F., Kellenberger, S., and Farmer, E.E.** (2013). GLUTAMATE RECEPTOR-LIKE genes mediate leaf-to-leaf wound signalling. *Nature* **500**: 422–426.
- Mur, L. a J., Kenton, P., Lloyd, A.J., Ougham, H., and Prats, E.** (2008). The hypersensitive response; The centenary is upon us but how much do we know? *J. Exp. Bot.* **59**: 501–520.
- Nallu, S., Hill, J.A., Don, K., Sahagun, C., Zhang, W., Meslin, C., Snell-Rood, E., Clark, N.L., Morehouse, N.I., Bergelson, J., Wheat, C.W., and Kronforst, M.R.** (2018). The molecular genetic basis of herbivory between butterflies and their host plants. *Nat. Ecol.*

Evol.

- Navarova, H., Bernsdorff, F., Doring, A.-C., and Zeier, J.** (2012). Pipecolic Acid, an Endogenous Mediator of Defense Amplification and Priming, Is a Critical Regulator of Inducible Plant Immunity. *Plant Cell* **24**: 5123–5141.
- Nguyen, C.T., Kurenda, A., Stolz, S., Chételat, A., and Farmer, E.E.** (2018). Identification of cell populations necessary for leaf-to-leaf electrical signaling in a wounded plant. *Proc. Natl. Acad. Sci.*: 201807049.
- Oerke, E.-C.** (2006). Crop losses to pests. *J. Agric. Sci.* **144**: 31–43.
- Oerke, E.C. and Dehne, H.W.** (2004). Safeguarding production - Losses in major crops and the role of crop protection. *Crop Prot.* **23**: 275–285.
- Olvera-Carrillo, Y. et al.** (2015). A conserved core of PCD indicator genes discriminates developmentally and environmentally induced programmed cell death in plants. *Plant Physiol.* **169**: pp.00769.2015.
- Pashalidou, F.G., Lucas-Barbosa, D., van Loon, J.J. a, Dicke, M., and Fatouros, N.E.** (2013). Phenotypic plasticity of plant response to herbivore eggs: effects on resistance to caterpillars and plant development. *Ecology* **94**: 702–13.
- Peschiutta, M.L., Scholz, F.G., Goldstein, G., and Bucci, S.J.** (2018). Oviposition by herbivorous insects induces changes in optical and mechanical properties of *Prunus avium* leaves. *Arthropod. Plant. Interact.* **0**: 0.
- Petzold-Maxwell, J., Wong, S., Arellano, C., and Gould, F.** (2011). Host plant direct defence against eggs of its specialist herbivore, *Heliothis subflexa*. *Ecol. Entomol.* **36**: 700–708.
- Pieterse, C.M.J., Van der Does, D., Zamioudis, C., Leon-Reyes, A., and Van Wees, S.C.M.** (2012). Hormonal Modulation of Plant Immunity. *Annu. Rev. Cell Dev. Biol.* **28**: 489–521.
- Pingali, P.L.** (2012). Green revolution: Impacts, limits, and the path ahead. *Proc. Natl. Acad. Sci. U. S. A.* **109**: 12302–12308.
- Ranf, S.** (2017). Sensing of molecular patterns through cell surface immune receptors. *Curr. Opin. Plant Biol.* **38**: 68–77.
- Reape, T.J., Molony, E.M., and McCabe, P.F.** (2008). Programmed cell death in plants: Distinguishing between different modes. *J. Exp. Bot.* **59**: 435–444.
- Reymond, P.** (2013). Perception, signaling and molecular basis of oviposition-mediated plant responses. *Planta* **238**: 247–58.
- Robert-Seilantiz, A., Grant, M., and Jones, J.D.G.** (2011). Hormone Crosstalk in Plant Disease and Defense: More Than Just JASMONATE-SALICYLATE Antagonism. *Annu. Rev. Phytopathol.* **49**: 317–343.
- Rojo, E., Martín, R., Carter, C., Zouhar, J., Pan, S., Plotnikova, J., Jin, H., Paneque, M., Sánchez-Serrano, J.J., Baker, B., Ausubel, F.M., and Raikhel, N. V.** (2004). VPEy Exhibits a Caspase-like Activity that Contributes to Defense against Pathogens. *Curr. Biol.* **14**: 1897–1906.
- Roux, M., Schwessinger, B., Albrecht, C., Chinchilla, D., Jones, A., Holton, N., Malinovsky, F.G., Tör, M., de Vries, S., and Zipfel, C.** (2011). The Arabidopsis Leucine-Rich Repeat Receptor-Like Kinases BAK1/SERK3 and BKK1/SERK4 Are Required for Innate Immunity to Hemibiotrophic and Biotrophic Pathogens. *Plant Cell* **23**: 2440–2455.
- Salguero-Linares, J. and Coll, N.S.** (2019). Plant proteases in the control of the hypersensitive response. *J. Exp. Bot.* **70**: 2087–2095.
- Salvesen, G.S., Hempel, A., and Coll, N.S.** (2015). Protease Signaling in Animal and Plant

Regulated Cell Death. FEBS J.: n/a-n/a.

- Saucedo-García, M., Guevara-García, A., González-Solís, A., Cruz-García, F., Vázquez-Santana, S., Markham, J.E., Lozano-Rosas, M.G., Dietrich, C.R., Ramos-Vega, M., Cahoon, E.B., and Gavilanes-Ruíz, M.** (2011). MPK6, sphinganine and the LCB2a gene from serine palmitoyltransferase are required in the signaling pathway that mediates cell death induced by long chain bases in Arabidopsis. *New Phytol.* **191**: 943–957.
- Schweizer, F., Bodenhausen, N., Lassueur, S., Masclaux, F.G., and Reymond, P.** (2013a). Differential Contribution of Transcription Factors to Arabidopsis thaliana Defense Against Spodoptera littoralis. *Front. Plant Sci.* **4**: 13.
- Schweizer, F., Fernández-Calvo, P., Zander, M., Diez-Diaz, M., Fonseca, S., Glauser, G., Lewsey, M.G., Ecker, J.R., Solano, R., and Reymond, P.** (2013b). Arabidopsis basic helix-loop-helix transcription factors MYC2, MYC3, and MYC4 regulate glucosinolate biosynthesis, insect performance, and feeding behavior. *Plant Cell* **25**: 3117–32.
- Serrano, M., Coluccia, F., Torres, M., L'Haridon, F., and Métraux, J.-P.** (2014). The cuticle and plant defense to pathogens. *Front. Plant Sci.* **5**: 274.
- Shah, J. and Zeier, J.** (2013). Long-distance communication and signal amplification in systemic acquired resistance. *Front. Plant Sci.* **4**: 30.
- Shapiro, A.M. and DeVay, J.E.** (1987). Hypersensitivity reaction of Brassica nigra L. (Cruciferae) kills eggs of Pieris butterflies (Lepidoptera: Pieridae). *Oecologia* **71**: 631–632.
- Stahl, E., Hilfiker, O. and Reymond, P.** (2018) Plant-arthropod interactions: who is the winner? *Plant J.* **93**: 703-728.
- Suzuki, Y., Sogawa, K., and Seino, Y.** (1996). Ovicidal Reaction of Rice Plants against the Whitebacked Planthopper, Sogatella furcifera HORVATH (Homoptera: Delphacidae). *Appl. Entomol. Zool.* **31**: 111–118.
- Tamiru, A., Khan, Z.R., and Bruce, T.J.** (2015). New directions for improving crop resistance to insects by breeding for egg induced defence. *Curr. Opin. Insect Sci.*
- Tao, Y., Xie, Z., Chen, W., Glazebrook, J., Chang, H.-S., Han, B., Zhu, T., Zou, G., and Katagiri, F.** (2003). Quantitative Nature of Arabidopsis Responses during Compatible and Incompatible Interactions with the Bacterial Pathogen Pseudomonas syringae. *Plant Cell* **15**: 317–330.
- Thomas, E.L. and van der Hoorn, R.A.L.** (2018). Ten prominent host proteases in plant-pathogen interactions. *Int. J. Mol. Sci.* **19**: 1–12.
- Thomma, B.P.H.J., Nürnberger, T., and Joosten, M.H.A.J.** (2011). Of PAMPs and Effectors: The Blurred PTI-ETI Dichotomy. *Plant Cell* **23**: 4–15.
- Torres, M.A., Dangl, J.L., and Jones, J.D.G.** (2002). Arabidopsis gp91phox homologues AtrbohD and AtrbohF are required for accumulation of reactive oxygen intermediates in the plant defense response. *Proc. Natl. Acad. Sci. U. S. A.* **99**: 517–522.
- Toyota, M., Spencer, D., Sawai-Toyota, S., Jiaqi, W., Zhang, T., Koo, A.J., Howe, G.A., and Gilroy, S.** (2018). Glutamate triggers long-distance, calcium-based plant defense signaling. *Science* (80-.). **361**: 1112–1115.
- Tsuda, K. and Katagiri, F.** (2010). Comparing signaling mechanisms engaged in pattern-triggered and effector-triggered immunity. *Curr. Opin. Plant Biol.* **13**: 459–465.
- Vellosillo, T., Vicente, J., Kulasekaran, S., Hamberg, M., and Castresana, C.** (2010). Emerging Complexity in Reactive Oxygen Species Production and Signaling during the Response of Plants to Pathogens. *Plant Physiol.* **154**: 444–448.
- Veloso, J. and van Kan, J.A.L.** (2018). Many Shades of Grey in Botrytis –Host Plant

Interactions. *Trends Plant Sci.* **0**: 1–10.

- Wang, D., Amornsiripanitch, N., and Dong, X.** (2006). A genomic approach to identify regulatory nodes in the transcriptional network of systemic acquired resistance in plants. *PLoS Pathog.* **2**: 1042–1050.
- Wang, J., Hu, M., Wang, J., Qi, J., Han, Z., Wang, G., Qi, Y., Wang, H.W., Zhou, J.M., and Chai, J.** (2019). Reconstitution and structure of a plant NLR resistosome conferring immunity. *Science* (80-.). **364**.
- Wildermuth, M.C., Dewdney, J., Wu, G., and Ausubel, F.M.** (2001). Isochorismate synthase is required to synthesize salicylic acid for plant defence. *Nature* **414**: 562–565.
- Wright, C. a and Beattie, G. a** (2004). *Pseudomonas syringae* pv. tomato cells encounter inhibitory levels of water stress during the hypersensitive response of *Arabidopsis thaliana*. *Proc. Natl. Acad. Sci.* **101**: 3269–3274.
- Wu, Y., Zhang, D., Chu, J.Y., Boyle, P., Wang, Y., Brindle, I.D., De Luca, V., and Després, C.** (2012). The *Arabidopsis* NPR1 Protein Is a Receptor for the Plant Defense Hormone Salicylic Acid. *Cell Rep.* **1**: 639–647.
- Yamasaki, M., Yoshimura, A., and Yasui, H.** (2003). Genetic basis of ovicidal response to whitebacked planthopper (*Sogatella furcifera* Horváth) in rice (*Oryza sativa* L.). *Mol. Breed.* **12**: 133–143.
- Yang, Y. et al.** (2014). Quantitative trait loci identification, fine mapping and gene expression profiling for ovicidal response to whitebacked planthopper (*Sogatella furcifera* Horvath) in rice (*Oryza sativa* L.). *BMC Plant Biol.* **14**: 145.
- Yoshimoto, K., Jikumaru, Y., Kamiya, Y., Kusano, M., Consonni, C., Panstruga, R., Ohsumi, Y., and Shirasu, K.** (2009). Autophagy negatively regulates cell death by controlling NPR1-dependent salicylic acid signaling during senescence and the innate immune response in *Arabidopsis*. *Plant Cell* **21**: 2914–27.
- Zhang, Y., Zhang, Y., Tessaro, M.J., Tessaro, M.J., Lassner, M., Lassner, M., Li, X., and Li, X.** (2003). Knockout Analysis of *Arabidopsis* Transcription Factors TGA2 , TGA5 , and TGA6 Reveals Their Redundant and Essential Roles in Systemic Acquired Resistance. *Plant Cell* **15**: 2647–2653.
- Zheng, X.-Y., Spivey, N.W., Zeng, W., Liu, P.-P., Fu, Z.Q., Klessig, D.F., He, S.Y., and Dong, X.** (2012). Coronatine promotes *Pseudomonas syringae* virulence in plants by activating a signaling cascade that inhibits salicylic acid accumulation. *Cell Host Microbe* **11**: 587–96.
- Zipfel, C.** (2014). Plant pattern-recognition receptors. *Trends Immunol.* **35**: 345–351.
- Zipfel, C., Robatzek, S., Navarro, L., Oakeley, E.J., Jones, J.D.G., Felix, G., and Boller, T.** (2004). Bacterial disease resistance in *Arabidopsis* through flagellin perception. *Nature* **428**: 764–767.

Chapter 1

Role of sphingolipids in *Pieris brassicae* egg-induced cell death in *Arabidopsis thaliana* and *Brassica nigra*

Raphaël Groux¹, Laetitia Fouillen², Esteban Alfonso¹, Sébastien Mongrand², Philippe Reymond¹.

¹Department of Plant Molecular Biology, University of Lausanne, 1015 Lausanne, Switzerland

²Laboratoire de Biogenèse Membranaire, UMR 5200 CNRS-Université de Bordeaux, 33883 Villenave-d'Ornon, France

Abstract

In *Brassicaceae*, hypersensitive-like (HR-like) cell death is a central component of direct defenses triggered against the eggs of the large white butterfly *Pieris brassicae*. The signaling pathway leading to cell death in the model plant *Arabidopsis thaliana* is partially dependent on salicylic acid (SA) accumulation, but downstream molecular components are unclear. Here, we analyzed transcriptomic data from *Arabidopsis* responses to *P. brassicae* eggs and found significant changes in sphingolipid metabolism genes. We report that eggs induce an accumulation of C16:0 ceramides in both *Arabidopsis* and *Brassica nigra*, and this pattern was consistent with a role as a SA-dependent cell death inducers. In addition, disruption of ceramide synthase activity led to a reduction in cell death while SA signalling and ROS levels were unchanged. Furthermore, we provide genetic evidence that the modification of fatty acyl chains of sphingolipids modulates cell death and SA-dependent signaling. Finally, we observe that ceramide synthases and fatty acid-modifying enzymes differently affect egg- or pathogen-induced cell death. Altogether, these results show that sphingolipids play a key and specific role during insect egg-triggered HR-like.

Introduction

The role of programmed cell death (PCD) during a plant's life is manifold: it is part of development by promoting cell and tissue differentiation, but it can also be the result of immune defense system activation (Coll et al., 2011; Reape and McCabe, 2010; Huysmans et al., 2017). The most studied form of pathogen-triggered PCD (pPCD) is termed the hypersensitive response (HR), a spectacular response triggered upon the recognition of adapted pathogens by resistance proteins that leads to macroscopic cell death, induction of defense gene expression, and pathogen resistance (Balint-Kurti, 2019). A meta-analysis of PCD-inducing conditions revealed that transcriptomic signatures of developmental PCD (dPCD) and pPCD are largely distinct (Olvera-Carrillo et al., 2015), suggesting that they are under different control regimes. More specifically, pPCD is dependent on salicylic acid (SA) accumulation and signaling (Balint-Kurti, 2019; Huysmans et al., 2017; Coll et al., 2011). In addition to immunity to pathogens, it was reported that hypersensitivity may also function as a defense strategy against immobile insect stages (Fernandes, 1990; Stuart, 2015). Interestingly, plants from the *Brassicales*, *Solanales* and *Fabales* orders were shown to induce localized cell death in response to oviposition by insects (Shapiro and DeVay, 1987; Petzold-Maxwell et al., 2011; Fatouros et al., 2016; Garza et al., 2001; Little et al., 2007; Geuss et al., 2017), a process hereafter called HR-like (Reymond, 2013). As a consequence, direct defense induction correlates with decreased egg survival and/or increased egg parasitism (Fatouros et al., 2016). As for pathogen-triggered HR, it was found that HR-like responses are associated with an accumulation of reactive oxygen species (ROS), SA and defense gene expression (Little et al., 2007; Geuss et al., 2017; Bonnet et al., 2017; Hilfiker et al., 2014). Studies in *Arabidopsis thaliana* reported that the signaling cascade involved in the response to eggs of the Large White Butterfly *Pieris brassicae* is similar to pathogen-triggered immunity (PTI) (Gouhier-Darimont et al. 2013). Notably, the induction of cell death was dependent on SA accumulation and signaling. The exact cause of the decreased egg survival associated with HR-like is not known, but data from *B. nigra* suggest that it could be due to water removal at the oviposition site (Griese et al., 2017), consistent with low water potential observed in tissues undergoing HR (Wright and Beattie, 2004). In addition, exposure to ROS was shown to increase egg mortality (Geuss et al., 2017). These data thus suggest that HR-like at oviposition sites may constitute an efficient defense strategy against insect eggs.

As it could decrease insect pressure before damage occurs, the introgression of egg-killing traits in cultivated crop species is desirable (Fatouros et al., 2016) and has been successfully

reported in *Oryza sativa* (Suzuki et al., 1996; Yamasaki et al., 2003; Yang et al., 2014). Despite this achievement, this strategy is still mostly overlooked as the genetic basis for these responses is usually unknown (Reymond, 2013; Fatouros et al., 2016). The use of *Arabidopsis* as a model plant to explore the genetic basis of the response to *P. brassicae* eggs has so far successfully identified PTI components as regulators of egg-induced HR-like (Gouhier-Darimont et al., 2013), and enabled the recent description of *LecRK-1.8* as a putative receptor for egg-derived molecules (Gouhier-Darimont et al., 2019). Nevertheless, the identity of cell-death inducing factors downstream of SA is unknown.

In contrast to animals, plants lack certain central components of PCD pathways, such as caspases (Coll et al., 2011; Salvesen et al., 2015), but instead rely on a variety of other proteases that fulfill similar functions (Salguero-Linares and Coll, 2019). The identification and characterization of lesion mimic mutants (LMM), which display spontaneous HR-like cell death along with elevated defenses, has largely contributed to shed light on processes involved in PCD (Bruggeman et al., 2015). In particular, several LMM were found to function in sphingolipid metabolism. The involvement of sphingolipids in PCD induction in animals is well described (Young et al., 2013), and their function appears to be conserved in plants (Townley et al., 2005). Sphingolipids differ from glycerolipids as they consist of a sphingoid long-chain base (LCB) linked via the amide bond to one fatty acid (FA) moiety (Ali et al., 2018). LCB backbones can be further modified through hydroxylation or desaturation, and FA side chains can be hydroxylated on their α -position. These molecules, called ceramides (Cer), can be further modified by the attachment of a polar head group consisting of a glucose or an inositol-glucuronic acid moiety, leading to the formation of complex sphingolipids such as GluCer (glucosylceramides) or GIPC (glycosyl inositol phospho ceramides), respectively. In plants, most sphingolipids found are complex (90%; Markham et al., 2013; Gronnier et al., 2016), whereas LCB and Cer are low abundant. Interestingly, both free LCB and Cer have been shown to induce PCD when exogenously applied to plants (Liang et al., 2003; Lachaud et al., 2011; Shi et al., 2007; Saucedo-García et al., 2011). Additionally, several fungal toxins such as Fumonisin B1 were shown to cause cell death through an accumulation of free LCB by inhibiting ceramide synthases (Berkey et al., 2012). In contrast, phosphorylated LCB and Cer were shown to promote cell survival (Ali et al., 2018a). While the mechanisms involved downstream of LCB/Cer are not clear, the modification of sphingolipid levels in the context of immune responses was shown to affect pathogen resistance (Magnin-Robert et al., 2015; Ternes et al., 2011; Wu et al., 2015b).

Here we report that eggs of *P. brassicae* trigger causes a change in expression of sphingolipid metabolism genes, together with an accumulation of ceramides in both *Arabidopsis* and *B. nigra*. Furthermore, we show that cell death induction is affected in

different ceramide synthase and fatty acid hydroxylases mutants, whereas ROS and SA accumulation are unaffected. Altogether, these data show that sphingolipids play a key role in the execution of egg-induced cell death, downstream of SA signaling.

Material and methods

Plant and insects growth conditions

All experiments described using *Arabidopsis thaliana* were conducted in the Col-0 background. Seeds of *Brassica nigra* were collected from a wild population in Wageningen (The Netherlands) as previously described (Bonnet et al., 2017). Plants were grown in growth chambers in short day conditions (10 h light, 22°C, 65% relative humidity, 100 $\mu\text{mol m}^{-2} \text{s}^{-1}$) and were 4 to 5 weeks old at the time of treatment. Seeds were stratified for 3 days at 4 °C after sowing. Larvae, eggs and butterflies of the Large White butterfly *Pieris brassicae* came from a population maintained on *Brassica oleracea* in a greenhouse as described previously (Reymond et al., 2000).

Oviposition and treatment with egg extract

P. brassicae eggs were collected and crushed with a pestle in Eppendorf tubes. After centrifugation (15 000 g, 3 min), the supernatant ('egg extract') was collected and stored at -20°C. Plants were 4-5 weeks old at the time of treatment. For each plant, two leaves were treated with 2 μl of egg extract. This amount corresponds to one egg batch of 18 eggs (E. Stahl, personal communication). A total of four plants were used for each experiment. After the appropriate time, egg extract was gently removed with a scalpel blade and treated leaves were stored in liquid nitrogen. Untreated plants were used as controls.

T-DNA insertion lines

T-DNA insertion lines for *loh1* (SALK_069253), *loh2* (SALK_018608), *loh3* (SALK_150849), *fah1* (SALK_140660), *fah2* (SAIL_862_H01) were kindly provided by Ivo Feussner (University of Göttingen); *sid2-1* from Christiane Nawrath (University of Lausanne), *npr1-1* and *ein2-1* from the Nottingham Arabidopsis Stock Center; *myb30* from Dominique Roby (LIPM INRA, Toulouse); *fad3fad7fad8* from Edward E. Farmer (University of Lausanne); *tga2tga3tga5tga6* from Corné Pieterse (Utrecht University).

Histochemical stainings (Trypan blue, DAB)

For visualization of cell death, egg extract was gently removed and leaves were submerged in lactophenol trypan blue solution (5 ml of lactic acid, 10 ml of 50% glycerol, 1 mg of trypan blue (Sigma), and 5 ml of phenol) at 28°C for 2–3 h. Hydrogen peroxide (H₂O₂) accumulation was measured with 3,3-diaminobenzidine (DAB; Sigma). Leaves were

submerged in a 1.0 mg ml⁻¹ DAB solution and incubated in the dark at room temperature for 6–8 h.

Superoxide radical (O₂⁻) was visualized with the sensitive dye nitroblue tetrazolium (NBT; Sigma). Leaves were submerged in a solution containing 0.02% NBT and 10 mM NaN₃ for 4 h at room temperature in the dark. After each staining, leaves were destained for in boiling 95% ethanol. Microscope images were saved as TIFF files and processed for densitometric quantification with ImageJ version 1.64 (NIH).

Salicylic acid quantifications

SA quantifications were performed using the bacterial biosensor *Acinetobacter* sp. ADPWH (DeFraia et al., 2008; Zvereva et al., 2016). Briefly, 6 leaf discs (0.7 cm, ~20mg) were ground in liquid nitrogen and extracted in 0.1M sodium acetate buffer (pH 5.6). Extracts were then centrifuged at 4°C for 15min at 16'000g. 50µL of extract were incubated with 5 µL of β-Glucosidase from almonds (0.5U/µl in acetate buffer, Sigma-Aldrich) during 90min at 37°C to release SA from SA-glucoside (SAG). 20µL of extract was then mixed with 60µL of LB and 50µL of a culture of *Acinetobacter* sp. ADPWH_lux (OD₆₀₀ = 0.4), and incubated for 1h at 37°C. Finally, luminescence was integrated using a 485±10nm filter for 1s. An SA standard curve diluted in untreated *sid2-1* extract amounts ranging from 0 to 60ng was read in parallel to allow quantification. SA amounts in samples were estimated by fitting a 3rd order polynomial regression on the standards.

Cultivation of bacteria and plant infection

Pseudomonas syringae pv. tomato DC3000 AvrRPM1 (Pst AvrRPM1) was streaked from a -80°C glycerol stock onto a low salt Luria Bertani (LB) medium (10 g L⁻¹ BactoTryptone, 5g L⁻¹ yeast extract, 5g L⁻¹ NaCl and 14 g L⁻¹ Bactoagar, pH 7.0) containing 50 µg mL⁻¹ of rifampicine. Bacteria were inoculated into 6 ml of liquid culture in LB with antibiotic and grown at 28°C overnight (O/N). For infection, bacterial cultures were centrifuged at 13'000 rpm for 1 min. The supernatant was discarded, the pellet washed thrice with 10 mM MgCl₂, and cells were finally resuspended in 10 mM MgCl₂ to the desired final OD₆₀₀.

Ion leakage measurement

Ion leakage measurements were performed according to a method reported previously (Johansson et al., 2015). Briefly, leaf discs from 5 week-old plants were punched out using a cork borer (diameter 0.7 cm). Leaf discs were placed in 50mL Falcon tubes containing 20mL of a bacterial suspension at OD₆₀₀=0.1 prepared as described above. Tubes were then placed in a SpeedVac concentrator without the rotor and pressure was decreased until the

solution starts boiling. This procedure was repeated several times until all leaf discs were successfully infiltrated (i.e. sunken at the bottom of the tubes). Leaf discs were thoroughly rinsed with deionized water and placed in dH₂O for another 10min for further rinsing. 4 fully infiltrated leaf discs were placed with 10mL dH₂O in 15 mL Falcon tubes. Solution conductivity was measured using a conductimeter (pH/Ion bench meter SE S500-K; Mettler-Toledo) at the desired time. For each genotype, five samples from different plants were prepared.

Botrytis cinerea infection assay

Botrytis cinerea strain BMM (Zimmerli et al., 2000) was grown on 1 x PDA (Potato Dextrose Agar, 39 g l⁻¹, Difco) for 10-14 days in darkness at 23°C. Spores were harvested in water and filtered through wool placed in a 5 ml tip to remove hyphae. Spores were diluted in half-strength PDB (Potato Dextrose Broth, 12 g l⁻¹, Difco) to a concentration of 5 x 10⁵ spores ml⁻¹ for inoculation. One 5 µl droplet of spore suspension was deposited on the adaxial surface of two leaves of 4-week-old plants. Inoculated plants were kept under a water-sprayed transparent lid to maintain high humidity in a growth chamber under dim light (around 2 µmol m⁻² s⁻¹) during the whole time of infection. Lesion size measurements were made using the ImageJ software version 1.49 (<http://imagej.nih.gov/ij>).

Determination of nonenzymatic lipid peroxidation

Frozen leaf material (25mg) was ground on liquid nitrogen, mixed with 0.5 ml of 0.1 % trichloroacetic acid (TCA), and centrifuged at 10.000 g for 15 min. 0.25 ml of the supernatant was mixed with 0.5 ml of 20 % TCA and 0.5 ml of 0.5 % thiobarbituric acid (TBA) and the mixture was incubated at 95 °C for 30 min to react MDA with TBA. Thereby a TBA-MDA complex is formed which is reported to have a specific absorbance at 532 nm. The specific absorbance of 532 nm and a nonspecific of 600 nm were measured with an UV-VIS spectrophotometer and the nonspecific absorbance was subtracted from the specific absorbance. The concentrations of MDA were calculated using Beer-Lambert's equation with an extinction coefficient for MDA of 155 mM⁻¹ cm⁻¹ (Heath and Packer, 1968) and expressed to the fresh weight. Because this assay is described to overestimate the absolute concentration of MDA we normalized data on MDA levels in untreated Col-0 leaves and depicted them as fold-changes.

2-hydroxy fatty acid (hFA) quantification

Fatty acid quantification was performed based on a previously published protocol (Cacas et al., 2016). Briefly, 25mg of frozen sample was spiked with 10 µg of 2-hydroxy-tetradecanoic acid (h14:0) as internal standard, and was transmethylated at 110°C overnight in 3 mL of

methanol containing 5% (v/v) sulfuric acid. After cooling, 3mL of NaCl (2.5%, w/v) was added, and methylated fatty acids were extracted in 1 mL of hexane. The organic phase was collected in a new tube, washed with 3mL of saline solution (200mM NaCl and 200 mM Tris, pH 8), centrifuged and the organic phase was dried under a gentle stream of nitrogen at room temperature. Free hydroxyl groups were derivatized at 110°C for 30min in 100 µL of N,O-bis(trimethylsilyl)trifluoroacetamide (BSTFA, Sigma) and pyridine (50:50, v/v), and surplus BSTFA was evaporated under nitrogen. Samples were finally dissolved in hexane and transferred into capped autosampling vials until analysis.

Quantitative analysis was performed using a HP-5MS capillary column (5% phenyl-methyl-siloxane, 30m x 250 mm, 0.25 mm film thickness; Agilent) with helium carrier gas at 1.5mL/min; injection was in splitless mode; injector temperature was set to 250 C; the oven temperature was held at 50°C for 1 min, then programmed with a 25°C/min ramp to 150°C (2min hold), and a 10°C/min ramp to 320°C (6min hold). Quantification of fatty acids and hydroxy-fatty acids was based on peak areas derived from specific ions in single-ion mode (SIM) and the respective internal standards. Ions used for quantifications are listed in the Supplementary Table 1.

Sphingolipid measurements by LC-MS/MS

For the analysis of sphingolipids by LC-MS/MS, lipids extracts were obtained using the Markham method described previously (Markham, 2013). Extracts were then incubated 1h at 50°C in 2 mL of methylamine solution (7ml methylamine 33% (w/v) in EtOH combined with 3mL of methylamine 40% (w/v) in water (Sigma Aldrich) in order to remove phospholipids. After incubation, methylamine solutions were split as follows: 1/3 for GlcCer and GIPC and 2/3 for LCB, and Ceramides, and then dried at 40°C under a stream of air. Finally, extracts for LCB and Cer quantifications were resuspended in 100 µL of THF containing synthetic internal lipid standards (LCB d17:1, LCB-P d17:1 and Cer d18:1/C17:0) was added, thoroughly vortexed and transferred into an LC vial. Likewise, extracts for GlcCer and GIPC were resuspended into 100 µL of THF/MeOH/H₂O (40:20:40, v/v) with 0.1% formic acid containing synthetic internal lipid standards (GluCer d18:1/C12:0 and GM1) was added. Samples were later incubated at 60°C for 20min, sonicated 2min and transferred into LC vials.

LC-MS/MS (multiple reaction monitoring mode) analyses were performed with a model QTRAP 6500 (ABSciex) mass spectrometer coupled to a liquid chromatography system (1290 Infinity II, Agilent). Analyses were performed in the positive mode. Nitrogen was used for the curtain gas (set to 30), gas 1 (set to 30), and gas 2 (set to 10). Needle

voltage was at +5500 V with needle heating at 400°C; the declustering potential was adjusted between +10 and +40 V. The collision gas was also nitrogen; collision energy varied from +15 to +60 eV on a compound-dependent basis.

Reverse-phase separations were performed at 40°C on a Supercosil ABZ+, 100x2.1 mm column and 5µm particles (Supelco). Eluent A was THF/ACN/5 mM Ammonium formate (3/2/5 v/v/v) with 0.1% formic acid and eluent B was THF/ACN/5 mM Ammonium formate (7/2/1 v/v/v) with 0.1% formic acid. The gradient elution program for LCB and Cer quantification was as follows: 0 to 1 min, 1% eluent B; 40 min, 80% eluent B; and 40 to 42, 80% eluent B. The gradient elution program for GluCer and GIPC quantification was as follows: 0 to 1 min, 15% eluent B; 31 min, 45% eluent B; 47.5 min, 70% eluent B; and 47.5 to 49, 70% eluent B. The flow rate was set at 0.2 mL/min, and 5 mL sample volumes were injected. A list of all sphingolipid species scanned during this procedure is available in Supplementary Table 2.

The areas of LC peaks were determined using MultiQuant software (version 3.0; ABSciex) for sphingolipids quantification. Due to the lack of authentic standards for phytoceramides and GIPCs, the most abundant species present in plant tissues, absolute quantification is impossible without strong assumptions and was therefore avoided. Areas of LC peaks for specific transitions were normalized to the signal of the standard from the same class (Cer, hCer, GluCer or GIPC) and normalized to dry weight.

RNA Extraction, Reverse-transcription and Quantitative Real-time PCR

Tissue samples were ground in liquid nitrogen, and total RNA was extracted using ReliaPrep™ RNA Tissue Miniprep (Promega) according to the manufacturer's instructions, including DnaseI treatment. Afterwards, cDNA was synthesized from 500 ng of total RNA using M-MLV reverse transcriptase (Invitrogen) and subsequently diluted eightfold with water. Quantitative real-time PCR reactions were performed using Brilliant III Fast SYBR-Green QPCR Master Mix on an QuantStudio 3 real-time PCR instrument (Life Technologies) with the following program: 95°C for 3min, then 40 cycles of 10s at 95°C, 20s at 60°C.

Values were normalized to the housekeeping gene *SAND* (At2g28390). The expression level of a target gene (TG) was normalized to the reference gene (RG) and calculated as normalized relative quantity (NRQ) as follows: $NRQ = E^{Ct_{RG}} / E^{Ct_{TG}}$. Primer efficiencies (E) were evaluated by five-step dilution regression. For each experiment, three biological replicates were analyzed. A list of all primers used in experiments can be found in Supplementary Table 3.

Transcript sequences for gene homologs in *B. nigra* were identified by BLAST using *Arabidopsis* CDS sequences on BrassicaDB (<http://brassicadb.org/brad/index.php>). Because of the lack of accessible genome sequences, designed primer sequences were then checked

for specificity using Primer BLAST against the “Brassica” mRNA database. Primer pairs that had no unspecific binding in other *Brassica* were tested by PCR on gDNA and cDNA from *B. nigra* for size and specificity.

Statistical Analyses

Data were analyzed using R software version 3.6 or GraphPad Prism 8.0.1.

Results

Eggs of *P. brassicae* induce biotic cell death markers in a SA- and ET-dependent manner

Different types of PCD exist in plants and meta-analysis of publically available transcriptomic data previously enabled the characterization of marker genes for different types of cell death:

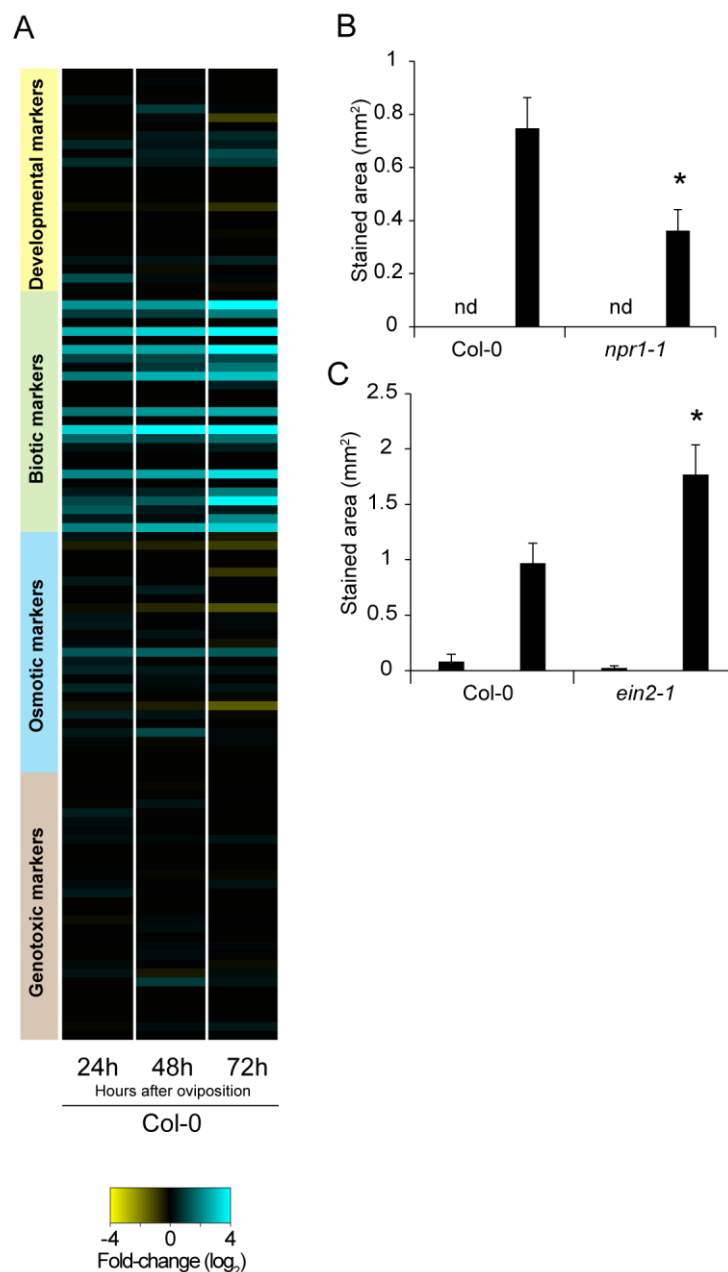


Figure 1. Hypersensitive-like cell death following *P. brassicae* oviposition induces markers of biotic PCD and is regulated by SA and ET. A. *Arabidopsis* plants oviposited by *P. brassicae* butterfly for 24h, 48h or 72h induce the expression of marker genes for biotic-related programmed cell death. Marker genes were described in Olvera-Carrillo et al. 2015 and microarray data were previously reported (Little et al 2007). B and C. Cell death as quantified by trypan blue staining after 3 days of egg extract treatments in *npr1-1* (B) and *ein2-1*(C) mutant plants. For each genotype, a total of 12 to 16 leaves from 6 to 8 plants were treated with 2 μ L of egg extract. Untreated leaves were used as controls. Data represent means \pm standard error (SEM). Statistical significance was assessed by two-sample t-test against Col-0 treated plants. *, P < 0.05. n.d., not determined.

biotic, osmotic, developmental and genotoxic (Olvera-Carrillo et al., 2015). We previously published transcriptomic data from *Arabidopsis* plants subjected to natural oviposition (Little et al., 2007) and used these expression profiles to explore the molecular signatures associated with egg-induced HR-like. We extracted expression data for the different PCD marker genes described in Olvera-Carrillo et al. 2015 24h, 48h and 72h after egg deposition by *P. brassicae*. Interestingly, marker genes for biotic cell death were found to be highly induced after egg perception, while markers for other types of PCD were weakly responsive (Fig. 1A). Biotic PCD is typically induced upon recognition of pathogens, and this process was shown to be regulated by the phytohormones ethylene (ET) and salicylic acid (SA) (Radojčić et al., 2018; Ciardi et al., 2001; Bouchez et al., 2007). To get a further insight into the regulation of egg-induced HR-like, we treated mutant plants for ET or SA signalling with *P. brassicae* egg extract and quantified cell death by trypan blue staining as previously reported (Gouhier-Darimont et al., 2013). Interestingly, the extent of cell death was reduced in *npr1-1* but increased in *ein2-1* (Fig. 1B), suggesting that SA and ET act as positive and negative regulators, respectively, of egg-induced HR-like. These results are consistent with the previously reported SA-dependence of egg-induced cell death (Gouhier-Darimont et al., 2013) but unveil the unexpected importance of ET during this response. Together, these data show that the recognition of *P. brassicae* eggs results in genetically encoded cell death and that this response is dependent on SA and ET signaling.

Oviposition by *P. brassicae* induces transcriptomic alterations in lipid metabolism genes

Lipid metabolism is central in plant development and some sectors have been shown to be involved in cell death during immunity (Lim et al., 2017; Siebers et al., 2016). We explored potential involvement of lipid metabolism during egg-induced responses. A global survey of transcriptomic alterations in genes related to lipid metabolism (AraLip database; <http://aralip.plantbiology.msu.edu/>) after *P. brassicae* oviposition was done using previously published expression data (Little et al., 2007). Only genes whose expression was significantly different at least at one time point and with a ratio $\geq|1.5|$ were kept. This analysis led to a list of 136 genes (out of 765 in the AraLip database) representative of all major lipid pathways (Fig. 2A). Data clustering showed that genes were either up- or downregulated over time, displaying a very sharp regulation process. Interestingly, genes involved in processes such as fatty acid (FA) synthesis, elongation or phospholipid synthesis were mostly downregulated while genes in sphingolipid biosynthesis, TAG degradation and oxylipin biosynthesis were mainly upregulated (Fig. 2B). Interestingly, both oxylipin and sphingolipids have previously been involved in the regulation of cell death (Siebers et al., 2016; Lim et al., 2017; Huby et al., 2019), hinting to a potential implication during egg-

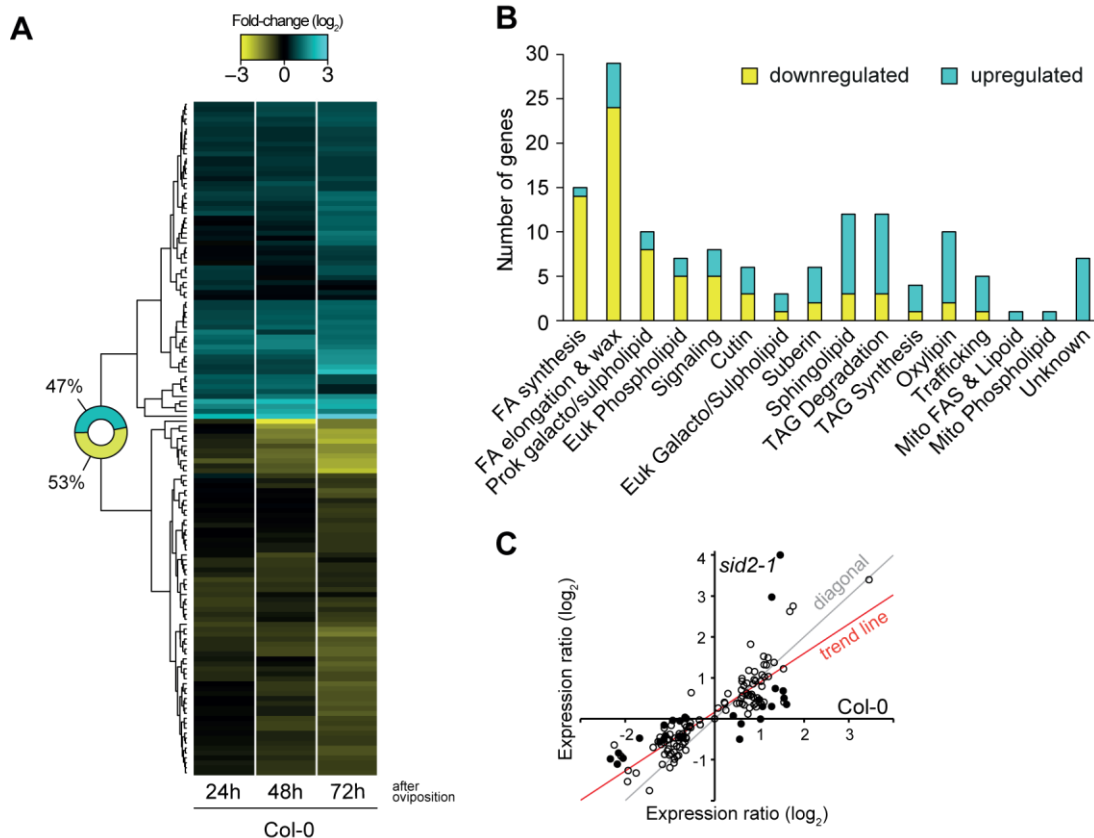


Figure 2. Transcriptomic alterations in lipid metabolism after insect egg deposition. A. Heatmap showing expression of genes involved in lipid metabolism 24h, 48h and 72h after oviposition by *P. brassicae* on *Arabidopsis* wild-type plants. Microarray data were taken from Little et al. 2007 and a list of genes specifically involved in lipid metabolism was obtained from the AraLip database. Only genes that were differentially regulated between control and treated plants ($P < 0.05$, Fold-change $> |1.5|$) in at least one time-point are shown. B. Amount of gene up- or down-regulated in each metabolic categories defined on the AraLip database. For sake of clarity, only one category is shown per gene. C. Comparison of transcript levels between Col-0 and *sid2-1* mutant plants 72h after egg deposition. Mean expression ratios (\log_2) in Col-0 and mutant plants were plotted against each other. Each circle represents one gene that is induced by eggs in Col-0. Filled circles are genes whose expression was significantly different in the mutant; open circles are genes whose expression was not altered. The grey line indicates perfect correspondence in expression ratios between wild-type and mutant, (i.e the diagonal) while the trend line of the dataset is indicated in red. A trend line closer to one of the axis indicates an overall higher gene induction in this particular genotype.

induced responses. As *P. brassicae* eggs trigger responses partially dependent on SA (Gouhier-Darimont et al., 2013; Bruessow et al., 2010), we examined whether these transcriptional alterations were dependent on SA accumulation by extending our analysis to previously published transcriptome data of oviposited *sid2-1* plants (Little et al., 2007). Overall, only a few genes had significantly altered transcript levels after oviposition in both *sid2-1* (Fig. 2C), indicating that the transcriptional reprogramming of lipid metabolism is mainly independent from SA accumulation. However, linear fitting of both datasets shows that overall, changes in gene expression were lower in *sid2-1* (as seen by regression line closer to the Col-0 axis), suggesting a role for SA in amplifying this response (Fig. 2C). These results show that eggs of *P. brassicae* induce transcriptional changes in lipid metabolism, including categories such as oxylipin and sphingolipid metabolisms which have previously been involved in cell death induction.

HR-like induction is independent from MYB30 and oxylipin synthesis

We further explored the intriguing possibility that lipid metabolism may play a role in cell death induction upon insect egg perception. MYB30 was previously shown to be involved in ETI triggered cell-death through the transcriptional regulation of VLCFA biosynthesis and accumulation (Raffaele et al., 2008), providing an interesting link between lipid metabolism and death induction. Because most VLCFA are found in sphingolipids and cuticular waxes (De Bigault Du Granrut and Cacas, 2016), the authors concluded that MYB30 induces cell death by promoting substrate accumulation for sphingolipid synthesis (Raffaele et al., 2008; De Bigault Du Granrut and Cacas, 2016). As *MYB30* expression was reported to be transiently induced before cell-death onset, we measured the expression of both *MYB30* and *FATB*, one of its target (Raffaele et al., 2008), during the first 24h after egg-extract treatment. However, neither of these genes was induced upon treatment and *FATB* expression was even repressed over time (Supplemental Fig. 1). In addition, microarray data showed that *MYB30* is repressed later during the egg-extract response, along with other MYB30-regulated genes (Little et al., 2007). Finally, cell death induction was not altered in a *myb30* knock-out line, indicating that it is not involved in the induction of HR-like (Fig. 3A). These

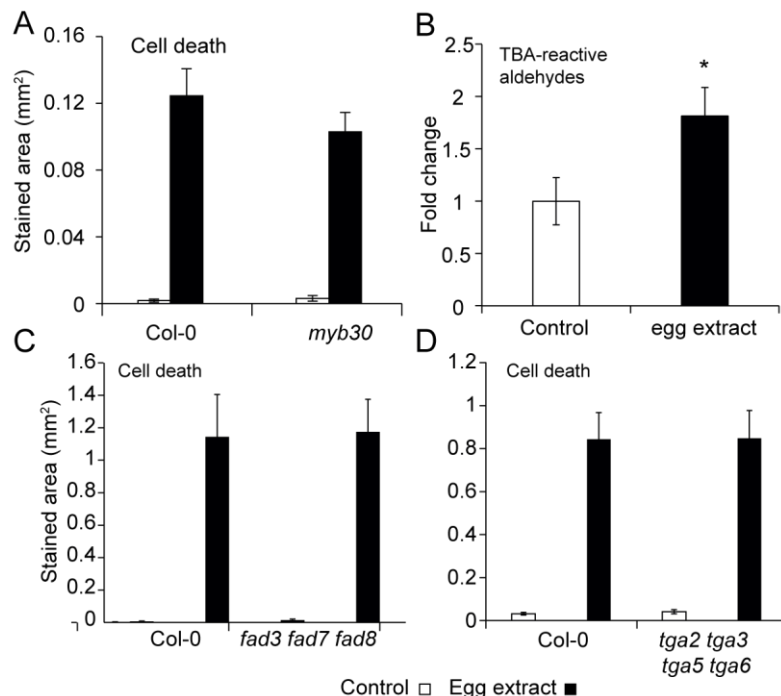


Figure 3. *P. brassicae* egg-induced cell death is independent from MYB30 and oxylipins. A, C and D. Cell death as quantified by trypan blue staining after 3 days of egg extract treatments in *myb30* (A), *fad3 fad7 fad8* (C) and *tga2 tga3 tga5 tga6* mutant plants. For each genotype, a total of 12 to 16 leaves from 6 to 8 plants were treated with 2 μ L of egg extract. Untreated leaves were used as controls. B. Relative nonenzymatic lipid peroxidation levels as measured by the quantification of TBA reactive aldehydes in Col-0 plants treated with egg-extract for 3 days. Data represent means \pm standard error (SEM). Statistical significance was assessed by two-sample t-test against Col-0 treated plants. *, $P < 0.05$.

data are in agreement with the observed FA synthesis/elongation transcriptional repression discussed above.

Lipid peroxydation plays a crucial role in the regulation of cell death through the production of oxylipins (Siebers et al., 2016; García-Marcos et al., 2013), and it was reported that important oxylipin production occurs upon induction of HR by bacterial pathogens (Andersson et al., 2006). This process occurs upon enzymatic or non-enzymatic polyunsaturated fatty acid oxydation, and one of the best known oxylipin is JA. We assessed the level of lipid peroxydation after 3 days of egg extract treatment by using the thiobarbituric acid (TBA) assay, which gives an indirect measure of lipid peroxydation through the detection of its byproducts. Interestingly, we observed that egg perception caused an increase in the level of lipid peroxydation in wild-type plants (Fig. 3B), a clear argument that oxylipins are indeed produced in response to eggs. We then genetically assessed whether lipid peroxydation was necessary for cell death induction by using the fatty acid desaturase *fad3 fad7 fad8* triple mutant which lacks tri-unsaturated fatty acids from which most oxylipins are derived (McConn and Browse, 1996; Weber et al., 2004). Trypan blue staining following egg extract treatment did not reveal any difference in the ability of *fad3 fad7 fad8* mutant plants to induce cell death, demonstrating that this process is independent from trienoic fatty acids and oxylipin production. Furthermore, the TGA transcription factors TGA2, TGA5 and TGA6 were shown to transduce responses downstream of oxylipins such as OPDA and phytoprostanes (Stotz et al., 2013; Mueller et al., 2008). Consistent with our previous results, the quadruple *tga2 tga3 tga5 tga6* mutant displayed wild-type levels of cell death upon egg extract treatment, again suggesting that oxylipins do not play a role during this response. These results provide critical indications that HR-like triggered by *P. brassicae* eggs is independent from MYB30 and from oxylipin-mediated signalling pathways.

Egg perception alters transcription of sphingolipid metabolism genes

Sphingolipids are composed of a sphingoid LCB (long-chain base) backbone, produced by the condensation of a serine with a fatty acid, amidified to a fatty acid moiety. A range of modifications can occur on LCB backbones such as hydroxylation or desaturation. These simple sphingolipids are named ceramides (Cer) and the usual nomenclature is to characterize them by both their LCB core structure as di- or tri-(e.g d18:0 for a dihydroxylated LCB with no unsaturation, t18:1 for a trihydroxylated LCB with one unsaturation and so on) and the fatty acid moiety (C16:0 or h16:0 for instance). These molecules can be modified by the attachment of a polar head group consisting of a glucose or an inositol-glucuronic acid moiety, leading to the formation of complex sphingolipids such as GluCer (glucosylceramides) or GIPC (glycosyl inositol phorpo ceramides), respectively.

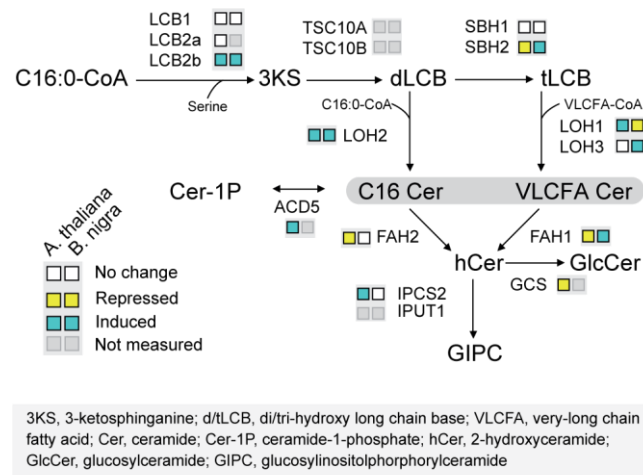


Figure 4. Transcription of sphingolipid biosynthetic genes is altered upon egg perception. Proteins involved in each step is indicated above the reaction arrow and substrates are indicated when appropriate. Expression data are indicated next to the gene name according to the legend below the scheme and are indicated as either up- or down-regulated independently of the degree of transcriptional change. Detailed expression data are available in supplementary fig. 2 and 3.

To further explore the potential role of sphingolipids during egg-induced cell death, we measured the expression of different *Arabidopsis* genes involved in sphingolipid metabolism and signaling by qPCR after treatment with egg-extract for 24 h, 48 h and 72 h. Additionally, we performed the same analysis in *B. nigra*, a plant species that was shown to develop severe HR-like lesions (Fatouros et al., 2016; Griese et al., 2017; Fatouros et al., 2014). Remarkably, the small subunit of the serine palmitoyltransferase *LCB2b*, which catalyzes the first step of LCB synthesis, as well as the ceramide synthase *LOH2* were consistently induced after 3 days of egg-extract treatment in both plant species (Fig. 4). Ceramide synthases catalyze the first step of ceramide synthesis through the attachment of a FA side chain on the LCB backbone. Sphingolipids are usually characterized by both their LCB core structure (e.g. d18:0 for a dihydroxylated LCB with no unsaturation, t18:1 for a trihydroxylated LCB with one unsaturation and so on) and the fatty acid moiety (C16:0 or h16:0 for instance). Interestingly, *LOH2* catalyzes the attachment of C16:0 FA on dihydroxy LCB (d18:X), whereas *LOH1* and *LOH3* have a broader substrate specificity and attach mainly VLCFA on trihydroxy LCB (t18:X) (Luttgeharm et al., 2016; Ternes et al., 2011; Luttgeharm et al., 2015). The fact that mainly *LOH2* was consistently induced in both plant species is indicative of an increased metabolic flux towards C16-Cer (Fig. 4), a class of known inducers of cell death in plants (Berkey et al., 2012). This provides a clear indication that sphingolipids may be involved in the regulation of HR-like. Complex sphingolipids (GluCer and GIPC) consist for the main part of a trihydroxylated LCB attached to 2-hydroxy FA (hFA). The latter step is catalyzed by *FAH1* and *FAH2* (Nagano et al., 2012). Genes involved in fatty-acid hydroxylation (*FAH1/FAH2*) and GluCer synthesis (*GCS*) were downregulated in *Arabidopsis*. This could indicate a decreased flux towards complex sphingolipids, possibly resulting in the accumulation of precursors (Cer and hCer). IN contrast, the induction of the

BnLOH3 and *BnFAH1* was observed in *B. nigra*, indicating a potential increased synthesis of complex sphingolipids. Altogether, these data further confirm that *P. brassicae* egg perception results in alterations of sphingolipid metabolism gene expression in two different plant species and suggest an increased flux towards cell death-inducing C16-Cer.

Ceramide synthase mutants show reduced cell death but intact upstream signaling

In order to further explore the link between egg-triggered responses and sphingolipid metabolism, we tested whether cell death induction was altered in mutant lacking ceramide synthases (*loh1*, *loh2* and *loh3*). Remarkably, both *loh2* and *loh3* displayed decreased cell death after three days of egg-extract treatment, whereas *loh1* did not show any alteration (Fig. 5A). These results are consistent with the previously observed induction of *LOH2* in response to eggs and demonstrates the involvement of sphingolipids in the signaling pathway leading to cell death. While previous studies highlighted the existence of a link between SA signaling and sphingolipids, it is still unclear whether sphingolipids act up- or

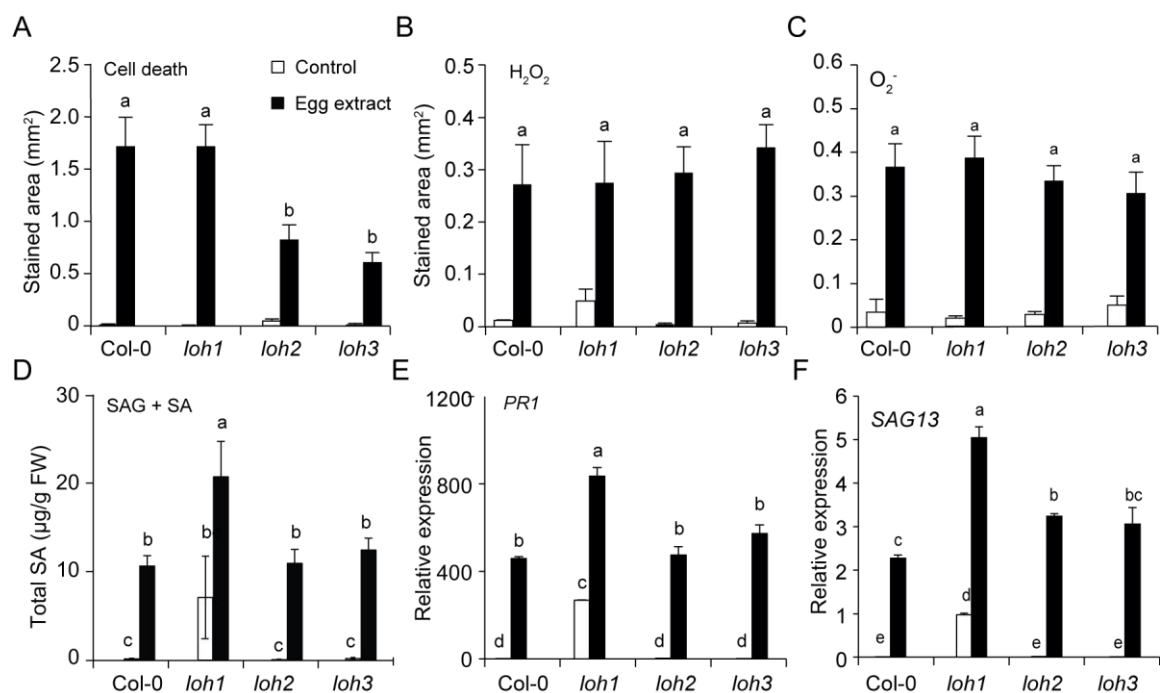


Figure 5. Egg-induced cell death is reduced in ceramide synthase mutants. A to C. Cell death (A), H₂O₂ (B) or O₂⁻ (C) levels after 3 days of egg extract treatments in ceramide synthase mutants. For each genotype, a total of 12 to 16 leaves from 6 to 8 plants were treated with 2μL of egg extract. Untreated leaves were used as controls. D. Total SA (SA + SAG) levels in ceramide synthase mutants after 3 days of egg extract treatment. Results from two independent experiments are shown (n = 8). E and F. Expression of the SA-dependent marker *PR-1* or the SA-independent marker *SAG13* in ceramide mutants after 3 days of egg extract treatment was monitored by qPCR. Means ± standard error (SEM) of three technical replicates are shown. Gene expression was normalized to the reference gene *SAND*. All experiments (except D) were repeated at least twice times with similar results. Different letters indicate significant differences at P<0.05 (ANOVA, followed by Tukey HSD for multiple comparisons).

downstream of SA accumulation and signaling during biotic interactions (Sánchez-Rangel et al., 2015). We previously reported that ROS and SA accumulation act as upstream signals in response to insect eggs (Gouhier-Darimont et al., 2013, 2019). We thus tested whether the lack of ceramide synthases *loh2* and *loh3* affected the production of these early signals. Remarkably, when we measured H₂O₂ and O²⁻ production, no difference could be detected between Col-0 and mutant lines (Fig. 5B and C), indicating that *loh2* and *loh3* act downstream of ROS production. Furthermore, total SA (SA+SAG) reached similar levels after egg extract treatment in Col-0 and *loh2* or *loh3*, while *loh1* displayed increased basal and induced SA levels (Fig. 4D). Moreover, no difference in the expression of the SA-dependent marker *PR1* and the partially SA-independent marker *SAG13* could be observed in *loh2* and *loh3* plants treated with egg extract (Fig. 4E and F). Despite this, *loh1* displayed increased basal and induced transcript levels for these marker genes, consistent with a previous study (Ternes et al., 2011). Altogether, these results demonstrate a role for ceramides in the induction of cell death downstream of ROS and SA signaling. These results suggest that sphingolipids act as executors of cell death but do not play a role in early signaling steps.

Fatty acid hydroxylation modulates egg-induced responses

2-hydroxylation of FA in ceramides is known to be crucial for complex sphingolipid synthesis (Ternes et al., 2011; Markham et al., 2011), and a link between 2-hydroxylation of FA and cell death was demonstrated (Nagano et al., 2012). The current model for sphingolipid synthesis suggests that α -hydroxylation occurs at the ceramide level through the activity of both isoforms of Fatty Acid Hydroxylase, FAH1 and FAH2 (Nagano et al., 2012; König et al., 2012). More specifically, FAH1 was shown to specifically hydroxylate VLCFA whereas FAH2 preferentially uses C16:0 FA as substrates. Interestingly, hVLCFA but not h16:0 fatty acids accumulated upon H₂O₂ treatment, suggesting that hVLCFA play a role in the suppression of cell death (Townley et al., 2005; Nagano et al., 2012). Based on our results demonstrating a role for ceramides in the induction of cell death following egg perception, we tested whether sphingolipid FA hydroxylation plays a role in response to eggs. Cell death was increased in the *fah1* mutant, but not in *fah2*, after three days of egg extract treatment (Fig. 6A), suggesting that hydroxylation of VLCFA in ceramides plays a role in cell death suppression during egg-induced HR-like. Further experiments revealed that while ROS production was not altered (Fig. 6B), basal and induced transcript levels of *PR1* and *SAG13* were elevated after egg extract treatment in *fah1* (Fig. 6C and D). Since ceramides appear to be downstream inducers of cell death, these phenotypes indicate that the increased cell death observed in *fah1* may be the result of pre-induced immune signaling. We next examined global FA 2-hydroxylation in response to insect eggs by GC-MS using a previously published method (Cacas et al., 2016). Surprisingly, we found that egg extract did not cause changes

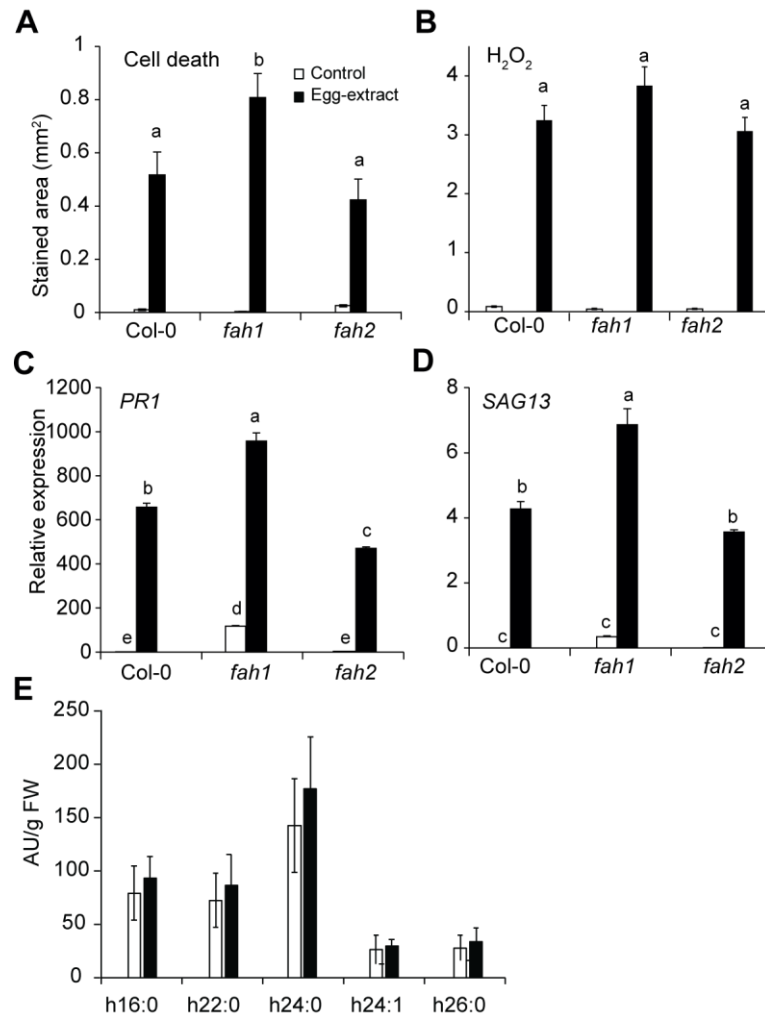


Figure 6. Fatty acid 2-hydroxylation modulates *P. brassicae* egg-induced cell death. A to B. Cell death (A) and H₂O₂ (B) levels after 3 days of egg extract treatments in *fah1* and *fah2* mutant plants. For each genotype, a total of 12 to 16 leaves from 6 to 8 plants were treated with 2 μ L of egg extract. Untreated leaves were used as controls. Expression of the SA-dependent marker *PR-1* (C) or the SA-independent marker *SAG13* (D) in fatty acid hydroxylase mutants after 3 days of egg extract treatment was monitored by qPCR. Means \pm standard error (SEM) of three technical replicates are shown. Gene expression was normalized to the reference gene *SAND*. All experiments (except D) were repeated at least twice times with similar results. Different letters indicate significant differences at $P < 0.05$ (ANOVA, followed by Tukey HSD for multiple comparisons). E. 2-hydroxy fatty acid (hFA) levels following three days of egg extract treatment were quantified by GC-MS as described in the methods. Mean \pm SEM from three biologically independent samples ($n = 3$) are shown.

in neither individual nor total hFA levels (Fig. 6E), suggesting that the phenotypes observed in *fah1* could be the result of a pre-sensitized immunity. Alternatively, hFA profiles from individual sphingolipid species may be altered while overall levels stay stable. These results thus provide additional evidence that ceramides play a role in egg-induced responses.

Sphingolipidome analysis reveals an accumulation of C16:0-containing ceramides in response to *P. brassicae* eggs

We provided clear genetical evidences for the involvement of ceramides as executors of cell death in response to *P. brassicae* egg perception. Our results point to a role for C16:0-containing ceramides and hVLCFA-containing sphingolipids. However, the large number of

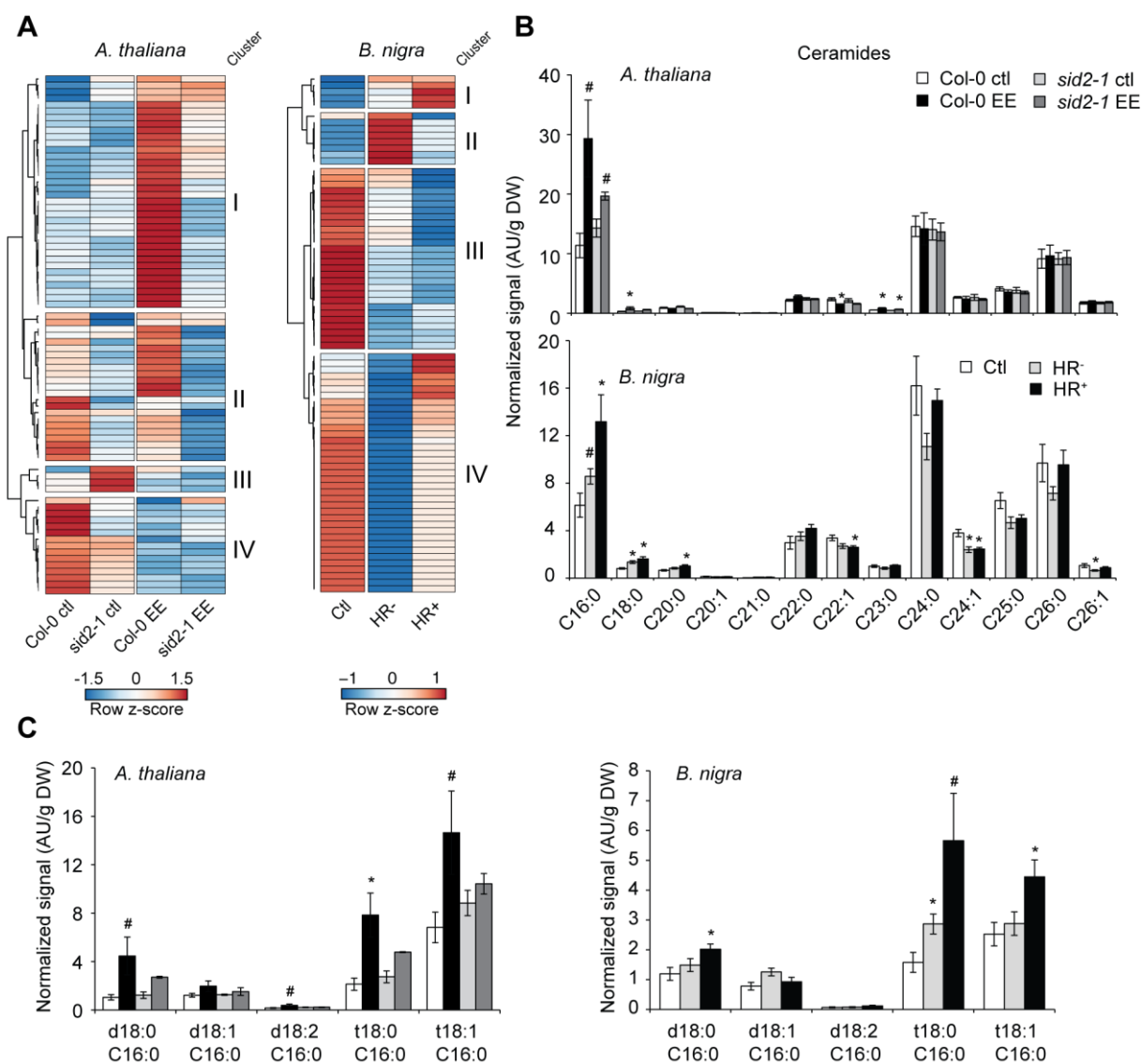


Figure 7. Egg extract induces changes in sphingolipid levels in both *Arabidopsis* and *B. nigra*. Leaves from either species were treated for 3 days with egg extract, and sphingolipids were extracted and analyzed by LC-MS/MS as described in methods. A. Heatmaps displaying sphingolipid levels for the different lipid classes (Cer, hCer, GluCer and GIPC) depending on LCB and FA present. Rows are centered and unit variance scaling is applied to rows. Both rows and columns are clustered using correlation distance and average linkage. Heatmaps were produced using the ClustVis online tool. A larger version with lipid annotations is available as supplementary material. B. Ceramide levels as a function of the FA side chain present. C. Levels of the different C16-containing ceramides after egg extract treatment in the different mutants and species. Data indicate mean \pm SEM from three to five independent samples, except *sid2 EE* which consists of only two samples. Statistical significance was determined using two-sample t-test between egg extract treated samples and their respective controls. #, $P < 0.1$; *, $P < 0.05$; **, $P < 0.01$.

sphingolipid species present in plants (> 200, Pata et al., 2010) makes the interpretation of sphingolipid-related mutants difficult. To resolve these issues, we sought to determine the sphingolipidome composition of *Arabidopsis* and *B. nigra* plants in response to egg extract treatment. Since we observed that the induction of cell death in *B. nigra* plants treated with egg extract was variable, we classified the response into no clear symptom (HR-) to severe cell death (HR+, Supplementary Fig. 3), in line with the phenotypes observed after natural oviposition (Shapiro and DeVay, 1987; Fatouros et al., 2014). For the analysis, we developed

an extended LC-MS/MS analytical method that covers all sphingolipid classes (except free LCB so far, see methods for details). Additionally, to explore the link between sphingolipid alterations and SA (Sánchez-Rangel et al., 2015), we included *sid2-1* in our analysis. Fig. 7A shows heatmaps representing the entire sphingolipid profiles measured in both plant species according to the FA side chain (see Supplementary Fig. 4 for heatmap with lipid annotations). We observed that sphingolipid profiles were altered in response to *P. brassicae* egg extract, in line with our previous results. Based on cell death phenotypes in *loh2* and *loh3*, cell death-inducing sphingolipid(s) should accumulate in response to egg extract. Accordingly, sphingolipid species found in cluster I in both datasets contained lipids that specifically accumulated upon egg extract treatment (Fig. 7A). Interestingly, this accumulation appeared to be largely SA-dependent in *Arabidopsis* and correlated with HR-like severity in *B. nigra*. We observed that cluster I in *B. nigra* only contained non-hydroxy ceramides (Supplementary Figure 4), and the same species were also found in cluster I from *Arabidopsis* data together with many GIPCs. Based on the similar accumulation pattern for certain ceramides in both plant species, these molecules represent ideal candidates as cell death-inducers. FA side chain distribution in Cer revealed a marked accumulation of C16:0 Cer following egg extract treatment in both *Arabidopsis* and *B. nigra* (Fig. 7B). More specifically, our result show that C16:0 Cer containing d18:0, t18:0 and t18:1 LCB were strongly accumulating in both plant species and this pattern is consistent with a SA-dependent cell-death inducing function. While *sid2-1* plants accumulated Cer after egg extract treatment, its extent was much lower than in wild-type plants and the differences observed were non-significant when individual Cer are considered (Fig. 7C and Supplementary Fig. 5A). Furthermore, GluCer and GIPC species did not display any pattern of accumulation compatible with a positive regulation of cell death (Supplementary Fig. 6 and 7), suggesting that C16:0 Cer are good candidates for this function. Surprisingly, hFA distribution in *Arabidopsis* was not significantly altered upon egg extract treatment, confirming our previous quantifications (Fig. 6E) but leaving the role of FA hydroxylation during this response unanswered. In *B. nigra* however, several GluCer (both hydroxy and non-hydroxy) species decreased in abundance after treatment, and this pattern correlated with symptom severity (Supplementary Fig. 6). Additionally, a large decrease (~50%) in the major serie A h24:0 GIPC could be observed in these plants (Supplementary Fig. 7A). Altogether, these results provide clear evidence that C16:0 Cer accumulate in response to egg perception in both *Arabidopsis* and *B. nigra* and thus constitute ideal candidates for cell death executors during this response. Furthermore, our data provide genetical and biochemical evidence that ceramides accumulate in a SA-dependent manner.

The impact of sphingolipid mutants during biotic stress depends on the interaction

The observed accumulation in C16:0 Cer is reminiscent of the sphingolipid profiles of plants infected with the pathogens *B. cinerea* and *P. syringae* pv. *tomato* (Magnin-Robert et al., 2015), suggesting that it might be a common response following infection. To better understand the specificities and commonalities of sphingolipid alterations during biotic stresses, we evaluated the transcriptional response of sphingolipid metabolic genes during interaction with different types of attackers such as oomycetes, fungi, bacteria or insects feeding by using publically available transcriptome data from Genevestigator. To our surprise, these data show that the pattern of sphingolipid-related gene expression triggered upon infestation is very similar independently of the attacker or feeding mode considered (Supplementary Fig. 8), suggesting that this might be a common immune response. Based on these similarities in sphingolipid accumulation and transcription, we evaluated the role of the different ceramide synthases (*loh*) and fatty acid hydroxylases (*fah*) during the interaction with an avirulent pathogen (*P. syringae* pv. *tomato* *AvrRPM1*) and the fungal pathogen *B. cinerea*. We observed that cell death, as measured by ion leakage, in response to *Pst* *AvrRpm1* was reduced in *loh1* and *fah1*, while the same mutants were more resistant to *B. cinerea* (Fig. 8A and B). Additionally, *fah2* was more susceptible to *B. cinerea* (Fig. 8B). These results strongly contrast with the genetic architecture of sphingolipid-mediated cell death upon insect egg perception, and show a different ceramide synthase requirement during pathogen-induced cell death. Moreover, *fah1* mutants display opposite phenotypes during egg- and pathogen-induced cell death, indicating that the impact of fatty acid

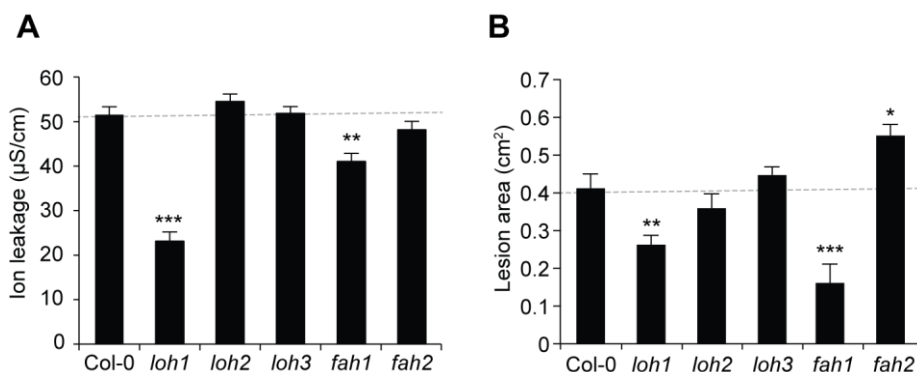


Figure 8. Impact of mutations in sphingolipid mutants on resistance against *P. syringae* pv. *tomato* *AvrRPM1* and *B. cinerea*. A. Cell death induced by the bacterial pathogen *Pst* *AvrRPM1* was quantified by ion leakage 8 hours post infection ($OD_{600}=0.1$ in the different *loh* and *fah* mutant lines). Data represent mean \pm SEM of five from samples ($n=5$). This experiment was replicated twice with similar results. B. The different plant genotypes were infected with a *B. cinerea* spore suspension and lesions were evaluated 3 days later. Bars represent mean \pm SEM of 13-16 leaves per genotype. This experiment was replicated twice with similar results. Statistical significance between mutant and wild-type plants was determined by one-way ANOVA, followed by Dunnett's multiple comparison test. *, $P < 0.05$; **, $P < 0.01$; ***, $P < 0.001$.

hydroxylation is also interaction-specific. These results show that, despite similar transcriptional and metabolic outputs, the genetic basis of sphingolipid-mediated cell death is dependent on the biotic interaction.

Discussion

A few years ago, a study from Gouhier-Darimont and colleagues identified for the first time the molecular pathway involved in the induction of a direct defense mechanism against insect eggs in a *Brassicaceous* species (Gouhier-Darimont et al., 2013). Despite this step forward, components required for PCD induction downstream of SA accumulation were still unclear. A growing body of evidence indicate that the response triggered by *P. brassicae* eggs are conserved in both *B. nigra* and *Arabidopsis* (Bonnet et al., 2017; Fatouros et al., 2014; Geiselhardt et al., 2013), demonstrating the relevance of using *Arabidopsis* as a model species to explore this interaction. By re-analysis of previously published transcriptomic data, we observed an activation of two lipid signaling pathways that were previously implicated in cell death induction: oxylipins and sphingolipids. While the role of oxylipins in cell death induction has been documented (Vollenweider et al., 2000; Alm eras et al., 2003; Garc a-Marcos et al., 2013; Montillet et al., 2005), we did not find evidence that they are involved in insect egg-induced cell death. Besides their role as structural components of membranes, the role of sphingolipids during PCD is a conserved feature throughout the eukaryotic kingdom (Young et al., 2013). Here we report that insect eggs trigger transcriptional and quantitative alterations of sphingolipid metabolism in both *Arabidopsis* and *B. nigra*. Despite differences in the profiles of complex sphingolipids from both species after egg extract treatment, a common and marked accumulation of C16:0-containing Cer could be observed. Remarkably, the accumulation of C16:0 Cer is a conserved hallmark of cell death induction in plants, animals and fungi (Berkey et al., 2012; Ali et al., 2018b; Young et al., 2013). Most of the accumulating C16:0 Cer contained t18:0 or t18:1 LCB which are not found in animals, confirming that the observed increase is not due to the potential presence of egg-derived lipids. We also observed that cell death induction is dependent on the ceramide synthases LOH2 and LOH3, raising the question of the specificity of each enzyme during this process. Previous works revealed that LOH2 is responsible for the production of most C16:0 Cer *in planta* (Markham et al., 2011), consistent with the observed accumulation of these molecules following egg treatment. Given that LOH3 was described as producing mainly VLCFA Cer, its role during egg-induced responses is not clear. A careful description of LOH function and substrate specificity revealed that LOH2 mainly catalyzes the attachment of C16:0 FA onto dihydroxy LCB (d18:0 and d18:1) with low affinity for trihydroxy LCB (t18:0 and t18:1), whereas LOH1 and LOH3 attach VLCFA onto trihydroxy LCB (Luttgeharm et al. 2016). Interestingly, *in vitro* ceramide synthase activity shows that LOH3, in contrast to LOH1, can also accept C16:0 substrates. Based on these results, we postulate that the observed

accumulation of C16:0 Cer after egg treatment may have different origins: LOH2 might be required for the production of d18:0 C16:0 Cer, and LOH3 for the production of t18:0/t18:1 C16:0 Cer. Sphingolipid quantification in the respective mutants would enable to address this intriguing possibility.

How LCBs or ceramides induce cell death is still not clear (Berkey et al., 2012; De Bigault Du Granrut and Cacas, 2016) but studies from plants and other organisms may provide insights into their function. Sphingolipids, outside of their role as structural lipids in plasma membranes (PM), are major constituents of lipid rafts (Mamode Cassim et al., 2019). Membrane microdomains, or lipid rafts, are patches of lipids and proteins that laterally segregate from the rest of the PM due to a high degree of intermolecular interactions between sphingolipids (De Bigault Du Granrut and Cacas, 2016; Cacas et al., 2012). Proteomic studies of raft-associated proteins show that many immune regulators accumulate in these structures (Morel et al., 2006) and studies in rice showed that alterations in microdomain sphingolipid composition can affect the abundance and function of PTI and cell death regulators in rafts (Ishikawa et al., 2015; Nagano et al., 2016). Additionally, phytoceramides were shown to perturb lipid rafts in yeast (Pacheco et al., 2013). These results depict a dynamic relationship between sphingolipid metabolism and membrane microdomains, suggesting that changes in the composition of certain sphingolipid classes could affect protein distribution and therefore raft function. In animal and yeast cells, ceramides have also been reported to have the ability to self-assemble so-called ceramide channels in mitochondria's outer membrane (MOM) and to promote the leakage of mitochondrial proteins (including cytochrome c), a hallmark point of no return for PCD (Siskind et al., 2002; Colombini, 2017). Under this model, Cer are thus direct cell death executors, but whether such structures can form in plant cells is currently unknown. Interestingly, C16:0 phytoceramides (with trihydroxy LCBs) were reported to have a higher pore-forming activity in rat mitochondria than dihydroxy-ceramides (Perera et al., 2012), demonstrating that these molecules have the ability to form pores. Remarkably, these structures were found to assemble at physiological ceramide concentrations and their function was shown to be under the regulation of apoptotic regulators (Colombini, 2017). Alternatively, Cer may function through their interaction with cell-death modulator/executor proteins as revealed by the recent identification in human mitochondria of the voltage-dependent anion channel VDAC2 as a critical effector of Cer-induced PCD (Dadsena et al., 2019). In plants, no protein interacting with Cer have been described thus far. However, the function of plant VDAC in PCD appears to be conserved when expressed in human cells, suggesting that VDAC channels may also act as Cer interactors in plants (Godbole et al.,

2003). Given their important role in PCD induction in plants, future research should aim at identifying the molecular mechanisms underlying ceramide-regulated cell death.

The role of sphingolipids in lipid raft structure and function may bring light on the phenotypes observed in *fah1* upon egg extract treatment. *fah1* mutant plants displayed increased cell death following egg extract treatment and this correlated with a higher basal and induced expression of SA-dependent and -independent markers *PR1* and *SAG13*, respectively. Despite a trend for certain GIPC with hFA, we found no clear alteration in overall hFA levels and distribution in different sphingolipid classes upon egg extract treatment. This suggests that hFA may not play a role after the response is triggered. As mentioned, two recent studies in rice reported that alterations in microdomain hFA levels resulted in the depletion of certain PTI and cell death modulators (Nagano et al., 2016; Ishikawa et al., 2015). These data may thus suggest that the increased cell death observed in *fah1* after egg extract treatment may be the result of altered signaling from plasma membrane microdomains, although this question would require additional work.

Some sphingolipid changes were observed only in one of the studied species. For instance, *B. nigra* plants displayed severely decreased GlcCer levels (-35%) and serie A GIPC (-36%). Since the vast majority of sphingolipids (~90%) are complex (Markham et al., 2013; Gronnier et al., 2016), the measured decrease in *B. nigra* is massive. While studies show that they can function as receptor for fungal toxins (Lenarčič et al., 2017) and accumulate in membrane microdomains (Gronnier et al., 2016), the function of complex sphingolipids such as GlcCer and GIPC during biotic stresses is unknown. Alternatively, the decrease in GIPC levels may be caused by an enzyme similar to the serie A GIPC-specific phospholipase D recently described (Hasi et al., 2019). However, since this change was observed in *B. nigra* but not in *Arabidopsis*, it is likely that GIPCs do not play a central role during cell death execution following egg perception.

The hypothesis that SA signaling and sphingolipid metabolism are somehow connected was based on the observation that certain sphingolipid mutants or FB1 treatment lead to increased defense gene expression or SA signaling/accumulation (Wang et al., 2008; Luttgeharm et al., 2015; Fang et al., 2016; König et al., 2012; Sánchez-Rangel et al., 2015). This led to postulate that the rise in Cer might precede SA accumulation (Sánchez-Rangel et al., 2015). In contrast, we found that *loh2* and *loh3* mutant plants displayed wild-type ROS, SA and *PR1* levels, although they showed a significantly reduced cell death. These results thus show that ceramides function downstream of egg-induced SA signaling. Additionally, we found that the increase in C16:0 Cer was largely reduced in *sid2-1*, showing that SA accumulation not only precedes but also contributes to Cer accumulation. However, we could

not observe any significant alteration in the induction of *LCB2b* and *LOH2* in *sid2-1* compared to Col-0 after egg extract treatment, suggesting that gene expression is not the only factor impacting gene expression. This hypothesis is consistent with the fact that *B. nigra* HR- plants induced gene expression to similar levels than HR+ plants, yet they displayed less pronounced C16:0 Cer accumulation. The reason for the discrepancy between gene expression and metabolite accumulation is not known but deserves further investigation. Finally, cell death in *ein2-1* mutants was increased as compared to wild-type plants, revealing that ET signaling contributes to the mounting of HR-like. Since ET was previously reported to negatively regulate sphingolipid metabolism and gene transcription (Wu et al., 2015a; Plett et al., 2009; Asai et al., 2000), the observed increase in cell death is consistent with this function. Furthermore, we observed that *LOH2* expression was higher upon egg extract treatment in *ein2-1* plants (Supplementary Fig. 9), in line with this hypothesis.

Altogether, our results show that sphingolipid metabolism plays a central role in the execution of HR-like after *P. brassicae* egg perception. The similarities observed between *Arabidopsis* and *B. nigra* strongly suggest that Cer play a role in HR-like in other *Brassicaceae* as well. Further research should aim at deciphering the exact mechanism by which shingolipids generate HR-like. On more applied aspect, a better understanding of the processes used by plants to trigger localized cell death in response to oviposition, and hence drastically impair egg development, may provide strategies to reduce insecticide use in agriculture (Fatouros et al., 2016).

Acknowledgments

We thank Steve Lassueur for the pictures of HR-like symptoms on *B. nigra* leaves; Alice Bacon for valuable help with sphingolipid extractions; Marion Rebeaud and Lisa Buttucaz for technical help during qPCR experiments.

References

- Ali, U., Li, H., Wang, X., and Guo, L.** (2018). Emerging Roles of Sphingolipid Signaling in Plant Response to Biotic and Abiotic Stresses. *Mol. Plant* **11**: 1328–1343.
- Alméras, E., Stolz, S., Vollenweider, S., Reymond, P., Mène-Saffrané, L., and Farmer, E.E.** (2003). Reactive electrophile species activate defense gene expression in *Arabidopsis*. *Plant J.* **34**: 205–216.
- Andersson, M.X., Hamberg, M., Kourtchenko, O., Brunnström, Å., McPhail, K.L., Gerwick, W.H., Göbel, C., Feussner, I., and Ellerström, M.** (2006). Oxylinin profiling of the hypersensitive response in *Arabidopsis thaliana*: Formation of a novel oxo-phytodienoic acid-containing galactolipid, arabidopside E. *J. Biol. Chem.* **281**: 31528–31537.
- Asai, T., Stone, J.M., Heard, J.E., Kovtun, Y., Yorgey, P., Sheen, J., and Ausubel, F.M.** (2000). Fumonisin B1-induced cell death in *Arabidopsis* protoplasts requires jasmonate-, ethylene-, and salicylate-dependent signaling pathways. *Plant Cell* **12**: 1823–1836.
- Balint-Kurti, P.** (2019). The plant hypersensitive response: concepts, control and consequences. *Mol. Plant Pathol.* **0**: 1163–1178.
- Berkey, R., Bendigeri, D., and Xiao, S.** (2012). Sphingolipids and plant defense/disease: the “death” connection and beyond. *Front. Plant Sci.* **3**: 68.
- De Bigault Du Granrut, A. and Cacas, J.-L.** (2016). How Very-Long-Chain Fatty Acids Could Signal Stressful Conditions in Plants? *Front. Plant Sci.* **7**: 1–13.
- Bonnet, C., Lassueur, S., Ponzio, C., Gols, R., Dicke, M., and Reymond, P.** (2017). Combined biotic stresses trigger similar transcriptomic responses but contrasting resistance against a chewing herbivore in *Brassica nigra*. *BMC Plant Biol.* **17**: 127.
- Bouchez, O., Huard, C., Lorrain, S., Roby, D., and Balagué, C.** (2007). Ethylene is one of the key elements for cell death and defense response control in the *Arabidopsis* lesion mimic mutant *vad1*. *Plant Physiol.* **145**: 465–477.
- Bruessow, F., Gouhier-Darimont, C., Bruchala, A., Metraux, J.-P., and Reymond, P.** (2010). Insect eggs suppress plant defence against chewing herbivores. *Plant J.* **62**: 876–885.
- Bruggeman, Q., Raynaud, C., Benhamed, M., and Delarue, M.** (2015). To die or not to die? Lessons from lesion mimic mutants. *Front. Plant Sci.* **6**: 1–22.
- Cacas, J. et al.** (2016). Revisiting Plant Plasma Membrane Lipids in Tobacco: A Focus on Sphingolipids. *Plant Physiol.* **170**: 367–384.
- Cacas JL, Furt F, Le Guédard M, Schmitter JM, Buré C, Gerbeau-Pissot P, Moreau P, Bessoule JJ, Simon-Plas F, Mongrand S** (2012). Lipids of plant membrane rafts. *Prog Lipid Res* **51**: 272–299
- Ciardi, J.A., Tieman, D.M., Jones, J.B., and Klee, H.J.** (2001). Reduced expression of the tomato ethylene receptor gene *leETR4* enhances the hypersensitive response to *Xanthomonas campestris* pv. *vesicatoria*. *Mol. Plant-Microbe Interact.* **14**: 487–495.
- Coll, N.S., Epple, P., and Dangl, J.L.** (2011). Programmed cell death in the plant immune system. *Cell Death Differ.* **18**: 1247–56.
- Colombini, M.** (2017). Ceramide channels and mitochondrial outer membrane permeability. *J. Bioenerg. Biomembr.* **49**: 57–64.
- Dadsena, S. et al.** (2019). Ceramides bind VDAC2 to trigger mitochondrial apoptosis. *Nat.*

Commun. **10**.

- DeFraia, C.T., Schmelz, E.A., and Mou, Z.** (2008). A rapid biosensor-based method for quantification of free and glucose-conjugated salicylic acid. *Plant Methods* **4**: 28.
- Fang, L. et al.** (2016). Loss of Inositol Phosphorylceramide Sphingolipid Mannosylation Induces Plant Immune Responses and Reduces Cellulose Content in Arabidopsis. *Plant Cell* **28**: 2991–3004.
- Fatouros, N.E., Cusumano, A., Danchin, E.G.J., and Colazza, S.** (2016). Prospects of herbivore egg-killing plant defenses for sustainable crop protection. *Ecol. Evol.* **6**: 6906–6918.
- Fatouros, N.E., Pineda, A., Huigens, M.E., Broekgaarden, C., Shimwela, M.M., Candia, I.A.F., Verbaarschot, P., and Bukovinszky, T.** (2014). Synergistic effects of direct and indirect defences on herbivore egg survival in a wild crucifer. *Proc. R. Soc. B Biol. Sci.* **281**: 20141254.
- Fernandes, G.W.** (1990). Hypersensitivity: A Neglected Plant Resistance Mechanism Against Insect Herbivores. *Environ. Entomol.* **19**: 1173–1182.
- García-Marcos, A., Pacheco, R., Manzano, A., Aguilar, E., and Tenllado, F.** (2013). Oxylin biosynthesis genes positively regulate programmed cell death during compatible infections with the synergistic pair potato virus X-potato virus Y and Tomato spotted wilt virus. *J. Virol.* **87**: 5769–83.
- Garza, R., Vera, J., Cardona, C., Barcenas, N., and Singh, S.P.** (2001). Hypersensitive response of beans to *Apion godmani* (Coleoptera: Curculionidae). *J. Econ. Entomol.* **94**: 958–962.
- Geiselhardt, S., Yoneya, K., Blenn, B., Drechsler, N., Gershenzon, J., Kunze, R., and Hilker, M.** (2013). Egg Laying of Cabbage White Butterfly (*Pieris brassicae*) on *Arabidopsis thaliana* Affects Subsequent Performance of the Larvae. *PLoS One* **8**: e59661.
- Geuss, D., Stelzer, S., Lortzing, T., and Steppuhn, A.** (2017). *Solanum dulcamara* 's response to eggs of an insect herbivore comprises ovicidal hydrogen peroxide production. *Plant. Cell Environ.* **40**: 2663–2677.
- Godbole, A., Varghese, J., Sarin, A., and Mathew, M.K.** (2003). VDAC is a conserved element of death pathways in plant and animal systems. *Biochim. Biophys. Acta - Mol. Cell Res.* **1642**: 87–96.
- Gouhier-Darimont, C., Schmiesing, A., Bonnet, C., Lassueur, S., and Reymond, P.** (2013). Signalling of *Arabidopsis thaliana* response to *Pieris brassicae* eggs shares similarities with PAMP-triggered immunity. *J. Exp. Bot.* **64**: 665–74.
- Gouhier-Darimont, C., Stahl, E., Glauser, G., and Reymond, P.** (2019). The *Arabidopsis* Lectin Receptor Kinase LecRK-I.8 Is Involved in Insect Egg Perception. *Front. Plant Sci.* **10**: 1–10.
- Griese, E., Dicke, M., Hilker, M., and Fatouros, N.E.** (2017). Plant response to butterfly eggs: inducibility, severity and success of egg-killing leaf necrosis depends on plant genotype and egg clustering. *Sci. Rep.* **7**: 7316.
- Gronnier, J., Germain, V., Gouguet, P., Cacas, J.-L., and Mongrand, S.** (2016). GIPC: Glycosyl Inositol Phospho Ceramides, the major sphingolipids on earth. *Plant Signal. Behav.* **11**: e1152438.
- Hasi, R.Y., Miyagi, M., Morito, K., Ishikawa, T., Kawai-Yamada, M., Imai, H., Fukuta, T., Kogure, K., Kanemaru, K., Hayashi, J., Kawakami, R., and Tanaka, T.** (2019). Glycosylinositol phosphoceramide-specific phospholipase D activity catalyzes transphosphatidylation. *J. Biochem.* **166**: 441–448.

- Heath, R.L., and Packer, L.** (1968). Photoperoxidation in isolated chloroplasts. I. Kinetics and stoichiometry of fatty acid peroxidation. *Archives Biochem. Biophysics* **125**: 189–198.
- Hilfiker, O., Groux, R., Bruessow, F., Kiefer, K., Zeier, J., and Reymond, P.** (2014). Insect eggs induce a systemic acquired resistance in *Arabidopsis*. *Plant J.* **80**: 1085–94.
- Huby, E., Napier, J.A., Baillieul, F., Michaelson, L. V., and Dhondt-Cordelier, S.** (2019). Sphingolipids: towards an integrated view of metabolism during the plant stress response. *New Phytol.*
- Huysmans, M., Lema A, S., Coll, N.S., and Nowack, M.K.** (2017). Dying two deaths — programmed cell death regulation in development and disease. *Curr. Opin. Plant Biol.* **35**: 37–44.
- Ishikawa, T., Aki, T., Yanagisawa, S., Uchimiya, H., and Kawai-Yamada, M.** (2015). Overexpression of BAX INHIBITOR-1 Links Plasma Membrane Microdomain Proteins to Stress. *Plant Physiol.* **169**: 1333–1343.
- Johansson, O.N., Nilsson, A.K., Gustavsson, M.B., Backhaus, T., Andersson, M.X., and Ellerström, M.** (2015). A quick and robust method for quantification of the hypersensitive response in plants. *PeerJ* **3**: e1469.
- König, S., Feussner, K., Schwarz, M., Kaever, A., Iven, T., Landesfeind, M., Ternes, P., Karlovsky, P., Lipka, V., and Feussner, I.** (2012). *Arabidopsis* mutants of sphingolipid fatty acid α -hydroxylases accumulate ceramides and salicylates. *New Phytol.* **196**: 1086–1097.
- Lachaud, C., Da Silva, D., Amelot, N., Béziat, C., Brière, C., Cotelle, V., Graziana, A., Grat, S., Mazars, C., and Thuleau, P.** (2011). Dihydrosphingosine-induced programmed cell death in tobacco BY-2 cells is independent of H₂O₂ production. *Mol. Plant* **4**: 310–8.
- Lenarčič, T. et al.** (2017). Eudicot plant-specific sphingolipids determine host selectivity of microbial NLP cytolysins. *Science* (80-). **358**: 1431–1434.
- Liang, H., Yao, N., Song, J.T., Luo, S., Lu, H., and Greenberg, J.T.** (2003). Ceramides modulate programmed cell death in plants. *Genes Dev.* **17**: 2636–2641.
- Lim, G., Singhal, R., Kachroo, A., and Kachroo, P.** (2017). Fatty Acid- and Lipid-Mediated Signaling in Plant Defense. *Annu. Rev. Phytopathol.* **55**: 505–536.
- Little, D., Gouhier-Darimont, C., Bruessow, F., and Reymond, P.** (2007a). Oviposition by pierid butterflies triggers defense responses in *Arabidopsis*. *Plant Physiol.* **143**: 784–800.
- Little, D., Gouhier-Darimont, C., Bruessow, F., and Reymond, P.** (2007b). Oviposition by pierid butterflies triggers defense responses in *Arabidopsis*. *Plant Physiol.* **143**: 784–800.
- Luttgeharm, K.D., Cahoon, E.B., and Markham, J.E.** (2016). Substrate specificity, kinetic properties and inhibition by fumonisin B1 of ceramide synthase isoforms from *Arabidopsis*. *Biochem. J.* **473**: 593–603.
- Luttgeharm, K.D., Chen, M., Mehra, A., Cahoon, R.E., Markham, J.E., and Cahoon, E.B.** (2015). Overexpression of *Arabidopsis* Ceramide Synthases Differentially Affects Growth, Sphingolipid Metabolism, Programmed Cell Death, and Mycotoxin Resistance. *Plant Physiol.* **169**: 1108–17.
- Magnin-Robert, M., Le Bourse, D., Markham, J.E., Dorey, S., Clément, C., Baillieul, F., and Dhondt-Cordelier, S.** (2015). Modifications of sphingolipid content affect tolerance to hemibiotrophic and necrotrophic pathogens by modulating plant defense responses in *Arabidopsis*. *Plant Physiol.* **169**: 2255–2274.

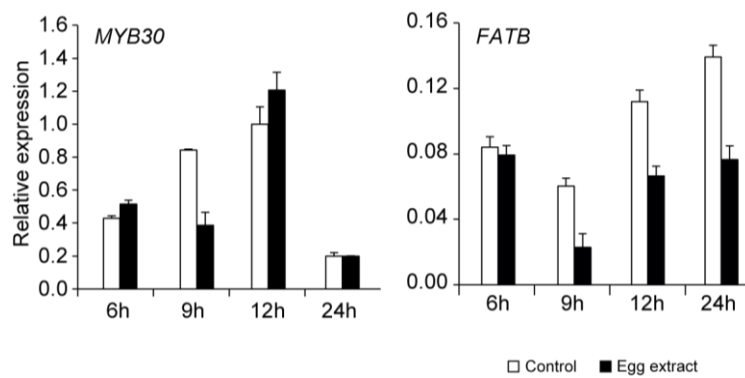
- Mamode Cassim, A., Gouguet, P., Gronnier, J., Laurent, N., Germain, V., Grison, M., Boutté, Y., Gerbeau-Pissot, P., Simon-Plas, F., and Mongrand, S.** (2019). Plant lipids: Key players of plasma membrane organization and function. *Prog. Lipid Res.* **73**: 1–27.
- Markham, J.E.** (2013). Detection and Quantification of Plant Sphingolipids by LC-MS. T. Munnik and I. Heilmann, eds (Humana Press: Totowa, NJ).
- Markham, J.E., Lynch, D. V., Napier, J.A., Dunn, T.M., and Cahoon, E.B.** (2013). Plant sphingolipids: Function follows form. *Curr. Opin. Plant Biol.* **16**: 350–357.
- Markham, J.E., Molino, D., Gissot, L., Bellec, Y., Hématy, K., Marion, J., Belcram, K., Palauqui, J.-C., Satiat-Jeunemaître, B., and Faure, J.-D.** (2011). Sphingolipids containing very-long-chain fatty acids define a secretory pathway for specific polar plasma membrane protein targeting in Arabidopsis. *Plant Cell* **23**: 2362–78.
- McConn, M. and Browse, J.** (1996). The Critical Requirement for Linolenic Acid Is Pollen Development, Not Photosynthesis, in an Arabidopsis Mutant. *Plant Cell* **8**: 403–416.
- Montillet, J., Chamnongpol, S., Rustérucchi, C., Dat, J., van de Cotte, B., Agnel, J., Battesti, C., Inzé, D., van Breusegem, F., and Triantaphylidès, C.** (2005). Fatty Acid Hydroperoxides and H₂O₂ in the Execution of Hypersensitive Cell Death in Tobacco Leaves. *Plant Physiol.* **138**: 1516–1526.
- Morel, J., Claverol, S., Mongrand, S., Furt, F., Fromentin, J., Bessoule, J.-J., Blein, J.-P., and Simon-Plas, F.** (2006). Proteomics of Plant Detergent-resistant Membranes. *Mol. Cell. Proteomics* **5**: 1396–1411.
- Mueller, S., Hilbert, B., Dueckershoff, K., Roitsch, T., Krischke, M., Mueller, M.J., Berger, S., Biowissenschaften, J., Biologie, P., and Wuerzburg, U.** (2008). General Detoxification and Stress Responses Are Mediated by Oxidized Lipids through TGA Transcription Factors in Arabidopsis. **20**: 768–785.
- Nagano, M., Ishikawa, T., Fujiwara, M., Fukao, Y., Kawano, Y., Kawai-Yamada, M., and Shimamoto, K.** (2016). Plasma Membrane Microdomains Are Essential for Rac1-RbohB/H-Mediated Immunity in Rice. *Plant Cell* **28**: 1966–1983.
- Nagano, M., Takahara, K., Fujimoto, M., Tsutsumi, N., Uchimiya, H., and Kawai-Yamada, M.** (2012). Arabidopsis Sphingolipid Fatty Acid 2-Hydroxylases (AtFAH1 and AtFAH2) Are Functionally Differentiated in Fatty Acid 2-Hydroxylation and Stress Responses. *Plant Physiol.* **159**: 1138–1148.
- Olvera-Carrillo, Y. et al.** (2015). A conserved core of PCD indicator genes discriminates developmentally and environmentally induced programmed cell death in plants. *Plant Physiol.* **169**: pp.00769.2015.
- Pacheco, A., Azevedo, F., Rego, A., Santos, J., Chaves, S.R., Côte-Real, M., and Sousa, M.J.** (2013). C2-phytoceramide perturbs lipid rafts and cell integrity in *Saccharomyces cerevisiae* in a sterol-dependent manner. *PLoS One* **8**: 1–12.
- Pata, M.O., Hannun, Y.A., and Ng, C.K.Y.** (2010). Plant sphingolipids: Decoding the enigma of the Sphinx. *New Phytol.* **185**: 611–630.
- Perera, M.N., Ganesan, V., Siskind, L.J., Szulc, Z.M., Bielawski, J., Bielawska, A., Bittman, R., and Colombini, M.** (2012). Ceramide channels: Influence of molecular structure on channel formation in membranes. *Biochim. Biophys. Acta - Biomembr.* **1818**: 1291–1301.
- Petzold-Maxwell, J., Wong, S., Arellano, C., and Gould, F.** (2011). Host plant direct defence against eggs of its specialist herbivore, *Heliothis subflexa*. *Ecol. Entomol.* **36**: 700–708.
- Plett, J.M., Cvetkovska, M., Makenson, P., Xing, T., and Regan, S.** (2009). Arabidopsis

ethylene receptors have different roles in Fumonisin B1-induced cell death. *Physiol. Mol. Plant Pathol.* **74**: 18–26.

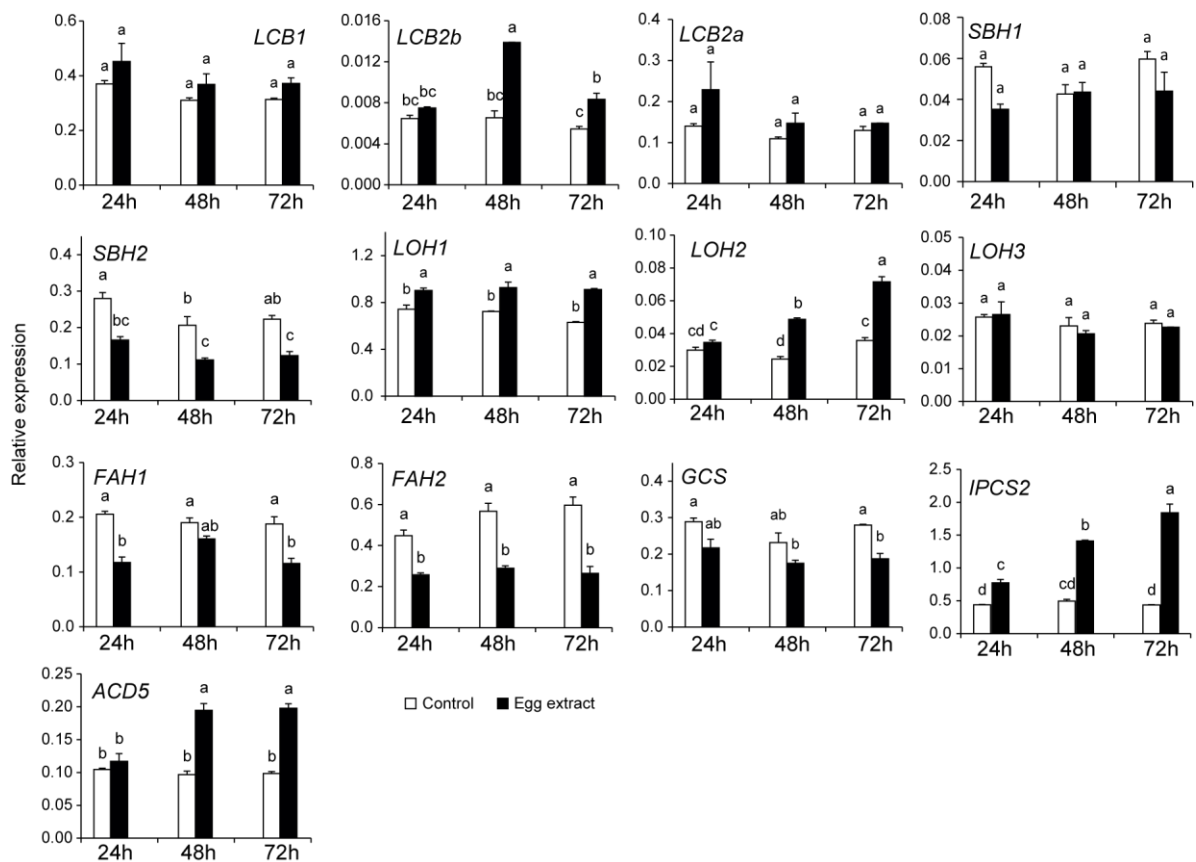
- Radojičić, A., Li, X., and Zhang, Y.** (2018). Salicylic Acid: A Double-Edged Sword for Programmed Cell Death in Plants. *Front. Plant Sci.* **9**: 1133.
- Raffaele, S., Vaillau, F., Leger, a, Joubes, J., Miersch, O., Huard, C., Blee, E., Mongrand, S., Domergue, F., and Roby, D.** (2008). A MYB transcription factor regulates very-long-chain fatty acid biosynthesis for activation of the hypersensitive cell death response in Arabidopsis. *Plant Cell* **20**: 752–767.
- Reape, T.J. and McCabe, P.F.** (2010). Apoptotic-like regulation of programmed cell death in plants. *Apoptosis* **15**: 249–256.
- Reymond, P.** (2013). Perception, signaling and molecular basis of oviposition-mediated plant responses. *Planta* **238**: 247–58.
- Salguero-Linares, J. and Coll, N.S.** (2019). Plant proteases in the control of the hypersensitive response. *J. Exp. Bot.* **70**: 2087–2095.
- Salvesen, G.S., Hempel, A., and Coll, N.S.** (2015). Protease Signaling in Animal and Plant Regulated Cell Death. *FEBS J.*: n/a-n/a.
- Sánchez-Rangel, D., Rivas-San Vicente, M., de la Torre-Hernández, M.E., Nájera-Martínez, M., and Plasencia, J.** (2015). Deciphering the link between salicylic acid signaling and sphingolipid metabolism. *Front. Plant Sci.* **6**: 1–8.
- Saucedo-García, M., Guevara-García, A., González-Solís, A., Cruz-García, F., Vázquez-Santana, S., Markham, J.E., Lozano-Rosas, M.G., Dietrich, C.R., Ramos-Vega, M., Cahoon, E.B., and Gavilanes-Ruíz, M.** (2011). MPK6, sphinganine and the LCB2a gene from serine palmitoyltransferase are required in the signaling pathway that mediates cell death induced by long chain bases in Arabidopsis. *New Phytol.* **191**: 943–957.
- Shapiro, A.M. and DeVay, J.E.** (1987). Hypersensitivity reaction of *Brassica nigra* L. (Cruciferae) kills eggs of *Pieris* butterflies (Lepidoptera: Pieridae). *Oecologia* **71**: 631–632.
- Shi, L., Bielawski, J., Mu, J., Dong, H., Teng, C., Zhang, J., Yang, X., Tomishige, N., Hanada, K., Hannun, Y.A., and Zuo, J.** (2007). Involvement of sphingoid bases in mediating reactive oxygen intermediate production and programmed cell death in Arabidopsis. *Cell Res.* **17100**: 1030–1040.
- Siebers, M., Brands, M., Wewer, V., Duan, Y., Hölzl, G., and Dörmann, P.** (2016). Lipids in plant–microbe interactions. *Biochim. Biophys. Acta - Mol. Cell Biol. Lipids* **1861**: 1379–1395.
- Siskind, L.J., Kolesnick, R.N., and Colombini, M.** (2002). Ceramide channels increase the permeability of the mitochondrial outer membrane to small proteins. *J. Biol. Chem.* **277**: 26796–26803.
- Stotz, H.U., Mueller, S., Zoeller, M., Mueller, M.J., and Berger, S.** (2013). TGA transcription factors and jasmonate-independent COI1 signalling regulate specific plant responses to reactive oxylipins. *J. Exp. Bot.* **64**: 963–975.
- Stuart, J.** (2015). Insect effectors and gene-for-gene interactions with host plants. *Curr. Opin. Insect Sci.* **9**: 56–61.
- Suzuki, Y., Sogawa, K., and Seino, Y.** (1996). Ovicidal Reaction of Rice Plants against the Whitebacked Planthopper, *Sogatella furcifera* HORVATH (Homoptera: Delphacidae). *Appl. Entomol. Zool.* **31**: 111–118.
- Ternes, P., Feussner, K., Werner, S., Lerche, J., Iven, T., Heilmann, I., Riezman, H., and Feussner, I.** (2011). Disruption of the ceramide synthase LOH1 causes spontaneous

- cell death in *Arabidopsis thaliana*. *New Phytol.* **192**: 841–854.
- Townley, H.E., McDonald, K., Jenkins, G.I., Knight, M.R., and Leaver, C.J.** (2005). Ceramides induce programmed cell death in *Arabidopsis* cells in a calcium-dependent manner. *Biol. Chem.* **386**: 161–166.
- Vollenweider, S., Weber, H., Stolz, S., Chételat, A., and Farmer, E.E.** (2000). Fatty acid ketodienes and fatty acid ketotrienes: Michael addition acceptors that accumulate in wounded and diseased *Arabidopsis* leaves. *Plant J.* **24**: 467–476.
- Wang, W. et al.** (2008). An inositolphosphorylceramide synthase is involved in regulation of plant programmed cell death associated with defense in *Arabidopsis*. *Plant Cell* **20**: 3163–79.
- Weber, H., Chételat, A., Reymond, P., and Farmer, E.E.** (2004). Selective and powerful stress gene expression in *Arabidopsis* in response to malondialdehyde. *Plant J.* **37**: 877–888.
- Wright, C. a and Beattie, G. a** (2004). *Pseudomonas syringae* pv. tomato cells encounter inhibitory levels of water stress during the hypersensitive response of *Arabidopsis thaliana*. *Proc. Natl. Acad. Sci.* **101**: 3269–3274.
- Wu, J., Wu, J., Yin, J., Zheng, P., and Yao, N.** (2015a). Ethylene Modulates Sphingolipid Synthesis in *Arabidopsis*. *Front. Plant Sci.* **6**: 1–11.
- Wu, J.X., Li, J., Liu, Z., Yin, J., Chang, Z.Y., Rong, C., Wu, J.L., Bi, F.C., and Yao, N.** (2015b). The *Arabidopsis* ceramidase AtACER functions in disease resistance and salt tolerance. *Plant J.* **81**: 767–780.
- Yamasaki, M., Yoshimura, A., and Yasui, H.** (2003). Genetic basis of ovicidal response to whitebacked planthopper (*Sogatella furcifera* Horváth) in rice (*Oryza sativa* L.). *Mol. Breed.* **12**: 133–143.
- Yang, Y. et al.** (2014). Quantitative trait loci identification, fine mapping and gene expression profiling for ovicidal response to whitebacked planthopper (*Sogatella furcifera* Horvath) in rice (*Oryza sativa* L.). *BMC Plant Biol.* **14**: 145.
- Young, M.M., Kester, M., and Wang, H.-G.** (2013). Sphingolipids: regulators of crosstalk between apoptosis and autophagy. *J. Lipid Res.* **54**: 5–19.
- Zvereva, A.S., Golyaev, V., Turco, S., Gubaeva, E.G., Rajeswaran, R., Schepetilnikov, M. V., Srour, O., Ryabova, L.A., Boller, T., and Pooggin, M.M.** (2016). Viral protein suppresses oxidative burst and salicylic acid-dependent autophagy and facilitates bacterial growth on virus-infected plants. *New Phytol.* **211**: 1020–1034.

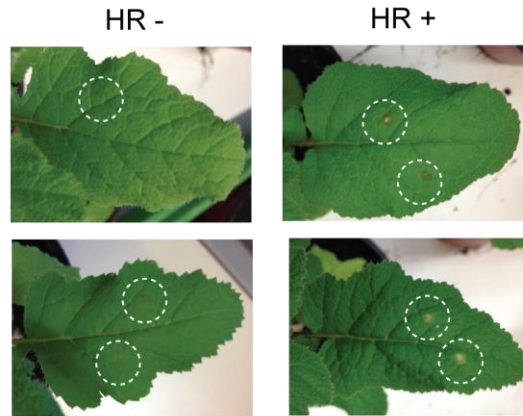
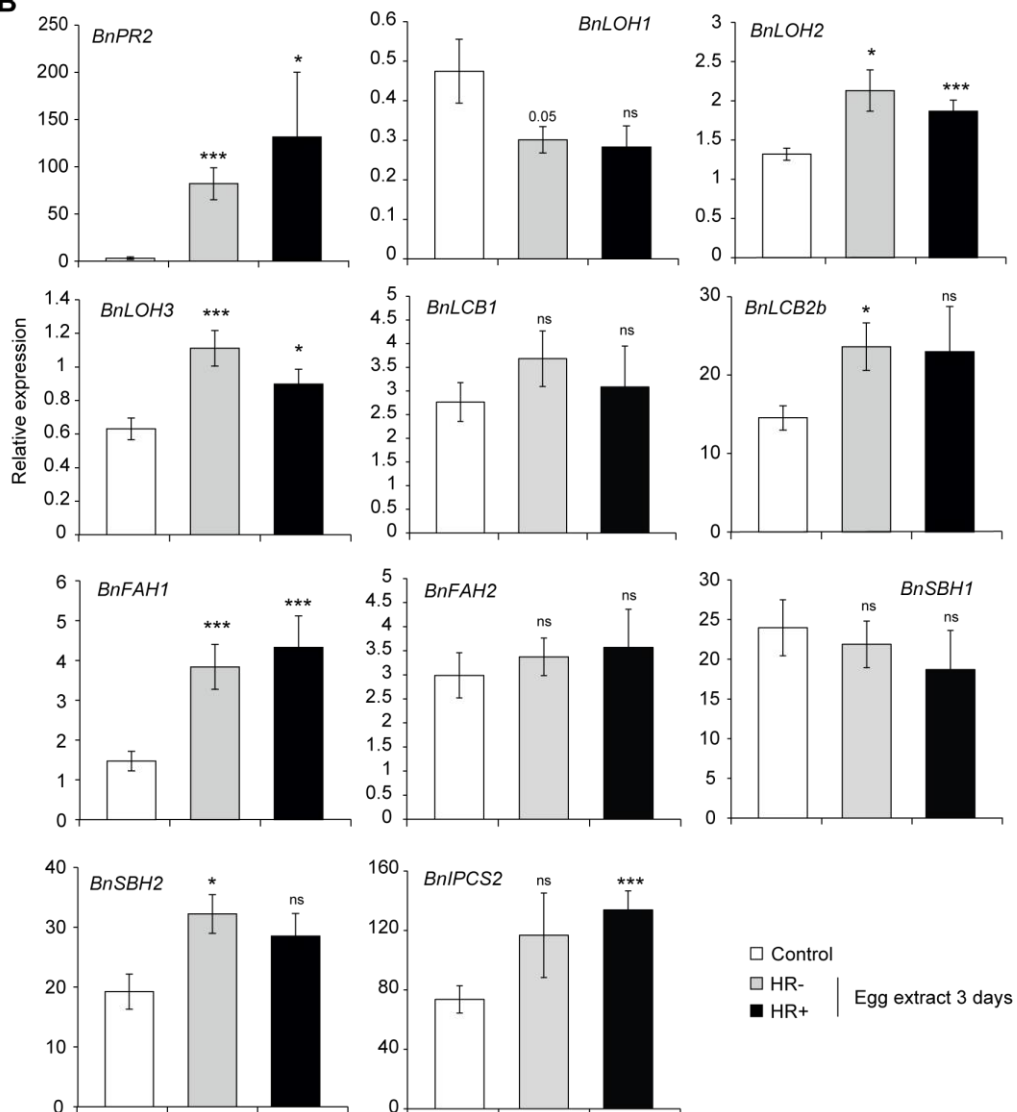
Supplementary Figures



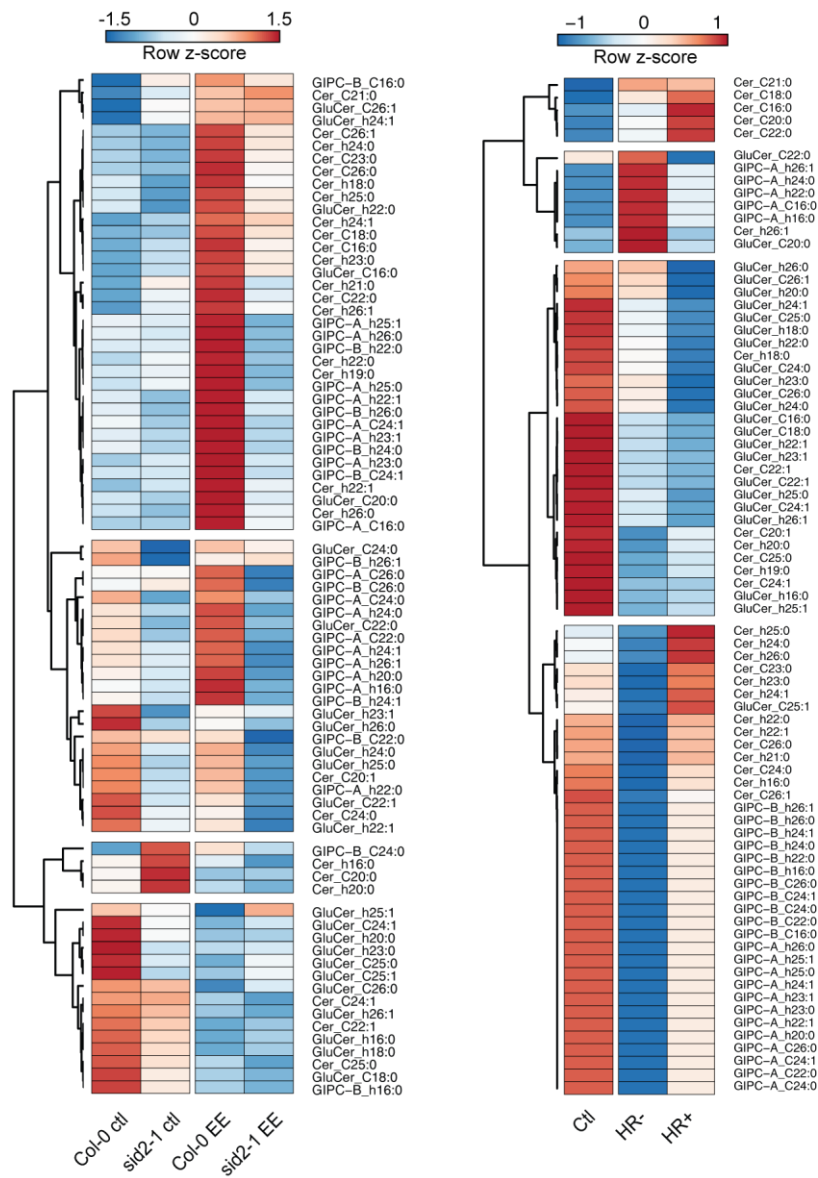
Supplementary Figure 1. Time-course expression of the *MYB30* and one of its target *FATB* after egg extract treatment was monitored by qPCR. Means \pm standard error (SEM) of three technical replicates are shown. Gene expression was normalized to the reference gene *SAND*. This experiment was repeated once with similar results.



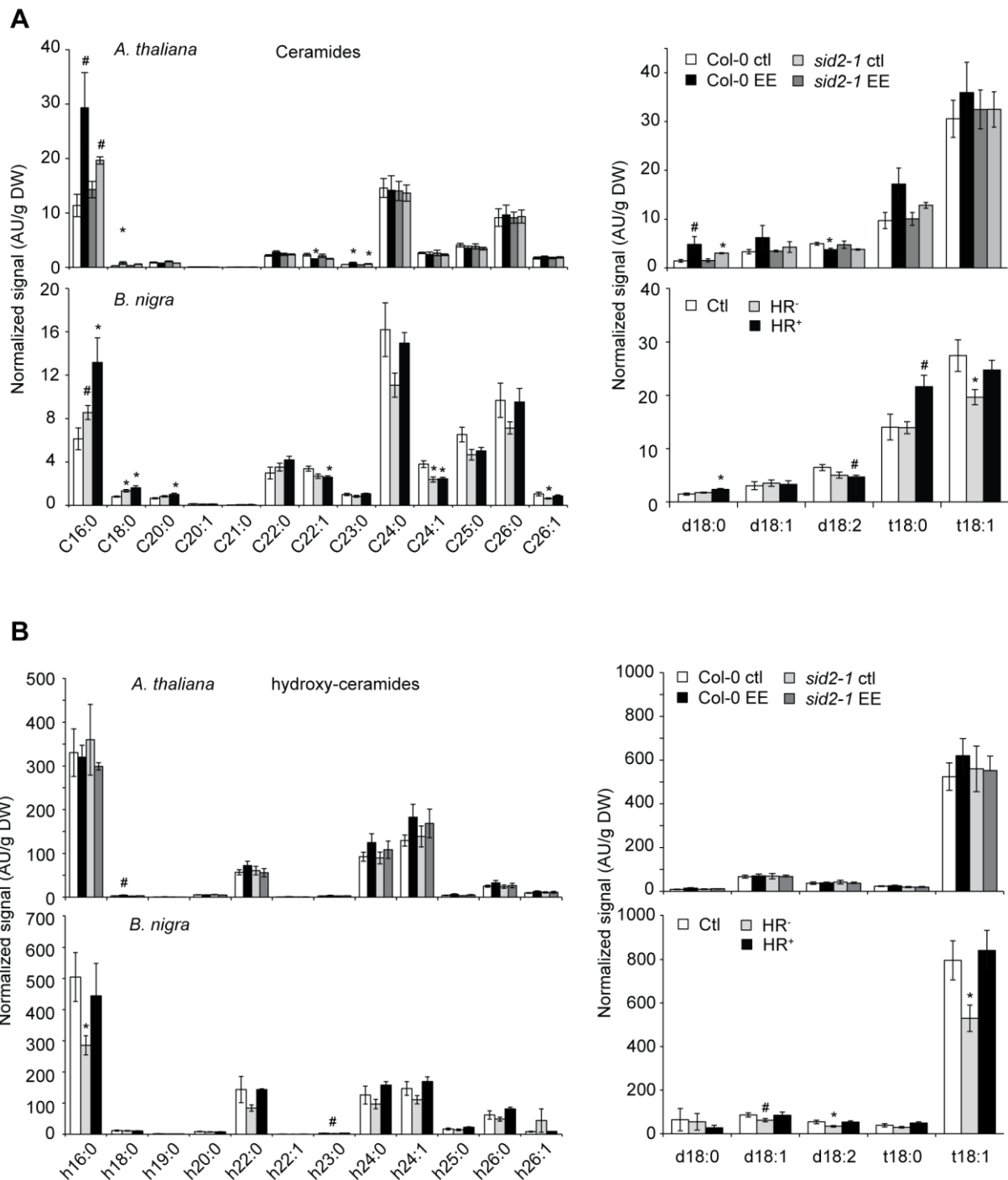
Supplementary Figure 2. Time-course expression of sphingolipid metabolism genes after egg extract treatment. Expression level of target genes was monitored by qPCR in wild-type plants after 1,2 and 3 days of egg extract treatment. Means \pm standard error (SEM) of three technical replicates are shown. Gene expression was normalized to the reference gene *SAND*. Experiments were repeated twice times with similar results. Different letters indicate significant differences at $P < 0.05$ (ANOVA, followed by Tukey HSD for multiple comparisons).

A**B**

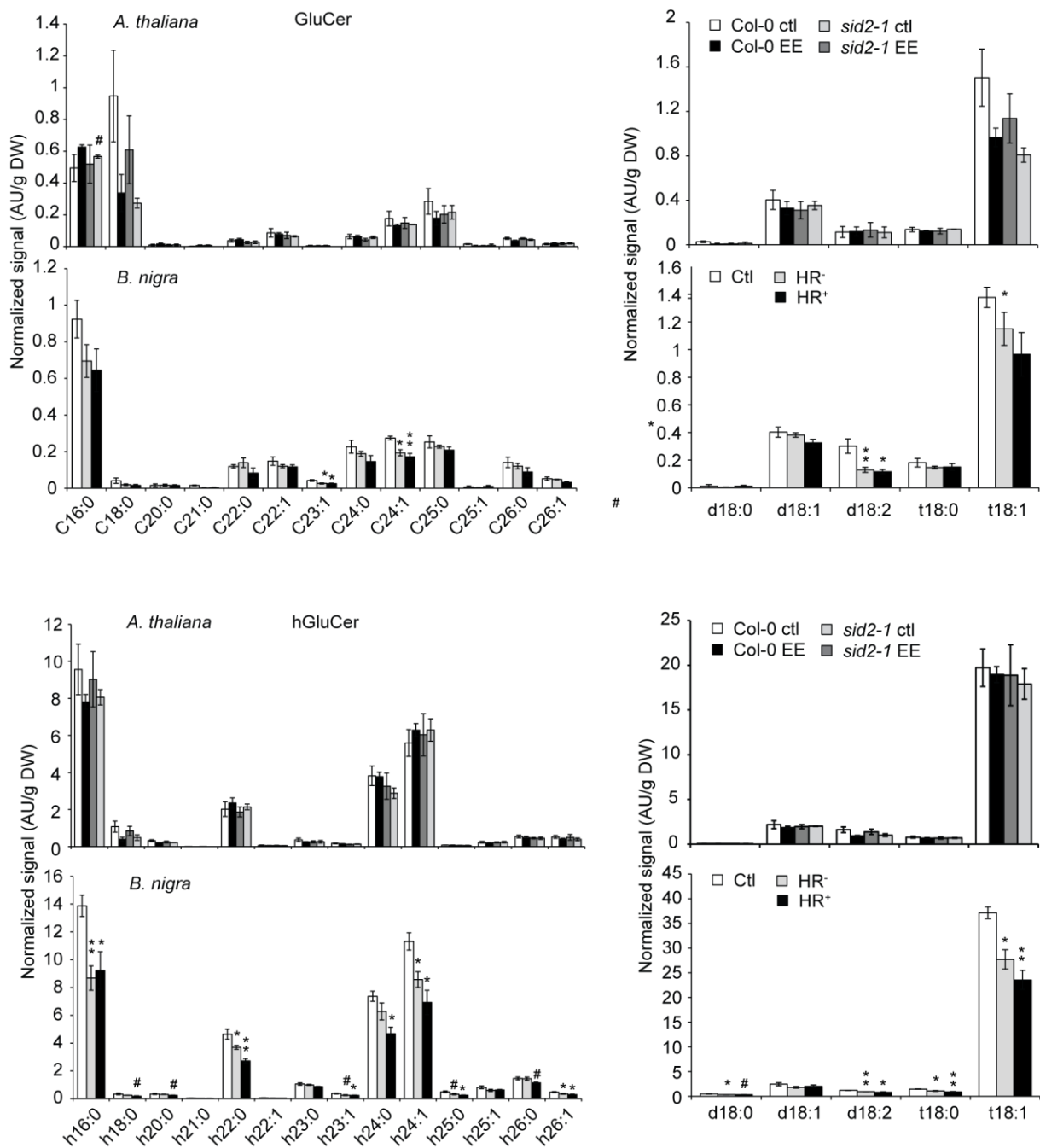
Supplementary Figure 3. A. Pictures of macroscopic HR-like symptoms triggered by *P. brassicae* egg extract after 3 days of treatment on *B. nigra*. B. Transcript levels of *B. nigra* sphingolipid genes in response to egg-extract were quantified by qPCR. Leaf samples were sorted according to the macroscopic symptoms developed (absence or presence of HR-like). Gene expression was normalized to the reference gene *BnSAND*. Means \pm standard error (SEM) of three to seven independent biological replicates ($n = 3-8$) are shown.



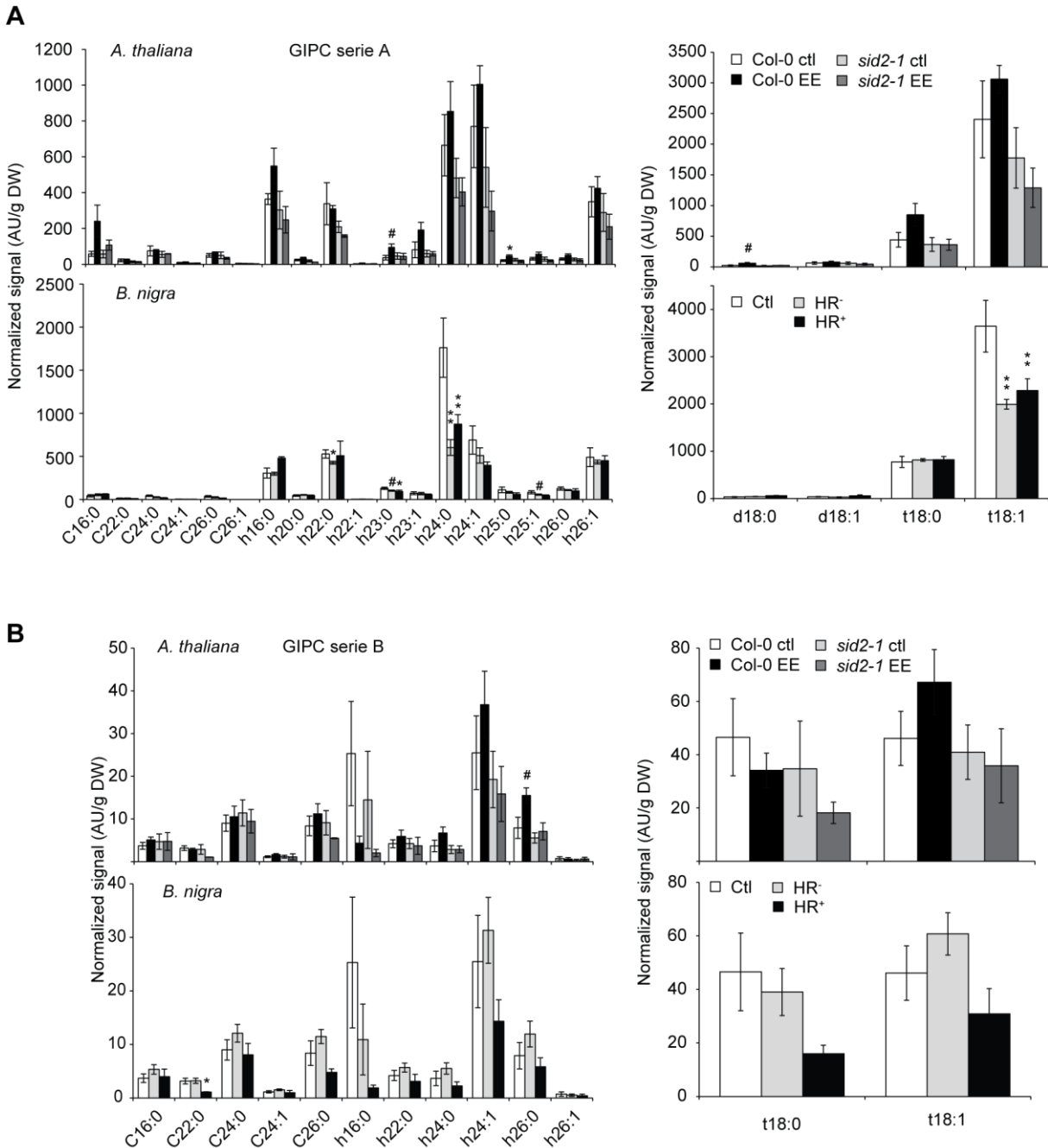
Supplementary Figure 4. Heatmaps displaying sphingolipid levels for the different lipid classes (Cer, hCer, GluCer and GIPC) depending on LCB and FA present as indicated on the right side. Sphingolipid content was quantified by LC-MS/MS as described in methods. Rows are centered and unit variance scaling is applied to rows. Both rows and columns are clustered using correlation distance and average linkage. Heatmaps were produced using the ClustVis online tool. Data indicate mean from three to five independent samples, except *sid2 EE* which consists of only two samples.



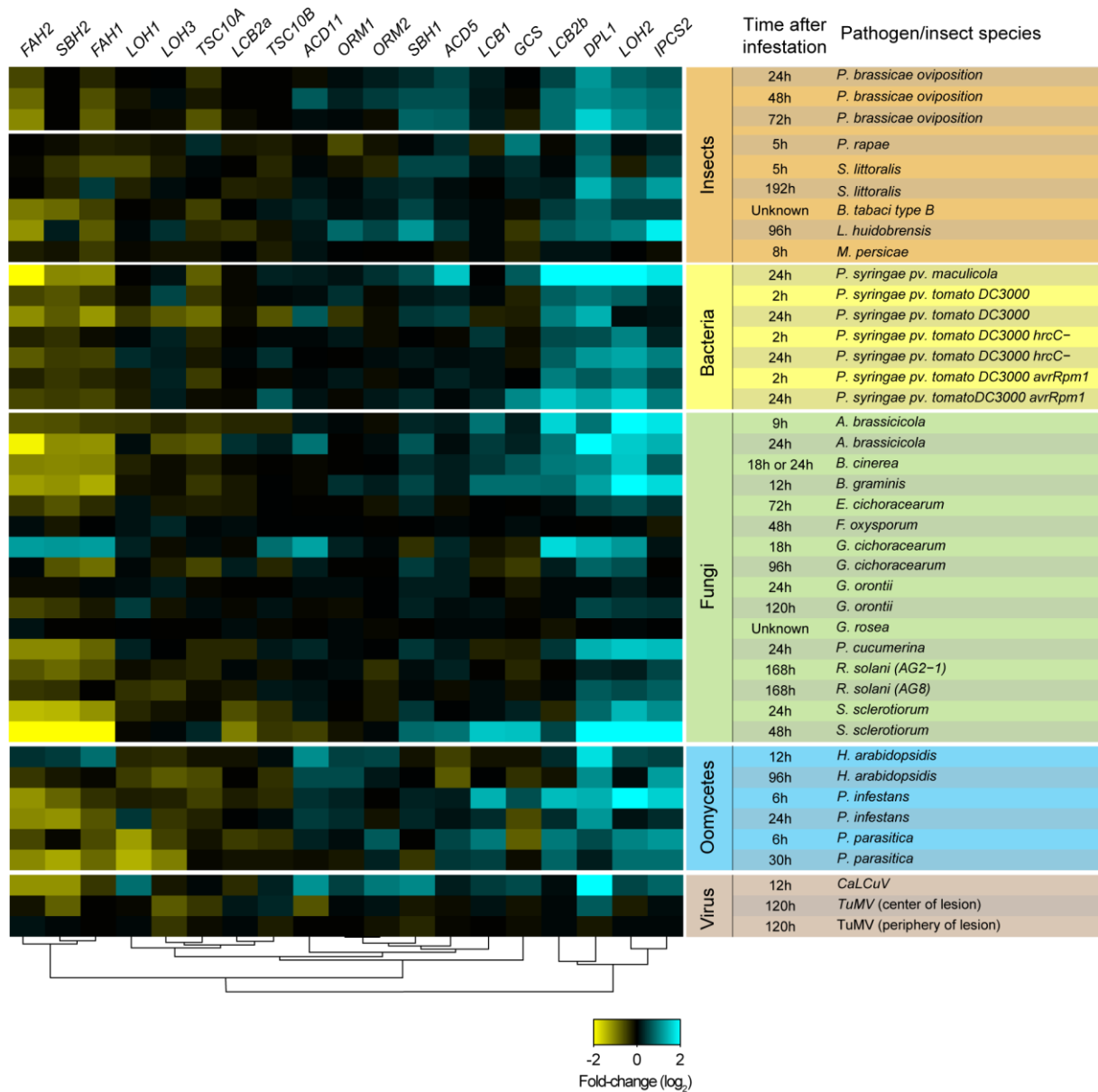
Supplementary Figure 5. Ceramide (A) and hydroxyl-ceramide (B) levels in *Arabidopsis* and *B. nigra* after 3 days of egg extract treatment depending on FA side chain (left panel) or LCB (right panel) present. Sphingolipid content was quantified by LC-MS/MS as described in methods. Data indicate mean \pm SEM from three to five independent samples, except *sid2 EE* which consists of only two samples. Statistical significance was determined using two-sample t-test between egg extract treated samples and their respective controls. #, $P < 0.1$; *, $P < 0.05$; **, $P < 0.01$.



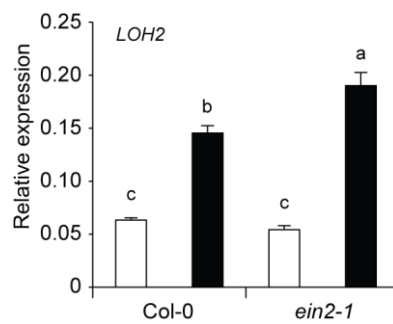
Supplementary Figure 6. GluCer (A) and hGluCer (B) levels in *Arabidopsis* and *B. nigra* after 3 days of egg extract treatment depending on FA side chain (left panel) or LCB (right panel) present. Sphingolipid content was quantified by LC-MS/MS as described in methods. Data indicate mean \pm SEM from three to five independent samples, except *sid2 EE* which consists of only two samples. Statistical significance was determined using two-sample t-test between egg extract treated samples and their respective controls. #, $P < 0.1$; *, $P < 0.05$; **, $P < 0.01$.



Supplementary Figure 7. GIPC serie A (A) and serie B (B) levels in *Arabidopsis* and *B. nigra* after 3 days of egg extract treatment depending on FA side chain (left panel) or LCB (right panel) present. Sphingolipid content was quantified by LC-MS/MS as described in methods. Data indicate mean \pm SEM from three to five independent samples, except *sid2 EE* which consists of only two samples. Statistical significance was determined using two-sample t-test between egg extract treated samples and their respective controls. #, $P < 0.1$; *, $P < 0.05$; **, $P < 0.01$.



Supplementary Figure 8. Diverse biotic stresses induce transcriptional alterations in sphingolipid metabolism. Relative expression levels of the selected sphingolipid genes in response to different attackers (insects, bacteria, fungi, oomycetes and virus) were obtained from Genevestigator. When more than two time-points were available, one early and one late time points were selected. Whole-genome expression data for *P. brassicae* oviposition or insect feeding and *P. rapae* or *S. littoralis* herbivory were obtained from previous publications (see methods for details).



Supplementary Figure 9. Involvement of ET signaling in sphingolipid gene transcription. Expression level of the the ceramide synthase *LOH2* in *ein2-1* plants after 3 days of egg extract treatment was monitored by qPCR. Means \pm standard error (SEM) of three technical replicates are shown. Gene expression was normalized to the reference gene *SAND*. Experiments were repeated twice times with similar results. Different letters indicate significant differences at $P < 0.05$ (ANOVA, followed by Tukey HSD for multiple comparisons).

Supplementary Tables

Supplementary Table 1 : List of ions used for specific compound identification and quantification. In all cases, the most abundant ion that could discriminate the compound of interest unequivocally from other co-eluting compound was chosen.

Compound	m/z
h14:0 (IS)	271
h16:0	299
h22:0	383
h24:1	73
h24:0	411
h26:0	439

Supplementary Table 2. List of all sphingolipid species targeted for LC-MS/MS analysis. LCB, Cer, GlcCer and GIPC designate distinct sphingolipid classes. d or t18:X represent di- or trihydroxy LCB, where X is the level of unsaturation. Fatty acid side chains are displayed as C (saturated) or h (2-hydroxy) FA in the following format N_{carbon}:unsaturation.

Name	Name
IS LCB_d17:1	GlCer_d18:2_h25:1
LCB_d17:0	GlCer_d18:2_h26:0
LCB_d18:0	GlCer_d18:2_h26:1
LCB_d18:1	GlCer_t18:0_C16:0
LCB_d18:2	GlCer_t18:0_C18:0
LCB_t18:0	GlCer_t18:0_C20:0
LCB_t18:1	GlCer_t18:0_C21:0
IS LCB_d17:1-P	GlCer_t18:0_C22:0
LCB_d17:0-P	GlCer_t18:0_C23:0
LCB_d18:0-P	GlCer_t18:0_C23:1
LCB_d18:1-P	GlCer_t18:0_C24:0
LCB_d18:2-P	GlCer_t18:0_C24:1
LCB_t18:0-P	GlCer_t18:0_C25:0
LCB_t18:1-P	GlCer_t18:0_C25:1
IS Cer d18:1_C17:0	GlCer_t18:0_C26:0
IS Cer d18:1_h17:0	GlCer_t18:0_C26:1
Cer d18:0_C16:0	GlCer_t18:0_h16:0
Cer d18:0_C17:0	GlCer_t18:0_h18:0
Cer d18:0_C18:0	GlCer_t18:0_h20:0
Cer d18:0_C19:0	GlCer_t18:0_h21:0
Cer d18:0_C20:0	GlCer_t18:0_h22:0
Cer d18:0_C20:1	GlCer_t18:0_h22:1
Cer d18:0_C21:0	GlCer_t18:0_h23:0
Cer d18:0_C22:0	GlCer_t18:0_h23:1
Cer d18:0_C22:1	GlCer_t18:0_h24:0
Cer d18:0_C23:0	GlCer_t18:0_h24:1
Cer d18:0_C24:0	GlCer_t18:0_h25:0
Cer d18:0_C24:1	GlCer_t18:0_h25:1
Cer d18:0_C25:0	GlCer_t18:0_h26:0
Cer d18:0_C26:0	GlCer_t18:0_h26:1
Cer d18:0_C26:1	GlCer_t18:1_C16:0
Cer d18:0_h16:0	GlCer_t18:1_C18:0
Cer d18:0_h17:0	GlCer_t18:1_C20:0
Cer d18:0_h18:0	GlCer_t18:1_C21:0
Cer d18:0_h19:0	GlCer_t18:1_C21:1
Cer d18:0_h20:0	GlCer_t18:1_C22:0
Cer d18:0_h20:1	GlCer_t18:1_C22:1
Cer d18:0_h21:0	GlCer_t18:1_C23:0
Cer d18:0_h22:0	GlCer_t18:1_C23:1

Cer d18:0_h22:1	GI Cer_t18:1_C24:0
Cer d18:0_h23:0	GI Cer_t18:1_C24:1
Cer d18:0_h24:0	GI Cer_t18:1_C25:0
Cer d18:0_h24:1	GI Cer_t18:1_C25:1
Cer d18:0_h25:0	GI Cer_t18:1_C26:0
Cer d18:0_h26:0	GI Cer_t18:1_C26:1
Cer d18:0_h26:1	GI Cer_t18:1_h16:0
Cer d18:1_C16:0	GI Cer_t18:1_h18:0
Cer d18:1_C18:0	GI Cer_t18:1_h20:0
Cer d18:1_C19:0	GI Cer_t18:1_h21:0
Cer d18:1_C20:0	GI Cer_t18:1_h22:0
Cer d18:1_C20:1	GI Cer_t18:1_h22:1
Cer d18:1_C21:0	GI Cer_t18:1_h23:0
Cer d18:1_C22:0	GI Cer_t18:1_h23:1
Cer d18:1_C22:1	GI Cer_t18:1_h24:0
Cer d18:1_C23:0	GI Cer_t18:1_h24:1
Cer d18:1_C24:0	GI Cer_t18:1_h25:0
Cer d18:1_C24:1	GI Cer_t18:1_h25:1
Cer d18:1_C25:0	GI Cer_t18:1_h26:0
Cer d18:1_C26:0	GI Cer_t18:1_h26:1
Cer d18:1_C26:1	IS_GM1
Cer d18:1_h16:0	GIPC-A d18:0_h16:0
Cer d18:1_h18:0	GIPC-A d18:1_h16:0
Cer d18:1_h19:0	GIPC-A t18:0_C16:0
Cer d18:1_h20:0	GIPC-A t18:0_h16:0
Cer d18:1_h20:1	GIPC-A t18:0_h20:0
Cer d18:1_h21:0	GIPC-A t18:0_h22:0
Cer d18:1_h22:0	GIPC-A t18:0_h22:1
Cer d18:1_h22:1	GIPC-A t18:0_h23:0
Cer d18:1_h23:0	GIPC-A t18:0_h23:1
Cer d18:1_h24:0	GIPC-A t18:0_h24:0
Cer d18:1_h24:1	GIPC-A t18:0_h24:1
Cer d18:1_h25:0	GIPC-A t18:0_h25:0
Cer d18:1_h26:0	GIPC-A t18:0_h25:1
Cer d18:1_h26:1	GIPC-A t18:0_h26:0
Cer d18:2_C16:0	GIPC-A t18:0_h26:1
Cer d18:2_C17:0	GIPC-A t18:1_C16:0
Cer d18:2_C18:0	GIPC-A t18:1_C22:0
Cer d18:2_C19:0	GIPC-A t18:1_C24:0
Cer d18:2_C20:0	GIPC-A t18:1_C24:1
Cer d18:2_C20:1	GIPC-A t18:1_C26:0
Cer d18:2_C21:0	GIPC-A t18:1_C26:1
Cer d18:2_C22:0	GIPC-A t18:1_h16:0
Cer d18:2_C22:1	GIPC-A t18:1_h20:0
Cer d18:2_C23:0	GIPC-A t18:1_h22:0
Cer d18:2_C24:0	GIPC-A t18:1_h22:1
Cer d18:2_C24:1	GIPC-A t18:1_h23:0
Cer d18:2_C25:0	GIPC-A t18:1_h23:1

Cer d18:2_C26:0	GIPC-A t18:1_h24:0
Cer d18:2_C26:1	GIPC-A t18:1_h24:1
Cer d18:2_h16:0	GIPC-A t18:1_h25:0
Cer d18:2_h17:0	GIPC-A t18:1_h25:1
Cer d18:2_h18:0	GIPC-A t18:1_h26:0
Cer d18:2_h19:0	GIPC-A t18:1_h26:1
Cer d18:2_h20:0	GIPC-A-NH2 d18:0_h16:0
Cer d18:2_h20:1	GIPC-A-NH2 d18:1_h16:0
Cer d18:2_h21:0	GIPC-A-NH2 t18:0_C16:0
Cer d18:2_h22:0	GIPC-A-NH2 t18:0_h16:0
Cer d18:2_h22:1	GIPC-A-NH2 t18:0_h20:0
Cer d18:2_h23:0	GIPC-A-NH2 t18:0_h22:0
Cer d18:2_h24:0	GIPC-A-NH2 t18:0_h22:1
Cer d18:2_h24:1	GIPC-A-NH2 t18:0_h23:0
Cer d18:2_h25:0	GIPC-A-NH2 t18:0_h23:1
Cer d18:2_h26:0	GIPC-A-NH2 t18:0_h24:0
Cer d18:2_h26:1	GIPC-A-NH2 t18:0_h24:1
Cer t18:0_C16:0	GIPC-A-NH2 t18:0_h25:0
Cer t18:0_C17:0	GIPC-A-NH2 t18:0_h25:1
Cer t18:0_C18:0	GIPC-A-NH2 t18:0_h26:0
Cer t18:0_C19:0	GIPC-A-NH2 t18:0_h26:1
Cer t18:0_C20:0	GIPC-A-NH2 t18:1_C16:0
Cer t18:0_C20:1	GIPC-A-NH2 t18:1_C22:0
Cer t18:0_C21:0	GIPC-A-NH2 t18:1_C24:0
Cer t18:0_C22:0	GIPC-A-NH2 t18:1_C24:1
Cer t18:0_C22:1	GIPC-A-NH2 t18:1_C26:0
Cer t18:0_C23:0	GIPC-A-NH2 t18:1_C26:1
Cer t18:0_C24:0	GIPC-A-NH2 t18:1_h16:0
Cer t18:0_C24:1	GIPC-A-NH2 t18:1_h20:0
Cer t18:0_C25:0	GIPC-A-NH2 t18:1_h22:0
Cer t18:0_C26:0	GIPC-A-NH2 t18:1_h22:1
Cer t18:0_C26:1	GIPC-A-NH2 t18:1_h23:0
Cer t18:0_h16:0	GIPC-A-NH2 t18:1_h23:1
Cer t18:0_h17:0	GIPC-A-NH2 t18:1_h24:0
Cer t18:0_h18:0	GIPC-A-NH2 t18:1_h24:1
Cer t18:0_h19:0	GIPC-A-NH2 t18:1_h25:0
Cer t18:0_h20:0	GIPC-A-NH2 t18:1_h25:1
Cer t18:0_h20:1	GIPC-A-NH2 t18:1_h26:0
Cer t18:0_h21:0	GIPC-A-NH2 t18:1_h26:1
Cer t18:0_h22:0	GIPC-A-NHAc d18:0_h16:0
Cer t18:0_h22:1	GIPC-A-NHAc d18:1_h16:0
Cer t18:0_h23:0	GIPC-A-NHAc t18:0_C16:0
Cer t18:0_h24:0	GIPC-A-NHAc t18:0_h16:0
Cer t18:0_h24:1	GIPC-A-NHAc t18:0_h20:0
Cer t18:0_h25:0	GIPC-A-NHAc t18:0_h22:0
Cer t18:0_h26:0	GIPC-A-NHAc t18:0_h22:1
Cer t18:0_h26:1	GIPC-A-NHAc t18:0_h23:0
Cer t18:1_C16:0	GIPC-A-NHAc t18:0_h23:1

Cer t18:1_C17:0	GIPC-A-NHAc t18:0_h24:0
Cer t18:1_C18:0	GIPC-A-NHAc t18:0_h24:1
Cer t18:1_C19:0	GIPC-A-NHAc t18:0_h25:0
Cer t18:1_C20:0	GIPC-A-NHAc t18:0_h25:1
Cer t18:1_C20:1	GIPC-A-NHAc t18:0_h26:0
Cer t18:1_C21:0	GIPC-A-NHAc t18:0_h26:1
Cer t18:1_C22:0	GIPC-A-NHAc t18:1_C16:0
Cer t18:1_C22:1	GIPC-A-NHAc t18:1_C22:0
Cer t18:1_C23:0	GIPC-A-NHAc t18:1_C24:0
Cer t18:1_C24:0	GIPC-A-NHAc t18:1_C24:1
Cer t18:1_C24:1	GIPC-A-NHAc t18:1_C26:0
Cer t18:1_C25:0	GIPC-A-NHAc t18:1_C26:1
Cer t18:1_C26:0	GIPC-A-NHAc t18:1_h16:0
Cer t18:1_C26:1	GIPC-A-NHAc t18:1_h20:0
Cer t18:1_h16:0	GIPC-A-NHAc t18:1_h22:0
Cer t18:1_h17:0	GIPC-A-NHAc t18:1_h22:1
Cer t18:1_h18:0	GIPC-A-NHAc t18:1_h23:0
Cer t18:1_h19:0	GIPC-A-NHAc t18:1_h23:1
Cer t18:1_h20:0	GIPC-A-NHAc t18:1_h24:0
Cer t18:1_h20:1	GIPC-A-NHAc t18:1_h24:1
Cer t18:1_h21:0	GIPC-A-NHAc t18:1_h25:0
Cer t18:1_h22:0	GIPC-A-NHAc t18:1_h25:1
Cer t18:1_h22:1	GIPC-A-NHAc t18:1_h26:0
Cer t18:1_h23:0	GIPC-A-NHAc t18:1_h26:1
Cer t18:1_h24:0	GIPC-B d18:0_h16:0
Cer t18:1_h24:1	GIPC-B d18:1_h16:0
Cer t18:1_h25:0	GIPC-B t18:0_C16:0
Cer t18:1_h26:0	GIPC-B t18:0_C22:0
Cer t18:1_h26:1	GIPC-B t18:0_C24:0
IS GluCer d18:1/c12:0	GIPC-B t18:0_C26:0
GlCer_d18:0_C16:0	GIPC-B t18:0_h16:0
GlCer_d18:0_C18:0	GIPC-B t18:0_h22:0
GlCer_d18:0_C20:0	GIPC-B t18:0_h24:0
GlCer_d18:0_C21:0	GIPC-B t18:0_h24:1
GlCer_d18:0_C22:0	GIPC-B t18:0_h25:0
GlCer_d18:0_C22:1	GIPC-B t18:0_h26:0
GlCer_d18:0_C23:0	GIPC-B t18:1_C16:0
GlCer_d18:0_C23:1	GIPC-B t18:1_C22:0
GlCer_d18:0_C24:0	GIPC-B t18:1_C24:0
GlCer_d18:0_C24:1	GIPC-B t18:1_C24:1
GlCer_d18:0_C25:0	GIPC-B t18:1_C26:0
GlCer_d18:0_C25:1	GIPC-B t18:1_C26:1
GlCer_d18:0_C26:0	GIPC-B t18:1_h16:0
GlCer_d18:0_C26:1	GIPC-B t18:1_h22:0
GlCer_d18:0_h16:0	GIPC-B t18:1_h24:0
GlCer_d18:0_h18:0	GIPC-B t18:1_h24:1
GlCer_d18:0_h20:0	GIPC-B t18:1_h25:0
GlCer_d18:0_h21:0	GIPC-B t18:1_h25:1

GlCer_d18:0_h22:0	GIPC-B t18:1_h26:0
GlCer_d18:0_h22:1	GIPC-B t18:1_h26:1
GlCer_d18:0_h23:0	GIPC-B-NH2 d18:0_h16:0
GlCer_d18:0_h23:1	GIPC-B-NH2 d18:1_h16:0
GlCer_d18:0_h24:0	GIPC-B-NH2 t18:0_C16:0
GlCer_d18:0_h24:1	GIPC-B-NH2 t18:0_C22:0
GlCer_d18:0_h25:0	GIPC-B-NH2 t18:0_C24:0
GlCer_d18:0_h25:1	GIPC-B-NH2 t18:0_C26:0
GlCer_d18:0_h26:0	GIPC-B-NH2 t18:0_h16:0
GlCer_d18:0_h26:1	GIPC-B-NH2 t18:0_h20:0
GlCer_d18:1_C16:0	GIPC-B-NH2 t18:0_h22:0
GlCer_d18:1_C18:0	GIPC-B-NH2 t18:0_h22:1
GlCer_d18:1_C20:0	GIPC-B-NH2 t18:0_h24:0
GlCer_d18:1_C21:0	GIPC-B-NH2 t18:0_h24:1
GlCer_d18:1_C22:0	GIPC-B-NH2 t18:0_h25:0
GlCer_d18:1_C22:1	GIPC-B-NH2 t18:0_h25:1
GlCer_d18:1_C23:0	GIPC-B-NH2 t18:0_h26:0
GlCer_d18:1_C23:1	GIPC-B-NH2 t18:0_h26:1
GlCer_d18:1_C24:0	GIPC-B-NH2 t18:1_C16:0
GlCer_d18:1_C24:1	GIPC-B-NH2 t18:1_C22:0
GlCer_d18:1_C25:0	GIPC-B-NH2 t18:1_C24:0
GlCer_d18:1_C25:1	GIPC-B-NH2 t18:1_C24:1
GlCer_d18:1_C26:0	GIPC-B-NH2 t18:1_C26:0
GlCer_d18:1_C26:1	GIPC-B-NH2 t18:1_C26:1
GlCer_d18:1_h16:0	GIPC-B-NH2 t18:1_h16:0
GlCer_d18:1_h18:0	GIPC-B-NH2 t18:1_h20:0
GlCer_d18:1_h20:0	GIPC-B-NH2 t18:1_h22:0
GlCer_d18:1_h21:0	GIPC-B-NH2 t18:1_h22:1
GlCer_d18:1_h22:0	GIPC-B-NH2 t18:1_h24:0
GlCer_d18:1_h22:1	GIPC-B-NH2 t18:1_h24:1
GlCer_d18:1_h23:0	GIPC-B-NH2 t18:1_h25:0
GlCer_d18:1_h23:1	GIPC-B-NH2 t18:1_h25:1
GlCer_d18:1_h24:0	GIPC-B-NH2 t18:1_h26:0
GlCer_d18:1_h24:1	GIPC-B-NH2 t18:1_h26:1
GlCer_d18:1_h25:0	GIPC-B-NHAc d18:0_h16:0
GlCer_d18:1_h25:1	GIPC-B-NHAc d18:1_h16:0
GlCer_d18:1_h26:0	GIPC-B-NHAc t18:0_C16:0
GlCer_d18:1_h26:1	GIPC-B-NHAc t18:0_C22:0
GlCer_d18:2_C16:0	GIPC-B-NHAc t18:0_C24:0
GlCer_d18:2_C18:0	GIPC-B-NHAc t18:0_C26:0
GlCer_d18:2_C20:0	GIPC-B-NHAc t18:0_h16:0
GlCer_d18:2_C21:0	GIPC-B-NHAc t18:0_h22:0
GlCer_d18:2_C22:0	GIPC-B-NHAc t18:0_h24:0
GlCer_d18:2_C22:1	GIPC-B-NHAc t18:0_h24:1
GlCer_d18:2_C23:0	GIPC-B-NHAc t18:0_h25:0
GlCer_d18:2_C23:1	GIPC-B-NHAc t18:0_h25:1
GlCer_d18:2_C24:0	GIPC-B-NHAc t18:0_h26:0
GlCer_d18:2_C24:1	GIPC-B-NHAc t18:0_h26:1

GlCer_d18:2_C25:0	GIPC-B-NHAc t18:1_C16:0
GlCer_d18:2_C25:1	GIPC-B-NHAc t18:1_C22:0
GlCer_d18:2_C26:0	GIPC-B-NHAc t18:1_C24:0
GlCer_d18:2_C26:1	GIPC-B-NHAc t18:1_C24:1
GlCer_d18:2_h16:0	GIPC-B-NHAc t18:1_C26:0
GlCer_d18:2_h18:0	GIPC-B-NHAc t18:1_C26:1
GlCer_d18:2_h20:0	GIPC-B-NHAc t18:1_h16:0
GlCer_d18:2_h21:0	GIPC-B-NHAc t18:1_h22:0
GlCer_d18:2_h22:0	GIPC-B-NHAc t18:1_h24:0
GlCer_d18:2_h22:1	GIPC-B-NHAc t18:1_h24:1
GlCer_d18:2_h23:0	GIPC-B-NHAc t18:1_h25:0
GlCer_d18:2_h23:1	GIPC-B-NHAc t18:1_h25:1
GlCer_d18:2_h24:0	GIPC-B-NHAc t18:1_h26:0
GlCer_d18:2_h24:1	GIPC-B-NHAc t18:1_h26:1

Supplementary table 3. List of primers used for quantitative PCR experiments.

Gene name	Gene ID	Primer ID	Sequence (3'-5')	Reference
SAND	At2g28390	SAND_fw	AACTCTATGCAGCATTTGATCCACT	
		SAND_rev	TGATTGCATATCTTTATCGCCATC	
PR1	At2g14610	PR1_fw	GTGGGTTAGCGAGAAGGCTA	
		PR1_rev	ACTTTGGCACATCCGAGTCT	
SAG13	At2g29350	SAG13_fw	GTCGTGCATGTCAATGTTGG	
		SAG13_rev	CCAAGGACAAACAGAGTTCCG	
MYB30	At3g28910	MYB30_fw	CAACGTCTTCTCTGCTGAA	Kosma et al 2009
		MYB30_rev	GTCTTCGGCGAGTTTTTCAC	
FATB	At1g08510	FATB_fw	CGTCGTCATTCTTTCCTGTA	Raffaele et al. 2008
		FATB_rev	AACCAACCTTTTTCCCATTA	
LOH1	AT3G25540	LOH1_fw	TCCGATTCTGAAAGCGATGATG	Wu et al. 2015
		LOH1_rev	ATTCCTAGTCTCCGTGTGGTT	
LOH2	AT3G19260	LOH2_fw	GGATTCTTCTTCTTGAGGCTTGTC	Wu et al. 2015
		LOH2_rev	CCGAGTAGCAGCATCATTCAAT	
LOH3	AT1G13580	LOH3_fw	CTCTCCTATATTGCTTGCTTGTCT	Wu et al. 2015
		LOH3_rev	AATCAGTCTTCGTCTCATCTTC	
LCB1	AT4G36480	LCB1_fw	CTTCTTAAAGCGTGGAGTCA	Wu et al. 2015
		LCB1_rev	TCTGCGGATTCTGTTGTCTAC	
LCB2a	AT5G23670	LCB2a_fw	TGGCTATATTGCTGGATCTAAGGA	Wu et al. 2015
		LCB2a_rev	GTGCGGAAGGAGTTGGTATG	
LCB2b	AT3G48780	LCB2b_fw	CAGGTGTTATCGCAGTCATCTT	Wu et al. 2015
		LCB2b_rev	GCACATTCGTGGTCTGGAAG	
ACD5	At5g51290	ACD5_fw	GTGTGGAATTTGGACGGAGAG	Bi et al. 2014
		ACD5_rev	CAGATGCGAACAGAGGTATAAGG	
FAH1	AT2G34770	FAH1_fw	ATGTGATGTACGATGTCACTC	This work
		FAH1_rev	CCAAATCCTTTGTCTGAATCC	
FAH2	AT4G20870	FAH2_fw	CAGCAACAGCTATTCTCTTGG	This work
		FAH2_rev	CTAAAGTGATGATTGAGGTGG	
IPCS2	AT2G37940	IPCS2_fw	CTGTGTTGCTCCCAGTAATC	This work
		IPCS2_rev	TGTCAATCTTCCCCTTACC	
GCS	AT2G19880	GCS_fw	TCAATCCATAAACTGGTCTGG	This work
		GCS_rev	TGAAGCTTTCTGAGGAGCTC	
SBH1	AT1G69640	SBH1_fw	CCACGATCAAAACCGTGGAC	This work
		SBH1_rev	TTTGAATCTTTAGTCGGGCG	
SBH2	AT1G14290	SBH2_fw	ATGATCATTGTGGAATGATGGC	This work
		SBH2_rev	CTCCATTGGCTCTTTTCTCC	
BnSAND	BniB003645	BnSAND_fw_2	TGCTAGGAGGGACTGATGC	Bonnet et al. 2017
		BnSAND_rev_2	AACCTTGTGCTCGACATTAG	
BnPR2	BniB029818	BnPR2_fw	GTGATAGATTTCTTGGTAAGCA	Bonnet et al. 2017
		BnPR2_rev	CACAATCTCCAAAAATTCGCC	
BnLOH1	BniB046986	BnLOH1_fw_1	TATCAGATTATAATGACTGTGG	This work
		BnLOH1_rev_1	AGCACAAGCAAGCAGAACAAG	
BnLOH2	BniB021107	BnLOH2_fw	GGCTTTTGTAGTACTGTTCTG	This work
		BnLOH2_rev	TCTTGATTAGGCCAACCGTG	
BnLOH3	BniB004139	BnLOH3_fw	TTCTCTATTGCTTGCTTGTCT	This work
		BnLOH3_rev	AACATCTTCACTAAGCTTGCC	
BnLCB1	BniB021240	BnLCB1_fw	AGGGGATGTGCTAACAAGC	This work
		BnLCB1_rev	TTCTTAGAGCTCACAAACCAAC	
BnLCB2b	BniB033113	BnLCB2b_fw	GTGGCAGTTGTGGTTGTTGG	This work
		BnLCB2b_rev	TTGATTCCGGTGAGGTCACC	
BnFAH1	BniB033988	BnFAH1_fw	TACGTGATGTACGATTAATCTC	This work
		BnFAH1_rev	CCAAATCCCTTGTCTTGAATCC	
BnFAH2	BniB037392	BnFAH2_fw	CGGTTTAATAGTTGCCTTTGG	This work
		BnFAH2_rev	CGTCTTGTGGGTGCTTGTGA	
BnIPCS2	BniB016748	BnIPCS2_fw	TTGGTTGGCTCACTGCTTTC	This work
		BnIPCS2_rev	GATTACCGGTAGCAACACCG	
BnSBH1	BniB037186	BnSBH1_fw	CCACGATCAAGACTGTGGAT	This work
		BnSBH1_rev	CTTTAAACTCTTGTAGTAGGACG	
BnSBH2	BniB033050	BnSBH2_fw	ATGATCACTGTGGAATGATGGC	This work
		BnSBH2_rev	CGAGAATCCTATCCACATG	

Chapter 2

***GLUTAMATE RECEPTOR-LIKE 2.7* is associated with insect egg-induced responses and is under balancing selection.**

Raphaël Groux, Gioia Lenzoni, Edward E. Farmer, Philippe Reymond.
Department of Plant Molecular Biology, University of Lausanne, 1015 Lausanne, Switzerland

Abstract

Plants from the *Brassicaceae* family induce a defense response that culminates in cell death (HR-like) upon the perception of insect eggs. While this response can subsequently impact egg survival, the molecular mechanisms are poorly understood. Here we use a genome-wide association (GWA) mapping approach to dissect the genetic structure of HR-like responses and SA accumulation in *Arabidopsis thaliana*. GWA mapping identified the putative amino-acid gated calcium channel *GLUTAMATE-LIKE RECEPTOR 2.7* as a major locus controlling these responses. Analysis of natural polymorphisms shows that two major haplotypes segregate at the species-wide level and suggests that balancing selection acts at this locus. Furthermore, accessions possessing the haplotype associated with low HR-like do not produce *GLR2.7* transcripts. However, disruption of *GLR2.7* in Col-0 background did not affect egg-induced defenses. Consistently, we observe that another uncharacterized locus additively regulates HR-like in the mapping panel, suggesting that it may compensate for the loss of *GLR2.7*. These results provide a further step in the elucidation of the mechanisms controlling HR-like in *Arabidopsis*.

Introduction

Plant responses to insects have received a great amount of interest in the past decades, yet the understanding of how plants respond to the perception of insect eggs is still lacking. Diverse plant responses to insect eggs have been described (Fatouros et al., 2016) and include morphological changes of plant tissues, such as the formation of cell death in *Brassica nigra* (Shapiro and DeVay, 1987) and *Phaseolus vulgaris* (Garza et al., 2001) or neoplasms in *Physalis sp.* (Petzold-Maxwell et al., 2011) and these responses usually correlate with a decreased egg survival (Fatouros et al., 2016). Unfortunately, in most cases the underlying genetic basis of such trait is unknown. The current model of plant immunity relies on the existence of membrane or cytoplasmic receptors that recognize specific molecules indicative of pathogen, herbivore or damage presence (Jones and Dangl, 2006; Tang et al., 2017). Downstream, phytohormonal jasmonic acid (JA) or salicylic acid (SA) pathways, depending on whether a chewing insect or a pathogen is perceived, further translate danger signals into cellular outputs (Pieterse et al., 2012; Erb and Reymond, 2019). Even though defenses against larvae of the specialist herbivore *Pieris brassicae* are dependent on a functional JA pathway (Erb and Reymond, 2019; Schweizer et al., 2013), it was recently found that eggs of the same species induce a transcriptional reprogramming similar to pathogen perception and trigger SA accumulation (Little et al., 2007; Bruessow et al., 2010; Lortzing et al., 2019; Gouhier-Darimont et al., 2013). In plants of the *Brassicales* order, this response further culminates into localized cell death underneath eggs or at the site of egg-extract application, a process named hypersensitive-like response (HR-like) based on the resemblance to the response triggered by adapted pathogens (Reymond, 2013; Hilker and Fatouros, 2015; Fatouros et al., 2016). Several studies in *Brassicaceae* have reported that HR-like symptoms induced by eggs from *Pieridae* species can result in egg desiccation, increased egg mortality, higher egg parasitism, and lower subsequent larval performance (Shapiro and DeVay, 1987; Fatouros et al., 2014; Pashalidou et al., 2013). Moreover, a synergistic effect of both direct and indirect defenses against *Pieris* eggs was observed in the black mustard *Brassica nigra* (Fatouros et al., 2014). These results show that HR-like symptoms can act as a direct defense response against insect eggs, therefore implying that appropriate immunity to different insect developmental stages can rely on contrasting mechanisms.

The genetics of egg-triggered immunity in different species is still poorly understood, but the accumulation of reactive oxygen species (ROS) together with SA was frequently observed in plants expressing HR-like (Little et al., 2007; Geuss et al., 2017; Bittner et al.,

2017; Bruessow et al., 2010; Bonnet et al., 2017). Studies with the model plant *Arabidopsis thaliana* have unveiled some aspects of the molecular basis of this response. *Arabidopsis* plants treated with *P. brassicae* egg extract displayed elevated PTI (pathogen-triggered immunity) marker genes as early as 3h after treatment, demonstrating that plants are able to perceive egg presence in a timely manner (Gouhier-Darimont et al., 2013). Additionally, SA-dependent signaling and biosynthesis were found to be required for cell death induction, similar to bacterial-induced HR (Balint-Kurti, 2019). Attempts to characterize so-called egg-associated molecular patterns (EAMPs) identified internal egg lipids associated with HR-like and other responses triggered by *P. brassicae* eggs (Little et al., 2007; Gouhier-Darimont et al., 2013, 2019). In addition, benzyl cyanide (BC), which is found in accessory reproductive glands of *P. brassicae*, induces leaf surface changes that arrest parasitoid wasps in *Brassica oleracea* and *Brassica nigra* (Fatouros et al., 2008). However, transcriptional responses triggered by BC and eggs only marginally intersect in either species (Fatouros et al., 2008, 2015). Additionally, while BC was found to induce cell death, this was not linked with an induction of *PR1* expression, (Fatouros et al., 2015), suggesting that the compound or its solvent (EtOH 70%) may be toxic and causes cell injury. Recently, several studies showed an involvement of the lectin receptor-like kinase LecRK-I.8 in egg-induced responses (Gouhier-Darimont et al., 2013, 2019; Wang et al., 2017), and data show that it functions upstream in the signaling pathways. However, the exact nature of its ligand during this response is not clear.

Our molecular knowledge of insect egg-triggered signaling in *Brassicaceae* is however still limited and despite similarities to PTI, data suggest that some aspects of egg-triggered immunity, such as the RBOHD/F-independent origin of ROS, are under the control of specific signaling components (Gouhier-Darimont et al., 2013). In *Arabidopsis*, mutation of *LECRK-I.8* does not fully abolish SA accumulation and *PR1* expression, indicating the potential presence of multiple receptors and/or EAMPs (Gouhier-Darimont et al., 2019). In rice (*Oryza sativa*), oviposition by *Sogatella furcifera* induces the formation of watery lesions together with the ovicidal substance benzyl benzoate (SEINO et al., 1996). The ability of different races to induce these lesions was found to vary (Yamasaki et al., 2003), and fine mapping of this trait lead to the identification of several QTLs potentially involved in this response (Yang et al., 2014). These results demonstrate the use of natural variation in the dissection of insect egg-triggered immunity in plants. We previously observed that HR-like symptoms vary among natural accessions in *Arabidopsis* upon *P. brassicae* egg extract treatment (Reymond, 2013), showing the existence of genetic variation in this response. Similarly, variation in the response was also observed in other *Brassicaceae* (Fatouros et al., 2015; Griese et al., 2017, 2019).

The ease of genetic manipulation and the recent development of high-quality SNP data/genome sequences from a large number of natural accessions makes *Arabidopsis* an ideal system to study the genetic basis of insect-egg induced responses by using a Genome-Wide Association (GWA) approach. The use of GWA mapping in *Arabidopsis* for the dissection of trait structure has massively increased over the past years and has been proven to be successful in the identification of natural variants involved in a variety of traits such as flowering, development and disease resistance (Atwell et al., 2010; Huard-Chauveau et al., 2013), but also for more complex traits critical to local adaptation (Xu et al., 2019; Ferrero-Serrano and Assmann, 2019; Kerdaffrec et al., 2016) or even combinations of abiotic and biotic stresses (Thoen et al., 2017; Davila Olivas et al., 2017).

Here we describe the existence of large natural variation in the extent of *P. brassicae* egg-induced HR-like symptoms and SA accumulation in *Arabidopsis*. GWA mapping revealed that two loci explain most of the variation observed, one of them being associated with both phenotypes measured. This suggests that the locus identified functions in early signaling steps. We further describe the genetic structure of this candidate gene and provide evidence for balancing selection maintaining variation at this locus.

Material and methods

Plant and insects growth conditions

All experiments described here were carried out in *Arabidopsis thaliana*. Plants were grown in growth chambers in short day conditions (10 h light, 22°C, 65% relative humidity, 100 $\mu\text{mol m}^{-2} \text{s}^{-1}$) and were 4 to 5 weeks old at the time of treatment. Larvae, eggs and butterflies of the Large White butterfly *Pieris brassicae* came from a population maintained on *Brassica oleracea* in a greenhouse (Reymond et al., 2000).

T-DNA insertion lines and HIF lines

Accessions used for GWA mapping were obtained from the NASC stock center and are listed in Supplementary Table 1. T-DNA insertion lines for *glr2.8* (SALK_111659) and *glr2.9* (SALK_125496) were obtained from the NASC stock center- *sid2-1* plants were obtained from Dr. Christiane Nawrath (University of Lausanne) and seeds of *glr2.7* T-DNA mutant line (SALK_121990) was obtained from Prof. Ted Farmer. Genotyping primers were designed with SIGNAL T-DNA verification tool for all lines used in this study.

Heterozygous inbred families (HIF) lines used for the validation of the *GLR2.7* locus were obtained from the Versailles Arabidopsis Stock Center (<http://publiclines.versailles.inra.fr>). Two crosses using lines containing different *GLR2.7* alleles were available, namely Col-0 x Bur-0 and Sha x Bay-0. Three independent HIF lines heterozygous for a genomic segment encompassing *GLR2.7* were selected in each cross. Lines were phenotyped for HR-like as described below.

Genome-wide association mapping and haplotype analysis

For GWA analysis, a set of 295 accessions from the HapMap panel (Horton et al., 2012) were used. Pools of 30 accessions were phenotyped every week over 2 days. Because of germination issues and low seed number, all plants for a given accession were phenotyped on the same day. To account for potential temporal effect, Col-0 plants originating from lab seed stocks were grown and phenotyped every week together with the accessions from the mapping panel. For each accession, 3 leaves from 3 to 6 plants were treated with egg-extract diluted 1:1 with deionized water leading to a total of 9 to 18 treated leaves. In parallel, 2 plants per accession were left untreated. Plants were left in the growth chamber for an additional 5 days until phenotyping. After 5 days, leaves were removed with forceps, symptoms were scored and pictures were taken as described below. One to three samples containing 6 randomly selected leaves were frozen in liquid nitrogen for further SA quantification.

GWA mapping was performed locally using custom scripts (Kerdaffrec et al., 2016) or on the GWAPP platform (<https://gwas.gmi.oeaw.ac.at/>, Seren et al., 2012) with the accelerated-mixed model (AMM) algorithm. This algorithm controls for population structure by computing a population-wide kinship matrix. Genotype data for ~250K SNP, full genome sequences of 1'135 accessions (The 1001 Genomes Consortium, 2016) or full imputed genotypes for 2029 lines (Togninalli et al., 2018) were used and only SNPs with a minor-allele frequency (MAF) > 0.05 were considered for analysis. To correct for genome-wide multiple testing, a Bonferonni corrected threshold of significance was computed by dividing $\alpha = 0.05$ by the number of SNPs used in the analysis. Based on the similar mapping profiles obtained using symptom score (Fig. 2A) and normalized symptom score (Supplementary Fig. 1) together with the identification of other good *a priori* candidates on chromosome 3 (L-type LecRKs, see chapter 3), we considered only non-normalized data for the current studies.

Haplotype analysis was based on significantly associated SNPs using the genotype data from GWAPP. Presence of premature stop codons in sequenced accessions was recovered from the POLYMORPH1001 Variant browser (<https://tools.1001genomes.org/polymorph/>). Both sets of data were used to explore phenotypic data.

Population-wide cladogram was built by calculating Euclidian distance between accessions from the kinship matrix, and clustering was subsequently performed using the “ward.d2” algorithm. Cladograms were further handled and annotated within the “ggtree” R package. Haplotype networks were built using the “ape” and “pegas” package by using the same sequence alignments as for phylogenetic trees.

Broad sense heritability

For each phenotype, broad sense heritability (H) was calculated using the following equations: $H = V_g/V_p$ and $V_p = V_g + V_e$, where V_g , V_p and V_e stand for genetic, phenotypic and environmental variance respectively. Since accessions are homozygous, V_e was estimated as the average intra-accession variance and V_p was the variance of the phenotype in the population.

Tajima's D and Fu and Li's F/D tests of neutrality

Sliding windows analysis of Tajima's D and Fu and Li's F/D tests were performed using DnaSP (version 6.12.03) with sliding windows of 100bp and a step size of 25bp, and significance threshold was set according to a 95% confidence limits published before (Tajima, 1989).

Oviposition and treatment with egg extract

For experiments with natural oviposition, plants were placed in a tent containing approximately 20 *P. brassicae* butterflies for a maximum of 8 h. Afterward, plants were kept in a growth chamber in plastic boxes until hatching of the eggs. Control plants were kept in the same conditions without butterflies.

P. brassicae eggs were collected and crushed with a pestle in Eppendorf tubes. After centrifugation (15 000 g, 3 min), the supernatant ('egg extract') was collected and stored at -20°C. Plants were 4-5 weeks old at the time of treatment. For each plant, two leaves were treated with 2 µl of egg extract. This amount corresponds to one egg batch of 18 eggs (E. Stahl, personal communication). A total of four plants were used for each experiment. After the appropriate time, egg extract was gently removed with a scalpel blade and treated leaves were stored in liquid nitrogen. Untreated plants were used as controls.

For GWA analysis, a large amount of egg-extract was prepared as described and aliquots were stored under N₂ at -80°C in order to ensure homogenous treatments during the entire experiment.

Symptom scoring

Symptoms were scored visually from the adaxial side of the leaves and were classified into the following categories: no symptom (leaf treated area is still lush green, score = 0), small chlorosis (<50% of the treated area, score = 1), large chlorosis (> 50%, score = 2), small necrosis (brown spots or transparent membrane on < 50% of the treated area, score = 3), large necrosis (> 50 %, score = 4) and spreading necrosis (necrosis not confined to the treated area, score = 5). Normalized symptom score was calculated by dividing the score of a given accession by the score of the lab Col-0 score from the same week.

Histochemical stainings (Trypan blue, DAB)

For visualization of cell death, egg extract was gently removed and leaves were submerged in lactophenol trypan blue solution (5 ml of lactic acid, 10 ml of 50% glycerol, 1 mg of trypan blue (Sigma), and 5 ml of phenol) at 28°C for 2–3 h. Hydrogen peroxide (H₂O₂) accumulation was measured with 3,3-diaminobenzidine (DAB; Sigma). Leaves were submerged in a 1.0 mg ml⁻¹ DAB solution and incubated in the dark at room temperature for 6–8 h. After each staining, leaves were destained for 10 min in boiling 95% ethanol. Microscope images were saved as TIFF files and processed for densitometric quantification with ImageJ (version 1.48).

Salicylic acid quantifications

SA quantifications were performed using the bacterial biosensor *Acinetobacter* sp. ADPWH (DeFraia et al., 2008; Zvereva et al., 2016). Briefly, 6 leaf discs (0.7 cm, ~20mg) were extracted in 0.1M sodium acetate buffer (pH 5.6). Extracts were then centrifuged at 4°C for 15min at 16'000g. 50µL of extract were incubated with 5 µL of β-Glucosidase from almonds (0.5U/µl in acetate buffer, Sigma-Aldrich) during 90min at 37°C to release SA from SA-glucoside (SAG). 20µL of extract was then mixed with 60µL of LB and 50µL of a culture of *Acinetobacter* sp. ADPWH_lux (OD₆₀₀ = 0.4), and incubated for 1h at 37°C. Finally, luminescence was integrated using a 485±10nm filter for 1s. A standard curve with SA amounts ranging from 0 to 60ng was read in parallel to allow quantification, and sample amounts were estimated by fitting a 3rd order polynomial regression on the standards.

RNA Extraction, Reverse-transcription and Quantitative Real-time PCR

Tissue samples were ground in liquid nitrogen, and total RNA was extracted using ReliaPrep™ RNA Tissue Miniprep (Promega) according to the manufacturer's instructions, including DnaseI treatment. Afterwards, cDNA was synthesized from 500 ng of total RNA using M-MLV reverse transcriptase (Invitrogen) and subsequently diluted eightfold with water. Quantitative real-time PCR reactions were performed using Brilliant III Fast SYBR-Green QPCR Master Mix on an QuantStudio 3 real-time PCR instrument (Life Technologies) with the following program: 95°C for 3min, then 40 cycles of 10s at 95°C, 20s at 60°C.

Values were normalized to the housekeeping gene *SAND* (At2g28390). The expression level of a target gene (TG) was normalized to the reference gene (RG) and calculated as normalized relative quantity (NRQ) as follows: $NRQ = E^{Ct_{RG}} / E^{Ct_{TG}}$. Primer efficiencies (E) were evaluated by five-step dilution regression. For each experiment, three biological replicates were analysed. A list of all primers used in experiments can be found in Supplementary Table 2.

Statistical Analyses

GWA mapping and subsequent analysis of the data obtained was performed with R software version 3.6. For boxplots, the thick line indicates the median, box edges represent 1st and 3rd quartile respectively, whiskers cover 1.5 times the interquartile space and dots represent extreme values. Boxplot width is proportional to the number of sample. When displayed, notches indicate an approximate confidence interval for median values. All other analyses using mutant lines were analyzed using GraphPad Prism 8.0.1.

Results

Arabidopsis accessions display natural variation in response to *P. brassicae* eggs

We observed that Arabidopsis accessions display varying degrees of HR-like symptoms after 5 days of treatment with *P. brassicae* egg extract (Fig. 1A), corresponding to the hatching time of real eggs. The existence of natural variation for this defense-related trait suggests that it is under genetic control, consistent with previous reports (Gouhier-Darimont et al., 2013, 2019). While most leaves exhibited some degree of chlorosis, symptoms usually ranged from no visible symptom to the formation of large patches of cell death (Fig. 1B). Moreover, symptoms were most of the time restricted to the area of egg application, but could exceptionally grow larger for both chlorosis and necrosis. However, because of the

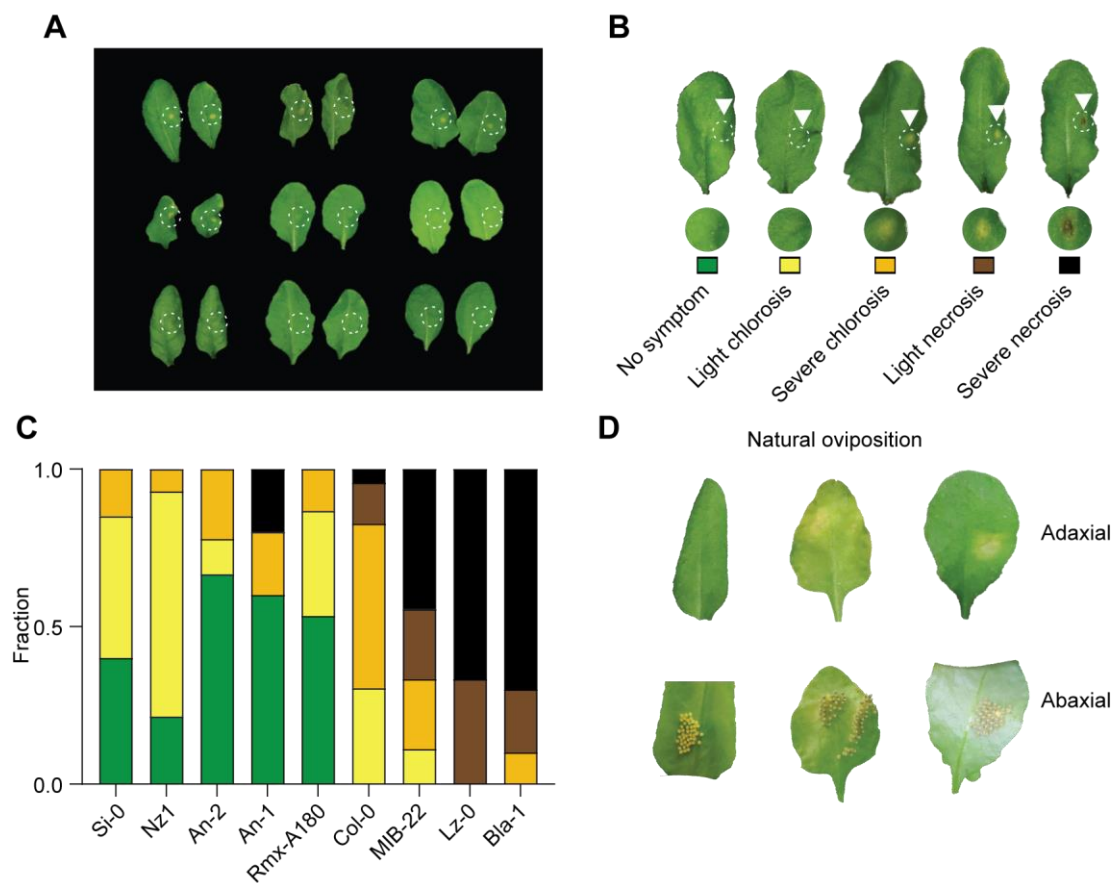


Figure 1. Insect-egg induced HR-like varies among natural *A thaliana* accessions

A. Representative picture of accessions displaying varying phenotypes after treatment with *P. brassicae* egg extract. B. Representative pictures of symptoms used for scoring in experiments. C. Proportion of each symptom class developed by some accessions shown in panel A as visualized from the adaxial side. D. Variation in HR-like triggered after natural oviposition by *P. brassicae* butterflies. In all experiments shown here, duration of treatment was 5 days as this corresponds to the hatching time of naturally oviposited *P. brassicae* eggs. The dashed circles indicate the site of treatment on the abaxial side of the leaf.

very low frequency of such events, we did not quantify those separately. This scoring scheme allows an easy quantification of this phenomenon (Fig.1C). To verify that application of *P. brassicae* egg extract mimics HR-like responses induced by real eggs, we tested whether naturally oviposited eggs could also induce some degree of variation in HR-like responses. In several accessions, we observed the formation of chlorotic or necrotic tissue localized around and underneath the egg clutches after 5 days (Fig. 1D) and this correlated with the severity of symptoms observed after egg extract treatment. This response was however less frequently observed, yet a parsimonious explanation might be that putative EAMPs may be more accessible in egg extract than in real eggs where the protective shell may slow down release of elicitors. In an effort to set conditions for a GWA mapping experiment using egg extract, we first performed initial tests on 3 selected accessions, using Col-0 as a control. Based on these experiments, we defined experimental conditions as follows: short day length (10L:14D), egg extracted diluted 1:1 with deionized water, and 3 leaves treated per plant (Supplementary Fig. 2A-C). Because such experiment requires a very large amount of egg extract, this allows to maximize the overall number of plant treated per accession and per block, thereby improving power, even though the use of “pure” egg-extract and/or long days conditions seem to increase symptom strength.

GWA mapping and identification of associated loci

We set out to investigate the genetic basis of insect egg-induced HR-like by performing a Genome-wide association study (GWAS) on a world-wide set of 295 Arabidopsis accessions. Symptom score and total SA (SA+SAG) were quantified in all accessions after 5 days of egg extract treatment and were used for mapping. The initial phenotype distribution (Supplementary Fig. 3) of symptom score displays a bimodal distribution, from the high number of accessions with score <1. This obvious departure from normality could suggest that some accessions may have lost to a large degree their ability to respond to *P. brassicae* egg extract, potentially through the loss of crucial upstream components. Broad sense heritability (H), which estimates the amount of phenotypic variance that is genetically encoded, was high for both symptom score (H = 0.56) and total SA (H = 0.87). This finding is consistent with previously reported H values for defense phenotypes (Yang et al. 2017). Initial mapping using an imputed genotype matrix for 2029 accessions (The 1001 Genomes Consortium, 2016) revealed a highly significant peak associated with symptom score and total SA levels ($-\log_{10} P = 15.96$ and 10.64 respectively) spanning over 10Kb on chromosome 2 (Fig. 2A and Supplementary Fig. 4 for total SA) and one marker reaching significance on chromosome 3 ($-\log_{10} P = 7.59$) that is only associated with symptom score. The description of this other locus will be the subject of a separate publication. As the genotype matrix used was produced by imputing missing genotypes based on a subset of accessions that were

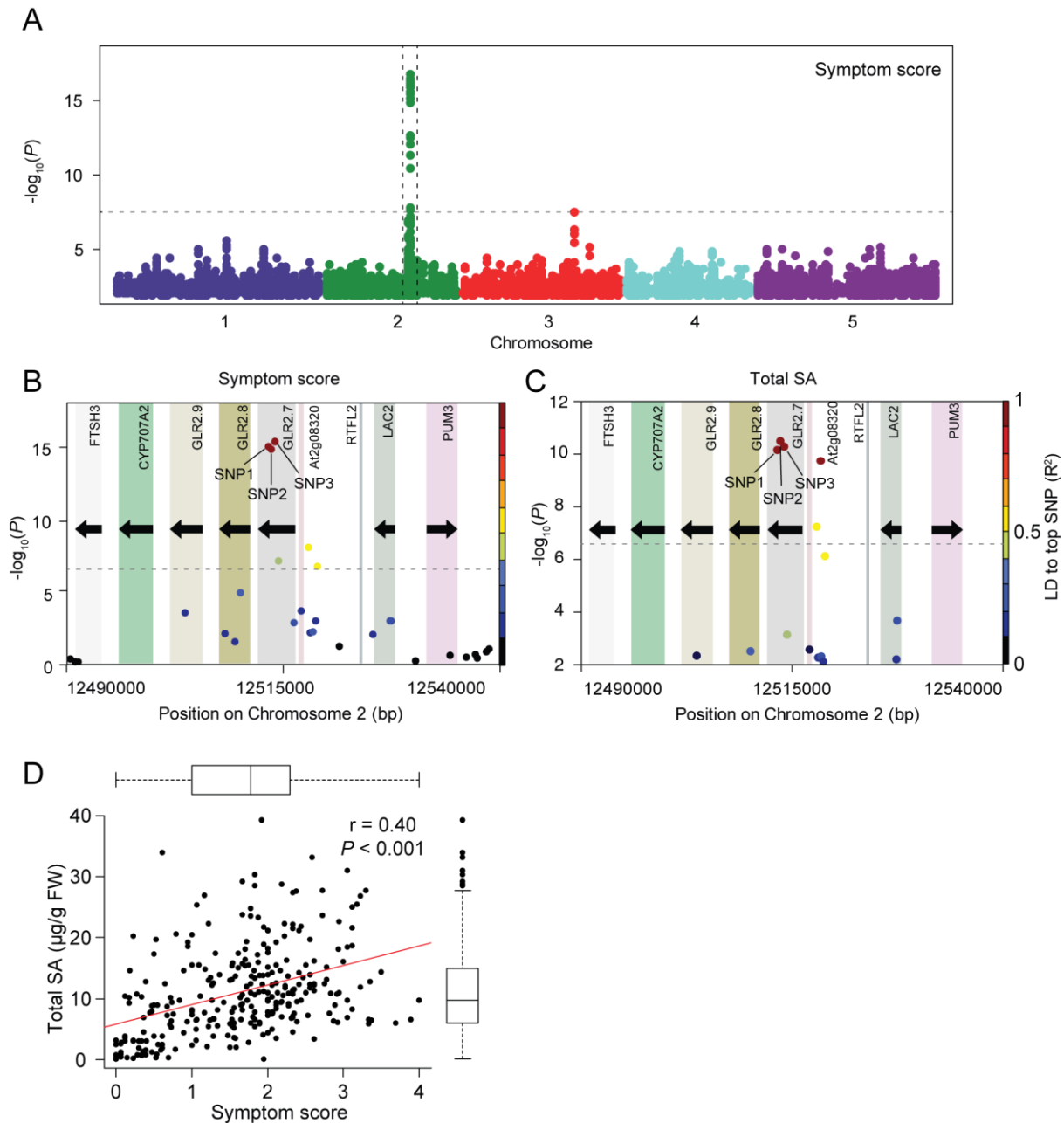


Figure 2. Genome-wide mapping of insect-egg induced responses
 A. Manhattan plot of GWA for symptom score after 5 days of *P. brassicae* egg-extract using an accelerated mixed-model. Full imputed genotypes for all 295 accessions were used for mapping. Chromosomes are displayed in different colors and the dashed line indicates the Bonferroni-corrected significance at threshold $\alpha = 0.05$. B and C. Local association plot of the GLR2.7 locus using the 250K genotype data for symptom score (B) and total SA levels (C). The x-axis represents genomic position on chromosome 2 and color boxes indicate genes. LD with the most significant SNP is indicated by a color scale. The dashed line indicates the Bonferroni corrected significance threshold at $\alpha = 0.05$. D. Population-wide relationship between total SA levels and symptoms score after 5 days of *P. brassicae* egg extract treatment. Boxplots (see material and methods for details) in outer margins indicate symptom score and total SA distributions. The red line indicates linear regression trendline, Pearson correlation coefficient and correlation significance are shown.

sequenced, we used the 250K SNP genotype data that was available for all used accessions for further investigation of specific markers. The 3 most significantly associated SNPs occurred within the coding region of *GLUTAMATE RECEPTOR-LIKE 2.7* (*GLR2.7*) for both phenotypes, while 2 additional markers are located in the promoter of the gene (Fig. 2B and

C). Interestingly, this locus contains two other clade 2 GLR members, *GLR2.8* and *GLR2.9*, which are the closest homologs of *GLR2.7* (Roy and Mukherjee, 2017). To further explore whether variation within *GLR2.7* could be causal for variation in HR-like and SA accumulation, we examined linkage disequilibrium (LD) between the top SNP and the other markers in a 50Kb window around the variant. We found that the most significantly associated SNPs in both scans were in very high LD with other SNPs located in the gene body of *GLR2.7*, while LD decayed rapidly around the gene for other markers (Fig. 2B and C). Both SNP1 and 2 appeared to be in very high LD with SNP3, while LD decayed rapidly around *GLR2.7* for other markers (Fig. 2B), suggesting that this gene might be involved in cell death induction and SA accumulation upon insect egg perception. To explore whether other genomic regions may be associated with HR-like or SA accumulation, we performed a conditional GWA scan by adding SNP3 as a cofactor. The resulting GWA scan showed no significant association left when SNP3 is taken into account (Supplementary Fig. 5A and B), confirming that the association observed *GLR2.7* accounts for most of the variation observed. As mentioned, SA was previously described to be necessary to induce cell death upon egg-extract perception (Gouhier-Darimont et al., 2013). Interestingly, we found that total induced SA and symptom score were moderately correlated ($r = 0.40$) in the entire mapping panel (Fig. 2D). This indicates that SA does not fully explain the strength of egg-induced HR-like and that other signaling components might also contribute, which is consistent with the partial reduction in cell death observed in *sid2-1* plants (Gouhier-Darimont et al., 2013). However, this could also be consistent with SA working in a more qualitative way as almost all accessions showed some degree of SA induction regardless of the degree of symptoms.

In order to explore how the identified region could contribute to the response, we

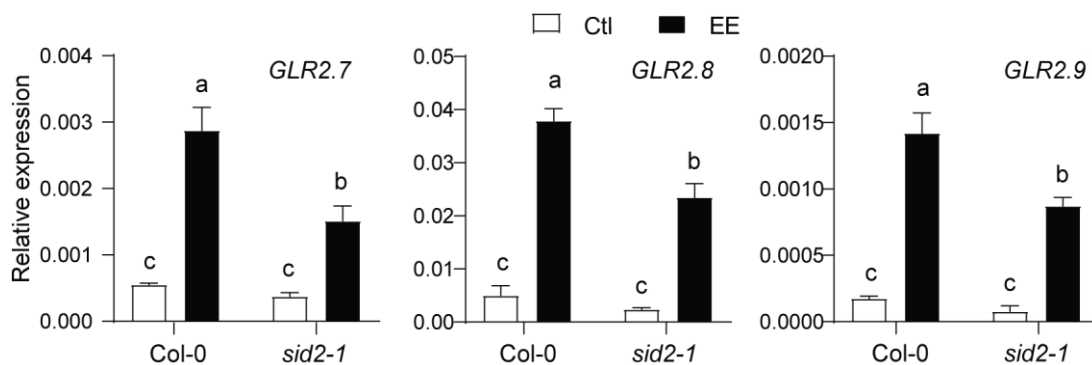


Figure 3. Expression of *GLR2.7*, *GLR2.8* and *GLR2.9*

A. Gene expression of different clade II *GLR* in Col-0 and *sid2-1* plants after three days of egg extract treatment. Transcript levels were monitored by qPCR and normalized to the reference gene *SAND*. Means \pm standard error (SEM) of three technical replicates are shown. Different letters indicate significant differences at $P < 0.05$ (ANOVA, followed by Tukey's HSD for multiple comparisons). This experiment was repeated twice with similar results.

measured gene expression of candidate genes after egg extract treatment. Transcripts of all *GLR* genes were significantly induced by egg extract (Fig. 3), and this induction was partially dependent on SA, as shown by lower transcript levels in *sid2-1*. Additionally, analysis of previously published microarray data showed that *GLR2.7* expression is induced after natural oviposition by *P. brassicae* and this effect was also partially SA-dependent (Little et al., 2007), further supporting these results. Finally, we explored whether this region had already been associated with another phenotype. We used the standardized AraGWAS catalog that encompasses many defense related phenotypes including insects and pathogens. Surprisingly, it appears that this region might be specifically linked to insect egg responses as we found that no previous GWA study had any significant association at this locus (Supplementary Fig. 6).

Different haplotypes of *GLR2.7* segregate in Arabidopsis populations

To get a further insight into the *GLR2.7* locus, we examined whether different haplotypes segregated in the population. By looking at all significantly associated markers within the *GLR2.7* gene sequence we found over 50 SNPs spanning the entire coding sequence and promoter (Fig. 4A), and most of them show similar P-values. As with the lower density SNP

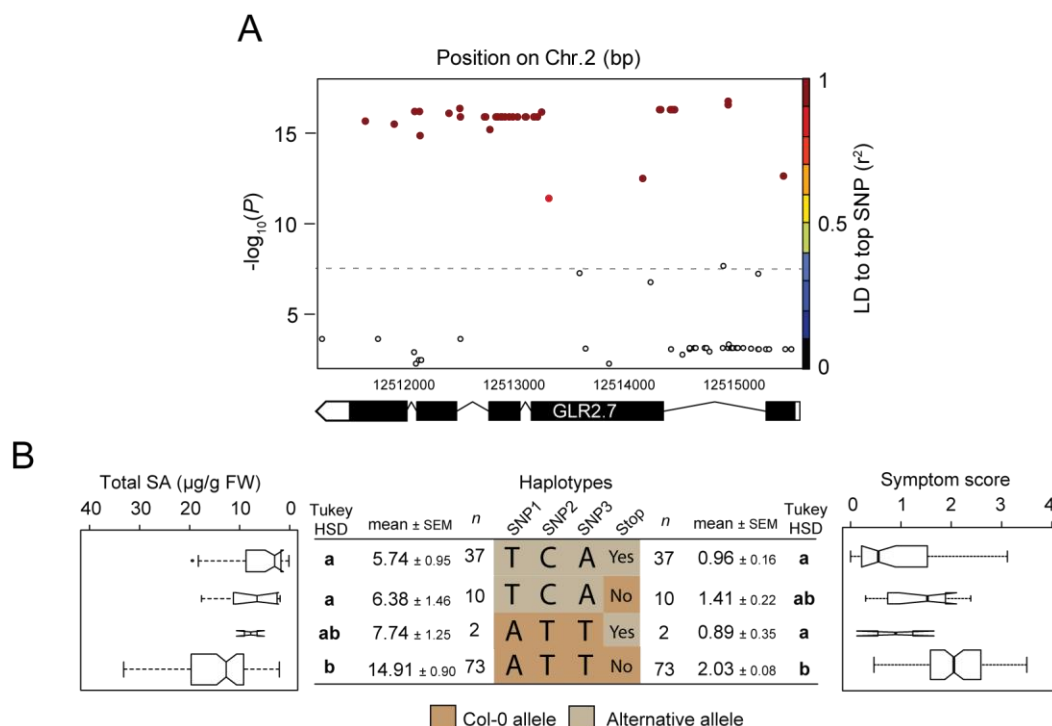


Figure 4. Local association and haplotype analysis of the *GLR2.7* locus

A. Local association plot of the *GLR2.7* locus using the full imputed genotype data. The x-axis represents genomic position on chromosome 2. LD with the most significant SNP is indicated by a color scale. The dashed line indicates the Bonferonni corrected significance threshold at $\alpha = 0.05$. B. The 3 selected SNPs from Fig.1 together with the presence/absence of a stop codon define 4 main haplotypes. For sake of clarity, only haplotypes containing at least 2 accessions are shown. Mean symptom score and total SA \pm SE is shown. Different letters indicate significant difference at $P < 0.05$ (ANOVA, followed by TukeyHSD for multiple comparison).

data, we found that all markers within the *GLR2.7* coding region were in very high LD (>0.8). The fact that many markers are genetically linked again supports the potential existence of distinct haplotypes segregating at this locus. Overall, out of all 54 significantly associated SNPs, 25 were found to induce non-synonymous changes in the protein sequence (Supplementary Table 3) and 1 was found to cause the appearance of a premature stop codon. As frameshifts and premature stop codons can lead to gene knock-out, we used the POLYMORPH 1001 database (<http://tools.1001genomes.org/polymorph/>) and extracted the list of high impact mutations in the accessions for which full genome sequences were available (125 / 295). Surprisingly, we found that 31% of these accessions contained a premature STOP codon and most of them were found in the first exon of the gene, suggesting that the protein might be truncated and therefore likely non-functional. To get a better insight into the population-wide genetic structure of this locus, we used the three significant SNPs (SNP1-3) identified in Fig. 2B and C together with the presence/absence of the premature STOP to define haplotypes of *GLR2.7*. As suspected, we found that SNP1-3 define mainly two haplotypes within the entire mapping population: one defined by the alleles TCA and associated with low symptom score (0.96 ± 0.16) and another one defined by the alleles ATT and associated with a strong symptom score (2.03 ± 0.08 , Fig. 4B). We thereafter named these two haplotypes *GLR2.7^{ATT}* and *GLR2.7^{TCA}* respectively. In contrast, other allelic series were either not present or contained a very low number ($n \leq 3$) of accessions and were therefore not further considered. By combining both analyses, we can observe that the presence of a premature stop codon leads to milder symptoms independently of the haplotype considered (Fig. 4B), indicating that the corresponding proteins might not be functional. Additionally, the vast majority of the stop codons were preferentially linked to the low symptom *GLR2.7^{TCA}* haplotype, thereby suggesting that the corresponding alleles might be natural knock-outs. Interestingly, Col-0 possesses the *GLR2.7^{ATT}* which is linked to high HR-like symptoms. Altogether, our data point to the existence of alleles at the *GLR2.7* locus that modulates the intensity of cell death and SA accumulation upon perception of *P. brassicae* eggs.

Haplotype-specific *GLR2.7* expression correlate with HR-like symptoms

As the latter analysis indicates the existence of distinct haplotypes of *GLR2.7*, we reasoned that differences in gene expression might underlie the differential phenotypes associated. We first used published RNAseq data from Arabidopsis accessions in order to explore this possibility (Kawakatsu et al., 2016). We extracted basal expression data for *GLR2.7* and nearby genes from accessions used in this study and stratified them based on the allele present at SNP3. All accessions harboring the *GLR2.7^{ATT}* haplotype displayed significantly higher level of transcripts in non-induced conditions (Supplementary Fig. 7), hinting to a

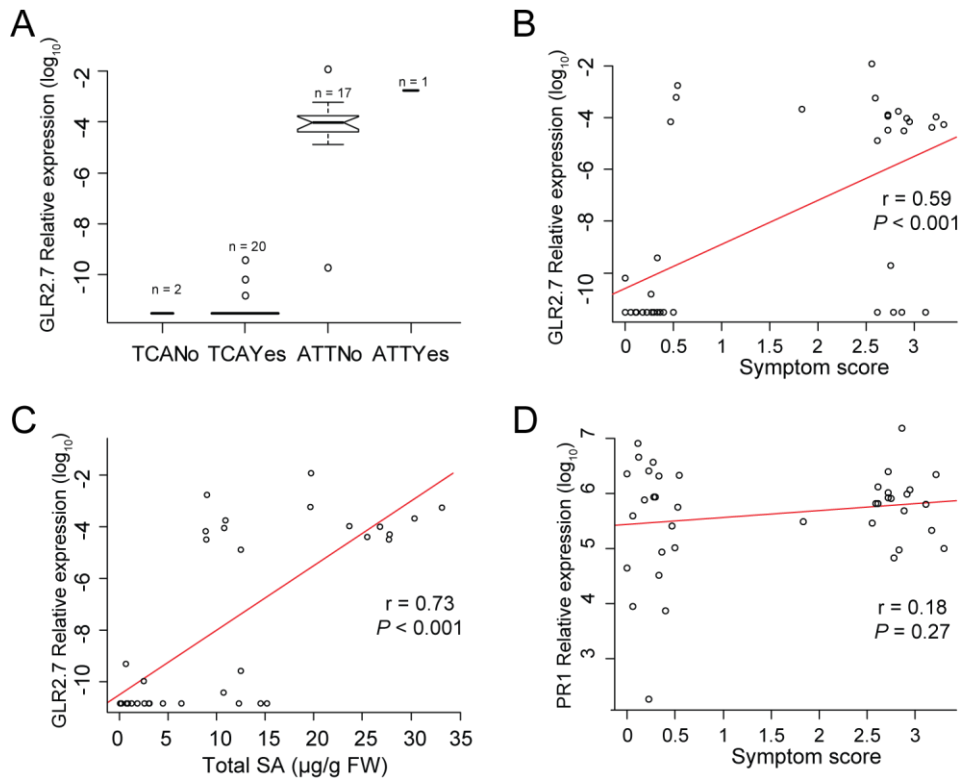


Figure 5. Targeted gene expression analysis in a panel of 40 accessions
 Average *GLR2.7* (A, B and C) or *PR1* (D) expression in 40 different accessions after 72h of egg-extract treatment. Transcript levels were plotted according to the haplotype defined previously (A) or against symptom scores of the respective accessions (B and D) or against total SA amounts (C). Gene expression was monitored by qPCR and target gene transcript level was normalized to the reference gene *SAND*. Means \pm standard error (SEM) of three technical replicates are shown. Expression data were corrected by adding half the smallest non-zero value in order to avoid zero values, and \log_{10} -transformed prior to analysis.

potential haplotype-dependent transcriptional regulation. To test whether this was also the case after egg-extract treatment, we measured transcript levels in a panel of 40 sequenced accessions from our mapping population that displayed either strong or low symptom scores, while SA + SAG values covered the entire distribution. Accessions containing the *GLR2.7^{TCA}* haplotype did not produce any *GLR2.7* transcripts after egg-extract treatment, while all accessions possessing the *GLR2.7^{ATT}* haplotype did (Fig. 5A), confirming that both haplotypes do not equally express *GLR2.7*. Additionally, we found clear and significant correlations between the level of *GLR2.7* expression and symptom strength or total SA (Fig. 5B and C), further supporting a link between transcript levels of this gene and egg-induced responses. Interestingly, *GLR2.7* transcript levels did not increase after egg treatment in several accessions displaying severe HR-like symptoms (Supplementary Fig. 8), potentially indicative the existence of additional accession-dependent factors. In contrast, when comparing the expression of all three *GLR* homologs in a subset of 10 accessions with high or low symptom scores, only *GLR2.7* had an expression pattern consistent with symptom score while *GLR2.8* and *GLR2.9* displayed no obvious correlation (Supplementary Fig. 9). Unexpectedly, the presence of a premature stop did not correlate with the pattern of *GLR2.7*

expression in any of the haplotype considered, potentially indicating that stop codons emerged after transcription was lost (Fig. 5A). We took advantage of the availability of high quality methylome data (Kawakatsu et al., 2016) for some of the accessions to investigate whether differential gene methylation (gbM) of *GLR2.7* could explain the variations in expression observed. However, gene body and promoter methylation was very low for *GLR2.7* and had no obvious correlation with symptom scores (Supplementary Fig. 10), suggesting that expression and gbM are not linked in this case. Consistently, recent studies indicate that gbM does not play a major role in transcription variation in *Arabidopsis* (Kawakatsu et al., 2016; Meng et al., 2016). Finally, while *PR1* is often used as a marker for *P. brassicae* egg-induced response, we could not observe any correlation between transcript levels of the marker gene *PR1* and symptom intensity in the accessions surveyed (Fig. 5D), suggesting that *PR1* might not be a good marker for all *P. brassicae* egg-induced responses. We can conclude that the low-symptom *GLR2.7^{TCA}* haplotype is a knock-out allele, while the presence of a full-length *GLR2.7* protein potentially enables plants to trigger strong HR-like symptoms upon insect egg perception.

Signatures of balancing selection at the *GLR2.7* locus

Genes that confer herbivore or pathogen resistance are advantageous in the presence of pest but are usually costly or detrimental to maintain in their absence (Vila-Aiub et al., 2011; van Velzen and Etienne, 2015; Ariga et al., 2017). Balancing selection is a process through which multiples alleles are maintained at intermediate frequency in a population, a process that is known to shape resistance loci (Bakker et al., 2006; Huard-Chauveau et al., 2013). Loci under balancing selection display highly diverged alleles and haplotype distribution is widespread across the geographical range of the considered species. As shown by the haplotype frequency distribution at the *GLR2.7* locus, two haplotypes defined by SNP1-3 are present at intermediate frequencies, while all others are found in very few individuals (Fig. 6A). To explore whether the distribution of *GLR2.7* haplotypes was caused by geographical or phylogenetical factors, we constructed a cladogram representing genome-wide distance between accessions by using the kinship matrix used for the GWA mapping. It appears clearly that both *GLR2.7^{ATT}* and *GLR2.7^{TCA}* haplotypes are homogeneously distributed among all populations of *Arabidopsis*, indicating that they are not confined by phylogenetical or geographical proximity (Fig. 6B). This is also true when considering premature stop codons. To further explore the genetic structure of *GLR2.7*, we used gene sequences from 125 accessions to build a haplotype network (Fig. 6C). These data show that the various alleles at this locus are structured into two deeply divergent haplotypes, separated by at least 12 mutations, corresponding to the ones defined previously. Interestingly, the *GLR^{TCA}* haplotype displays high intra-haplotype divergence as shown by the presence of rare alleles.

This is indicative of relaxed selection or drift occurring as a result of pseudogenization of this

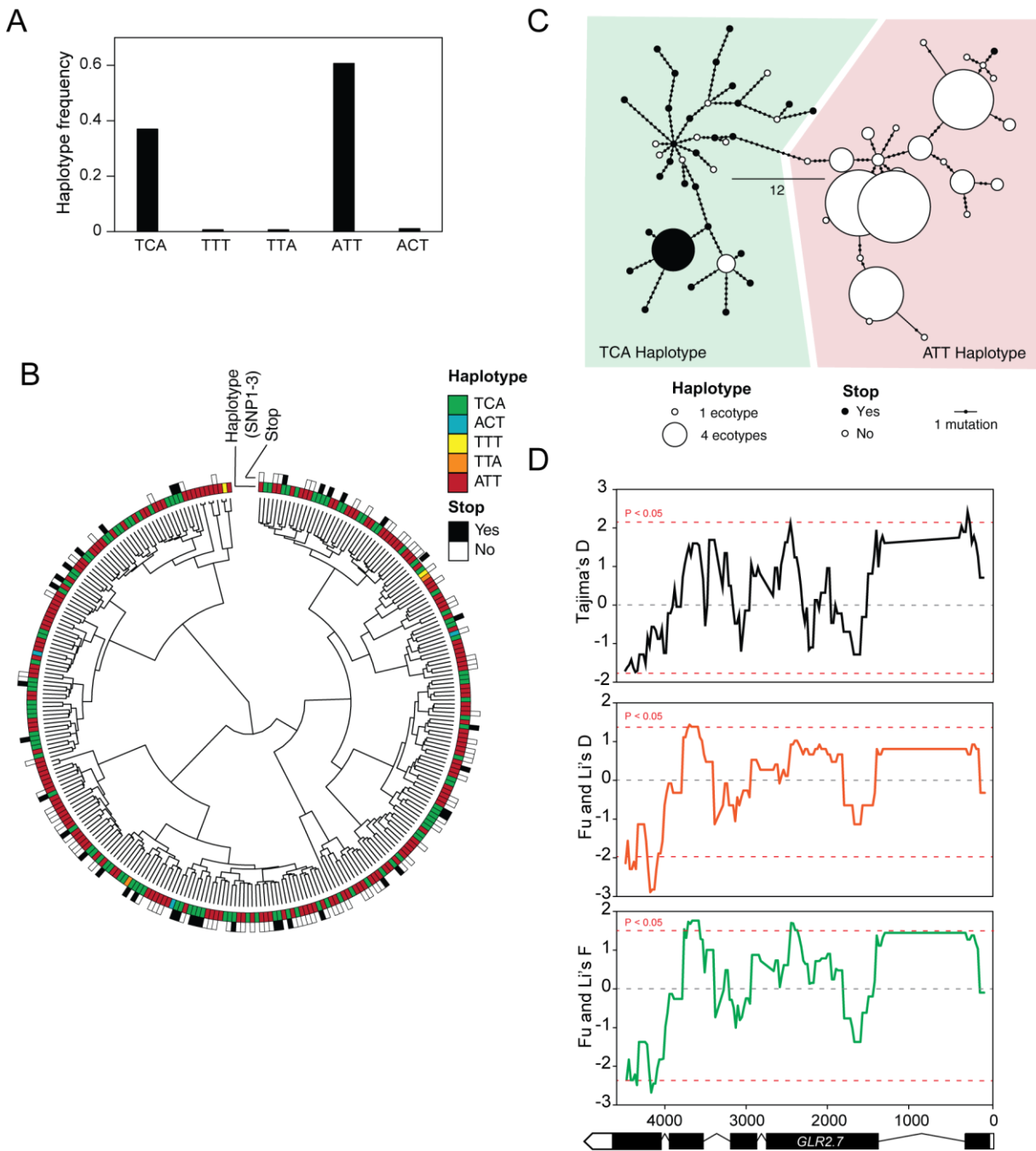


Figure 6. Various signatures of balancing selection at the *GLR2.7* locus.

A. Frequency of the haplotypes within a world-wide set of *Arabidopsis* accessions. B. Cladogram constructed from a genome-wide kinship matrix of the 295 accessions used in this study. The two outermost circles indicate haplotype and presence of a premature stop codon (for the sequenced accessions only). C. Haplotype network of the *GLR2.7* locus in the 125 sequenced accessions. Circles represent haplotypes and lines represent the number of step-wise mutations separating two haplotypes. Circles are colored according to the presence or absence of stop within a haplotype. D. Sliding window analysis of Tajima's D, Wu and Li's D and F statistics along the *GLR2.7* coding region using a window size of 200bp and a step size of 25bp. A subset of 125 accessions for which available full genome sequences was used for this analysis. For Wu and Li's statistical tests, *Arabidopsis lyrata* was used as an outgroup. The red dashed line indicate significance threshold at $P < 0.05$. The gene structure of *GLR2.7* is shown below.

gene in some accessions. The broad geographical presence of both haplotypes and their deep divergence suggests that they might be ancient polymorphisms and have been maintained through selection. Several statistical tests - such as Tajima's D and Fu and Li's F or D - have been described to test the hypothesis that a sequence evolves neutrally by comparing the amount of variation observed and the variation expected for a given sequence. Deviations from neutrality are identified by either positive or negative test values, indicating balancing or purifying selection respectively. Tajima's D is known to be sensitive to the species demography and we therefore also computed the Fu and Li's D and F statistics (Tajima, 1989; Fu and Li, 1993), which incorporate an outgroup sequence (here *Arabidopsis lyrata*) to better discriminate signatures of selection from demographic history. All three tests statistics displayed consistently positive values on most parts of the *GLR2.7* gene sequence (Fig. 6C) with some stretches reaching significance, therefore clearly indicating that this locus does not evolve neutrally. Altogether, these results show that two deeply diverged haplotypes of *GLR2.7* segregate in natural *Arabidopsis* populations, and we provide evidence that balancing selection may be maintaining variation at this locus.

GLR2.7 regulates HR-like in a background-dependent manner

Altogether, these results clearly point to *GLR2.7* as showing signs that variation in its sequence, which results in gene knock-out in low-symptom accessions, is causal for the differences observed in HR-like and SA amounts after egg-extract perception. We isolated a T-DNA insertion line (SALK_121990) that has a T-DNA insertion in the second exon of *GLR2.7*. Quantitative real-time PCR revealed the absence of transcript produced at this locus, confirming that the mutant is a knock-out (Supplementary Fig. 11). After 3 days of egg extract treatment, we could not observe any difference in HR-like symptoms or by using trypan blue staining between wild-type and *glr2.7* mutant plants (Fig. 8A and B). Moreover, SA + SAG amounts were also similar together with *PR1* transcript levels (Fig. 8C and D). These results are surprising given the amount of evidence suggesting a role of *GLR2.7* in these phenotypes. Initially, GWA mapping revealed the existence of two peaks on chromosome 2 and 3 associated with symptom scoring (Fig. 2A). We wondered whether some form of epistasis might be existing between both loci and further expanded the haplotypes defined using SNP1-3 in *GLR2.7* by including the top SNP found on chromosome 3. We observed that the combination of alleles from both loci shows an additive behavior on symptom distribution (Fig. 8E), suggesting that the presence of one or the other "strong" allele leads to intermediate HR-like symptoms. As it happens, Col-0 accession possesses the strong symptom-associated allele at both loci, potentially indicating that the knocking-out of *GLR2.7* could be rescued by the presence of another variant on chromosome 3. These data suggest that the phenotype conferred by *GLR2.7* may be background-dependent. To

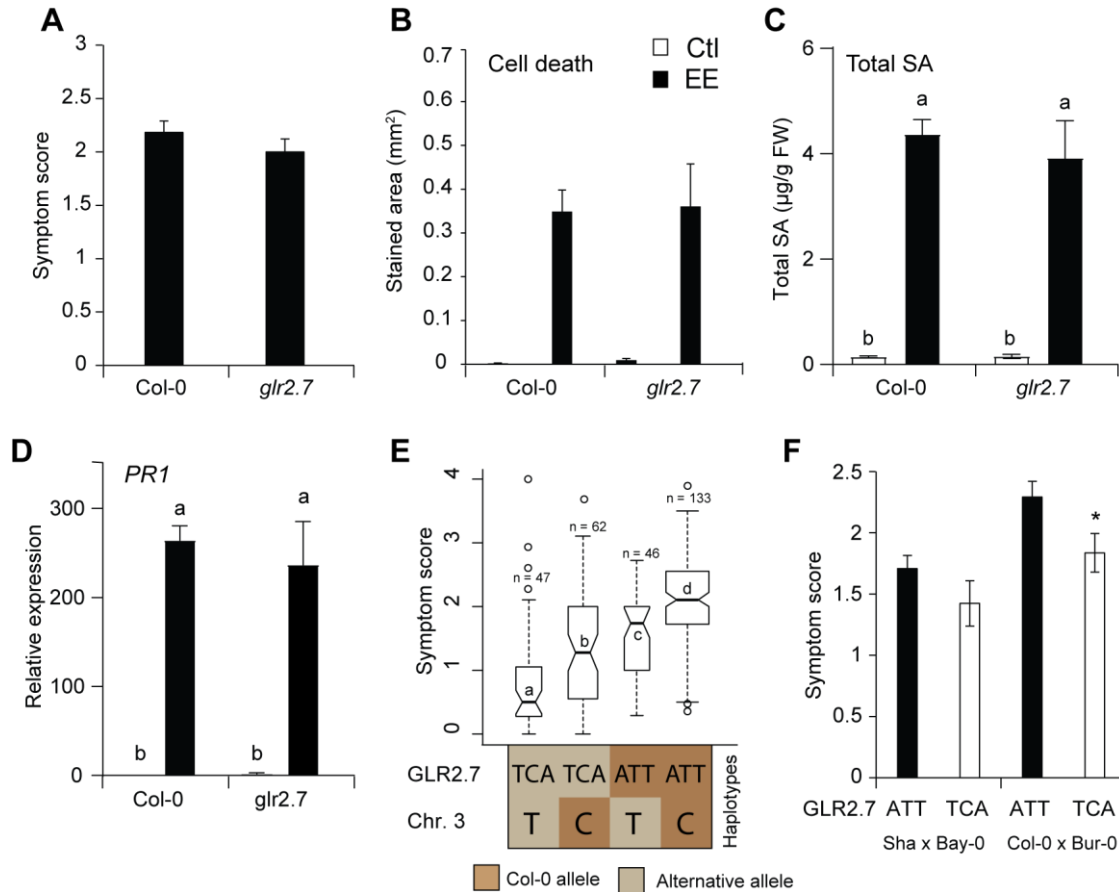


Figure 7. Egg-extract phenotypes in the *glr2.7* mutant and evidence for epistasis between the two associated loci. Average symptom score as visualized from the adaxial side after 5 days of treatment with egg extract. Means \pm standard error (SEM) from 12-18 leaves are shown. This experiment was repeated twice with similar results. B. Cell death as quantified by trypan blue staining after 3 days of egg extract treatment. Untreated leaves were used as controls. Means \pm standard error (SEM) from 8-20 leaves are shown. This experiment was repeated twice with similar results. C. Total salicylic acid (SA + SAG) was quantified in 7 mm diameter leaf discs ($n=6$) after 3 days of egg extract treatment. Quantifications were performed using 4 plants per genotype by using a bacterial biosensor. Means \pm standard error (SEM) of three independent experiment are shown ($n = 10-12$). D. Expression of the marker gene *PR1* after 72h of egg-extract treatment. Transcript levels were monitored by qPCR and normalized to the reference gene *SAND*. Means \pm standard error (SEM) of three technical replicates are shown. This experiment was repeated twice with similar results. E. Epistasis analysis using the haplotypes defined at the *GLR2.7* locus and the significant SNP of the second association peak observed in Fig. 2. Average symptom score from 295 accessions is shown. n indicates the number of accessions in each haplotype and different letters indicates significant differences at $P < 0.05$ (ANOVA, followed by Tukey HSD for multiple comparisons). F. Scoring of HIF lines segregating for the *GLR2.7* locus derived from two different crosses. Each comparison was performed on 3 or 4 independent lines. *, $P < 0.05$ (Student t-test).

to explore this idea, we used available heterozygous inbred family (HIF) lines from two different crosses segregating at the *GLR2.7* locus to address this possibility. Symptom scoring show that plants possessing the strong *GLR2.7^{ATT}* haplotype display higher symptoms than lines containing the pseudogenized *GLR2.7^{TCA}* haplotype in the lines derived from the Col-0 x Bur-0 cross, but not in the Sha x Bay-0 cross (Fig. 8F). Therefore the impact of *GLR2.7* haplotypes on HR-like symptom is background-dependent.

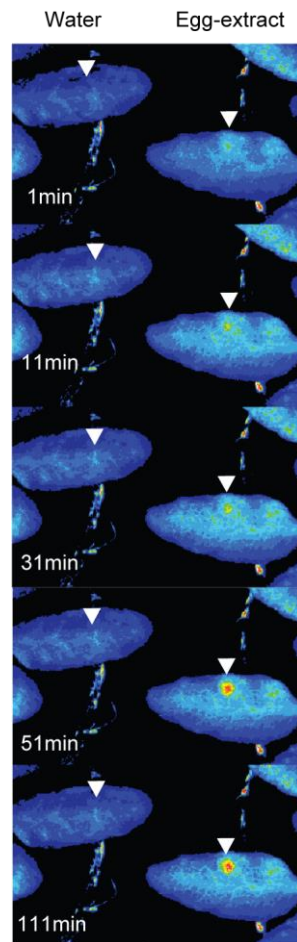


Figure 8. *P. brassicae* egg extract induces long lasting cytosolic calcium influx
 False-colored image of two *pUBQ10::GCaMP3* expressing plants treated with water or *P. brassicae* egg-extract. Fluorescence was imaged at the indicated time points after treatment. Arrowheads indicate the site of treatment on the abaxial side of leaves. For better visualization, contrast of all images was increased. This experiment was repeated twice with similar results.

P. brassicae egg-extract triggers long lasting cytosolic calcium influxes in leaves

Members of the *GLR* gene family are described as amino-acid gated Ca^{2+} permeable channels (Price et al., 2012). Even though their function during immune responses is not clear, several studies provide evidence that some yet unknown *GLR* may be responsible for PAMP-induced Ca^{2+} influx in tobacco and Arabidopsis (Kwaaitaal et al., 2011; Vatsa et al., 2011). We tested whether egg extract application triggers Ca^{2+} influx, potentially indicative of *GLR* function. We used the previously published *UBQ10::GCaMP3* line (Nguyen et al., 2018) to monitor cytosolic Ca^{2+} influx during this response. We observed a fast increase in cytosolic Ca^{2+} levels within the first 10min after egg extract application, and this sustained increase remained for more than 1 hour (Fig. 7). As water deposition did not trigger any response, we conclude that the observed increase in Ca^{2+} is not caused by mechanical stimulation. These data further support the potential role of a *GLR* channel during egg-induced responses.

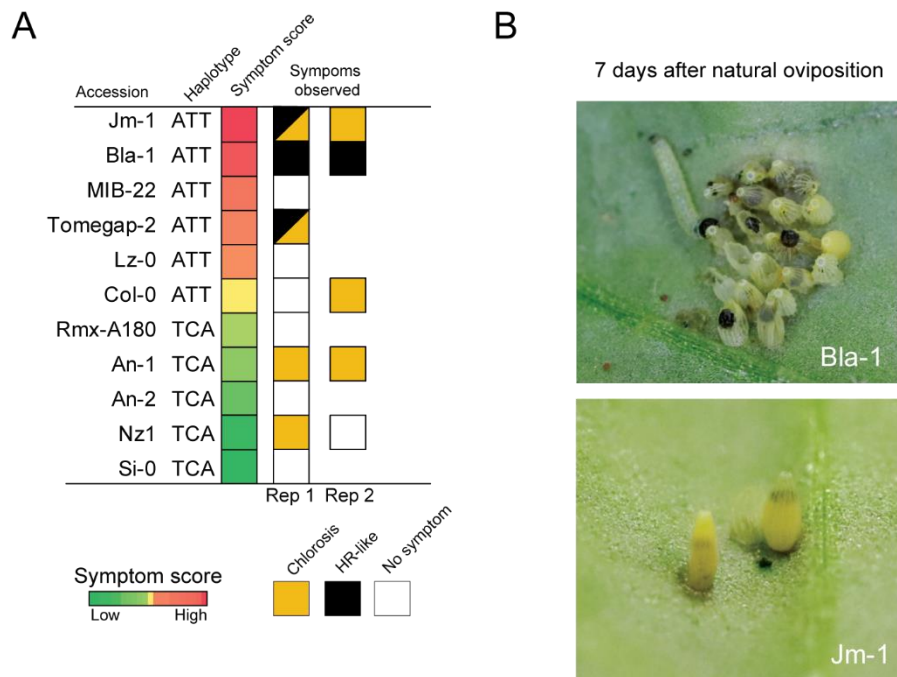


Figure 9. Correlation between HR-like symptoms and egg survival on accessions with low or high symptoms. A. Summary of the symptoms observed in different accessions 5 days after natural oviposition by *P. brassicae* in two independent experiments. Replicate 1 consisted of 4 plants per accessions and replicate 2 contained 5-8 plants per accessions. Butterflies were allowed to lay eggs on all accessions simultaneously and symptoms were noted 5 days after, corresponding to the natural hatching time of *P. brassicae*. Each plant received 1-5 egg batches on different leaves. B. Close-up pictures of dead egg batches 2 days after the natural hatching time on accessions Bla-1 and Jm-1. All eggs and emerging larvae are dead on the pictures as indicated by the absence of emergence after 7 days. In both cases, dead eggs were found on leaves displaying HR-like severe symptoms.

Symptoms and survival of *P. brassicae* eggs on different accessions

Based on the reported impact of HR-like symptoms on the survival of *P. brassicae* eggs, we explored whether the differential symptoms observed on diverse ecotypes treatment could translate into increased mortality upon natural oviposition. Butterflies laid around 1-5 egg batches on every plant and symptoms were observed 4 and 5 days after oviposition. We could observe that, globally, symptoms seem to correlate with the identity of the *GLR2.7* haplotype and with the strength of symptoms observed with egg extract (Fig. 9A), consistent with the identification of this region as being potentially involved in the response to eggs. Secondly, we observed few event where egg batches failed to hatch or larvae died while emerging as late as 7 days after oviposition on accessions carrying the *GLR2.7^{ATT}* haplotype (Fig. 9B). This indicates that the HR-like symptoms upon natural oviposition in Arabidopsis might be *GLR2.7*-dependent and that these symptoms can lead to increased egg mortality. It should be noted that these events were rare, making a proper quantification more complicated than on other species like *B. nigra*. Altogether, these data support a role *GLR2.7* during egg-induced HR-like response and provide evidence for an impact of this response on egg survival in Arabidopsis.

Discussion

The use of natural variation helps revealing unprecedented levels of details in the interactions between plant and insects by studying traits whose variation has been shaped through selection and drift, as opposed to the variation induced/observed in lab conditions (Tonsor et al., 2005). The understanding of plant responses to insect eggs is still scarce at the molecular levels but could provide useful tools for pest control (Fatouros et al., 2016; Tamiru et al., 2015). Here we identified of a novel locus associated with the severity of cell death developed upon the perception of insect eggs in *Arabidopsis*.

It is quite fascinating to observe such extensive variation in the response to *P. brassicae* eggs and egg extract in natural *Arabidopsis* accessions. Together with many phenotypes previously described such as cell death, ROS and SA accumulation, gene expression and the induction of systemic acquired resistance (SAR; (Little et al., 2007; Bruessow et al., 2010; Gouhier-Darimont et al., 2013, 2019), this observation further supports that egg extract can fully mimic the response to real *P. brassicae* eggs and thus represents a useful tool to dissect this response. Furthermore, this also seems to hold true for *B. nigra* (Bonnet et al., 2017). It is however noteworthy that *Arabidopsis* develops overall weaker HR-like symptoms than *B. nigra* and this could explain why no correlation between the severity of cell death and egg mortality was observed in *Arabidopsis* signaling mutants (Gouhier-Darimont et al., 2013). We could however observe few events where *P. brassicae* eggs failed to hatch on different accessions, and this correlated with the intensity of HR-like symptoms. Despite differences in overall intensity, there is increasing evidence that *Arabidopsis* and *B. nigra* trigger a similar, if not identical, response as shown by the presence of cell death (Shapiro and DeVay, 1987), defense gene expression and SA accumulation (Bonnet et al., 2017), and more recently sphingolipid profiles (see Chapter 1). Whether the difference in egg mortality between species truly depends on the absolute strength of the HR-like will deserve future attention.

Altogether, we provide clear evidence that the locus identified by the GWA mapping is causal for the variation in HR-like and SA levels observed. The results presented here reveal that i) the response of *Arabidopsis* to eggs of *P. brassicae* has a polygenic structure, with two loci accounting for a large proportion of the variation observed; ii) the *GLR2.7* haplotype associated with lower symptoms is not transcribed; iii) Ca^{2+} influx is an early response to egg extract. The first conclusion is consistent with the fact that quantitative disease resistance (QDR) is usually under the control of multiple genes (Roux et al., 2014; Corwin and Kliebenstein, 2017). The large effect associated with the *GLR2.7* locus in the accession panel most likely indicates it is an upstream component of the egg-induced response,

consistent with the strong association observed with total SA levels. Unfortunately, no function for this gene has so far been described. Plant *GLRs* are generally regarded as amino acid gated Ca^{2+} channels (Wudick et al., 2018). Consistent with an involvement of *GLR2.7*, we observed a fast and long lasting cytosolic Ca^{2+} increase after egg extract treatment. Intriguingly, this sustained Ca^{2+} wave resembles the response triggered by avirulent pathogens (Grant et al., 2000). To date, this is the fastest response to *P. brassicae* eggs to be observed. Furthermore, a fast diffusion of EAMP through the cuticle is consistent with the current hypothesis that egg lipids are responsible for this response (Müller and Riederer, 2005). The genetic structure observed at the *GLR2.7* provides strong evidence that it is involved in egg-induced responses. First of all, *GLR2.7* was found to be associated with both HR-like symptoms and SA levels, while variation in symptoms seems to involve a second identified locus. Despite being mildly correlated, both traits thus appear to have a partially overlapping genetic structures. Secondly, GWAS meta-analysis strongly suggests that this locus is specific to the response to insect eggs, as it was not associated with any other defense phenotype. Moreover, we observed that the *GLR2.7* locus consists mainly of two diverged haplotypes present through the entire *Arabidopsis* population studied. Both haplotypes are found at intermediate frequency independently of any geographic pattern, strongly suggesting that balancing selection contributes to their long-term maintenance (Wu et al., 2017). This hypothesis is further supported by the presence significant and positive Tajima's D and Fu and Li's D/F statistics in the coding sequence of *GLR2.7*. Recombination between homologous loci can blur selection signatures, potentially explaining why Tajima's D is significant only on short sequences (Koenig et al., 2019). Different selective processes can ultimately lead to the maintenance of genetic population and these are collectively referred to as balancing selection (Delph and Kelly, 2014). This type of selective process is opposed to purifying selection which eventually leads to a reduction in genetic variation. Remarkably, similar signatures of selection were previously observed at immune loci in *Arabidopsis* (Lastra et al., 2014; Todesco et al., 2010; Huard-Chauveau et al., 2013) and in the *Capsella* genus (Koenig et al., 2019). Given that *GLR2.7* was identified in a process related to direct defenses against insect eggs, it is conceivable the presence of a strong allele could confer a selective advantage in natural *Arabidopsis* populations exposed to insect oviposition by promoting stronger HR-like.

Finally, expression data show that accession possessing the *GLR2.7*^{TCA} do not produce transcript and accumulate premature stop codons. This is similar to the presence/absence genotype observed at the *RPM1* locus (Rose et al., 2012) or the production of a truncated transcript produced in some accessions at the *RKS1* locus (Huard-Chauveau et al., 2013) where, in both cases, higher resistance is associated with the

presence of a full length transcript. Moreover, several studies reported the existence of a presence/absence HR-like phenotype in *Brassicaceae* in response to oviposition by *P. brassicae* and *P. rapae* (Fatouros et al., 2015; Griese et al., 2019), consistent with the expression pattern and a potential role of *GLR2.7* during insect egg induced HR-like. Finally, HIF lines segregating for the *GLR2.7* locus confirmed that this region impacts symptom severity. However, this effect was background-dependent, suggesting the existence of additional loci interacting with the *GLR2.7* locus. QTL mapping using RILs derived from the same crosses would help identify these background-specific interactors. Altogether, our results are consistent with a specific role of *GLR2.7* in HR-like during insect egg-induced responses.

The potential role of *GLR2.7* in insect egg-induced responses

The identification of a *GLUTAMATE RECEPTOR-LIKE* gene as being associated with insect egg-induced cell death and SA induction raises several questions in terms of mechanism and function. This gene family was first described based on their homology to animal ionotropic glutamate receptors (iGluRs), yet phylogenetical analyses indicate that plant and animal GLRs diverged from a common ancestor. Phylogeny of *GLRs* in land plants indicates the existence of 4 main clades: clade I seems specific to *Brassicaceae* and clade II and III are present only in angiosperms (De Bortoli et al., 2016). As opposed to iGluR in animals which are mainly involved in neurotransmission, plant *GLRs* were shown to play roles in various developmental processes and stress responses (Lam et al., 1998; Price et al., 2012; De Bortoli et al., 2016). Consistent with our finding, this gene family was previously reported to be involved in pathogen and herbivore-triggered immunity (Kwaaitaal et al., 2011; Li et al., 2013; Mousavi et al., 2013). Plant *GLRs* are generally regarded as amino acid gated ion channels able to conduct Ca^{2+} (Wudick et al., 2018), although in most cases ligands are not known. In comparison to animal *iGluRs*, data gathered so far on plant *GLRs* indicate that they might have a broad ligand specificity: glutamate, but also glycine and more than 10 other amino acids, as well as more complex ligands such as glutathione may function as *GLR* agonists (Weiland et al., 2016). This is in line with the finding that the binding pocket appears to have diverged from human iGluRs, suggesting a plant-specific diversification of binding capabilities (Dubos et al., 2003). A structural modeling and docking approach of *GLR2.9*, a close homolog of *GLR2.7*, revealed that glycine is a probable agonist of the channel and that DNQX, an inhibitor of animal *iGluRs*, likely binds the ligand binding site (Dubos et al., 2003), suggesting a potentially conserved function in amino-acid sensing. Interestingly, extracellular concentrations of amino acids have been shown to increase after pathogen detection in tomato (Solomon and Oliver, 2001) and in common bean (O'Leary et al., 2016). Moreover, one study shows that active exocytosis of glutamate occurs upon

cryptogenin detection in tobacco cells, and PAMP-dependent Ca^{2+} fluxes were reduced in the presence of endocytosis and vesicle trafficking (Vatsa et al., 2011). This suggests that some *GLRs* may function by perceiving a secondary induced amino acid signal upon PTI induction. Consistent with this hypothesis, levels of several free amino-acids were found to increase after treatment with egg extract (Supplementary Fig. 12, data from Hilfiker et al., 2014). However, the origin (cellular or apoplastic) of the amino acids quantified is not known. Such mechanism is somewhat reminiscent of the perception of extracellular nucleotides by LecRK-I.8 and DORN1 (also known as LecRK-I.9). Both receptors were shown to bind NAD(P) and ATP respectively, and as mentioned LecRK-I.8 was also found to be involved in the perception of insect eggs (Wang et al., 2018; Gouhier-Darimont et al., 2013, 2019). Extracellular nucleotides are considered as damage-associated molecular patterns (DAMP) that are released upon tissue disruption and/or by some active process (Cao et al., 2014; Mou, 2017). Interestingly, DORN1-dependent perception of extracellular ATP (eATP) was shown to trigger Ca^{2+} fluxes, and chemical inhibition of Ca^{2+} channels inhibited downstream responses triggered by eNAD (Wang et al., 2018; Zhang and Mou, 2009). This is indicative of a link between LecRK receptors and calcium channels during early responses to DAMPs. However, in both cases the identity of the downstream Ca^{2+} channels is not known. Given that multiple clade I LecRK receptors may together be involved in the response to *P. brassicae* eggs (Gouhier-Darimont et al., 2019), it is tempting to speculate that *GLR2.7* alone or together with some other clade II GLR may participate in a similar signaling cascade downstream of clade I LecRKs. More work is clearly needed to test these hypotheses.

In conclusion, we have identified *GLR2.7* as a component of the insect egg perception pathway in Arabidopsis. While our data show that the genomic segment containing *GLR2.7* modulates HR-like, this effect was background-dependent, suggesting the existence of additional interacting loci. Future studies should focus on the precise description of *GLR2.7* and Ca^{2+} influx during this response. Moreover, the identification of the ligand responsible for *GLR2.7* activity will provide exciting insight into the way plants respond to insect eggs.

Acknowledgments

We would like to thank Envel Kerdaffrec for his help during GWA analyses and for sharing custom R scripts. We thank Dany Buffat for his technical assistance during the screening. We are also grateful to Nicolas Salamin and Anna Marcionetti for advices regarding the selection analyses.

References

- Ariga, H. et al.** (2017). NLR locus-mediated trade-off between abiotic and biotic stress adaptation in *Arabidopsis*. *Nat. Plants* **3**: 17072.
- Atwell, S. et al.** (2010). Genome-wide association study of 107 phenotypes in *Arabidopsis thaliana* inbred lines. *Nature* **465**: 627–31.
- Bakker, E.G., Toomajian, C., Kreitman, M., and Bergelson, J.** (2006). A Genome-Wide Survey of R Gene Polymorphisms in *Arabidopsis*. *Plant Cell* **18**: 1803–1818.
- Balint-Kurti, P.** (2019). The plant hypersensitive response: concepts, control and consequences. *Mol. Plant Pathol.* **0**: 1163–1178.
- Bittner, N., Trauer-Kizilelma, U., and Hilker, M.** (2017). Early plant defence against insect attack: involvement of reactive oxygen species in plant responses to insect egg deposition. *Planta* **245**: 993–1007.
- Bonnet, C., Lassueur, S., Ponzio, C., Gols, R., Dicke, M., and Reymond, P.** (2017). Combined biotic stresses trigger similar transcriptomic responses but contrasting resistance against a chewing herbivore in *Brassica nigra*. *BMC Plant Biol.* **17**: 127.
- De Bortoli, S., Teardo, E., Szabò, I., Morosinotto, T., and Alboresi, A.** (2016). Evolutionary insight into the ionotropic glutamate receptor superfamily of photosynthetic organisms. *Biophys. Chem.* **218**: 14–26.
- Bruessow, F., Gouhier-Darimont, C., Bruchala, A., Metraux, J.-P., and Reymond, P.** (2010). Insect eggs suppress plant defence against chewing herbivores. *Plant J.* **62**: 876–885.
- Cao, Y., Tanaka, K., Nguyen, C.T., and Stacey, G.** (2014). Extracellular ATP is a central signaling molecule in plant stress responses. *Curr. Opin. Plant Biol.* **20**: 82–7.
- Corwin, J.A. and Kliebenstein, D.J.** (2017). Quantitative Resistance: More Than Just Perception of a Pathogen. *Plant Cell* **29**: 655–665.
- Davila Olivas, N.H., Kruijer, W., Gort, G., Wijnen, C.L., van Loon, J.J.A., and Dicke, M.** (2017). Genome-wide association analysis reveals distinct genetic architectures for single and combined stress responses in *Arabidopsis thaliana*. *New Phytol.* **213**: 838–851.
- DeFraia, C.T., Schmelz, E.A., and Mou, Z.** (2008). A rapid biosensor-based method for quantification of free and glucose-conjugated salicylic acid. *Plant Methods* **4**: 28.
- Delph, L.F. and Kelly, J.K.** (2014). On the importance of balancing selection in plants. *New Phytol.* **201**: 45–56.
- Dubos, C., Huggins, D., Grant, G.H., Knight, M.R., and Campbell, M.M.** (2003). A role for glycine in the gating of plant NMDA-like receptors. *Plant J.* **35**: 800–810.
- Erb, M. and Reymond, P.** (2019). Molecular Interactions Between Plants and Insect Herbivores. *Annu. Rev. Plant Biol.* **70**: 1–31.
- Fatouros, N.E., Broekgaarden, C., Bukovinszkyne’Kiss, G., van Loon, J.J. a, Mumm, R., Huigens, M.E., Dicke, M., and Hilker, M.** (2008). Male-derived butterfly anti-aphrodisiac mediates induced indirect plant defense. *Proc. Natl. Acad. Sci. U. S. A.* **105**: 10033–8.
- Fatouros, N.E., Cusumano, A., Danchin, E.G.J., and Colazza, S.** (2016). Prospects of herbivore egg-killing plant defenses for sustainable crop protection. *Ecol. Evol.* **6**: 6906–6918.
- Fatouros, N.E., Paniagua Voirol, L.R., Drizou, F., Doan, Q.T., Pineda, A., Frago, E., and**

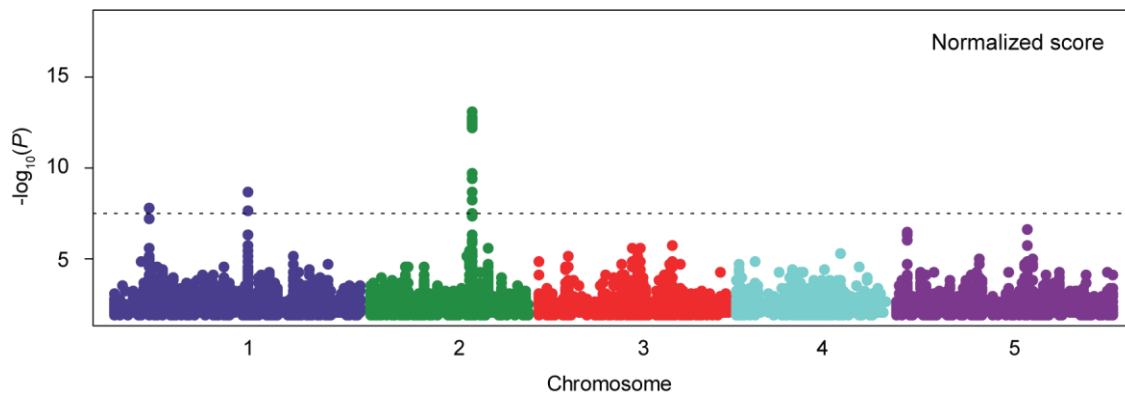
- van Loon, J.J. a.** (2015). Role of Large Cabbage White butterfly male-derived compounds in elicitation of direct and indirect egg-killing defenses in the black mustard. *Front. Plant Sci.* **6**: 1–9.
- Fatouros, N.E., Pineda, A., Huigens, M.E., Broekgaarden, C., Shimwela, M.M., Candia, I.A.F., Verbaarschot, P., and Bukovinszky, T.** (2014). Synergistic effects of direct and indirect defences on herbivore egg survival in a wild crucifer. *Proc. R. Soc. B Biol. Sci.* **281**: 20141254.
- Ferrero-Serrano, Á. and Assmann, S.M.** (2019). Phenotypic and genome-wide association with the local environment of *Arabidopsis*. *Nat. Ecol. Evol.* **3**: 274–285.
- Fu, Y.X. and Li, W.H.** (1993). Statistical tests of neutrality of mutations. *Genetics* **133**: 693–709.
- Garza, R., Vera, J., Cardona, C., Barcenas, N., and Singh, S.P.** (2001). Hypersensitive Response of Beans to *Apion godmani* (Coleoptera: Curculionidae). *J. Econ. Entomol.* **94**: 958–962.
- Geuss, D., Stelzer, S., Lortzing, T., and Steppuhn, A.** (2017). *Solanum dulcamara* 's response to eggs of an insect herbivore comprises ovicidal hydrogen peroxide production. *Plant. Cell Environ.* **40**: 2663–2677.
- Gouhier-Darimont, C., Schmiesing, A., Bonnet, C., Lassueur, S., and Reymond, P.** (2013). Signalling of *Arabidopsis thaliana* response to *Pieris brassicae* eggs shares similarities with PAMP-triggered immunity. *J. Exp. Bot.* **64**: 665–74.
- Gouhier-Darimont, C., Stahl, E., Glauser, G., and Reymond, P.** (2019). The *Arabidopsis* Lectin Receptor Kinase LecRK-I.8 Is Involved in Insect Egg Perception. *Front. Plant Sci.* **10**: 1–10.
- Grant, M., Brown, I., Adams, S., Knight, M., Ainslie, A., and Mansfield, J.** (2000). The RPM1 plant disease resistance gene facilitates a rapid and sustained increase in cytosolic calcium that is necessary for the oxidative burst and hypersensitive cell death. *Plant J.* **23**: 441–450.
- Griese, E., Dicke, M., Hilker, M., and Fatouros, N.E.** (2017). Plant response to butterfly eggs: inducibility, severity and success of egg-killing leaf necrosis depends on plant genotype and egg clustering. *Sci. Rep.* **7**: 7316.
- Griese, E., Pineda, A., Pashalidou, F.G., Iradi, E.P., and Hilker, M.** (2019). Plant responses to butterfly oviposition partly explain preference-performance relationships on different brassicaceous species. *bioRxiv*.
- Hilfiker, O., Groux, R., Bruessow, F., Kiefer, K., Zeier, J., and Reymond, P.** (2014). Insect eggs induce a systemic acquired resistance in *Arabidopsis*. *Plant J.* **80**: 1085–94.
- Hilker, M. and Fatouros, N.E.** (2015). Plant Responses to Insect Egg Deposition. *Annu. Rev. Entomol.* **60**: 493–515.
- Horton, M.W. et al.** (2012). Genome-wide patterns of genetic variation in worldwide *Arabidopsis thaliana* accessions from the RegMap panel. *Nat. Genet.* **44**: 212–6.
- Huard-Chauveau, C., Perchepied, L., Debieu, M., Rivas, S., Kroj, T., Kars, I., Bergelson, J., Roux, F., and Roby, D.** (2013). An Atypical Kinase under Balancing Selection Confers Broad-Spectrum Disease Resistance in *Arabidopsis*. *PLoS Genet.* **9**.
- Jones, J.D.G. and Dangl, J.L.** (2006). The plant immune system. *Nat. Rev.* **444**: 323–329.
- Kawakatsu, T. et al.** (2016). Epigenomic Diversity in a Global Collection of *Arabidopsis thaliana* Accessions. *Cell* **166**: 492–505.
- Kerdaffrec, E., Filiault, D.L., Korte, A., Sasaki, E., Nizhynska, V., Seren, Ü., and Nordborg, M.** (2016). Multiple alleles at a single locus control seed dormancy in Swedish *Arabidopsis*. *Elife* **5**: 1–24.

- Koenig, D., Hagmann, J., Li, R., Bemm, F., Slotte, T., Nueffer, B., Wright, S.I., and Weigel, D.** (2019). Long-term balancing selection drives evolution of immunity genes in *capsella*. *Elife* **8**: 1–27.
- Kwaaitaal, M., Huisman, R., Maintz, J., Reinstädler, A., and Panstruga, R.** (2011). Ionotropic glutamate receptor (iGluR)-like channels mediate MAMP-induced calcium influx in *Arabidopsis thaliana*. *Biochem. J.* **440**: 355–373.
- Lam, H.-M., Chiu, J., Hsieh, M.-H., Meisel, L., Oliveira, I.C., Shin, M., and Coruzzi, G.** (1998). Glutamate-receptor genes in plants. *Nature* **396**: 125–126.
- Lastra, R.O. et al.** (2014). The long-term maintenance of a resistance polymorphism through diffuse interactions. *Nature* **512**: 436–440.
- Li, F., Wang, J., Ma, C., Zhao, Y., Wang, Y., Hasi, A., and Qi, Z.** (2013). Glutamate Receptor-Like Channel3.3 Is Involved in Mediating Glutathione-Triggered Cytosolic Calcium Transients, Transcriptional Changes, and Innate Immunity Responses in *Arabidopsis*. *PLANT Physiol.* **162**: 1497–1509.
- Little, D., Gouhier-Darimont, C., Bruessow, F., and Reymond, P.** (2007). Oviposition by pierid butterflies triggers defense responses in *Arabidopsis*. *Plant Physiol.* **143**: 784–800.
- Lortzing, V., Oberländer, J., Lortzing, T., Tohge, T., Steppuhn, A., Kunze, R., and Hilker, M.** (2019). Insect egg deposition renders plant defence against hatching larvae more effective in a salicylic acid-dependent manner. *Plant. Cell Environ.* **42**: 1019–1032.
- Meng, D., Dubin, M., Zhang, P., Osborne, E.J., Stegle, O., Clark, R.M., and Nordborg, M.** (2016). Limited Contribution of DNA Methylation Variation to Expression Regulation in *Arabidopsis thaliana*. *PLOS Genet.* **12**: e1006141.
- Mou, Z.** (2017). Extracellular pyridine nucleotides as immune elicitors in *arabidopsis*. *Plant Signal. Behav.* **12**: e1388977.
- Mousavi, S.A.R., Chauvin, A., Pascaud, F., Kellenberger, S., and Farmer, E.E.** (2013). GLUTAMATE RECEPTOR-LIKE genes mediate leaf-to-leaf wound signalling. *Nature* **500**: 422–426.
- Müller, C. and Riederer, M.** (2005). Plant Surface Properties in Chemical Ecology. *J. Chem. Ecol.* **31**: 2621–2651.
- Nguyen, C.T., Kurenda, A., Stolz, S., Chételat, A., and Farmer, E.E.** (2018). Identification of cell populations necessary for leaf-to-leaf electrical signaling in a wounded plant. *Proc. Natl. Acad. Sci.*: 201807049.
- O’Leary, B.M., Neale, H.C., Geilfus, C.M., Jackson, R.W., Arnold, D.L., and Preston, G.M.** (2016). Early changes in apoplast composition associated with defence and disease in interactions between *Phaseolus vulgaris* and the halo blight pathogen *Pseudomonas syringae* Pv. *phaseolicola*. *Plant Cell Environ.* **39**: 2172–2184.
- Pashalidou, F.G., Lucas-Barbosa, D., van Loon, J.J. a, Dicke, M., and Fatouros, N.E.** (2013). Phenotypic plasticity of plant response to herbivore eggs: effects on resistance to caterpillars and plant development. *Ecology* **94**: 702–13.
- Petzold-Maxwell, J., Wong, S., Arellano, C., and Gould, F.** (2011). Host plant direct defence against eggs of its specialist herbivore, *Heliothis subflexa*. *Ecol. Entomol.* **36**: 700–708.
- Pieterse, C.M.J., Van der Does, D., Zamioudis, C., Leon-Reyes, A., and Van Wees, S.C.M.** (2012). Hormonal Modulation of Plant Immunity. *Annu. Rev. Cell Dev. Biol.* **28**: 489–521.
- Price, M.B., Jelesko, J., and Okumoto, S.** (2012). Glutamate Receptor Homologs in Plants: Functions and Evolutionary Origins. *Front. Plant Sci.* **3**: 1–10.

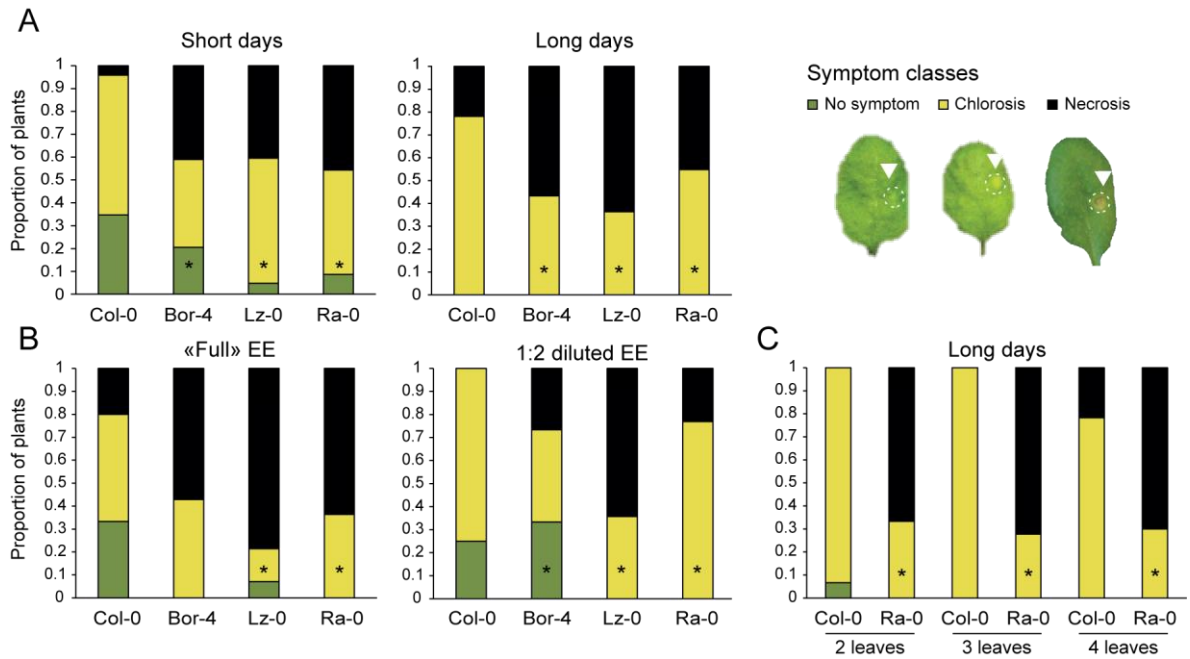
- Reymond, P.** (2013). Perception, signaling and molecular basis of oviposition-mediated plant responses. *Planta* **238**: 247–58.
- Rose, L., Atwell, S., Grant, M., and Holub, E.B.** (2012). Parallel Loss-of-Function at the RPM1 Bacterial Resistance Locus in *Arabidopsis thaliana*. *Front. Plant Sci.* **3**: 1–16.
- Roux, F., Voisin, D., Badet, T., Balagué, C., Barlet, X., Huard-Chauveau, C., Roby, D., and Raffaele, S.** (2014). Resistance to phytopathogens e tutti quanti: Placing plant quantitative disease resistance on the map. *Mol. Plant Pathol.* **15**: 427–432.
- Roy, B.C. and Mukherjee, A.** (2017). Computational analysis of the glutamate receptor gene family of *Arabidopsis thaliana*. *J. Biomol. Struct. Dyn.* **35**: 2454–2474.
- Schweizer, F., Fernández-Calvo, P., Zander, M., Diez-Diaz, M., Fonseca, S., Glauser, G., Lewsey, M.G., Ecker, J.R., Solano, R., and Reymond, P.** (2013). *Arabidopsis* basic helix-loop-helix transcription factors MYC2, MYC3, and MYC4 regulate glucosinolate biosynthesis, insect performance, and feeding behavior. *Plant Cell* **25**: 3117–32.
- Seino, Y., Suzuki, Y., and Sogawa, K.** (1996). An Ovicidal Substance Produced by Rice Plants in Response to Oviposition by the Whitebacked Planthopper, *Sogatella furcifera* (HORVATH) (Homoptera: Delphacidae). *Appl. Entomol. Zool.* **31**: 467–473.
- Seren, Ü., Vilhjálmsson, B.J., Horton, M.W., Meng, D., Forai, P., Huang, Y.S., Long, Q., Segura, V., and Nordborg, M.** (2012). GWAPP: A web application for genome-wide association mapping in *Arabidopsis*. *Plant Cell* **24**: 4793–805.
- Shapiro, A.M. and DeVay, J.E.** (1987). Hypersensitivity reaction of *Brassica nigra* L. (Cruciferae) kills eggs of *Pieris* butterflies (Lepidoptera: Pieridae). *Oecologia* **71**: 631–632.
- Solomon, P.S. and Oliver, R.P.** (2001). The nitrogen content of the tomato leaf apoplast increases during infection by *Cladosporium fulvum*. *Planta* **213**: 241–249.
- Tajima, F.** (1989). Statistical Method for Testing the Neutral Mutation Hypothesis by DNA Polymorphism. *Genetics*: 585–595.
- Tamiru, A., Khan, Z.R., and Bruce, T.J.** (2015). New directions for improving crop resistance to insects by breeding for egg induced defence. *Curr. Opin. Insect Sci.*
- Tang, D., Wang, G., and Zhou, J.-M.** (2017). Receptor Kinases in Plant-Pathogen Interactions: More Than Pattern Recognition. *Plant Cell* **29**: 618–637.
- The 1001 Genomes Consortium** (2016). 1,135 Genomes Reveal the Global Pattern of Polymorphism in *Arabidopsis thaliana*. *Cell* **166**: 481–491.
- Thoen, M.P.M. et al.** (2017). Genetic architecture of plant stress resistance: multi-trait genome-wide association mapping. *New Phytol.* **213**: 1346–1362.
- Todesco, M. et al.** (2010). Natural allelic variation underlying a major fitness trade-off in *Arabidopsis thaliana*. *Nature* **465**: 632–636.
- Togninalli, M., Seren, Ü., Meng, D., Fitz, J., Nordborg, M., Weigel, D., Borgwardt, K., Korte, A., and Grimm, D.G.** (2018). The AraGWAS Catalog: a curated and standardized *Arabidopsis thaliana* GWAS catalog. *Nucleic Acids Res.* **46**: D1150–D1156.
- Tonsor, S.J., Alonso-Blanco, C., and Koornneef, M.** (2005). Gene function beyond the single trait: Natural variation, gene effects, and evolutionary ecology in *Arabidopsis thaliana*. *Plant, Cell Environ.* **28**: 2–20.
- Vatsa, P., Chiltz, A., Bourque, S., Wendehenne, D., Garcia-Brugger, A., and Pugin, A.** (2011). Involvement of putative glutamate receptors in plant defence signaling and NO production. *Biochimie* **93**: 2095–2101.
- van Velzen, E. and Etienne, R.S.** (2015). The importance of ecological costs for the evolution of plant defense against herbivory. *J. Theor. Biol.* **372**: 89–99.

- Vila-Aiub, M.M., Neve, P., and Roux, F.** (2011). A unified approach to the estimation and interpretation of resistance costs in plants. *Heredity (Edinb)*. **107**: 386–394.
- Wang, C., Zhou, M., Zhang, X., Yao, J., Zhang, Y., and Mou, Z.** (2017). A lectin receptor kinase as a potential sensor for extracellular nicotinamide adenine dinucleotide in *Arabidopsis thaliana*. *Elife* **6**: 1–23.
- Wang, L., Wilkins, K.A., and Davies, J.M.** (2018). *Arabidopsis* DORN1 extracellular ATP receptor; activation of plasma membrane K⁺- and Ca²⁺-permeable conductances. *New Phytol.*: 1301–1304.
- Weiland, M., Mancuso, S., and Baluska, F.** (2016). Signalling via glutamate and GLRs in *Arabidopsis thaliana*. *Funct. Plant Biol.* **43**: 1.
- Wu, Q., Han, T.S., Chen, X., Chen, J.F., Zou, Y.P., Li, Z.W., Xu, Y.C., and Guo, Y.L.** (2017). Long-term balancing selection contributes to adaptation in *Arabidopsis* and its relatives. *Genome Biol.* **18**: 1–15.
- Wudick, M.M., Michard, E., Oliveira Nunes, C., and Feijó, J.A.** (2018). Comparing plant and animal glutamate receptors: Common traits but different fates? *J. Exp. Bot.* **69**: 4151–4163.
- Xu, Y.-C., Niu, X.-M., Li, X.-X., He, W., Chen, J.-F., Zou, Y.-P., Wu, Q., Zhang, Y.E., Busch, W., and Guo, Y.-L.** (2019). Adaptation and Phenotypic Diversification in *Arabidopsis* through Loss-of-Function Mutations in Protein-Coding Genes. *Plant Cell* **31**: 1012–1025.
- Yamasaki, M., Yoshimura, A., and Yasui, H.** (2003). Genetic basis of ovicidal response to whitebacked planthopper (*Sogatella furcifera* Horváth) in rice (*Oryza sativa* L.). *Mol. Breed.* **12**: 133–143.
- Yang Y, Xu J, Leng Y, Xiong G, Hu J, Zhang G, Huang L, Wang L, Guo L, Li J, et al.** (2014). Quantitative trait loci identification, fine mapping and gene expression profiling for ovicidal response to whitebacked planthopper (*Sogatella furcifera* Horvath) in rice (*Oryza sativa* L.). *BMC Plant Biol.* **14**: 145.
- Yang R** (2017). Genome-wide estimation of heritability and its functional components for flowering, defense, ionomics, and developmental traits in a geographically diverse population of *Arabidopsis thaliana*. *Genome* **60**: 572–580
- Zhang, X. and Mou, Z.** (2009). Extracellular pyridine nucleotides induce PR gene expression and disease resistance in *Arabidopsis*. *Plant J.* **57**: 302–312.
- Zvereva, A.S., Golyaev, V., Turco, S., Gubaeva, E.G., Rajeswaran, R., Schepetilnikov, M. V., Srour, O., Ryabova, L.A., Boller, T., and Pooggin, M.M.** (2016). Viral protein suppresses oxidative burst and salicylic acid-dependent autophagy and facilitates bacterial growth on virus-infected plants. *New Phytol.* **211**: 1020–1034.

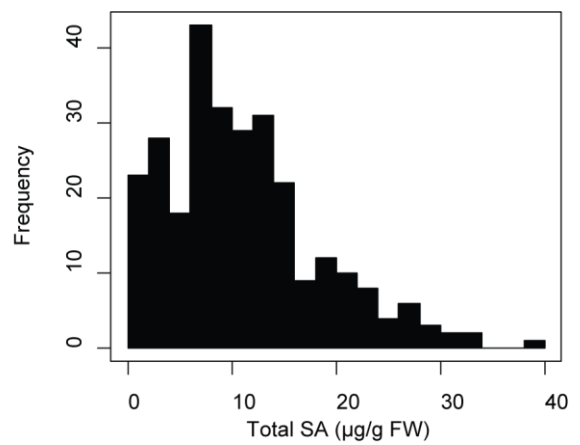
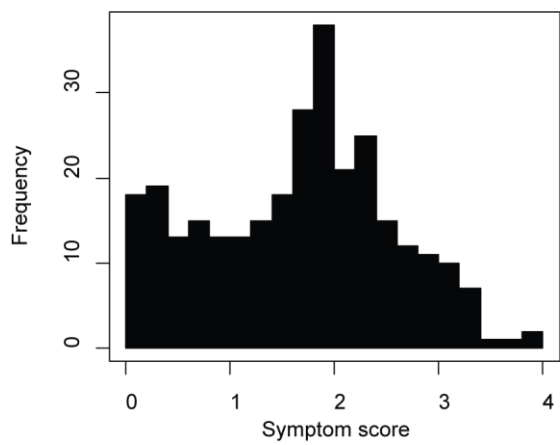
Supplementary Figures



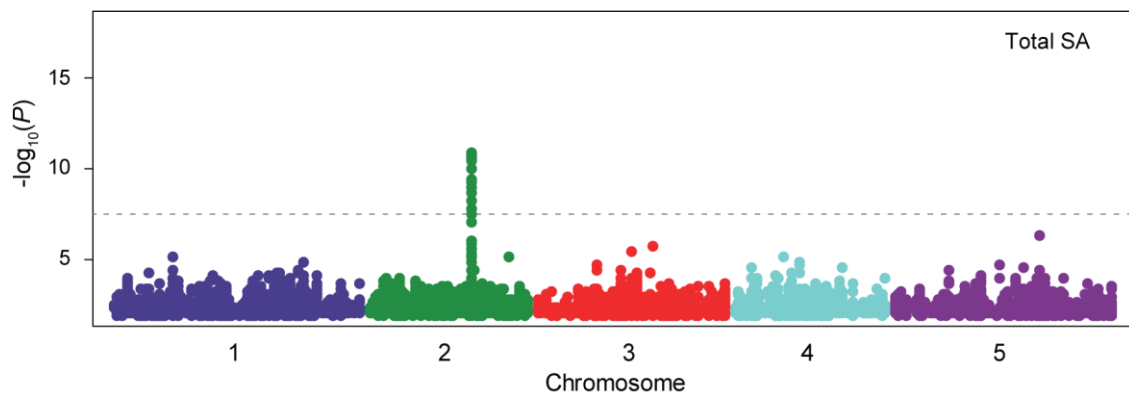
Supplementary Figure 1. Manhattan plot of GWA mapping for normalized score after 5 days of *P. brassicae* egg extract treatment using an accelerated mixed-model. Full imputed genotypes for all 295 accessions was used for mapping. Chromosomes are displayed in different colors and the dashed line indicate the Bonferonni-corrected significance at threshold $\alpha = 0.05$.



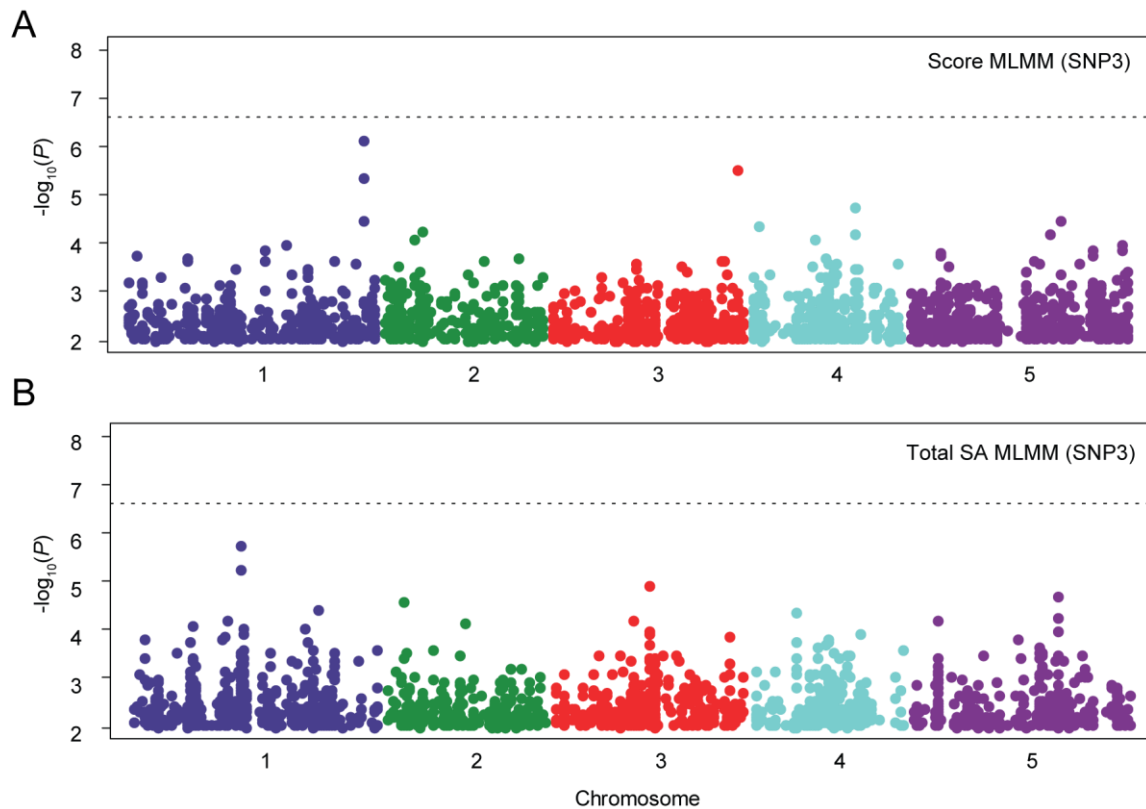
Supplementary Figure 2. A. Symptom distribution according to growth conditions after 5 days of egg-extract treatment. B. Symptom distribution depending on whether the egg extract was diluted 1:2 in distilled water or not (Full EE). C. Symptom distribution in Col-0 and Ra-0 after treatment of two, three or four leaves per plant. Unless otherwise specified, all experiments were carried out in short days condition and two leaves per plants were treated with -extract. Symptoms were observed from the adaxial side of the leaves and classified according to the legend on the right. Asterisks denote significant differences between a given accession and Col-0 at $P < 0.05$ (Fisher's exact test).



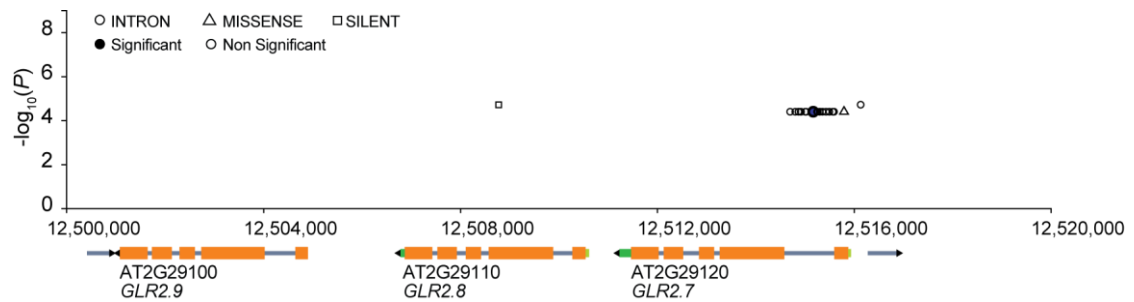
Supplementary Figure 3. Histograms representing the distribution of symptom scores and total SA after 5 days of egg extract treatment in the mapping population.



Supplementary Figure 4. Manhattan plot of GWA mapping for total SA after 5 days of *P. brassicae* egg extract treatment using an accelerated mixed-model. Full imputed genotypes for all 295 accessions was used for mapping. Chromosomes are displayed in different colors and the dashed line indicate the Bonferonni-corrected significance at threshold $\alpha = 0.05$.

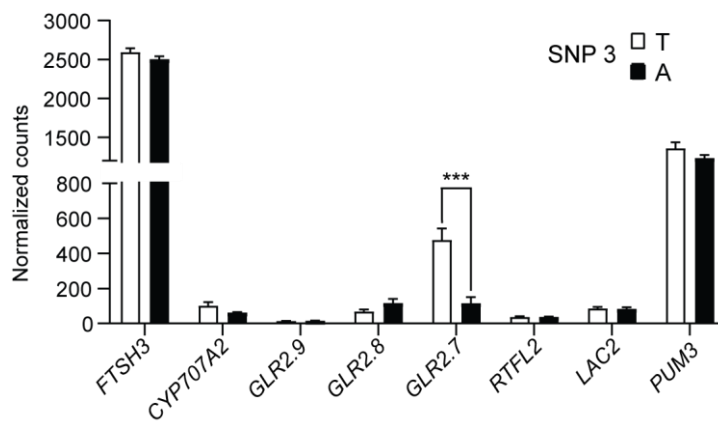


Supplementary Figure 5. GWA mapping using the multi-locus mixed model (MLMM) method. Manhattan plots for symptom score (A) or total SA (B) data using the multi-locus mixed model. Both plots were produced by incorporating the most significant marker (SNP3) as a cofactor for the MLMM algorithm. The chromosomes are displayed in different colors and the x-axis represent genomic position of markers. The dashed line indicates the Bonferonni corrected significance threshold at $\alpha = 0.05$.

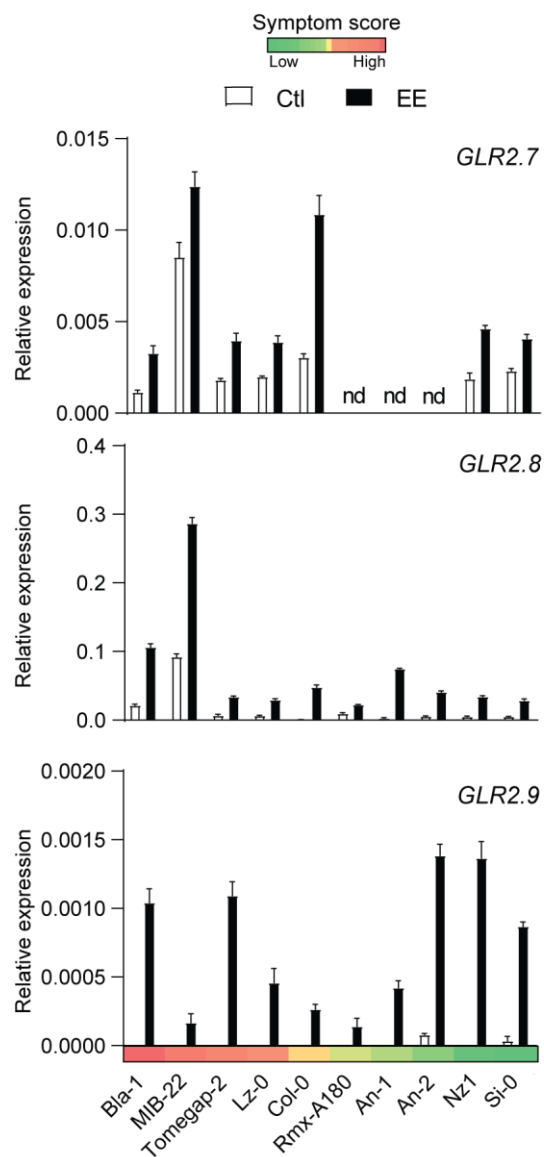


Supplementary Figure 6. Meta-analysis of association at the *GLR2.7* locus

Screenshot of associations from the AraGWAS database at the *GLR2.7* locus. X-axis represents genomic position along chromosome 2 and gene structures are shown below. Markers are shown depending on their genic position and on significance. Significance threshold were calculated based on permutations for each phenotype as described in Togninalli et al. 2018. Notice that none of the displayed marker reached significance. Only markers with MAF > 5% and MAC > 5 are shown.



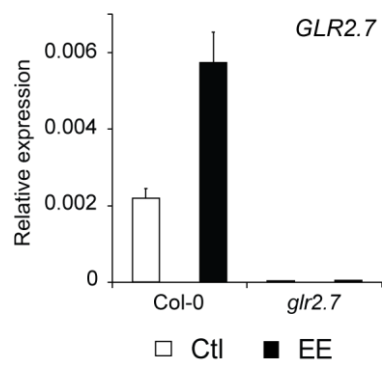
Supplementary Figure 7. Basal expression of genes in the vicinity of the *GLR2.7* locus
 RNA-seq data were selected for the accessions used in this study and expression levels are shown depending on the allele identified at SNP3 for all genes annotated in the vicinity of *GLR2.7*. Significance was assessed by 2-way ANOVA followed by TukeyHSD. ***, $P < 0.001$.



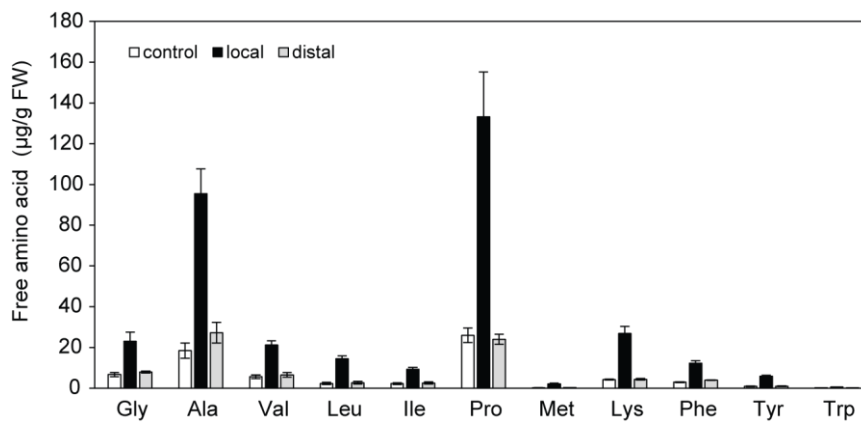
Supplementary Figure 9. *Glutamate Receptor-Like* expression in 10 ecotypes with low and high symptoms
 Expression of *GLR2.7* (A), *GLR2.8* (B) or *GLR2.9*(C) in 10 accessions after 72h of egg-extract treatment. Colors above accession names represent average symptom score. Gene expression was monitored by qPCR and target gene transcript level was normalized to the reference gene SAND. Means \pm standard error (SE) of three technical replicates are shown. This experiment was repeated twice with similar results.



Supplementary Figure 10. Levels of cytosine methylation around *GLR2.7* in diverse accessions. Snapshot of the 1001 Epigenomes browser (<http://neomorph.salk.edu/1001.php>) showing the levels of cytosine methylation in *GLR2.7*, *GLR2.8* and *GLR2.9* in various accessions arranged according to their symptom score (next to accessions names). Only accessions that were used for gene expression analysis were considered. The different sequence contexts for cytosine methylation are shown with different colors.



Supplementary Figure 11. Expression of *GLR2.7* in the T-DNA insertion line SALK_121990 after 72h of egg-extract treatment. Gene expression was monitored by qPCR and target gene transcript level was normalized to the reference gene *SAND*. Means \pm standard error (SE) of three technical replicates are shown. This experiment was repeated once with similar results.



Supplementary Figure 12. Free amino acid levels after egg extract treatment

Free amino acid levels were quantified in local or distal leaves following 5 days of treatment with *P. brassicae* egg-extract. For sake of clarity, only amino acids whose levels were changing upon treatment are displayed. The data reproduced here are taken from Hilfiker et al. 2014 with permission. Refer to the the publication for additional details.

Supplementary Tables

Supplementary table 1. List of the 295 diverse accessions used in this study. Name, accession ID and NASC line number are provided. Longitude and Latitude refer to geographical coordinates of the collection site, while “sequenced” indicates whether a given accession was sequenced as part of the 1001 Genomes project.

Accession name	Accession ID	NASC number	Country	Latitude	Longitude	Sequenced?
ALL1-2	1	N76089	FRA	45.2667	1.48333	
ALL1-3	2	N76090	FRA	45.2667	1.48333	
CAM-16	23	N76107	FRA	48.2667	-4.58333	
CAM-61	66	N76108	FRA	48.2667	-4.58333	
CUR-3	81	N76115	FRA	45	1.75	
JEA	91	N76148	FRA	43.6833	7.33333	
LAC-3	94	N76157	FRA	47.7	6.81667	
LAC-5	96	N76158	FRA	47.7	6.81667	
LDV-58	149	N76163	FRA	48.5167	-4.06667	
MIB-15	166	N76181	FRA	47.3833	5.31667	
MIB-22	173	N76182	FRA	47.3833	5.31667	
MIB-28	178	N76183	FRA	47.3833	5.31667	
MIB-84	223	N76184	FRA	47.3833	5.31667	
MOG-37	242	N76189	FRA	48.6667	-4.06667	
PAR-3	258	N76205	FRA	46.65	-0.25	
PAR-4	259	N76206	FRA	46.65	-0.25	
PAR-5	260	N76207	FRA	46.65	-0.25	
ROM-1	267	N76221	FRA	45.5333	4.85	
TOU-A1-115	281	N76252	FRA	46.6667	4.11667	
TOU-A1-116	282	N76253	FRA	46.6667	4.11667	
TOU-A1-43	321	N76255	FRA	46.6667	4.11667	
TOU-A1-62	328	N76256	FRA	46.6667	4.11667	
TOU-A1-96	357	N76258	FRA	46.6667	4.11667	
TOU-C-3	362	N76259	FRA	46.6667	4.11667	
TOU-E-11	366	N76260	FRA	46.6667	4.11667	
TOU-H-12	373	N76261	FRA	46.6667	4.11667	
TOU-H-13	374	N76262	FRA	46.6667	4.11667	
TOU-I-17	378	N76263	FRA	46.6667	4.11667	
TOU-I-6	380	N76265	FRA	46.6667	4.11667	
TOU-J-3	383	N76266	FRA	46.6667	4.11667	
VOU-1	390	N76299	FRA	46.65	0.166667	
VOU-2	392	N76300	FRA	46.65	0.166667	
LI-OF-095	641	N76165	USA	40.7777	-72.9069	
Belmonte-4-94	957	N76095	ITA	42.1167	12.4833	
KBS-Mac-8	1716	N76151	USA	42.405	-85.398	
MNF-Pot-48	1859	N76187	USA	43.595	-86.2657	
MNF-Pot-68	1867	N76188	USA	43.595	-86.2657	
MNF-Jac-32	1967	N76186	USA	43.5187	-86.1739	
Map-42	2057	N76180	USA	42.166	-86.412	Yes
Paw-3	2150	N76208	USA	42.148	-86.431	
Pent-1	2187	N76209	USA	43.7623	-86.3929	
SLSP-30	2274	N76228	USA	43.665	-86.496	
Ste-3	2290	N76232	USA	42.03	-86.514	
UKSW06-202	4802	N76292	UK	50.4	-4.9	
UKSE06-062	4997	N76280	UK	51.3	0.5	
UKSE06-192	5056	N76281	UK	51.3	0.5	
UKSE06-272	5116	N76282	UK	51.3	0.4	

Accession name	Accession ID	NASC number	Country	Latitude	Longitude	Sequenced?
UKSE06-349	5158	N76284	UK	51.3	0.4	
UKSE06-351	5160	N76285	UK	51.3	0.4	
UKSE06-414	5202	N76286	UK	51.3	0.4	
UKSE06-429	5207	N76287	UK	51.3	0.4	
UKSE06-466	5232	N76288	UK	51.2	0.4	
UKSE06-520	5264	N76290	UK	51.3	1.1	
UKSE06-628	5341	N76291	UK	51.1	0.4	
UKNW06-059	5380	N76275	UK	54.4	-3	
UKNW06-060	5381	N76276	UK	54.4	-3	
UKNW06-386	5565	N76277	UK	54.6	-3.1	
UKNW06-436	5606	N76278	UK	54.7	-3.4	
UKNW06-460	5628	N76279	UK	54.7	-3.4	
Bur-0	5719	N76105	IRL	53.08	-9.0755	
UKID22	5729	N76271	UK	54.7	-3.4	
UKID37	5742	N76272	UK	51.3	1.1	
UKID80	5785	N76274	UK	54.7	-2.9	
App1-16	5832	N76092	SWE	56.3333	15.9667	Yes
Bor-1	5837	N76099	CZE	49.4013	16.2326	Yes
DralV1-14	5896	N76119	CZE	49.4112	16.2815	
DralV6-16	5987	N76122	CZE	49.4112	16.2815	
DralV6-35	6005	N76123	CZE	49.4112	16.2815	
Duk	6008	N76124	CZE	49.1	16.2	Yes
Fja1-2	6019	N76131	SWE	56.06	14.29	Yes
Fja1-5	6020	N76132	SWE	56.06	14.29	Yes
Lom1-1	6042	N76174	SWE	56.09	13.9	Yes
Lov-5	6046	N76175	SWE	62.801	18.079	Yes
Or-1	6074	N76201	SWE	56.4573	16.1308	Yes
Rev-2	6076	N76219	SWE	55.6942	13.4504	Yes
Sparta-1	6085	N76229	SWE	55.7097	13.2145	Yes
T1040	6094	N76233	SWE	55.6494	13.2147	Yes
T1060	6096	N76234	SWE	55.6472	13.2225	Yes
T1080	6098	N76235	SWE	55.6561	13.2178	Yes
T1110	6100	N76236	SWE	55.6	13.2	Yes
T1130	6102	N76237	SWE	55.6	13.2	Yes
T690	6124	N76241	SWE	55.8378	13.3092	Yes
Tad01	6169	N76243	SWE	62.8714	18.3447	Yes
TDr-1	6188	N76245	SWE	55.7683	14.1386	Yes
TDr-3	6190	N76248	SWE	55.7686	14.1381	
TDr-8	6194	N76249	SWE	55.7706	14.1342	Yes
TDr-18	6203	N76247	SWE	55.7714	14.1208	Yes
Tomegap-2	6242	N76250	SWE	55.7	13.2	Yes
Tottarp-2	6243	N76251	SWE	56.27373	13.90045	Yes
Udul1-34	6318	N76269	CZE	49.2771	16.6314	
UII3-4	6413	N76295	SWE	56.06	13.97	Yes
ZdrI2-25	6449	N76308	CZE	49.3853	16.2544	
Bg2	6709	N76096	USA	47.6479	-122.305	
CIBC2	6727	N28140	UK	51.4083	-0.6383	
CIBC5	6730	N28142	UK	51.4083	-0.6383	
Cold Spring Harbor Lab-5	6744	N28181	USA	40.8585	-73.4675	Yes
NFC20	6847	N28550	UK	51.4083	-0.6383	
Ag-0	6897	N76087	FRA	45	1.3	Yes
An-1	6898	N76091	BEL	51.2167	4.4	Yes
Bay-0	6899	N76094	GER	49	11	

Accession name	Accession ID	NASC number	Country	Latitude	Longitude	Sequenced?
Bor-4	6903	N76100	CZE	49.4013	16.2326	Yes
Br-0	6904	N76101	CZE	49.2	16.6166	Yes
C24	6906	N76106	POR	40.2077	-8.42639	
CIBC17	6907	N76111	UK	51.4083	-0.6383	Yes
Col-0	6909	N76113	USA	38.3	-92.3	Yes
Ct-1	6910	N76114	ITA	37.3	15	
Cvi-0	6911	N76116	CPV	15.1111	-23.6167	Yes
Edi-0	6914	N76126	UK	55.9494	-3.16028	
Fab-4	6918	N76128	SWE	63.0165	18.3174	Yes
Ga-0	6919	N76133	GER	50.3	8	Yes
Got-7	6921	N76136	GER	51.5338	9.9355	
HR-5	6924	N76144	UK	51.4083	-0.6383	Yes
Kin-0	6926	N76153	USA	44.46	-85.37	Yes
Kno-18	6928	N76154	USA	41.2816	-86.621	
Ler-1	6932	N76164	GER	47.984	10.8719	Yes
LL-0	6933	N76172	ESP	41.59	2.49	Yes
Lz-0	6936	N76179	FRA	46	3.3	
Mrk-0	6937	N76191	GER	49	9.3	
Mt-0	6939	N76192	LIB	32.34	22.46	
Mz-0	6940	N76193	GER	50.3	8.3	Yes
Nd-1	6942	N76197	GER	50	10	
NFA-10	6943	N76198	UK	51.4083	-0.6383	Yes
Oy-0	6946	N76203	NOR	60.39	6.19	
Pu2-23	6951	N76215	CZE	49.42	16.36	Yes
Ra-0	6958	N76216	FRA	46	3.3	Yes
Rennes-1	6959	N76218	FRA	48.5	-1.41	Yes
Se-0	6961	N76226	ESP	38.3333	-3.53333	Yes
Sha	6962	N76227	TJK	38.35	68.48	
Tamm-2	6968	N76244	FIN	60	23.5	Yes
Ts-1	6970	N76268	ESP	41.7194	2.93056	Yes
UII2-3	6973	N76293	SWE	56.0648	13.9707	Yes
UII2-5	6974	N76294	SWE	56.0648	13.9707	Yes
Uod-7	6976	N76296	AUT	48.3	14.45	Yes
Van-0	6977	N76297	CAN	49.3	-123	
Wa-1	6978	N28804	POL	52.3	21	
Wei-0	6979	N76301	SUI	47.25	8.26	Yes
Ws-0	6980	N76303	RUS	52.3	30	
Wt-5	6982	N76304	GER	52.3	9.3	Yes
Yo-0	6983	N76305	USA	37.45	-119.35	
Zdr-6	6985	N76306	CZE	49.3853	16.2544	
Alc-0	6988	N76088	ESP	40.49	-3.36	
Amel-1	6990	N28014	NED	53.448	5.73	Yes
Ann-1	6994	N28049	FRA	45.9	6.13028	
An-2	6996	N28017	BEL	51.2167	4.4	
Aa-0	7000	N28007	GER	50.9167	9.57073	Yes
Baa-1	7002	N28054	NED	51.3333	6.1	Yes
Bs-2	7004	N28097	SUI	47.5	7.5	
Benk-1	7008	N28064	NED	52	5.675	Yes
Ba-1	7014	N28053	UK	56.5459	-4.79821	Yes
Bla-1	7015	N76097	ESP	41.6833	2.8	
Boot-1	7026	N28091	UK	54.4	-3.2667	Yes
Bsch-0	7031	N28099	GER	50.0167	8.6667	Yes
Blh-1	7034	N76098	CZE	48.3	19.85	
Blh-2	7035	N28090	CZE	48	19	

Accession name	Accession ID	NASC number	Country	Latitude	Longitude	Sequenced?
Ca-0	7062	N28128	GER	50.2981	8.26607	Yes
Cnt-1	7064	N28160	UK	51.3	1.1	Yes
Cha-0	7069	N28133	SUI	46.0333	7.1167	
Chat-1	7071	N28135	FRA	48.0717	1.33867	Yes
Cit-0	7075	N28158	FRA	43.3779	2.54038	
Co-2	7078	N28163	POR	40.12	-8.25	
Co-4	7080	N28165	POR	40.12	-8.25	
Com-1	7092	N28193	FRA	49.416	2.823	Yes
Da-0	7094	N28200	GER	49.8724	8.65081	Yes
Di-1	7098	N28208	FRA	47	5	
Db-0	7100	N28202	GER	50.3055	8.324	
Do-0	7102	N28210	GER	50.7224	8.2372	Yes
Dra-2	7105	N28214	CZE	49.4167	16.2667	
Ede-1	7110	N28217	NED	52.0333	5.66667	
Ep-0	7123	N28236	GER	50.1721	8.38912	
Es-0	7126	N28241	FIN	60.1997	24.5682	Yes
Est-0	7128	N28243	RUS	58.3	25.3	
Fr-4	7135	N28268	GER	50.1102	8.6822	
Fi-1	7139	N28252	GER	50.5	8.0167	
Ga-2	7141	N28274	GER	50.3	8	
Gel-1	7143	N28279	NED	51.0167	5.86667	Yes
Ge-1	7145	N28277	SUI	46.5	6.08	
Gü -1	7150	N28332	GER	50.3	8	
Gö-0	7151	N28282	GER	51.5338	9.9355	
Gr-5	7158	N28326	AUT	47	15.5	Yes
Ha-0	7163	N28336	GER	52.3721	9.73569	Yes
Hau-0	7164	N28343	DEN	55.675	12.5686	Yes
Hn-0	7165	N28350	GER	51.3472	8.28844	Yes
Hey-1	7166	N28344	NED	51.25	5.9	
Hh-0	7169	N28345	GER	54.4175	9.88682	Yes
Jm-1	7178	N28373	CZE	49	15	
Kelsterbach -2	7188	N28382	GER	50.0667	8.5333	
Kl-5	7199	N28394	GER	50.95	6.9666	Yes
Kr-0	7201	N28419	GER	51.3317	6.55934	
Kro-0	7206	N28420	GER	50.0742	8.96617	
Li-3	7224	N28454	GER	50.3833	8.0666	
Li-5:2	7227	N28457	GER	50.3833	8.0666	
Li-6	7229	N28459	GER	50.3833	8.0666	
Li-7	7231	N28461	GER	50.3833	8.0666	Yes
Mnz-0	7244	N28495	GER	50.001	8.26664	Yes
Mc-0	7252	N28490	UK	54.6167	-2.3	
Mh-0	7255	N28492	POL	50.95	20.5	Yes
Nw-0	7258	N28573	GER	50.5	8.5	Yes
Nw-2	7260	N28575	GER	50.5	8.5	
Nz1	7263	N28578	NZL	-37.7871	175.283	
No-0	7275	N28564	GER	51.0581	13.2995	
Ob-1	7277	N28580	GER	50.2	8.5833	
Old-1	7280	N28583	GER	53.1667	8.2	Yes
Or-0	7282	N28587	GER	50.3827	8.01161	Yes
Ors-1	7283	N28848	ROU	44.7203	22.3955	
Ors-2	7284	N28849	ROU	44.7203	22.3955	
Petergof	7296	N76211	RUS	59	29	Yes
Pla-0	7300	N28640	ESP	41.5	2.25	
Rhen-1	7316	N28685	NED	51.9667	5.56667	Yes

Accession name	Accession ID	NASC number	Country	Latitude	Longitude	Sequenced?
Sh-0	7331	N28734	GER	51.6832	10.2144	
Sei-0	7333	N28729	ITA	46.5438	11.5614	Yes
Si-0	7337	N28739	GER	50.8738	8.02341	Yes
Sp-0	7343	N28743	GER	52.5339	13.181	Yes
Sg-1	7344	N28732	GER	47.6667	9.5	Yes
Ty-0	7351	N28786	UK	56.4278	-5.23439	
Tha-1	7353	N28758	NED	52.08	4.3	Yes
Ting-1	7354	N28759	SWE	56.5	14.9	Yes
Tiv-1	7355	N28760	ITA	41.96	12.8	
Tscha-1	7372	N28779	AUT	47.0748	9.9042	Yes
Tsu-0	7373	N28780	JPN	34.43	136.31	Yes
Uk-1	7378	N28787	GER	48.0333	7.7667	Yes
Utrecht	7382	N28795	NED	52.0918	5.1145	Yes
Wag-3	7390	N28808	NED	51.9666	5.6666	
Wag-4	7391	N28809	NED	51.9666	5.6666	
Wag-5	7392	N28810	NED	51.9666	5.6666	
Ws	7397	N28823	RUS	52.3	30	
Wc-2	7405	N28814	GER	52.6	10.0667	
Wt-3	7408	N28833	GER	52.3	9.3	
Wl-0	7411	N28822	GER	47.9299	10.8134	Yes
Zu-1	7418	N28847	SUI	47.3667	8.55	Yes
Nc-1	7430	N28527	FRA	48.6167	6.25	Yes
N13	7438	N76194	RUS	61.36	34.15	
N4	7446	N28510	RUS	61.36	34.15	
N7	7449	N28513	RUS	61.36	34.15	
WAR	7477	N28812	USA	41.7302	-71.2825	Yes
PHW-10	7479	N28610	UK	51.2878	0.0565	
PHW-13	7482	N28613	UK	51.2878	0.0565	
PHW-20	7490	N28620	UK	51.2878	0.0565	
PHW-26	7496	N28626	UK	50.6728	-3.8404	
PHW-28	7498	N28628	UK	50.35	-3.5833	
PHW-31	7502	N28631	UK	51.4666	-3.2	
PHW-33	7504	N28633	NED	52.25	4.5667	
PHW-36	7507	N28636	FRA	48.6103	2.3086	
PHW-37	7508	N28637	FRA	48.6103	2.3086	
Var2-1	7516	N76298	SWE	55.58	14.334	Yes
Omo2-1	7518	N76200	SWE	56.14	15.78	
Lp2-2	7520	N76176	CZE	49.38	16.81	Yes
Lp2-6	7521	N76177	CZE	49.38	16.81	Yes
Mr-0	7522	N76190	ITA	44.15	9.65	
Pna-17	7523	N76213	USA	42.0945	-86.3253	Yes
Rmx-A180	7525	N76220	USA	42.036	-86.511	Yes
Pro-0	8213	N76214	ESP	43.25	-6	
Fei-0	8215	N76129	POR	40.5	-8.32	
Lis-2	8222	N76170	SWE	56.0328	14.775	Yes
Bro1-6	8231	N76102	SWE	56.3	16	Yes
Hod	8235	N76141	CZE	48.8	17.1	Yes
HSm	8236	N76146	CZE	49.33	15.76	Yes
PHW-3	8239	N76155	GER	51	7	Yes
Liarum	8241	N76166	SWE	55.9473	13.821	Yes
Lillo-1	8242	N76167	SWE	56.1494	15.7884	Yes
Ba1-2	8256	N76093	SWE	56.4	12.9	Yes
Bu-0	8271	N76103	GER	50.5	9.5	
Can-0	8274	N76109	ESP	29.2144	-13.4811	

Accession name	Accession ID	NASC number	Country	Latitude	Longitude	Sequenced?
Cen-0	8275	N76110	FRA	49	0.5	
Dra3-1	8283	N76117	SWE	55.76	14.12	Yes
Gd-1	8296	N76134	GER	53.5	10.5	
Ge-0	8297	N76135	SUI	46.5	6.08	Yes
Gr-1	8300	N76137	AUT	47	15.5	
Hi-0	8304	N76140	NED	52	5	
Hov4-1	8306	N76142	SWE	56.1	13.74	Yes
Hs-0	8310	N76145	GER	52.24	9.44	
In-0	8311	N76147	AUT	47.5	11.5	Yes
Ka-0	8314	N76149	AUT	47	14	
Lc-0	8323	N76159	UK	57	-4	
Lip-0	8325	N76168	POL	50	19.3	
Lis-1	8326	N76169	SWE	56.0328	14.775	Yes
Lm-2	8329	N76173	FRA	48	0.5	
Lund	8335	N76178	SWE	55.71	13.2	Yes
Na-1	8343	N76195	FRA	47.5	1.5	Yes
Ost-0	8351	N76202	SWE	60.25	18.37	Yes
Pa-1	8353	N76204	ITA	38.07	13.22	
Per-1	8354	N76210	RUS	58	56.3167	Yes
Rak-2	8365	N76217	CZE	49	16	Yes
Rsch-4	8374	N76222	RUS	56.3	34	
Sanna-2	8376	N76223	SWE	62.69	18	Yes
Sap-0	8378	N76224	CZE	49.49	14.24	
St-0	8387	N76231	SWE	59	18	Yes
Ta-0	8389	N76242	CZE	49.5	14.5	
Sav-1	8412	N76225	CZE	49.1833	15.8833	
Kelsterbach -4	8420	N76152	GER	50.0667	8.5333	Yes
Fja1-1	8422	N76130	SWE	56.06	14.29	Yes
Kas-2	8424	N76150	IND	35	77	Yes
Lisse	8430	N76171	NED	52.25	4.5667	
11ME1.32	8610	N76083	USA	42.093	-86.359	
328PNA054	8692	N76085	USA	42.0945	-86.3253	
11PNA4.101	8796	N76084	USA	42.0945	-86.3253	

Supplementary Table 2. List of primers used for quantitative-PCR experiments.

Gene name	Gene ID	Primer ID	Sequence (3'-5')	Reference
SAND	At2g28390	SAND_fw	AACTCTATGCAGCATTGATCCACT	
		SAND_rev	TGATTGCATATCTTTATCGCCATC	
PR1	At2g14610	PR1-Fw	GTGGGTTAGCGAGAAGGCTA	
		PR1-Rv	ACTTTGGCACATCCGAGTCT	
GLR2.7	AT2G29120	GLR2.7_fw	AGTTATCCTTTCTCAGAATTCC	This work
		GLR2.7_rev	CAATATGTTGCATTTCTTCGCC	
GLR2.8	AT2G29110	GLR2.8_fw	CAATACTGCTCCAAATATGCC	This work
		GLR2.8_rev	CCTGTCAAAGGTGAATTCCTG	
GLR2.9	AT2G29100	GLR2.9_fw	TCAATCCTGCTCTAAATATGTC	This work
		GLR2.9_rev	CTCGATTTGTTGCGTTACATTG	

Supplementary Table 3. List of all significantly associated mutations in the *GLR2.7* coding region. Mutations in bold indicate non-synonymous substitutions as compared to Col-0 reference allele.

Position on Chr. 2	Mutation
12511933	P802Q
12512197	S749C
12512383	F687Y
12512425	L673R
12512429	K672Q
12513017	S582
12513027	R579K
12513065	V566
12513122	R547
12513134	I543
12513164	A533
12513166	A533T
12513316	E520D
12513317	E520G
12513390	I496V
12513391	E495D
12513467	K470T
12513470	K469M
12513471	K469*
12513472	V468
12513495	M461L
12513499	G459
12513533	D448V
12513601	K425
12514453	T141
12515737	K53Q

Chapter 3

L-type LECTIN RECEPTOR KINASE-I.1 contributes to insect egg-induced cell death

Raphaël Groux, Caroline Gouhier-Darimont, Philippe Reymond.

Department of Plant Molecular Biology, University of Lausanne, 1015 Lausanne, Switzerland

Abstract

In *Arabidopsis thaliana*, a hypersensitive-like response (HR-like) is triggered underneath the eggs of the large white butterfly *Pieris brassicae*, and this response is dependent on salicylic acid (SA) accumulation and signaling. Previous reports indicate that the clade I L-type lectin receptor kinase LecRK-I.8 is possibly involved in egg perception. Genome-wide association (GWA) mapping was used to better characterize the genetic structure of HR-like and discover loci that contribute to this response. We report here the identification of LecRK-I.1, a close homolog of LecRK-I.8, and show that two main haplotypes segregate amongst natural *Arabidopsis* accessions and account for the observed variation. In addition, signatures of balancing selection at this locus suggest that this locus may be ecologically important. Functionally, disruption of LecRK-I.1 resulted in decreased HR-like while SA-dependent signaling was unaffected, suggesting that it is specifically involved in the induction of cell death. Furthermore, we provide evidence that LecRK-I.1 functions in the same pathway than LecRK-I.8. Altogether, our result show that the response to eggs of *P. brassicae* are controlled by LecRKs that operate at various steps of the signaling pathway.

Introduction

Despite representing a future threat, eggs of herbivorous insects deposited on plant surfaces are immobile and inert structures. Plants are able to sense egg presence and respond accordingly through diverse defense outputs (Reymond, 2013; Hilker and Fatouros, 2015). Two often co-occurring strategies have been described as impacting egg survival: direct defenses such as tissue growth (Desurmont and Weston, 2011; Petzold-Maxwell et al., 2011; Doss et al., 2000) or cell death (Shapiro and DeVay, 1987; Fatouros et al., 2014; Garza et al., 2001) leading to egg crushing by surrounding tissues or egg desiccation/drop off, and indirect defense through the release of chemicals that attract natural predators of eggs (Fatouros et al., 2012; Hilker and Meiners, 2006). Additionally, the production of benzyl cyanide, an ovicidal substance, at the oviposition site was reported in *Oryza sativa* (Suzuki et al., 1996; Yamasaki et al., 2003). While these defense mechanisms increase egg mortality individually, some studies found that the co-induction of both direct and indirect defense strategies synergistically impact egg survival (Fatouros et al., 2014). Even though such defenses can efficiently reduce insect pressure before damage occurs, one study indicate these traits may have been lost during maize domestication (Tamiru et al., 2015), similar to what is observed for other defense-related traits (Chen et al., 2015). Introgression of egg-killing traits in cultivated varieties has been reported in *Oryza sativa* (Suzuki et al., 1996; Yamasaki et al., 2003; Yang et al., 2014), however it is still a mostly unexploited strategy due to a lack of mechanistic understanding of these responses at the molecular and cellular levels (Reymond, 2013; Fatouros et al., 2016). Plants from the *Brassicales* and *Solanales* order respond to oviposition through the induction of cell death (Fatouros et al., 2016, 2014; Kalske et al., 2014; Petzold-Maxwell et al., 2011), a process that resembles the hypersensitive response (HR) triggered by certain adapted pathogens. Based on this intriguing similarity, this type of insect egg-triggered response is referred to as hypersensitive-like response (HR-like). Recent progress in the exploration of HR-like in response to insect eggs revealed that reactive oxygen species (ROS) accumulate at oviposition sites (Little et al., 2007; Geuss et al., 2017; Bittner et al., 2017). Moreover, salicylic acid (SA), one of the major phytohormone regulating plant immunity, was found to accumulate in response to oviposition in plant species expressing HR-like symptoms (Bruessow et al., 2010; Geuss et al., 2017; Bonnet et al., 2017), consistent with the fact that HR induction in response to bacterial pathogens is strictly dependent on the accumulation of SA (Balint-Kurti, 2019). This suggests that signaling pathways leading to cell death may be similar in different plant species considered. In *Arabidopsis thaliana*, cell death induction

upon egg extract treatment was reduced in SA synthesis and signaling mutants, demonstrating that this response is partially SA-dependent (Gouhier-Darimont et al., 2013). In *Brassica nigra*, only plants expressing HR-like symptoms displayed elevated *PR1* transcript levels, a widely used SA marker gene, again suggesting that SA accumulation is required for HR-like induction (Fatouros et al., 2014; Bonnet et al., 2017). These results indicate that the response to insect eggs is similar to pathogen-triggered immunity (PTI), as demonstrated elegantly in *Arabidopsis* (Gouhier-Darimont et al., 2013). However, knowledge of elicitor-receptor pairs involved in this sector of plant immunity is still scarce, but a recent report showed that the *Arabidopsis* L- (legume) type *LecRK-I.8* is impaired in most *P. brassicae* egg-induced responses (Gouhier-Darimont et al., 2019). This suggests that it functions upstream in this signaling cascade, thereby making *LecRK-I.8* a credible candidate for the perception of egg-associated molecular patterns (EAMP). Lectin-like receptor kinases (LecRKs) have been implicated in a myriad of immune-related processes such as PTI (Takahashi et al., 2007), chitin perception (Miya et al., 2007), e- (extracellular) ATP and eNAD⁺/eNADP⁺ perception (Choi et al., 2014; Wang et al., 2019), bacterial short chain 3OH-FA perception (Kutschera et al., 2019), mycorrhization (Labbé et al., 2019) and insect resistance (Gilardoni et al., 2011; Liu et al., 2015).

Despite the similarities to PTI and the discovery of *LecRK-I.8*, the genetic architecture of the response to insect eggs is still incomplete and lacks the identification of most early and late modulators of this response. Transcriptomic responses to oviposition by *Pieris brassicae* showed that it largely overlaps with pathogen response (Little et al., 2007), but not completely, suggesting that both responses are somewhat different. In support of this hypothesis, ROS production following *P. brassicae* egg extract treatment was independent on the NADPH oxidases RBOHD/F (Gouhier-Darimont et al., 2013), while this pathway is crucial for pathogen-triggered ROS accumulation (Torres et al., 2002; Morales et al., 2016). Moreover, *lecRK-I.8* plants did not show altered resistance to a bacterial pathogen (Gouhier-Darimont et al., 2019), suggesting that it may be specifically involved in egg perception

In order to further explore the molecular components of insect-egg induced responses in *Arabidopsis*, we previously performed a genome-wide association study (GWAS) using a set of 295 natural accessions. We found that two genomic loci were strongly associated with HR-like symptom induction (see chapter 2). The main peak of association was found to reside in *GLUTAMATE-LIKE RECEPTOR 2.7*, which encodes an amino acid gated calcium channel featuring signatures of balancing selection, and show that accessions displaying low HR-like symptoms lost the ability to transcribe this gene. However, *GLR2.7* knock-out in the Col-0 background did not lead to significant impact, suggesting that another locus may be

genetically interacting during this response. In an effort to further explore the results of this large GWAS, we report here that the second peak on chromosome 3 identifies the clade I L-type *LecRK-I.1*, a close homolog of *LecRK-I.8*, as the gene causal for the association observed on chromosome 3. We found that *LecRK-I.1* displays phenotypic additivity with *GLR2.7*, indicating that the two regulators work in parallel pathways. In addition to the putative EAMP receptor *LecRK-I.8*, we found that *LecRK-I.1* is specifically involved in the regulation of cell death following insect egg perception, hence providing additional indications for the specificity of this immune response.

Material and methods

Plant and insects growth conditions

All experiments described here were carried out in *Arabidopsis thaliana*. Plants were grown in growth chambers in short day conditions (10 h light, 22°C, 65% relative humidity, 100 $\mu\text{mol m}^{-2} \text{s}^{-1}$) and were 4 to 5 weeks old at the time of treatment. Larvae, eggs and butterflies of the Large White butterfly *Pieris brassicae* came from a population maintained on *Brassica oleracea* in a greenhouse (Reymond et al., 2000).

T-DNA insertion lines and CRISPR-Cas9 mutants

Accessions used for GWA mapping were obtained from the NASC stock center and are listed in supplementary table 1. T-DNA insertion lines for *lecrk-1.1* (SALK_066416), *lecrk-1.2* (SAIL_847_F07), *lecrk-1.3* (SALK_087804C), *lecrk-1.4* (SALK_091901), *lecrk-1.5* (GABI_777H06), *lecrk-1.6* (GABI_353G10) and *lecrk-1.8* (SALK_066416) were described previously (Gouhier-Darimont et al., 2019). Genotyping primers were designed with SIGNAL T-DNA verification tool for all lines used in this study.

Genome-wide association mapping and haplotype analysis

For GWA analysis, a set of 295 accessions from the HapMap panel (Horton et al., 2012) were used. Pools of 30 accessions were phenotyped every week over 2 days. Because of germination issues and low seed number, all plants for a given accession were phenotyped on the same day. To account for potential temporal effect, Col-0 plants originating from lab seed stocks were grown and phenotyped every week together with the accessions from the mapping panel. For each accession, 3 leaves from 3 to 6 plants were treated with egg-extract diluted 1:1 with deionized water leading to a total of 9 to 18 treated leaves. In parallel, 2 plants per accession were left untreated. Plants were left in the growth chamber for an additional 5 days until phenotyping. After 5 days, leaves were removed with forceps, symptoms were scored and pictures were taken as described below. One to three samples containing 6 randomly selected leaves were frozen in liquid nitrogen for further SA quantification.

GWA mapping was performed locally using custom scripts (Kerdaffrec et al., 2016) or on the GWAPP platform (<https://gwas.gmi.oeaw.ac.at/>, Seren et al., 2012) with the accelerated-mixed model (AMM) algorithm. This algorithm controls for population structure by computing a population-wide kinship matrix. Genotype data for ~250K SNP, full genome sequences of 1'135 accessions (The 1001 Genomes Consortium, 2016) or full imputed

genotypes for 2029 lines (Togninalli et al., 2018) were used and only SNPs with a minor-allele frequency (MAF) > 0.05 were considered for analysis. To correct for genome-wide multiple testing, a Bonferonni corrected threshold of significance was computed by dividing $\alpha = 0.05$ by the number of SNPs used in the analysis. Based on the similar mapping profiles obtained using symptom score (Chapter 2, Fig. 2A) and normalized symptom score (Chapter 2, Supplementary Fig. 1) together with the identification of other good *a priori* candidates on chromosome 3 (L-type LecRKs), we considered only non-normalized data for the current studies.

Haplotype analysis was based on significantly associated SNPs using the genotype data from GWAPP. Presence of premature stop codons in sequenced accessions was recovered from the POLYMORPH1001 Variant browser (<https://tools.1001genomes.org/polymorph/>). Both sets of data were used to explore phenotypic data.

Population-wide cladogram was built by calculating Euclidian distance between accessions from the kinship matrix, and clustering was subsequently performed using the “ward.d2” algorithm. Cladograms were further handled and annotated within the “ggtree” R package. Haplotype networks were built using the “ape” and “pegas” package by using the same sequence alignments as for phylogenetic trees.

Tajima’s D and Fu and Li’s F/D tests of neutrality

Sliding windows analysis of Tajima’s D and Fu and Li’s F/D tests were performed using DnaSP (version 6.12.03) with sliding windows of 100bp and a step size of 25bp, and significance threshold was set according to a 95% confidence limits published before (Tajima, 1989).

Oviposition and treatment with egg extract

For experiments with natural oviposition, plants were placed in a tent containing approximately 20 *P. brassicae* butterflies for a maximum of 8 h. Afterwards, plants were kept in a growth chamber in plastic boxes until hatching of the eggs. Control plants were kept in the same conditions without butterflies.

P. brassicae eggs were collected and crushed with a pestle in Eppendorf tubes. After centrifugation (15 000 g, 3 min), the supernatant (‘egg extract’) was collected and stored at -20°C. Plants were 4-5 weeks old at the time of treatment. For each plant, two leaves were treated with 2 μ l of egg extract. This amount corresponds to one egg batch of 18 eggs (E. Stahl, personal communication). A total of four plants were used for each experiment. After

the appropriate time, egg extract was gently removed with a scalpel blade and treated leaves were stored in liquid nitrogen. Untreated plants were used as controls.

For GWA analysis, a large amount of egg-extract was prepared as described and aliquots were stored under N₂ at -80°C in order to ensure homogenous treatments during the entire experiment.

Symptom scoring

Symptoms were scored visually from the adaxial side of the leaves and were classified into the following categories: no symptom (leaf treated area is still lush green, score = 0), small chlorosis (<50% of the treated area, score = 1), large chlorosis (> 50%, score = 2), small necrosis (brown spots or transparent membrane on < 50% of the treated area, score = 3), large necrosis (> 50 %, score = 4) and spreading necrosis (necrosis not confined to the treated area, score = 5). Normalized symptom score was calculated by dividing the score of a given accession by the score of the lab Col-0 score from the same week.

Histochemical stainings (Trypan blue, DAB)

For visualization of cell death, egg extract was gently removed and leaves were submerged in lactophenol trypan blue solution (5 ml of lactic acid, 10 ml of 50% glycerol, 1 mg of trypan blue (Sigma), and 5 ml of phenol) at 28°C for 2–3 h. Hydrogen peroxide (H₂O₂) accumulation was measured with 3,3-diaminobenzidine (DAB; Sigma). Leaves were submerged in a 1.0 mg ml⁻¹ DAB solution and incubated in the dark at room temperature for 6–8 h. After each staining, leaves were destained for 10 min in boiling 95% ethanol. Microscope images were saved as TIFF files and processed for densitometric quantification with ImageJ (version 1.48).

Salicylic acid quantifications

SA quantifications were performed using the bacterial biosensor *Acinetobacter sp.* ADPWH (DeFraia et al., 2008; Zvereva et al., 2016). Briefly, 6 leaf discs (0.7 cm, ~20mg) were ground in liquid nitrogen and extracted in 0.1M sodium acetate buffer (pH 5.6). Extracts were then centrifuged at 4°C for 15min at 16'000g. 50µL of extract were incubated with 5 µL of β-Glucosidase from almonds (0.5U/µl in acetate buffer, Sigma-Aldrich) during 90min at 37°C to release SA from SA-glucoside (SAG). 20µL of extract was then mixed with 60µL of LB and 50µL of a culture of *Acinetobacter sp.* ADPWH_lux (OD₆₀₀ = 0.4), and incubated for 1h at 37°C. Finally, luminescence was integrated using a 485±10nm filter for 1s. An SA standard curve diluted in untreated *sid2-1* extract amounts ranging from 0 to 60ng was read in parallel to allow quantification. SA amounts in samples were estimated by fitting a 3rd order polynomial regression on the standards.

RNA Extraction, Reverse-transcription and Quantitative Real-time PCR

Tissue samples were ground in liquid nitrogen, and total RNA was extracted using ReliaPrep™ RNA Tissue Miniprep (Promega) according to the manufacturer's instructions, including DnaseI treatment. Afterwards, cDNA was synthesized from 500 ng of total RNA using M-MLV reverse transcriptase (Invitrogen) and subsequently diluted eightfold with water. Quantitative real-time PCR reactions were performed using Brilliant III Fast SYBR-Green QPCR Master Mix on an QuantStudio 3 real-time PCR instrument (Life Technologies) with the following program: 95°C for 3min, then 40 cycles of 10s at 95°C, 20s at 60°C.

Values were normalized to the housekeeping gene *SAND* (At2g28390). The expression level of a target gene (TG) was normalized to the reference gene (RG) and calculated as normalized relative quantity (NRQ) as follows: $NRQ = E^{Ct_{RG}} / E^{Ct_{TG}}$. Primer efficiencies (E) were evaluated by five-step dilution regression. For each experiment, three biological replicates were analyzed. A list of all primers used in experiments can be found in Supplementary Table 1.

Statistical Analyses

GWA mapping and subsequent analysis of the data obtained was performed with R software version 3.6. For boxplots, the thick line indicates the median, box edges represent 1st and 3rd quartile respectively, whiskers cover 1.5 times the interquartile space and dots represent extreme values. Boxplot width is proportional to the number of sample. When displayed, notches indicate an approximate confidence interval for median values. All other analyses using mutant lines were analyzed using GraphPad Prism 8.0.1.

Results

Identification of a minor genetic locus associated with *P. brassicae* egg-induced symptoms

We previously reported that natural *Arabidopsis* accessions display large variation in SA accumulation and HR-like symptoms triggered upon *P. brassicae* egg extract perception (see Chapter 2). In order to investigate the genetic basis of insect egg-induced HR-like, we performed a Genome-wide association study (GWAS) by using both symptom score and total SA (SA + SAG) levels after 5 days of egg extract treatment for mapping. Genome-wide association (GWA) mapping using 295 accessions and a full imputed genotype matrix (The 1001 Genomes Consortium, 2016) revealed the existence of two loci associated with the degree of cell death induced by egg extract (Fig. 1A). The major peak of association on chromosome 2 was found to lie within the coding sequence of *GLUTAMATE RECEPTOR-like 2.7* (see chapter 2). Besides this peak, we observed the existence of another significantly associated marker ($-\log_{10} P = 7.59$) on chromosome 3 (Fig. 1A). Interestingly, this peak was absent from the GWA scan using total SA (see Chapter 2). By taking a closer look at this

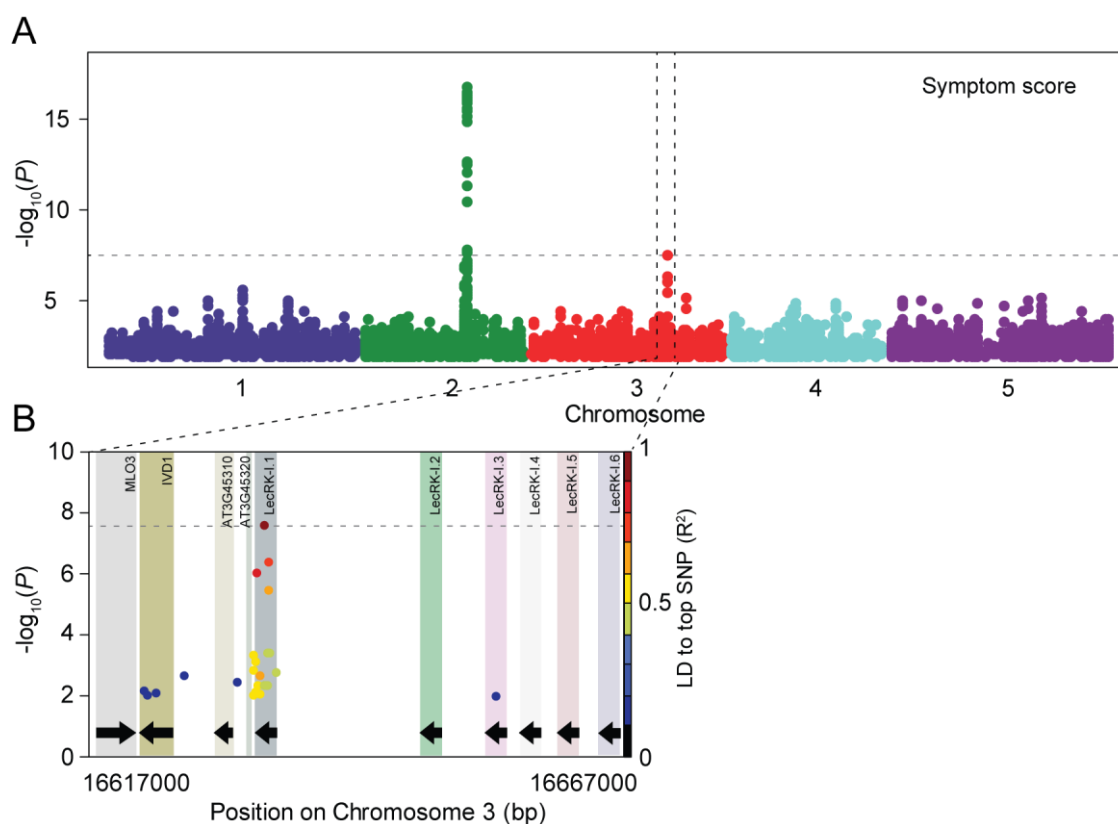


Figure 1. Genome-wide mapping of insect-egg induced HR-like symptoms

A. Manhattan plot of GWA for symptom score after 5 days of *P. brassicae* egg-extract using an accelerated mixed-model. Full imputed genotypes for all 295 accessions were used for mapping. Chromosomes are displayed in different colors and the dashed line indicates the Bonferroni-corrected significance at threshold $\alpha = 0.05$. B. Local association plot of a 50kb region surrounding the most significant marker. The x-axis represents genomic position on chromosome 2 and color boxes indicate genes. LD with the most significant SNP is indicated by a color scale. The dashed line indicates the Bonferroni corrected significance threshold at $\alpha = 0.05$.

genomic region, we found that this marker sits within the coding sequence of the L-type *LECTIN RECEPTOR KINASE-I.1* (Fig. 1B). Moreover, this genomic locus encompasses 5 other tandem duplicated L-type clade I *LecRK* genes. We found that high linkage disequilibrium (LD) with other surrounding markers was only observed for SNPs found in the gene sequence of *LecRK-I.1* (Fig. 1B), suggesting that this gene may be causal for the differences in HR-like symptoms observed. Additionally, expression of *LecRK-I.1* to *LecRK-I.6*, together with other clade I *LecRKs*, was previously found to be induced upon egg extract treatment (Gouhier-Darimont et al., 2019), further supporting this hypothesis. We then determined whether this locus was previously identified in other publically available GWAS scans. According to the araGWAS database (Togninalli et al., 2018), marker at the *LecRK-I.1* locus are not associated with any of the defense-related or developmental phenotypes available, suggesting that it may play a role specifically during *P. brassicae* egg-induced response (Supplementary fig. 1).

LecRK-I.1 is involved in cell death triggered upon egg perception

In order to test whether clade I *LecRKs* found in this region could be involved in the response to eggs of *P. brassicae*, we tested whether the lack of a single *LecRK* using T-DNA insertion lines lead to alterations in different egg-induced responses. Additionally, we used the CRISPR-Cas9 technology to delete the entire cluster of *LecRK-I.1* to *LecRK-I.6* (hereafter named *ccl.1-I.6*) in order to explore whether redundancy among these genes exists (Supplementary Fig. 2). Symptom score was found to be significantly reduced in *lecRK-I.1* mutant but not in knock-out lines from surrounding homologs (Fig. 2A). Consistently, deletion of the gene cluster lead to a similar reduction in symptoms. We then quantified cell death at the site of egg extract application by trypan blue staining and observed a similar pattern (Fig. 2B). These results clearly show that *LecRK-I.1*, but not other homologs from the genomic cluster, is involved in the induction of HR-like in response to insect eggs. Because altered SA signaling in the *lecRK-I.1* mutant could account for the reduction in cell death, we next quantified SA levels in plant treated with egg extract for 3 days. Indeed, total SA levels were lower in *lecRK-I.1* after 3 days of treatment compared to wild-type plants, however this trend was not statistically significant (Fig. 2C). Interestingly, we observed a similar result in the *lecRK-I.6* mutant and a significant reduction in *lecRK-I.3*, indicating that multiple *LecRKs* may regulate SA signaling. Removal of all six *LecRKs* using the *ccl.1-I.6* line resulted in reduced SA levels after egg extract treatment (Fig. 2C), further supporting that one or more clade I *LecRK* may participate in SA accumulation. We also monitored gene expression of the SA-dependent marker gene *PR1*. However, we did not observe any difference in the expression in any of the mutant line tested (Fig. 2D), indicating the existence of SA-independent processes. These results are consistent with a previous study that did not find significant

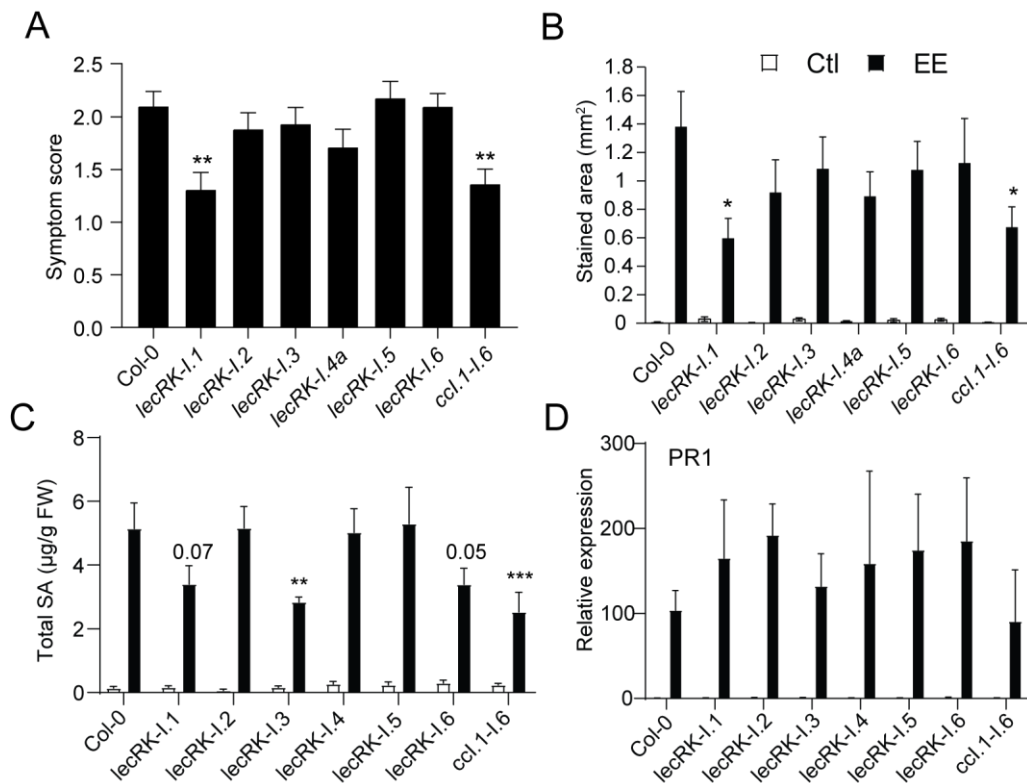


Figure 2. *LecRK-I.1* plays a role in the induction of HR-like symptoms following insect egg perception.

A. Average symptom score as visualized from the adaxial side after 5 days of treatment with egg extract. Means \pm standard error (SEM) from three independent experiment is shown (n= 12-23 for each experiment). B. Cell death as quantified by trypan blue staining after 3 days of egg extract treatment. Untreated leaves were used as controls. Means \pm standard error (SEM) from 8-20 leaves are shown. This experiment was repeated once with similar results. C. Total salicylic acid (SA + SAG) was after 3 days of egg extract treatment. Measurements were done on 4 plants per treatment by using a bacterial biosensor, untreated plants were used as control. Means \pm standard error (SEM) of three independent experiment are shown (n= 12). D. Expression of the marker gene *PR1* after 3 days of egg-extract treatment. Transcript levels were monitored by qPCR and normalized to the reference gene *SAND*. Means \pm standard error (SEM) of three independent biological replicates are shown. Stars indicate significant difference with Col-0 (ANOVA followed by Dunnet's test). *, P < 0.05; **, P < 0.01; ***, P < 0.001.

alterations in *PR1* induction in these mutants following egg extract treatment (Gouhier-Darimont et al., 2019). Altogether, these results demonstrate a role for *LecRK-I.1* in the regulation of cell death after insect egg perception, while providing evidence that different clade I *LecRKs* regulate SA levels during this response.

LecRK-I.1 haplotypes correlate with egg-induced symptoms

The identification of natural variation in *LecRK-I.1* as being associated with the inducibility of HR-like responses among *Arabidopsis* accessions indicates that protein variants of this gene may alter protein function(s) or gene expression. As mentioned, we observed that a single marker reached genome-wide significance (SNP3) while four other SNPs had intermediate P-values ($-\log_{10} P > 4$), all within the coding sequence of *LecRK-I.1* (Fig. 3A and B). Interestingly, three out of five SNPs result in amino acid changes: one (SNP5) in the putative carbohydrate-binding lectin-like domain (I228R), and two in the kinase domain (R356K ,SNP3; I602V ,SNP1), while the two other associated markers lead to silent mutations (Fig.

3B). Additionally, linkage analysis revealed that all markers are in moderate to strong LD with SNP3, indicating the potential existence of haplotypes segregating in the population (Fig. 3A). Based on the haplotypes defined by SNP1-5, we next determined that only 5 haplotypes are present in the Arabidopsis population used for GWA mapping (Fig. 3C), with two of them being present at rather high frequency compared to the other three. According to the phenotype distribution of these haplotypes, it appears that variants present in the lectin domain do not correlate with altered symptoms, suggesting that they do not impact this response. However, non Col-0 alleles for markers in the kinase domain are associated with significantly lower symptoms (Fig. 3C), potentially indicating that differential kinase function may underlie natural variation in egg-induced cell death. To explore this possibility, we examined whether these variants are found in functional sub domains of the kinase. Based on annotation from the UNIPROT database, we found that R356K lies in the predicted ATP binding site. We then performed homology-based modelling using SWISSMODEL (<https://swissmodel.expasy.org>) to predict the 3D topology of the LecRK-I.1 kinase domain in order to assess whether this amino acid change could potentially alter kinase function. We

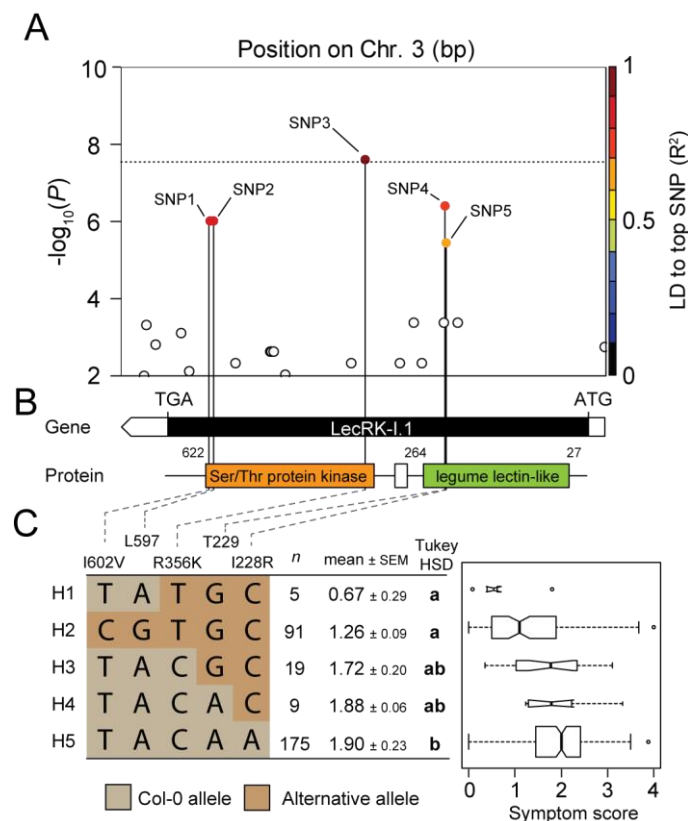


Figure 3. Local association and haplotype analysis of the *LecRK-I.1* locus

A. Local association plot of the *LecRK-I.1* locus. The x-axis represents genomic position on chromosome 2. LD of markers ($-\log_{10} P > 4$) with the most significant SNP is indicated by a color scale. The dashed line indicates the Bonferonni corrected significance threshold at $\alpha = 0.05$. B. Gene and protein domain organization according to UNIPROT. C. Haplotype analysis using the five most significant SNPs in the *LecRK-I.1* gene. Mean symptom score \pm SEM is shown and n indicates the number of accession present in each haplotype. Different letters indicate significant difference at $P < 0.05$ (ANOVA, followed by TukeyHSD for multiple comparison).

found that even though R356 is indeed proximal to the ATP binding site, the residue's side chain was not within 4Å of the ATP molecule and is exposed to the solvent in the model obtained (P. Jimenez Sandoval, results not shown). It is thus unlikely to interact with ATP within the active site. Moreover, we found that this position does not seem to be conserved in the structure of other plant kinases such as BAK1, and in all cases side chains were exposed to the solvent. Finally, the predicted amino acid change (R to K) does not lead to significant steric or charge modification at this site. This was also true for the other kinase variant, and the lectin variant appeared to be outside of the canonical lectin-binding or multimerization interface and is also solvent exposed (P. Jimenez Sandoval, personal communication). These results suggest that the identified variant may not be involved in canonical kinase or receptor function based on knowledge obtained from homologous proteins. We also determined whether multiple independent frameshifts and/or premature stop codon may be present in natural variants at this locus, potentially leading to the production of a truncated protein. We found that 18% of the sequenced accessions (23/125) possessed such variants (Supplementary Fig. 3A), yet this does not correlates with any difference in symptom distribution independently of the haplotype considered (Supplementary Fig. 3B). Moreover, premature STOP codons occurred within the first 20 first amino acid of the sequence. This suggests that these frameshifts and premature stops may not necessarily lead to the production of non-functional proteins, possibly through the existence of alternative start sites. Collectively, our results point to a role for variation in the *LecRK-I.1* genic sequence in modulating HR-like symptoms triggered by *P. brassicae* eggs. However, the link between

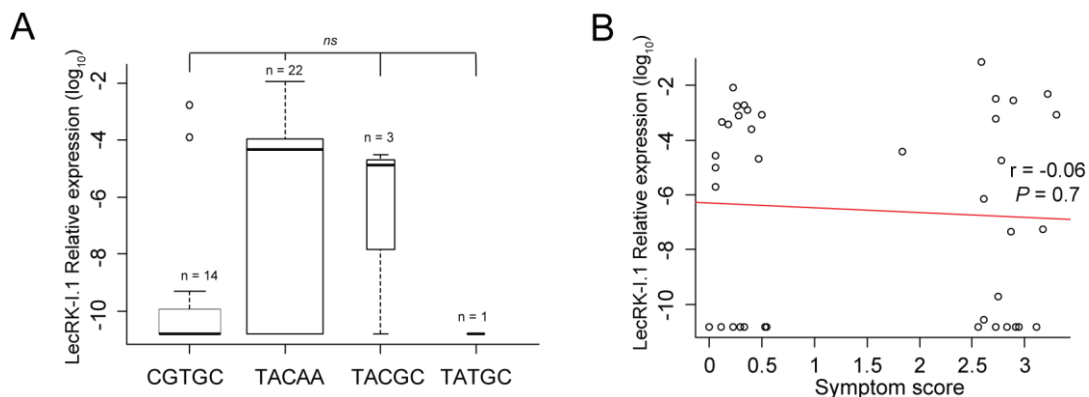


Figure 4. Natural *LecRK-I.1* haplotypes are not differentially expressed upon egg extract perception
LecRK-I.1 expression in 40 different accessions with low and high symptoms after 72h of egg-extract treatment. A. Transcript levels were plotted according to the haplotype defined previously. B. Transcript levels do not correlate with symptom scores of the respective accessions. Gene expression was monitored by qPCR and target gene transcript level was normalized to the reference gene *SAND*. Means of three technical replicates are shown. Expression data were corrected by adding half the smallest non-zero value in order to avoid zero values, and \log_{10} -transformed prior to analysis. *Ns*, not significant (ANOVA, $P > 0.05$). Pearson correlation coefficient (r) and corresponding P value (P) between *LecRK-I.1* transcript level and symptom score are shown in (B).

variation in the coding of this gene and the resulting phenotype is still unclear.

LecRK-I.1 variants are not associated with altered expression

The absence of any obvious impact of the variation identified within the *LecRK-I.1* coding sequence may indicate that an alternative process is involved. We determined whether differences in gene expression may correlate with haplotype identity and HR-like symptoms by measuring *LecRK-I.1* transcript levels following egg extract treatment in 40 accessions with high or low symptoms. Gene expression was highly variable in the accessions surveyed, and expression was even undetectable in certain lines (Supplementary Fig. 4). However, we found no significant association between haplotype identity and *LecRK-I.1* expression levels (Fig. 4A). Analysis of publicly available RNA-seq data from different accessions allowed for a similar analysis using SNP3 to split the data. Consistent with our experiments, none of the allele at this position was associated with altered *LecRK-I.1* transcript levels (Supplementary Fig. 5). Altogether these data suggest that variation in *LecRK-I.1* expression is not responsible for the variation in HR-like observed between accessions.

Signatures of selection at the *LecRK-I.1* locus

Based on the haplotype analysis, we found that only five *LecRK-I.1* haplotypes segregate in the mapping population used in this study. To get a closer look, we calculated haplotype frequencies using SNP1-5 described earlier. As mentioned before, two haplotypes appear to be present at high frequencies, while the three remaining haplotypes are much less frequent (< 7%, Fig. 5A). This could indicate that haplotypes may be distributed in two subpopulations due to adaptation to a type of environment for example, or that selection is acting at this loci and is maintaining variation. To disentangle these hypotheses, we constructed a cladogram representing genetic distance by using the kinship matrix used during the GWA mapping and superimposed haplotype identity for each accession (Fig. 5B). While it does appear that some low frequency haplotypes could be specific to certain wild populations, the two main haplotypes appear to have a very broad distribution in the entire *Arabidopsis* population used for mapping. The absence of any obvious link with phylogenetical or geographical history suggests that selection may be acting at this locus. To test the hypothesis that *LecRK-I.1* gene sequence does not evolve neutrally, we measured Tajima's D statistic along the coding sequence by using a sliding window (Fig. 5C). Tajima's D compares the number of variants observed with the number of mutations expected for a similar sequence under neutral evolution (Tajima, 1989), thereby indicating any departure from neutrality. We found that Tajima's D had a mainly positive value along the gene sequence of *LecRK-I.1*, and two short stretches were found to be significantly positive (Fig. 5C). This result is indicative that *LecRK-I.1* is not evolving neutrally. Because Tajima's D is sensitive to demographic history,

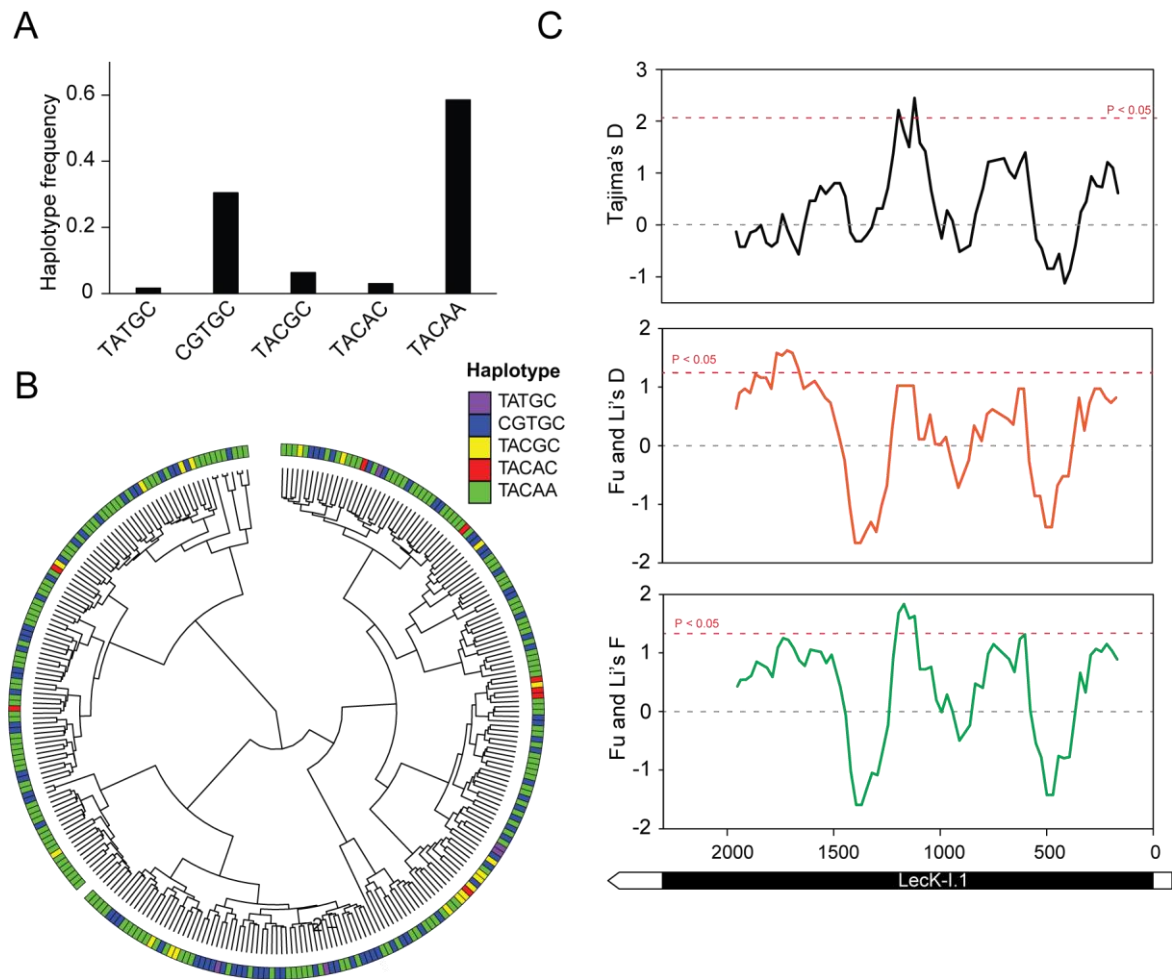


Figure 5. Signatures of selection at the *LecRK-I.1* locus.

A. Frequency of the different haplotypes in the accession panel used for mapping. B. Cladogram constructed from a genome-wide kinship matrix of the 295 accessions used in this study. The outermost circle indicate haplotype present in a given accession. C. Sliding window analysis of Tajima's D, and Fu and Li's D and F statistics along the *LecRK-I.1* coding region using a window size of 200bp and a step size of 25bp. A subset of 125 accessions for which available full genome sequences was used for this analysis. The red dashed line indicate significance threshold at $P < 0.05$. The gene structure of *LecRK-I.1* is shown below.

we also performed a sliding window analysis of Fu and Li's D and F statistics, which takes into account the species history by including an outgroup (*Arabidopsis lyrata*). We observed that the pattern and sign of Fu and Li's statistics were very similar to Tajima's D (Fig. 5C), further supporting the hypothesis that this locus is not evolving neutrally.

LecRK-I.1 and LecRK-I.8 function in the same pathway

Based on the previously reported identification of LecRK-I.8, a close homolog of LecRK-I.1 (Hofberger et al., 2015; Bouwmeester and Govers, 2009), as an early component of EAMP perception, we wondered whether both genes may function in the same signaling cascade or if they are involved in parallel pathways. We crossed *lecRK-I.1* with *lecRK-I.8* and measured HR-like symptoms in the single and double mutants. Both single mutants displayed a similar reduction of symptom after egg extract treatment. However, the double mutant did not show

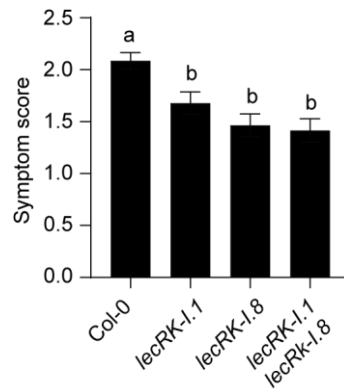


Figure 6. LecRK-I.1 genetically interacts with LecRK-I.8.

Average symptom score as visualized from the adaxial side after 5 days of treatment with egg extract. Means \pm standard error (SEM) from three independent experiment is shown (n= 12-23 for each experiment). Different letters indicate significant difference at $P < 0.05$ (ANOVA followed by Tukey's HSD test for multiple comparison).

a more severe phenotype, strongly suggesting that LecRK-I.1 and LecRK-I.8 act in the same pathway (Fig. 6A). These data are supported by the finding that egg extract-induction of *PR1* expression is similarly altered in single and double mutants (C. Gouhier-Darimont, personal communication).

Discussion

The recent description of *LecRK-I.8* as an upstream regulator of the insect egg-triggered signaling pathway opened the exciting possibility that it could be involved in EAMP perception (Gouhier-Darimont et al., 2019). However, several phenotypes including cell death were not completely abolished in the *lecRK-I.8* mutant, indicating a potential redundancy with other EAMP potential receptor(s) or that *LecRK-I.8* works as a modulator of the response. Multiple lines of evidence suggest that other clade I L-type LecRKs may be involved in this response as shown by their collective induction following egg extract treatment (Gouhier-Darimont et al., 2019). We describe here the identification of LecRK-I.1 as a component of the insect egg-triggered signaling pathway in Arabidopsis that specifically affects the induction of HR-like during this interaction. We show that a knock-out mutant of the L-type LecRK-I.1 leads to reduced HR-like symptoms and cell death following *P. brassicae* egg extract treatment, while only a trend in the reduction of total SA was observed. Moreover, double knock-out of both *LecRK-I.1* and *LecRK-I.8* did not result in a further reduction of HR-like symptoms, suggesting that both proteins function in the same transduction pathway or are part of the same complex. Other clade I *LecRK* mutants showed reduced SA levels and this was further confirmed by deleting all 6 receptors found in tandem at the locus. These results shows that multiple LecRKs are involved in the response to eggs by controlling different aspect of this pathway. Surprisingly, only LecRK-I.1 and LecRK-I.8 affect the induction of cell death following egg perception and only the *LecRK-I.1* locus displays natural variation.

Despite the absence of known ligand for LecRK-I.1 and most other clade I L-type LecRKs. It has been reported that LecRK-I.1 possesses a putative RGD-binding motif (Gouget et al., 2006) and that it may participate in plasma membrane-cell wall interactions. Whether insect eggs trigger changes in cell wall properties is not known, but epicuticular wax patterns were shown to be altered upon *P. brassicae* oviposition on Arabidopsis (Blenn et al., 2012). Because of mutations in invariant residues involved in carbohydrate binding, the binding pockets of plant lectin are unlikely to bind sugars (Bouwmeester and Govers, 2009). However, the conserved hydrophobicity of the resulting cavity could recognize more hydrophobic ligands. Given the lipidic nature of EAMP (Bruessow et al., 2010; Gouhier-Darimont et al., 2019), this would be consistent with a role for L-type LecRKs in egg perception. To date, the G-type LecRK LORE was found to recognize medium chain 3-OH fatty acids (Kutschera et al., 2019), further supporting the hypothesis that some LecRK may recognize hydrophobic ligands in EAMP. Alternatively, the identified LecRKs could also be

involved in the perception of secondary signals such as DAMPs as suggested by the identification of LecRK-I.8 and LecRK-VI.2 has potential receptors for eNAD⁺ and eNADP⁺ (Wang et al., 2017, 2019). The direct perception of EAMP by LecRK-I.1 is unlikely given that only a subset of responses are affected in the corresponding mutant. Based on genetics, we provide evidence that LecRK-I.1 and LecRK-I.8 function as parts the same pathway/complex. We therefore postulate that LecRK-I.1 might serve as a secondary signaling hub that controls LecRK-I.8-dependent cell death. A more detailed evaluation of egg-triggered phenotypes in single and double mutants will help address this hypothesis.

We found that natural variation in the *LecRK-I.1* gene sequence was associated with HR-like symptoms, but not with SA levels, consistent with the phenotypes observed in the *lecRK-I.1* mutant. Two main haplotypes of this gene segregate at the population level and in particular one variant in the kinase domain was significantly associated with HR-like symptoms. Evaluation of *LecRK-I.1* expression in accessions indicates that transcript levels are not associated with haplotype identity, therefore suggesting that functional variation at the LecRK-I.1 protein sequence results in differential activity. Given the success of homology modelling in the study of LecRK-I.9/DORN1 and its ATP-binding site (Nguyen et al., 2016), we addressed this question using a similar approach. Unfortunately, our results suggests that none of the identified variant would significantly affect the lectin binding pocket or the kinase domain. *In vitro* kinase assay using the different variants of the kinase domain would help address this question directly. Recently, LecRKVI.2 was shown to interact with the central immune co-receptor BAK1 (Huang et al., 2014; Wang et al., 2019), and both genes were found to be necessary for proper eNAD⁺ and eNADP⁺-induced signaling. Given the critical nature of such interactions for signal transduction, solvent-exposed natural variants associated with reduced HR-like symptoms could affect the binding of putative co-receptors and partners of LecRK-I.1. Moreover, LecRK homo- and heterodimerization was reported (Wang and Bouwmeester, 2017; Bellande et al., 2017), suggesting that a similar process might underlie LecRK-I.1 function and such interaction may be affected by the natural variants identified.

At the genomic level, L-type LecRKs are organized in clusters of tandem repeats that arose through local and whole genome duplication events (Hofberger et al., 2015). Clade I L-type LecRK genes appear to be mostly *Brassicaceae*-specific (Hofberger et al., 2015; Wang and Bouwmeester, 2017) and most of them have been involved in immunity. In particular, clade I L-type LecRKs originated following the At- α whole genome duplication event (50Mya), and LecRKs that were duplicated during this period show signs of positive selection (Hofberger et al., 2015). Consistent with this study, we found that the two major haplotypes

defined at the *LecRK-I.1* locus segregate at intermediate to high frequencies and have a wide distribution across the different Arabidopsis population used. The presence of such diverged polymorphisms in different populations indicate that they are ancient and have been maintained by selection. Consistent with the latter hypothesis, we found that the *LecRK-I.1* locus does not evolve neutrally, as indicated by positive Tajima's D as well as Fu and Li's D/F statistics. Positive values for these statistics are considered as signatures of balancing selection, a type of selection that is observed in immunity-related or resistance genes for instance (Bakker et al., 2006; Vila-Aiub et al., 2011; Huard-Chauveau et al., 2013; van Velzen and Etienne, 2015; Ariga et al., 2017). Balancing selection collectively refers to processes by which genetic variation is maintained in a population, as opposed to purifying selection that reduces variation (Delph and Kelly, 2014; Wu et al., 2017). Different selective processes can ultimately lead to the maintenance of genetic variation such as overdominance (or heterozygote advantage), frequency-dependent selection or environmental heterogeneity (spatially varying selection). Identification of the exact mode of balancing selection acting at this locus deserves further investigation. Nevertheless, the fact that *LecRK-I.1* displays strong signatures of balancing selection highlights the ecological importance of this gene in natural Arabidopsis populations.

In our GWAS experiment, we identified that the severity of HR-like symptoms triggered by *P. brassicae* egg extract was associated with another locus. We previously reported that variation at the *GLR2.7* locus results in loss of transcription, and this correlated with symptom severity and SA accumulation (see chapter 2). To our surprise, knockout of this gene in the Col-0 background did not result in decreased cell death following egg perception, pointing to the possible existence of epistatic loci present in the genome of certain accessions. To this end, we explored whether epistasis could occur between both loci identified by GWAS mapping. By analyzing symptom distribution, we found that the different haplotypes at either loci additively contribute to HR-like symptoms (see chapter 2), suggesting that both genes may function in parallel pathways. This hint to the possibility that the loss of *GLR2.7* may be somehow compensated by the presence of the strong haplotype at the *LecRK-I.1* locus. Interestingly, DORN1-dependent perception of eATP was shown to trigger Ca^{2+} fluxes, and chemical inhibition of Ca^{2+} channels inhibited downstream responses triggered by eNAD (Wang et al., 2018; Zhang and Mou, 2009), showing that calcium channels are necessary for the function of at least one clade I LecRK. Double mutant generation together with *in vivo* validation of potential interactions will help resolve this question. Remarkably, meta-analysis of publically available GWAS data show that neither *GLR2.7* nor *LecRK-I.1* have been associated with any other defense phenotype tested, raising the exciting possibility that these genes function specifically in response to insect

eggs. The identification of ligands for both receptors as well as a better understanding of their interaction and role in insect egg-triggered immunity will provide valuable insights into their function. While the results presented here allow to move forward in the mechanistic understanding of the induction of cell death response in *Arabidopsis*, it is not known whether this gene may also play a role in crop species such as cabbage or canola. Interestingly, induction of HR-like in *B. nigra* also correlates with higher egg parasitism, indicating that both defense mechanisms may be under a similar regulation (Fatouros et al., 2014). The identification of this locus allows the study of this region in other *Brassicaceae* and to screen available germplasms for existing variation in order to demonstrate a role for these genes in different plant species.

Acknowledgments

We would like to thank Envel Kerdaffrec for his help during GWA analyses and for sharing custom R scripts. We thank Dany Buffat for his technical assistance during the screening. We are also grateful to Nicolas Salamin and Anna Marcionetti for advices regarding the selection analyses.

References

- Ariga, H. et al.** (2017). NLR locus-mediated trade-off between abiotic and biotic stress adaptation in *Arabidopsis*. *Nat. Plants* **3**: 17072.
- Bakker, E.G., Toomajian, C., Kreitman, M., and Bergelson, J.** (2006). A Genome-Wide Survey of R Gene Polymorphisms in *Arabidopsis*. *Plant Cell* **18**: 1803–1818.
- Balint-Kurti, P.** (2019). The plant hypersensitive response: concepts, control and consequences. *Mol. Plant Pathol.* **0**: 1163–1178.
- Bellande, K., Bono, J.J., Savelli, B., Jamet, E., and Canut, H.** (2017). Plant lectins and lectin receptor-like kinases: How do they sense the outside? *Int. J. Mol. Sci.* **18**.
- Bittner, N., Trauer-Kizilelma, U., and Hilker, M.** (2017). Early plant defence against insect attack: involvement of reactive oxygen species in plant responses to insect egg deposition. *Planta* **245**: 993–1007.
- Blenn, B., Bandoly, M., Küffner, A., Otte, T., Geiselhardt, S., Fatouros, N.E., and Hilker, M.** (2012). Insect egg deposition induces indirect defense and epicuticular wax changes in *Arabidopsis thaliana*. *J. Chem. Ecol.* **38**: 882–92.
- Bonnet, C., Lassueur, S., Ponzio, C., Gols, R., Dicke, M., and Reymond, P.** (2017). Combined biotic stresses trigger similar transcriptomic responses but contrasting resistance against a chewing herbivore in *Brassica nigra*. *BMC Plant Biol.* **17**: 127.
- Bouwmeester, K. and Govers, F.** (2009). *Arabidopsis* L-type lectin receptor kinases: Phylogeny, classification, and expression profiles. *J. Exp. Bot.* **60**: 4383–4396.
- Bruessow, F., Gouhier-Darimont, C., Bruchala, A., Metraux, J.-P., and Reymond, P.** (2010). Insect eggs suppress plant defence against chewing herbivores. *Plant J.* **62**: 876–885.
- Chen, Y.H., Gols, R., and Benrey, B.** (2015). Crop Domestication and Its Impact on Naturally Selected Trophic Interactions. *Annu. Rev. Entomol.* **60**: 35–58.
- Choi, J., Tanaka, K., Cao, Y., Qi, Y., Qiu, J., Liang, Y., Lee, S.Y., and Stacey, G.** (2014). Identification of a plant receptor for extracellular ATP. *Science* (80-.). **343**: 290–294.
- DeFraia, C.T., Schmelz, E.A., and Mou, Z.** (2008). A rapid biosensor-based method for quantification of free and glucose-conjugated salicylic acid. *Plant Methods* **4**: 28.
- Delph, L.F. and Kelly, J.K.** (2014). On the importance of balancing selection in plants. *New Phytol.* **201**: 45–56.
- Desurmont, G.A. and Weston, P.A.** (2011). Aggregative oviposition of a phytophagous beetle overcomes egg-crushing plant defences. *Ecol. Entomol.* **36**: 335–343.
- Doss, R.P., Oliver, J.E., Proebsting, W.M., Potter, S.W., Kuy, S., Clement, S.L., Williamson, R.T., Carney, J.R., and DeVilbiss, E.D.** (2000). Bruchins: Insect-derived plant regulators that stimulate neoplasm formation. *Proc. Natl. Acad. Sci.* **97**: 6218–6223.
- Fatouros, N.E., Cusumano, A., Danchin, E.G.J., and Colazza, S.** (2016). Prospects of herbivore egg-killing plant defenses for sustainable crop protection. *Ecol. Evol.* **6**: 6906–6918.
- Fatouros, N.E., Lucas-Barbosa, D., Weldegergis, B.T., Pashalidou, F.G., van Loon, J.J. a, Dicke, M., Harvey, J. a, Gols, R., and Huigens, M.E.** (2012). Plant volatiles induced

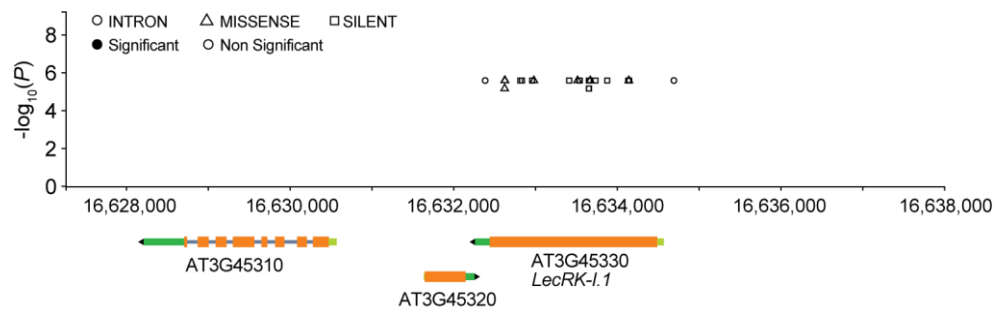
by herbivore egg deposition affect insects of different trophic levels. *PLoS One* **7**: e43607.

- Fatouros, N.E., Pineda, A., Huigens, M.E., Broekgaarden, C., Shimwela, M.M., Candia, I.A.F., Verbaarschot, P., and Bukovinszky, T.** (2014). Synergistic effects of direct and indirect defences on herbivore egg survival in a wild crucifer. *Proc. R. Soc. B Biol. Sci.* **281**: 20141254.
- Fu, Y.X. and Li, W.H.** (1993). Statistical tests of neutrality of mutations. *Genetics* **133**: 693–709.
- Garza, R., Vera, J., Cardona, C., Barcenas, N., and Singh, S.P.** (2001). Hypersensitive response of beans to *Apion godmani* (Coleoptera: Curculionidae). *J. Econ. Entomol.* **94**: 958–962.
- Geuss, D., Stelzer, S., Lortzing, T., and Steppuhn, A.** (2017). *Solanum dulcamara* 's response to eggs of an insect herbivore comprises ovicidal hydrogen peroxide production. *Plant. Cell Environ.* **40**: 2663–2677.
- Gilardoni, P.A., Hettenhausen, C., Baldwin, I.T., and Bonaventure, G.** (2011). *Nicotiana attenuata* lectin receptor kinase1 suppresses the insect-mediated inhibition of induced defense responses during *manduca sexta* herbivory. *Plant Cell* **23**: 3512–3532.
- Gouget, A., Senchou, V., Govers, F., Sanson, A., Barre, A., Rougé, P., Pont-Lezica, R., and Canut, H.** (2006). Lectin Receptor Kinases Participate in Protein-Protein Interactions to Mediate Plasma Membrane-Cell Wall Adhesions in *Arabidopsis*. *Plant Physiol.* **140**: 81–90.
- Gouhier-Darimont, C., Schmiesing, A., Bonnet, C., Lassueur, S., and Reymond, P.** (2013). Signalling of *Arabidopsis thaliana* response to *Pieris brassicae* eggs shares similarities with PAMP-triggered immunity. *J. Exp. Bot.* **64**: 665–74.
- Gouhier-Darimont, C., Stahl, E., Glauser, G., and Reymond, P.** (2019). The *Arabidopsis* Lectin Receptor Kinase LecRK-I.8 Is Involved in Insect Egg Perception. *Front. Plant Sci.* **10**: 1–10.
- Hilker, M. and Fatouros, N.E.** (2015). Plant Responses to Insect Egg Deposition. *Annu. Rev. Entomol.* **60**: 493–515.
- Hilker, M. and Meiners, T.** (2006). Early herbivore alert: insect eggs induce plant defense. *J. Chem. Ecol.* **32**: 1379–97.
- Hofberger, J.A., Nsibo, D.L., Govers, F., Bouwmeester, K., and Schranz, M.E.** (2015). A Complex Interplay of Tandem- and Whole-Genome Duplication Drives Expansion of the L-Type Lectin Receptor Kinase Gene Family in the Brassicaceae. *Genome Biol. Evol.* **7**: 720–734.
- Horton, M.W. et al.** (2012). Genome-wide patterns of genetic variation in worldwide *Arabidopsis thaliana* accessions from the RegMap panel. *Nat. Genet.* **44**: 212–6.
- Huang, P.Y., Yeh, Y.H., Liu, A.C., Cheng, C.P., and Zimmerli, L.** (2014). The *Arabidopsis* LecRK-VI.2 associates with the pattern-recognition receptor FLS2 and primes *Nicotiana benthamiana* pattern-triggered immunity. *Plant J.* **79**: 243–255.
- Huard-Chauveau, C., Perchepped, L., Debieu, M., Rivas, S., Kroj, T., Kars, I., Bergelson, J., Roux, F., and Roby, D.** (2013). An Atypical Kinase under Balancing Selection Confers Broad-Spectrum Disease Resistance in *Arabidopsis*. *PLoS Genet.* **9**.
- Kalske, A., Muola, A., Mutikainen, P., and Leimu, R.** (2014). Preference for outbred host plants and positive effects of inbreeding on egg survival in a specialist herbivore. *Proc. R. Soc. B Biol. Sci.* **281**: 20141421.
- Kerdaffrec, E., Filiault, D.L., Korte, A., Sasaki, E., Nizhynska, V., Seren, Ü., and Nordborg, M.** (2016). Multiple alleles at a single locus control seed dormancy in

- Swedish Arabidopsis. *Elife* **5**: 1–24.
- Kutschera, A. et al.** (2019). Bacterial medium-chain 3-hydroxy fatty acid metabolites trigger immunity in Arabidopsis plants. *Science* (80-.). **181**: 178–181.
- Labbé, J. et al.** (2019). Mediation of plant–mycorrhizal interaction by a lectin receptor-like kinase. *Nat. Plants* **5**: 676–680.
- Little, D., Gouhier-Darimont, C., Bruessow, F., and Reymond, P.** (2007). Oviposition by pierid butterflies triggers defense responses in Arabidopsis. *Plant Physiol.* **143**: 784–800.
- Liu, Y. et al.** (2015). A gene cluster encoding lectin receptor kinases confers broad-spectrum and durable insect resistance in rice. *Nat. Biotechnol.* **33**: 301–305.
- Miya, A., Albert, P., Shinya, T., Desaki, Y., Ichimura, K., Shirasu, K., Narusaka, Y., Kawakami, N., Kaku, H., and Shibuya, N.** (2007). CERK1, a LysM receptor kinase, is essential for chitin elicitor signaling in Arabidopsis. *Proc. Natl. Acad. Sci. U. S. A.* **104**: 19613–19618.
- Morales, J., Kadota, Y., Zipfel, C., Molina, A., and Torres, M.** (2016). The Arabidopsis NADPH oxidases RbohD and RbohF display differential expression patterns and contributions during plant immunity.
- Nguyen, C.T., Tanaka, K., Cao, Y., Cho, S.H., Xu, D., and Stacey, G.** (2016). Computational analysis of the ligand binding site of the extracellular ATP receptor, DORN1. *PLoS One* **11**: 1–20.
- Petzold-Maxwell, J., Wong, S., Arellano, C., and Gould, F.** (2011). Host plant direct defence against eggs of its specialist herbivore, *Heliothis subflexa*. *Ecol. Entomol.* **36**: 700–708.
- Reymond, P.** (2013). Perception, signaling and molecular basis of oviposition-mediated plant responses. *Planta* **238**: 247–58.
- Seren, Ü., Vilhjálmsson, B.J., Horton, M.W., Meng, D., Forai, P., Huang, Y.S., Long, Q., Segura, V., and Nordborg, M.** (2012). GWAPP: A web application for genome-wide association mapping in *Arabidopsis*. *Plant Cell* **24**: 4793–805.
- Shapiro, A.M. and DeVay, J.E.** (1987). Hypersensitivity reaction of *Brassica nigra* L. (Cruciferae) kills eggs of *Pieris* butterflies (Lepidoptera: Pieridae). *Oecologia* **71**: 631–632.
- Suzuki, Y., Sogawa, K., and Seino, Y.** (1996). Ovicidal Reaction of Rice Plants against the Whitebacked Planthopper, *Sogatella furcifera* HORVATH (Homoptera: Delphacidae). *Appl. Entomol. Zool.* **31**: 111–118.
- Tajima, F.** (1989). Statistical Method for Testing the Neutral Mutation Hypothesis by DNA Polymorphism. *Genetics*: 585–595.
- Takahashi, F., Yoshida, R., Ichimura, K., Mizoguchi, T., Seo, S., Yonezawa, M., Maruyama, K., Yamaguchi-Shinozaki, K., and Shinozaki, K.** (2007). The Mitogen-Activated Protein Kinase Cascade MKK3–MPK6 Is an Important Part of the Jasmonate Signal Transduction Pathway in Arabidopsis. *Plant Cell* **19**: 805–818.
- Tamiru, A., Khan, Z.R., and Bruce, T.J.** (2015). New directions for improving crop resistance to insects by breeding for egg induced defence. *Curr. Opin. Insect Sci.*
- The 1001 Genomes Consortium** (2016). 1,135 Genomes Reveal the Global Pattern of Polymorphism in *Arabidopsis thaliana*. *Cell* **166**: 481–491.
- Togninalli, M., Seren, Ü., Meng, D., Fitz, J., Nordborg, M., Weigel, D., Borgwardt, K., Korte, A., and Grimm, D.G.** (2018). The AraGWAS Catalog: a curated and standardized *Arabidopsis thaliana* GWAS catalog. *Nucleic Acids Res.* **46**: D1150–D1156.

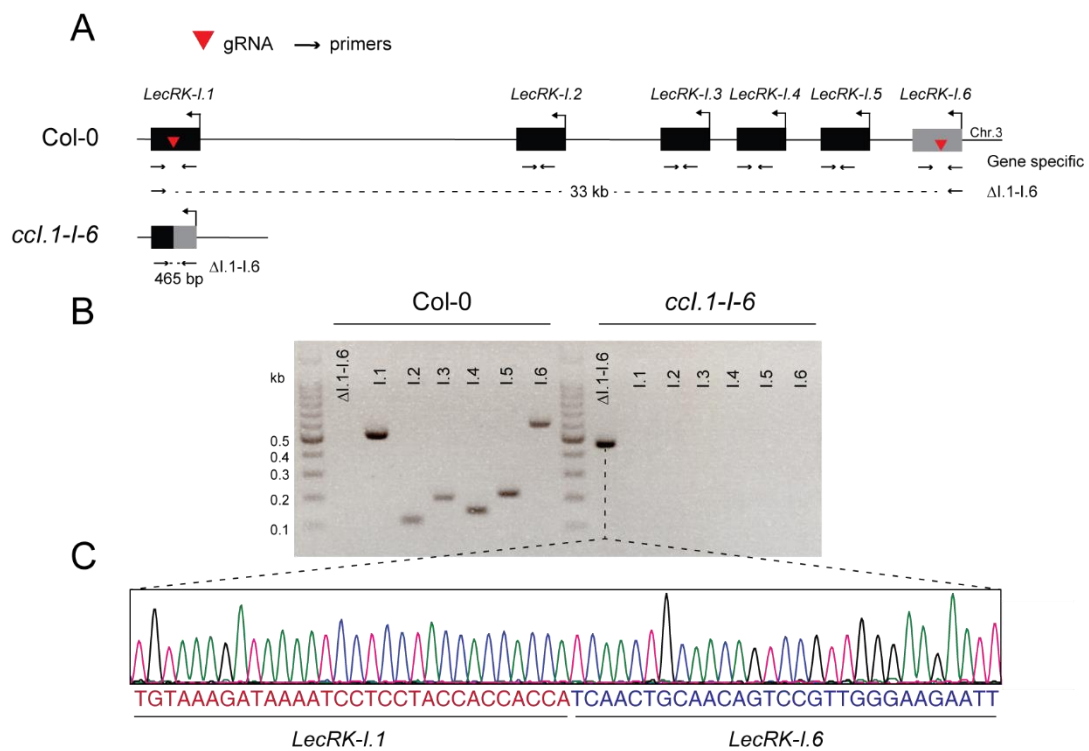
- Torres, M.A., Dangl, J.L., and Jones, J.D.G.** (2002). Arabidopsis gp91phox homologues AtrbohD and AtrbohF are required for accumulation of reactive oxygen intermediates in the plant defense response. *Proc. Natl. Acad. Sci. U. S. A.* **99**: 517–522.
- van Velzen, E. and Etienne, R.S.** (2015). The importance of ecological costs for the evolution of plant defense against herbivory. *J. Theor. Biol.* **372**: 89–99.
- Vila-Aiub, M.M., Neve, P., and Roux, F.** (2011). A unified approach to the estimation and interpretation of resistance costs in plants. *Heredity (Edinb).* **107**: 386–394.
- Wang, C., Huang, X., Li, Q., Zhang, Y., Li, J.L., and Mou, Z.** (2019). Extracellular pyridine nucleotides trigger plant systemic immunity through a lectin receptor kinase/BAK1 complex. *Nat. Commun.* **10**: 4810.
- Wang, C., Zhou, M., Zhang, X., Yao, J., Zhang, Y., and Mou, Z.** (2017). A lectin receptor kinase as a potential sensor for extracellular nicotinamide adenine dinucleotide in *Arabidopsis thaliana*. *Elife* **6**: 1–23.
- Wang, L., Wilkins, K.A., and Davies, J.M.** (2018). Arabidopsis DORN1 extracellular ATP receptor; activation of plasma membrane K⁺ and Ca²⁺-permeable conductances. *New Phytol.*: 1301–1304.
- Wang, Y. and Bouwmeester, K.** (2017). L-type lectin receptor kinases: New forces in plant immunity. *PLOS Pathog.* **13**: e1006433.
- Wu, Q., Han, T.S., Chen, X., Chen, J.F., Zou, Y.P., Li, Z.W., Xu, Y.C., and Guo, Y.L.** (2017). Long-term balancing selection contributes to adaptation in *Arabidopsis* and its relatives. *Genome Biol.* **18**: 1–15.
- Yamasaki, M., Yoshimura, A., and Yasui, H.** (2003). Genetic basis of ovicidal response to whitebacked planthopper (*Sogatella furcifera* Horváth) in rice (*Oryza sativa* L.). *Mol. Breed.* **12**: 133–143.
- Yang, Y. et al.** (2014). Quantitative trait loci identification, fine mapping and gene expression profiling for ovicidal response to whitebacked planthopper (*Sogatella furcifera* Horvath) in rice (*Oryza sativa* L.). *BMC Plant Biol.* **14**: 145.
- Zhang, X. and Mou, Z.** (2009). Extracellular pyridine nucleotides induce PR gene expression and disease resistance in *Arabidopsis*. *Plant J.* **57**: 302–312.
- Zvereva, A.S., Golyaev, V., Turco, S., Gubaeva, E.G., Rajeswaran, R., Schepetilnikov, M. V., Srour, O., Ryabova, L.A., Boller, T., and Pooggin, M.M.** (2016). Viral protein suppresses oxidative burst and salicylic acid-dependent autophagy and facilitates bacterial growth on virus-infected plants. *New Phytol.* **211**: 1020–1034.

Supplementary figures



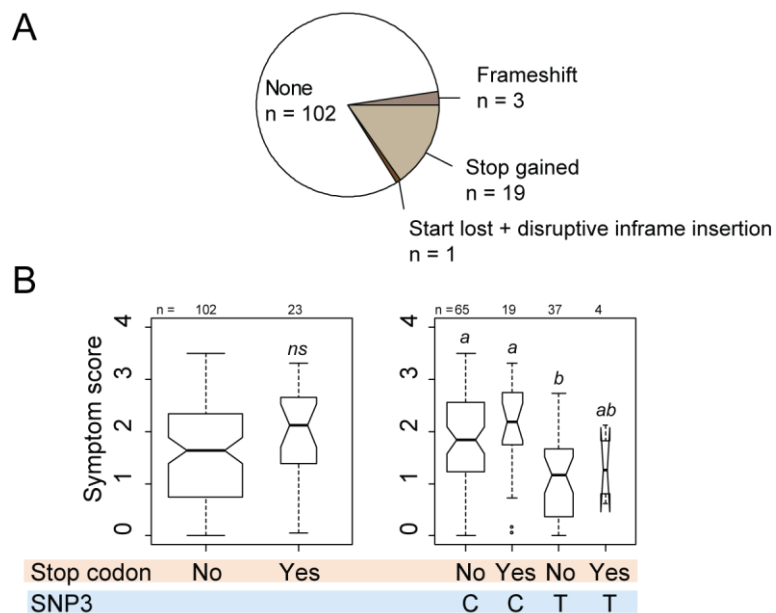
Supplementary figure 1. Meta-analysis of association at the *LecRK-I.1* locus

Screenshot of associations from the AraGWAS database at the *LecRK-I.1* locus. X-axis represents genomic position along chromosome 3 and gene structures are shown below. Markers are shown depending on their genic position and on significance. Significance threshold were calculated based on permutations for each phenotype as described in Togninalli et al. 2018. Notice that none of the displayed marker reached significance. Only markers with MAF > 5% and MAC > 5 are shown.



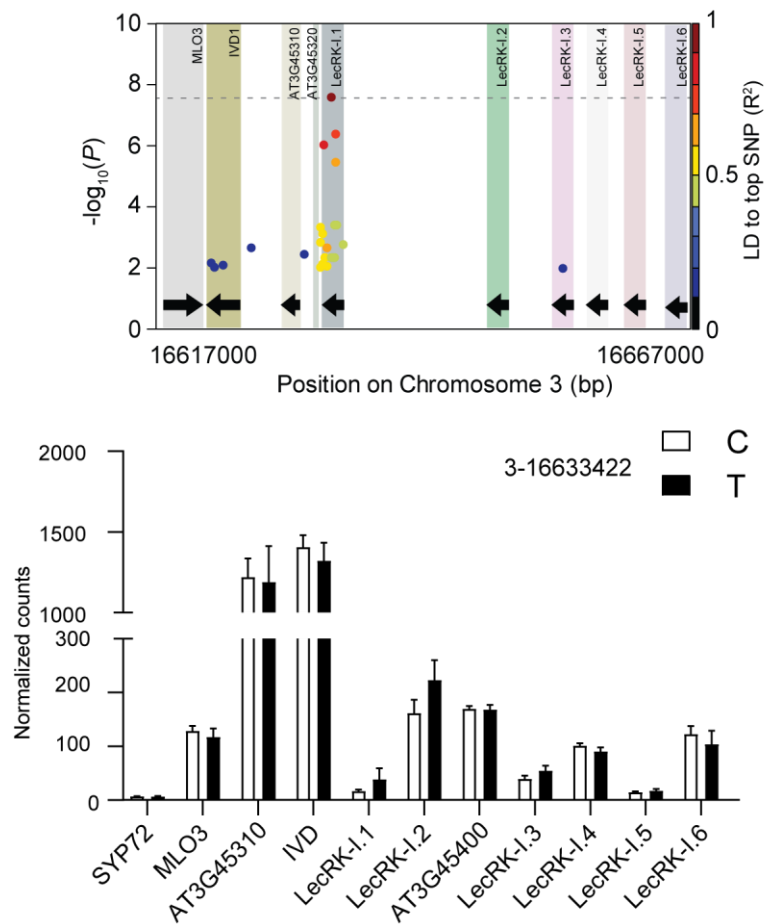
Supplementary figure 2. Deletion of *LecRK-I.1* to *LecRK-I.6* using CRISPR-Cas9.

A. Genomic cluster on chromosome 3 containing *LecRK-I.1* to *LecRK-I.6*. The two gRNA used to delete this six gene cluster are indicated with a red triangle. A simulation of the resulting chromosomal locus is depicted below. Arrows indicate the primers used for genotyping and the size of the respective PCR products is shown. B. PCR analysis of the *ccl.1-I-6* line using primers to identify the presence of a successful deletion ($\Delta I.1-I.6$) and gene specific primers (I.1 to I.6). C. The PCR product using the deletion-specific primers was sequenced and blasted against the *A. thaliana* genome. Blast results reveal that the 33Kb region was successfully deleted.



Supplementary figure 3. Disruptive variation in *LecRK-I.1* do not correlate with symptoms

A. Proportion of sequences accessions from our panel that contained premature stop codons and or frameshifts in their *LecRK-I.1* gene sequence. Different colors indicate the different types of disruptive polymorphisms found as annotated on POLYMORPH1001 (<https://tools.1001genomes.org/polymorph/>). N indicates the number of accessions that possessed a given type of variation. B. HR-like symptom score distribution depending on the presence of disruptive variation (left panel) and evaluation of the effect of this variation depending on the allele present at SNP3. Different letters indicate significant difference at $P < 0.05$ (Two-way ANOVA, followed by TukeyHSD for multiple comparison). *ns*, not significant.



Supplementary figure 5. Basal expression of genes in the vicinity of the *LecRK-I.1* locus
 Publicly available RNA-seq data were selected for the accessions used in this study and expression levels for all genes in a 50kb region around *LecRK-I.1* is shown depending on the allele present at SNP3. Only accessions that were used in this study were considered for analysis.

Supplementary Tables

Supplementary Table 1. List of primers used for quantitative-PCR experiments.

Gene name	Gene ID	Primer ID	Sequence (3'-5')	Reference
SAND	At2g28390	SAND_fw	AACTCTATGCAGCATTGATCCACT	
		SAND_rev	TGATTGCATATCTTTATCGCCATC	
PR1	At2g14610	PR1-Fw	GTGGGTTAGCGAGAAGGCTA	
		PR1-Rv	ACTTTGGCACATCCGAGTCT	
LecRK-1.1	At3g45330	LecRK-1.1_fw	CCCGATCGAAAAGCATTCA	Gouhier-Darimont et al. 2019
		LecRK-1.1_rev	GTTTTCTCCGGTTTCTTGGG	

General discussion

The aim of this thesis was to get a better understanding of the mechanisms that regulate *P. brassicae* egg-induced cell death. Through the use of different approaches, we characterized the role of sphingolipids in the execution of this response, together with the identification of two genes that affect HR-like in natural Arabidopsis populations. The functional validation of these mechanisms was successful and therefore demonstrate the interest of addressing biological questions through different strategies. While this work extends our conceptual understanding of how cell death is triggered in response to insect eggs in Arabidopsis and *B. nigra*, it also raises a great deal of questions. While most of the results were discussed in each chapter individually, some more general questions remain.

Is the egg-induced HR-like a form of ETI? Based on the previously described mechanisms of ETI outputs (Cui et al., 2013), the response to insect eggs shares intriguing similarities. As mentioned, it requires functional SA biosynthesis and signaling (Gouhier-Darimont et al., 2013), triggers hypersensitive-like cell death together with an increase in C16:0 Cer (Chapter 1), induces sustained MPK3/6 activation (O. Hilfiker, unpublished) and calcium fluxes (Chapter 2), consistent with previously reported ETI responses (Magnin-Robert et al., 2015; Tsuda et al., 2013; Grant et al., 2000). Previous attempts at characterizing EAMP identified eliciting activity in lipidic fractions (Bruessow et al., 2010). This hypothesis was further supported by the fact that the *LecRK-1.8* mutant also displays decreased gene expression and cell death in response to treatment with a lipid-derived SPE fraction from *P. brassicae* eggs (Gouhier-Darimont et al., 2019). To the best of our knowledge, no lipid effector has been described in plants, in particular not within the conceptual framework of ETI as described in the Zig-Zag model. Moreover, previously performed GWA mapping using effector-bearing pathogens resulted in the identification of NLR genes (Atwell et al., 2010; Iakovidis et al., 2016). GWA mapping on HR-like triggered by insect eggs, however, did not result in the identification of any NLR gene, which would be an indication that it triggers a canonical ETI (Cui et al., 2013). Mapping of HR-like was performed using a quantitative phenotype because egg-triggered HR-like in Arabidopsis was clearly identified as such (Gouhier-Darimont et al., 2013; Reymond, 2013). Quantitative traits are thought to be controlled by many loci (Corwin and Kliebenstein, 2017). In contrast, qualitative phenotype, such as the HR triggered by many effectors, usually map to single loci (such as a NLR), although ETI has been considered a quantitative trait (Iakovidis et al., 2016). With this in mind, we also performed GWA mapping by treating HR-like symptoms as a binary trait (0 = no necrotic symptom, 1 = at least one leaf with necrosis; data not shown). While this analysis revealed once again *GLR2.7* as a main QTL, a clear signal was present

in the gene sequence of *LOH3*. This provides further independent evidence that the results presented in Chapter 1 are functionally important. Given that the role of sphingolipids was validated, it would be interesting to evaluate what is the impact of natural variants on the protein sequence and function of *LOH3* during egg-induced responses. Despite the phenotypic resemblance with ETI/HR, HR-like triggered by *P. brassicae* eggs does not seem to rely on NLR(s), but rather possesses a highly polygenic structure. Altogether, these results confirm that HR-like is not a canonical ETI response in the sense of the Zig-Zag model (Jones and Dangl, 2006). This finding is consistent a growing body of evidence showing that there might be less distinction between PTI and ETI, as they exhibit similar defense responses but with different amplitude (Kanyuka and Rudd, 2019; Thomma et al., 2011).

The identification of *GLR2.7* and *LecRK-I.1* as regulators of insect egg-induced cell death is interesting for different reasons. First, these genes were not isolated in previous screens and GWAS, suggesting that they might play a specific role during egg-induced HR-like. Secondly, *GLR2.7* was associated with both HR-like and SA accumulation, an expected signature for an upstream component in a signaling pathway, and *LecRK-I.1* is a homolog of *LecRK-I.8* and seems to be part of the same signaling complex. Finally, both genes harbored clear signatures of balancing selection. The long term maintenance of these polymorphisms could indicate that both genes may play an important role in natural Arabidopsis populations. Its maintenance could be due to a so-called “cost of resistance”, whereby the allele associated with resistance is costly to maintain or displays negative pleiotropy. The ACQOS (acquired osmotolerance) locus, which codes for several NLR genes, was recently reported to be involved in a trade-off involving bacterial resistance and osmotolerance (Ariga et al., 2017). In the case of the well-studied *RPM1* locus, field experiment showed that the expression of this NLR in the absence of disease reduced seed production by 9% (Tian et al., 2003). Finally, the long term maintenance of the NLR *RPS5* was suggested to originate from diffuse interactions with multiple effectors/pathogens (Lastra et al., 2014). As a result, fluctuations in oviposition incidence together with the possibility that *LecRK-I.1* and *GLR2.7* may work in response to oviposition by multiple species, or play additional roles, could potentially explain the maintenance of these alleles in different populations. For each accession, careful evaluation of herbivore pressure, incidence of diverse biotic and abiotic factors, and microenvironmental conditions will help to address these hypotheses.

How does SA signaling lead to ceramide accumulation? We observed that the disruption of SA synthesis led to a reduction in *LOH2* induction upon egg extract treatment, suggesting that SA may participate in the transcriptional regulation of sphingolipid metabolism. This finding is corroborated by the fact that SA was previously reported to alter the

expression of several sphingolipid genes in a similar manner than insect eggs (Shi et al., 2015). As mentioned, LecRK-I.8 is responsible for part of the SA-dependent egg-induced responses. We noticed that the expression of sphingolipid genes seemed to be reduced in *lecRK-I.8* upon egg extract treatment (data not shown), further supporting this hypothesis. Additional replicates will help address this question. The identity of the regulators downstream of SA are unknown but several hypotheses exist based on the literature. For instance, WRKY18 and WRKY40, two transcription factors (TF) induced during PTI, were found to bind to the promoters of *LOH2* and *IPCS2* upon elicitation (Birkenbihl et al., 2017). In line with the possibility that they could play a role during oviposition, microarray data show that both TF genes are induced (Little et al., 2007). Preliminary data using single and double WRKY mutants suggest that cell death may be affected in these mutants (data not shown). A next step will be to validate these results and to test whether this is correlated with alterations in the transcriptional regulation of sphingolipid metabolism. ET was also shown to negatively impact the transcriptional and metabolic status of sphingolipid metabolism (Wu et al., 2015), and we observed that ET insensitivity using *ein2-1* mutant plants resulted in increased cell death and *LOH2* expression in response to eggs. It thus appears that sphingolipid metabolism may be regulated by a balance between SA and ET. Further work is needed to confirm this interesting possibility. Finally, it would be interesting to evaluate the potential connections between LecRK-I.1/I.8 or GLR2.7 with sphingolipid metabolism.

Based on our data, we propose the following simplified hypothetical model for the regulation of insect-egg triggered HR-like in Arabidopsis (Fig. 1). Following the recognition of

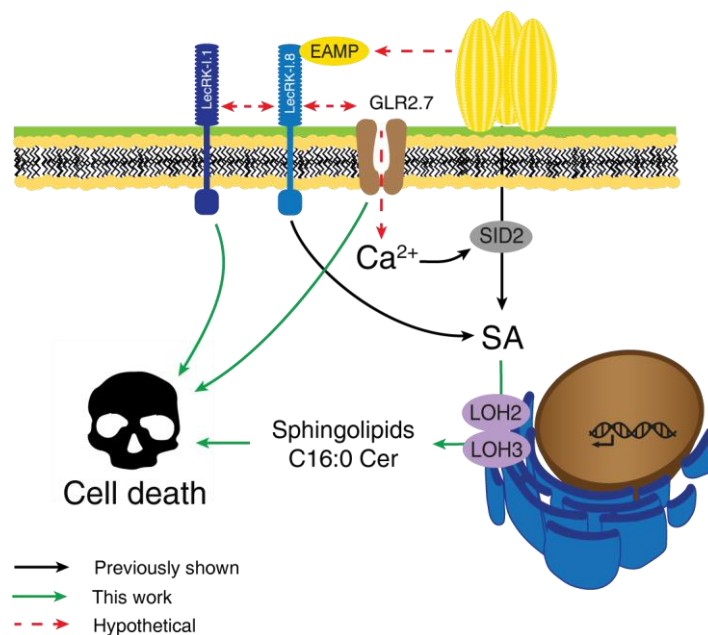


Figure 4. Simplified model of the mechanisms involved in insect egg-induced HR-like. Refer to the main text for a description.

egg-associated molecular patterns (EAMP), potentially by the L-type clade I LecRK-I.8, an early Ca^{2+} influx occurs and SA accumulates via the activity of SID2. Previous studies reported that the SID2 signaling module is regulated by Ca^{2+} , indicating that the observed Ca^{2+} influx could activate SA accumulation. While we could show an involvement of GLR2.7 during egg-induced cell death, its exact role remains unclear. As GLRs are described as ligand-gated calcium channels and GLR2.7 was associated with both HR-like and SA accumulation, we postulate that the early calcium influx observed upon egg treatment may be dependent on GLR2.7 and further activates SA accumulation. Accumulating SA then stimulates sphingolipid metabolism, leading to an accumulation of C16:0 ceramides via the activity of the ceramide synthases LOH2 and LOH3. Cell death is then induced by the high levels of C16:0 found in the cell via an unknown mechanism. In parallel, we postulate that LecRK-I.1 is activated downstream of LecRK-I.8, possibly via a direct interaction, leading to a modulation of egg-induced cell death. The hypothesis of direct interaction is likely based on the fact that LecRKs were shown to homo- and heterodimerize.

In conclusion, we identified three new mechanisms participating in the regulation of HR-like induced by insect eggs. While the role of sphingolipids in PCD was known, our results expand the current knowledge about downstream executors of cell death during HR-like. Furthermore, we identified two loci associated with egg-induced responses in natural *Arabidopsis* accessions. While the exact function of these genes is still lacking, they belong to gene families known to be involved in immune responses and therefore provide a valuable insight into the regulation of HR-like. Despite a lack of functional understanding for some of these processes, the identification of genomic regions involved in direct defenses against insect eggs provides a valuable resource for breeders. In the near future, it will be interesting to test whether the two identified loci are also potentially involved in HR-like in other *Brassicaceae*. Given the successful identification of ceramide accumulation as a common mechanism in both *Arabidopsis* and *B. nigra*, it is likely that at least part of the genetic structure of HR-like is conserved in *Brassicaceae*.

References

- Ariga, H. et al.** (2017). NLR locus-mediated trade-off between abiotic and biotic stress adaptation in *Arabidopsis*. *Nat. Plants* **3**: 17072.
- Atwell, S. et al.** (2010). Genome-wide association study of 107 phenotypes in *Arabidopsis thaliana* inbred lines. *Nature* **465**: 627–31.
- Birkenbihl, R.P., Kracher, B., Roccaro, M., and Somssich, I.E.** (2017). Induced Genome-Wide Binding of Three *Arabidopsis* WRKY Transcription Factors during Early MAMP-Triggered Immunity. *29*: 20–38.
- Bruessow, F., Gouhier-Darimont, C., Bruchala, A., Metraux, J.-P., and Reymond, P.** (2010). Insect eggs suppress plant defence against chewing herbivores. *Plant J.* **62**: 876–885.
- Corwin, J.A. and Kliebenstein, D.J.** (2017). Quantitative Resistance: More Than Just Perception of a Pathogen. *Plant Cell* **29**: 655–665.
- Cui, H., Tsuda, K., and Parker, J.E.** (2013). Effector-Triggered Immunity: From Pathogen Perception to Robust Defense. *Annu. Rev. Plant Biol.* **66**: 141210140145001.
- Gouhier-Darimont, C., Schmiesing, A., Bonnet, C., Lassueur, S., and Reymond, P.** (2013). Signalling of *Arabidopsis thaliana* response to *Pieris brassicae* eggs shares similarities with PAMP-triggered immunity. *J. Exp. Bot.* **64**: 665–74.
- Gouhier-Darimont, C., Stahl, E., Glauser, G., and Reymond, P.** (2019). The *Arabidopsis* Lectin Receptor Kinase LecRK-I.8 Is Involved in Insect Egg Perception. *Front. Plant Sci.* **10**: 1–10.
- Grant, M., Brown, I., Adams, S., Knight, M., Ainslie, A., and Mansfield, J.** (2000). The RPM1 plant disease resistance gene facilitates a rapid and sustained increase in cytosolic calcium that is necessary for the oxidative burst and hypersensitive cell death. *Plant J.* **23**: 441–450.
- Iakovidis, M., Teixeira, P.J.P.L., Exposito-Alonso, M., Cowper, M.G., Law, T.F., Liu, Q., Vu, M.C., Dang, T.M., Corwin, J.A., Weigel, D., Dangl, J.L., and Grant, S.R.** (2016). Effector Triggered Immune Response in *Arabidopsis thaliana* Is a Quantitative Trait. *Genetics* **1**: 1–45.
- Jones, J.D.G. and Dangl, J.L.** (2006). The plant immune system. *Nat. Rev.* **444**: 323–329.
- Kanyuka, K. and Rudd, J.J.** (2019). Cell surface immune receptors: the guardians of the plant's extracellular spaces. *Curr. Opin. Plant Biol.* **50**: 1–8.
- Lastra, R.O. et al.** (2014). The long-term maintenance of a resistance polymorphism through diffuse interactions. *Nature* **512**: 436–440.
- Little, D., Gouhier-Darimont, C., Bruessow, F., and Reymond, P.** (2007). Oviposition by pierid butterflies triggers defense responses in *Arabidopsis*. *Plant Physiol.* **143**: 784–800.
- Magnin-Robert, M., Le Bourse, D., Markham, J.E., Dorey, S., Clément, C., Baillieul, F., and Dhondt-Cordelier, S.** (2015). Modifications of sphingolipid content affect tolerance to hemibiotrophic and necrotrophic pathogens by modulating plant defense responses in *Arabidopsis*. *Plant Physiol.* **169**: 2255–2274.
- Reymond, P.** (2013). Perception, signaling and molecular basis of oviposition-mediated plant responses. *Planta* **238**: 247–58.
- Shi, C., Yin, J., Liu, Z., Wu, J.-X., Zhao, Q., Ren, J., and Yao, N.** (2015). A systematic simulation of the effect of salicylic acid on sphingolipid metabolism. *Front. Plant Sci.* **6**: 186.
- Thomma, B.P.H.J., Nürnberger, T., and Joosten, M.H.A.J.** (2011). Of PAMPs and

Effectors: The Blurred PTI-ETI Dichotomy. *Plant Cell* **23**: 4–15.

Tian, D., Traw, M.B., Chen, J.Q., Kreitman, M., and Bergelson, J. (2003). Fitness costs of R-gene-mediated resistance in *Arabidopsis thaliana*. *Nature* **423**: 74–77.

Tsuda, K., Mine, A., Bethke, G., Igarashi, D., Botanga, C.J., Tsuda, Y., Glazebrook, J., Sato, M., and Katagiri, F. (2013). Dual Regulation of Gene Expression Mediated by Extended MAPK Activation and Salicylic Acid Contributes to Robust Innate Immunity in *Arabidopsis thaliana*. *PLoS Genet.* **9**.

Wu, J., Wu, J., Yin, J., Zheng, P., and Yao, N. (2015). Ethylene Modulates Sphingolipid Synthesis in *Arabidopsis*. *Front. Plant Sci.* **6**: 1–11.

Acknowledgments

First and foremost, I would like to express my deep gratitude to my supervisor Philippe for all these years. The projects were not easy deals, but you always allowed me to explore many aspects independently while (trying to) refraining my curiosity and helping me focus on the important results and stories I was developing. This freedom helped me become the independent and creative researcher I am today. Trust is a beautiful gift, and I hope I proved myself worthy of deserving it. Thank you.

We always say that good lab/group atmosphere largely contributes to the success and well-being of researchers, and this has never failed in the past years. I had the chance to spend most of my time in the lab surrounded by a handful of truly inspiring and crazy people. Thank you Esteban for the great time we had, I am incredibly grateful that we spent all this time together. Things were often crazy with you, but this was all I needed when experiments fail. Elia, my favourite science nerd (yes you are) but also one of the craziest person I've met. Thank you for all the good (and bad) discussions we had about anything. Fabian, you never failed your reputation and I am really happy that you were around for a good part of my time in the lab. Caroline, of course, you taught me so many things (even though I would always try to argue) and helped me a great deal for some important experiments. I will be forever grateful for the atmosphere we had, this was truly something: serious when needed, quite stupid the rest of the time. How do people work in so many other labs? Many thanks also to the lab alumni, we had great fun at the time!

Virginie, just thank you for your endless support and tolerance towards me. I am not always easy, but you made it a lot easier for me. Thank you. I am also grateful to my entire family for their support, but especially for all the good times we had together. I am pretty lucky to have you all so close to me. My parents in particular, you also deserve a medal for surviving my university years and all that came with it.

As I am always super in advance when it comes to deadlines (sorry Philippe), I'll spend the next 5 minutes finishing this. So, endless gratitude to the entire department, past and present, I met some amazing people and I really enjoyed spending the past 6 years with you guys. I had a blast. Thanks to all my friends, close and less close. You mean the world to me and nothing would be the same without you all. Special thanks to Charles-Edouard Goy, my biology teacher in highschool, for believing in me and for transmitting this passion for Life. I am late and tired, but thank to all the people I met on the road to this day. We are defined by our relations, and I was lucky enough to always meet amazing people.

I would like to express a deep gratitude to all the people that contributed to this work in one way or another. I believe Science is always a collective effort, and I cannot deny this. Many thanks to my experts Sébastien Mongrand, Fabrice Roux and Matthias Erb for reading and discussing this work with me.

I would like to thank all the bands that provided a soundtrack for these years. This was important. Finally, nothing would have been possible without you my dear Caffeine.